
**Gene expression profiling in acute
leukemias: New insights into biology
and a global approach to the
diagnosis of leukemia using
microarray technology**

Dissertation
an der Fakultät für Biologie
der Ludwig-Maximilians-Universität
München

vorgelegt von
Alexander Kohlmann
aus Neumarkt i.d. OPf.

München, den 1. Dezember 2004

Diese Arbeit wurde im Labor für spezielle Leukämie-Diagnostik im
Klinikum der Ludwig-Maximilians-Universität München – Großhadern
unter Anleitung von Herrn Professor Dr. Dr. T. Haferlach durchgeführt.

Erstgutachter: Professor Dr. Thomas Cremer

Zweitgutachter: Professor Dr. Heinrich Leonhardt

Sondervotum: Professor Dr. Dr. Torsten Haferlach

Tag der mündlichen Prüfung: 26. Oktober 2005

Contents

Contents.....	IV
List of figures.....	VI
List of tables.....	VII
Abbreviations.....	VIII
1. Summary.....	1
2. Introduction.....	3
2.1 Microarrays and the era of functional genomics.....	3
2.2 Leukemia.....	7
2.3 Gene expression profiling in the field of hematology.....	12
2.4 Questions addressed in this work.....	14
3. Methods and Protocols.....	15
3.1 Description of patient samples.....	15
3.2 Diagnostic procedures.....	15
3.3 Microarray target preparation.....	18
3.3.1 Isolation of total RNA.....	19
3.3.2 Synthesis of ds cDNA.....	21
3.3.3 Cleanup of ds cDNA.....	23
3.3.4 Synthesis of biotin-labeled cRNA.....	25
3.3.5 Cleanup of biotin-labeled cRNA.....	26
3.3.6 Fragmenting the cRNA.....	28
3.3.7 Target hybridization.....	29
3.3.8 Microarrays.....	31
3.3.9 Microarray washing and staining.....	33
3.3.10 Microarray scanning and image analysis.....	35
3.3.11 Quality assessment.....	36
3.3.12 Data sets and scaling procedure.....	38
3.4 Microarray data analysis.....	39
3.4.2 Estimation of prediction performance.....	43
3.4.3 Hierarchical clustering.....	44
3.4.4 Principal component analysis.....	45
3.4.5 Classification of samples based on gene expression patterns.....	46
3.4.6 Functional gene annotation.....	48
3.4.7 Network analysis.....	49
3.4.8 Software.....	50
4. Results.....	51
4.1 Gene expression profiling in AML.....	51
4.2 Gene expression profiling in ALL.....	67
4.3 Gene expression profiling in t(11q23)/ <i>MLL</i> leukemias.....	73
4.4 Gene expression profiling as potential diagnostic method.....	82

5. Discussion	107
5.1 Specific patterns in AML with reciprocal rearrangements	107
5.2 Molecular characterization of ALL using microarrays.....	113
5.3 Novel insights into the biology of t(11q23)/ <i>MLL</i> leukemias	116
5.4 Microarray technology as a potential diagnostic platform.....	121
5.5 Concluding remarks	129
6. References	131
7. Appendix	146
7.1 Chemicals, enzymes, and reagents	146
7.2 Instrumentation and technical equipment.....	148
7.3 Buffers and solutions.....	149
Publications.....	153
Patent applications.....	155
Danksagung	157
Lebenslauf	158

List of figures

Figure 1.	Different types of microarray platforms.....	4
Figure 2.	Fluorescence image of a microarray (Affymetrix U133A).....	6
Figure 3.	Affymetrix chip design.....	6
Figure 4.	Interlaboratory tests in cytomorphology.....	11
Figure 5.	Gene expression analysis overview.....	18
Figure 6.	Overview about the data analysis workflow.....	39
Figure 7.	Hierarchical cluster analysis workflow.....	44
Figure 8.	Principal component analysis workflow.....	45
Figure 9.	Multiple-tree model computation.....	46
Figure 10.	Concept of SVM-based classification.....	47
Figure 11.	Classification task.....	47
Figure 12.	Network details on node shapes, edge labels, and types.....	49
Figure 13.	Unsupervised hierarchical clustering of AML with t(15;17), t(8;21), and inv(16).....	51
Figure 14.	Unsupervised PCA of AML with t(15;17), t(8;21), and inv(16).....	52
Figure 15.	Supervised analysis of AML with t(15;17), t(8;21), and inv(16).....	53
Figure 16.	PCA of three AML subtypes based on 13 genes.....	54
Figure 17.	Multiple-tree classifier for AML with t(15;17), t(8;21), and inv(16).....	55
Figure 18.	Hierarchical clustering using 36 genes from both classifiers.....	57
Figure 19.	Transition from U95Av2 arrays to the U133 array design.....	58
Figure 20.	Morphology of APL samples.....	59
Figure 21.	Class discovery: APL vs. other AML subclasses.....	60
Figure 22.	Network visualizing differences when comparing APL to other AML subclasses.....	61
Figure 23.	PCA based on genes from the GO category blood coagulation.....	62
Figure 24.	Supervised analysis to discriminate APL subtypes.....	63
Figure 25.	Differences in expression of genes with function in granulation or maturation in APL.....	66
Figure 26.	Analysis of adult ALL samples using U95Av2 microarrays.....	67
Figure 27.	Analysis of adult ALL samples using U133A microarrays.....	68
Figure 28.	PCA including heterogeneous precursor B-ALL cases.....	69
Figure 29.	Hierarchical clustering including heterogeneous precursor B-ALL cases.....	70
Figure 30.	Zoomed image of subtree 5 out of Figure 29.....	71
Figure 31.	Heterogeneous precursor B-ALL in the context of pediatric markers.....	72
Figure 32.	PCA including various acute leukemia subtypes.....	73
Figure 33.	Hierarchical clustering of 363 ALL and AML samples.....	74
Figure 34.	Network distinguishing t(11q23)/ <i>MLL</i> leukemias from other acute leukemia subtypes.....	75
Figure 35.	Unsupervised PCA of adult ALL and AML with t(11q23)/ <i>MLL</i>	76
Figure 36.	Unsupervised hierarchical clustering of adult ALL and AML with t(11q23)/ <i>MLL</i>	76
Figure 37.	Differentially expressed genes between ALL and AML with t(11q23)/ <i>MLL</i>	78
Figure 38.	Supervised identification of differentially expressed genes in t(11q23)/ <i>MLL</i> leukemias.....	79
Figure 39.	Unsupervised analysis of t(11q23)/ <i>MLL</i> samples with various partner genes.....	80
Figure 40.	Pattern robustness in AML with recurrent chromosomal aberrations.....	83
Figure 41.	Analysis of varying sample handling and operator parameters.....	85
Figure 42.	Concordance between cytochemistry and gene expression.....	87
Figure 43.	Protein expression and mRNA abundance in a subset of diagnostic antigens.....	89
Figure 44.	Pediatric markers according to Yeoh et al. can classify adult patients.....	95
Figure 45.	Pediatric markers according to Armstrong et al. can classify adult patients.....	96
Figure 46.	Overlapping t(11q23)/ <i>MLL</i> markers from two pediatric cohorts classify adult patients.....	97
Figure 47.	Overall survival in cytogenetically defined AML subgroups.....	99
Figure 48.	Hierarchical cluster analysis of 937 samples representing 13 classes.....	103
Figure 49.	Three-dimensional PCA visualizing distinctions of leukemia subtypes.....	104
Figure 50.	Identification of c-ALL/Pre-B-ALL samples with or without t(9;22).....	105
Figure 51.	Distinction between immature and cortical T-ALL samples.....	106
Figure 52.	Overview of <i>MLL</i> translocation partners.....	116

List of tables

Table 1.	Minimal set of 13 genes sufficient for accurate class prediction	54
Table 2.	Identified genes for the classification of AML with t(15;17), t(8;21), and inv(16).....	56
Table 3.	Morphological and genetic differences in the APL cohort.....	64
Table 4.	Linear regression analyses for top 20 discriminative genes (M3 vs. M3v).....	65
Table 5.	<i>MLL</i> partner gene confusion matrix determined by 10-fold CV.....	81
Table 6.	<i>MLL</i> partner gene confusion matrix determined by resampling	81
Table 7.	Classification accuracies for various parameters.....	83
Table 8.	Patients for comparison of flow cytometry and microarray analyses	88
Table 9.	Comparisons of protein expression and mRNA abundance in acute leukemia	90
Table 10.	Comparisons of protein expression and mRNA abundance in AML.....	91
Table 11.	Comparisons of protein expression and mRNA abundance in precursor B-ALL	92
Table 12.	Comparisons of protein expression and mRNA abundance in precursor T-ALL	93
Table 13.	Classification of three adult ALL subtypes based on pediatric markers.....	94
Table 14.	Prediction of t(11q23)/ <i>MLL</i> aberrations in adult ALL using pediatric markers.....	96
Table 15.	Prediction of <i>MLL</i> aberrations using overlapping t(11q23)/ <i>MLL</i> -specific genes.....	97
Table 16.	Number of samples and patient characteristics.....	98
Table 17.	Confusion matrix for prediction of 13 groups as determined by 10-fold CV.....	100
Table 18.	Confusion matrix for prediction of 13 groups as determined by resampling	101
Table 19.	Sensitivities and specificities for leukemia classification in 13 subgroups	102
Table 20.	Confirmation of genes correlated with AML with t(15;17), t(8;21), and inv(16).....	110

Abbreviations

μ	micro
μm	micrometer
ALL	acute lymphoblastic leukemia
AML	acute myeloid leukemia
APL	acute promyelocytic leukemia
ATP	adenosine triphosphate
ATRA	all-trans retinoic acid
bp	base pair
BSA	bovine serum albumin
cDNA	complementary DNA
CLL	chronic lymphatic leukemia
CML	chronic myeloid leukemia
CV	cross-validation
DEPC	diethyl pyrocarbonate
DNA	deoxyribonucleic acid
dNTP	deoxynucleotide triphosphate
ds	double-stranded
dT	deoxythymidine
DTT	dithiothreitol
<i>E. coli</i>	<i>Escherichia coli</i>
EDTA	ethylenediaminetetraacetic acid
EGIL	European Group on Immunological Classification of Leukemia
FAB	French-American-British
FDR	false discovery rate
FISH	fluorescence in situ hybridization
FITC	fluorescein-isothiocyanate
FLT3-LM	<i>FLT3</i> gene length mutation
g	gram
<i>g</i>	acceleration (9.80665 m/s ²)
G	giga
G-band	Giemsa dark chromosome band
GO	gene ontology
h	hour
Ig	immunoglobulin
IVT	in vitro transcription
k	kilo
l	liter
LOOCV	leave-one-out cross-validation
M	molar
MES	2-morpholinoethanesulfonic acid
min	minute
ml	milliliter
mM	millimolar
MRD	minimal residual disease
mRNA	messenger RNA
nm	nanometer
OH	hydroxyl group
PBS	phosphate buffered saline
PCA	principal component analysis
PCR	polymerase chain reaction
PE	phycoerythrin
RNA	ribonucleic acid
RNase	ribonuclease
rpm	rotations per minute
RPMI	cell culture medium (Roswell Park Memorial Institute)
RT-PCR	reverse transcriptase-polymerase chain reaction
s	second
SAM	significance analysis of microarrays
SAPE	streptavidin, R-phycoerythrin conjugate
SSPE	sodium chloride-sodium phosphate-EDTA buffer
SVM	support vector machine
Tris	Tris(hydroxymethyl)aminomethane
Tween-20	polyoxyethylenesorbitan monolaurate
U	unit
w/v	percentage weight per volume
WBC	white blood cell
WHO	World Health Organization

1. Summary

The application of global gene expression profiling allows to obtain detailed molecular fingerprints of underlying gene expression in any cell of interest. In this work gene expression profiles were generated from a comprehensive cohort of leukemia patients and healthy donors referred to and diagnosed in the Laboratory for Leukemia Diagnostics, Munich, Germany, which is a nation-wide reference center for the diagnosis of hematologic malignancies. Thoroughly characterized clinical samples were analyzed by high-density microarrays interrogating the expression status of more than 33,000 transcripts.

In one specific aspect of this work the potential application of gene expression signatures for the prediction and classification of specific leukemia subtypes was assessed. Today the diagnosis and subclassification of leukemias is based on a controlled application of various techniques including cytomorphology, cytogenetics, fluorescence in situ hybridization, multiparameter flow cytometry, and PCR-based methods. The diagnostic procedure is performed according to a specific algorithm, but is time-consuming, cost-intensive, and requires expert knowledge. Based on a very low number of candidate genes it is demonstrated in this work that prognostically relevant acute leukemia subtypes can be classified using microarray technology. Moreover, in an expanded analysis including 937 patient samples representing 12 distinct clinically relevant acute and chronic leukemia subtypes and healthy, non-leukemia bone marrow specimens a diagnostic prediction accuracy of ~95% was achieved. Thus, given these results it can be postulated that the occurring patterns in gene expression would be so robust that they would allow to predict the leukemia subtype using global gene expression profiling technology. This finding is further substantiated through the demonstration that reported differentially expressed genes from the literature, namely pediatric gene expression signatures representing various acute lymphoblastic leukemia (ALL) subtypes, can be used to independently predict the corresponding adult ALL subtypes. Furthermore, it could be demonstrated that microarrays both confirm and reproduce data from standard diagnostic procedures, but also provide very robust results. Parameters such as partial RNA degradation, shipment time of the samples, varying periods of storage of the samples, or target preparations at different time points from either bone marrow or peripheral blood specimens by different operators did not dramatically influence the diagnostic gene expression signatures.

In another major aspect of this work gene expression signatures were examined in detail to obtain new insights into the underlying biology of acute promyelocytic leukemia (APL) and t(11q23)/*MLL* leukemias. In APL, microarrays led to a deeper understanding of morphological and clinical characteristics. Firstly, genes which have a functional relevance in blood coagulation were found to be differentially expressed when APL was compared to other acute myeloid leukemia (AML) subtypes. Secondly, a supervised pairwise comparison between the two different APL phenotypes, M3 and its variant M3v, for the first time revealed differentially expressed genes encoding for biological functions and pathways such as granulation and maturation. With

respect to 11q23 leukemias it could be demonstrated that leukemias with rearrangements of the *MLL* gene are characterized by a common specific gene expression signature. Additionally, in unsupervised and supervised data analysis algorithms ALL and AML cases with t(11q23)/*MLL* segregated according to the lineage, i.e., myeloid or lymphoid, respectively. This segregation could be explained by a highly differing transcriptional program. Through the use of biological network analyses essential regulators of early B cell development, *PAX5* and *EBF*, were shown to be associated with a clear B-lineage commitment in lymphoblastic t(11q23)/*MLL* leukemias. Also, the influence of the different *MLL* translocation partners on the transcriptional program was directly assessed. But interestingly, gene expression profiles did not reveal a clear distinct pattern associated with one of the analyzed partner genes. Taken together, the identified molecular expression pattern of *MLL* fusion gene samples and biological networks revealed new insights into the aberrant transcriptional program in t(11q23)/*MLL* leukemias. In addition, a series of analyses was targeted to obtain new insights into the underlying biology in heterogeneous B-lineage leukemias not positive for *BCR/ABL* or *MLL* gene rearrangements. It could be demonstrated that the genetically more heterogeneous precursor B-ALL samples intercalate with *BCR/ABL*-positive cases, but their profiles were clearly distinct from T-ALL and t(11q23)/*MLL* cases.

In conclusion, various unsupervised and supervised data analysis strategies demonstrated that defined leukemia subtypes can be characterized on the basis of distinct gene expression signatures. Specific gene expression patterns reproduced the taxonomy of this hematologic malignancy, provided new insights into different disease subtypes, and identified critical pathway components that might be considered for future therapeutic intervention. Based on these results it is now further possible to develop a one-step diagnostic approach for the diagnosis of leukemias using a customized microarray.

2. Introduction

2.1 Microarrays and the era of functional genomics

Both biology and medicine are undergoing a revolution that is based on the accelerating determination of DNA sequences, including the completion of whole genomes of a growing number of organisms (Wheeler et al., 2004). In parallel to the sequencing efforts, a wide range of technologies with tremendous potential has grown that can take advantage of the vast quantity of genetic information that is now available. The field of functional genomics seeks to devise and apply these technologies, such as microarrays, to analyze the full complement of genes and proteins encoded by an organism in order to understand the functions of genes and proteins (Fields et al., 1999).

Microarrays for gene expression monitoring

The interval between the first draft assembly (Lander et al., 2001; Venter et al., 2001) and the closure of the human genome announced in April 2003 has seen big increases in human mRNA coverage, expressed sequence tags (EST) production, and continual refinement of automated genome annotation. The available data today are converging to a basal number of well below 30,000 protein-coding genes, which could even be as low as 25,000 (Southan, 2004). However, still with the sequence information alone it will not be possible to fully understand gene function, expression and regulation. Cellular processes are governed by the repertoire of expressed genes, and the levels and timing of their expression. Microarrays are a suitable tool to measure the expression of a large number of mRNAs in parallel (Young, 2000).

The basic concept behind microarrays is the precise positioning of DNA-probes that are designed to specifically monitor the mRNA abundance of genes of interest in a highly parallel manner on a solid support so that they can act as molecular detectors (Holloway et al., 2002). This determination of the relative concentration of mRNAs is based on hybridization of entire mRNA populations to high-density arrays of oligonucleotides and results in the generation of specific gene expression signatures, i.e., groups of genes with similar patterns of expression across a set of samples (Staudt, 2003). Common to all gene expression profiling approaches is the heteroduplex formation: Structural features of nucleic acids enable every nucleic acid strand to recognize complementary sequences through base pairing (Southern et al., 1999). After the process of hybridization, complementary and fluorescently tagged nucleotides can be detected. As such, microarrays allow the reproducible and quantitative monitoring of the expression levels of very large numbers of genes and provide a molecular fingerprint of the transcriptome (Lockhart and Winzeler, 2000).

Principally, in microarray experiments, the DNA probes are deposited, i.e., arrayed, on a substrate such as a glass slide, nylon membrane, or silicon wafer (Bowtell, 1999). The cDNA or cRNA target, generated from a sample input RNA that has been labeled, is hybridized to the microarray. A scanner then measures fluorescence at the site of each unique probe. Two major types of microarray technologies exist (Figure 1). The first is based on standard

microscopic glass slides on which cDNAs or long oligonucleotides (typically 60-mers) have been deposited (spotted) (Duggan et al., 1999). The second is based on photolithographic techniques to synthesize 25-mer oligonucleotides on a silicon wafer and constitutes the patented technology of Affymetrix, Inc. (Lockhart et al., 1996). These differences can impact experimental design and interpretation, but it is becoming clear that robust and reproducible gene expression data can be generated on multiple platforms (Wright et al., 2003). During the past few years powerful algorithms have been developed and adapted to mine microarray data. More recently, also applications to interpret gene expression signatures in terms of pathways and networks have evolved (Slonim, 2002).

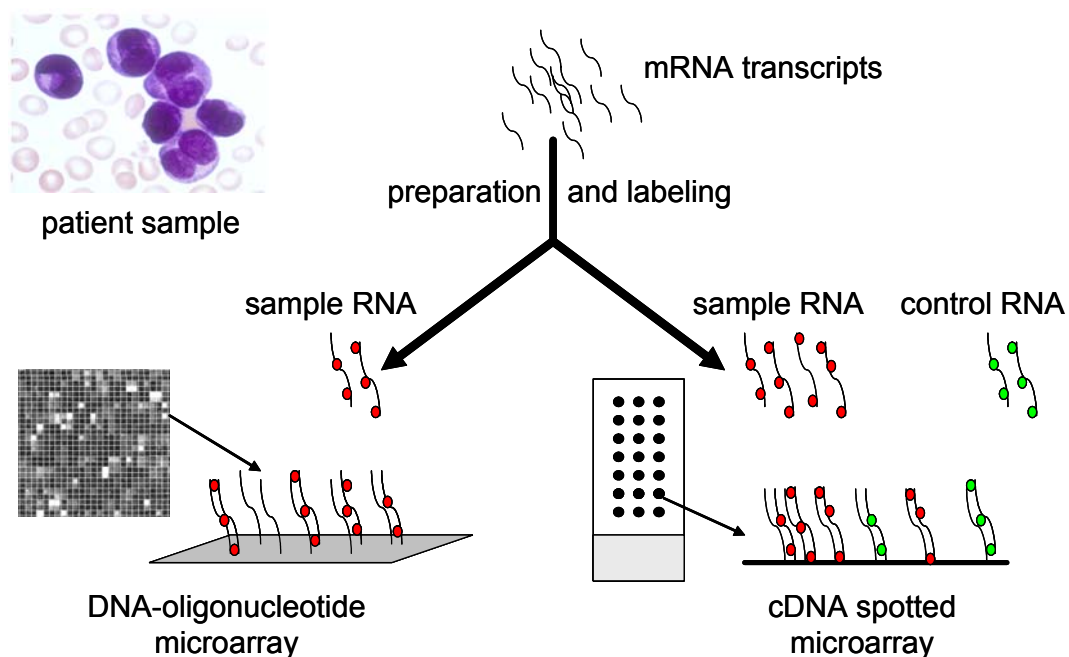


Figure 1. **Different types of microarray platforms.** Microarray platforms vary according to: (A) the solid support used (such as glass slides or silicon wafers), (B) the surface modifications with various substrates, (C) the type and length of DNA fragments on the array (such as cDNA or oligonucleotides), (D) whether the gene fragments are presynthesized and deposited or synthesized in situ, (E) the machinery used to place the fragments on the array (such as ink-jet printing, spotting, mask or micromirror-based in situ synthesis), and (F) the method of sample preparation. Currently, combinations of these variables are used to generate two main types of microarrays: in situ synthesized DNA-oligonucleotide arrays (left), and spotted glass slide arrays (right).

Glass slide microarrays

Glass slide microarrays were first produced in Patrick Brown's laboratory at Stanford University (Schena et al., 1995). In glass slide microarray studies RNA species from the test sample and from the reference sample are pairwise studied as an equivalent mixture in which the control RNA is the reference for expressing the gene transcript levels in the target sample (Figure 1). Various direct and indirect labeling methods for the sample have been developed (Holloway et al., 2002). The majority of expression analysis labeling protocols

are based on the reverse transcription of mRNA, either from highly purified poly(A) mRNA, or total RNA extracts and often include amplification steps (Van Gelder et al., 1990). In most protocols, one sample is labeled with the Cy3 (green) fluorochrome, the other with Cy5 (red). The labeled cRNA molecules hybridize to the corresponding cDNA or long oligonucleotides, of which the exact position on the array is known. The binding of the target to the probe is detected by scanning the array, typically using either a scanning confocal laser, or a charge coupled device (CCD) camera-based reader. After scanning, software calculations provide the ratios between green and red fluorescence for each spot, corresponding to the relative abundance of mRNA from a particular gene in the target sample vs. the reference sample (Duggan et al., 1999).

However, the technical difficulties in the reproducible production of glass slide microarrays should not be underestimated (Holloway et al., 2002). Much of this variation is introduced systematically during the spotting of the DNA onto the slide surface (Rickman et al., 2003) and many of the initial cDNA clone sets were compromised by contamination with T1 phage, by multiple clones in individual wells, and by incorrect sequence assignment (Halgren et al., 2001). Thus, given the lack of a gold standard for the production of glass slide microarrays using current technologies, there is a high degree of variation in the quality of data derived from glass slide microarray experiments. This poor reproducibility not only adds to the cost of a given study, but also leads to data sets that are difficult to interpret (Holloway et al., 2002).

DNA-oligonucleotide microarrays

Microarrays manufactured by Affymetrix, Inc., also known as the so-called GeneChips, use only one color and generate a gene expression profile of one sample in each analysis (Figure 2). The results obtained from these absolute expression analyses are conducive to building large databases.

GeneChip probe arrays are manufactured in a series of cycles that are highly reproducible and can be performed in a controlled environment through a technology that combines photolithography and solid-phase DNA synthesis (Lockhart et al., 1996). Each surface-bound oligonucleotide (probe) is located in a specific area on the array called a probe cell. Each probe cell contains millions of copies of a given oligonucleotide. Initially, a silicon wafer is coated with linkers containing photolabile protecting groups. Then, a photolithographic mask is applied that exposes selected portions of the probe array to ultraviolet light. Illumination removes the photolabile protecting groups enabling selective nucleoside phosphoramidite addition only at the previously exposed sites. Next, a different mask is applied and the cycle of illumination and chemical coupling is performed again. By repeating this cycle, a specific set of oligonucleotide probes is synthesized with each probe type in a known location. Thus, given a reference sequence, a probe array can be designed that consists of a highly dense collection of complementary probes with virtually no constraints on design parameters. The amount of nucleic acid information encoded on the array in the form of different probes is limited only by the physical size of the array and the achievable lithographic resolution (Lipshutz et al., 1999). Target mRNAs present at a frequency of 1:300,000 are unambiguously detected. The detection is quantitative over more than three orders of magnitude (Lockhart et al., 1996).

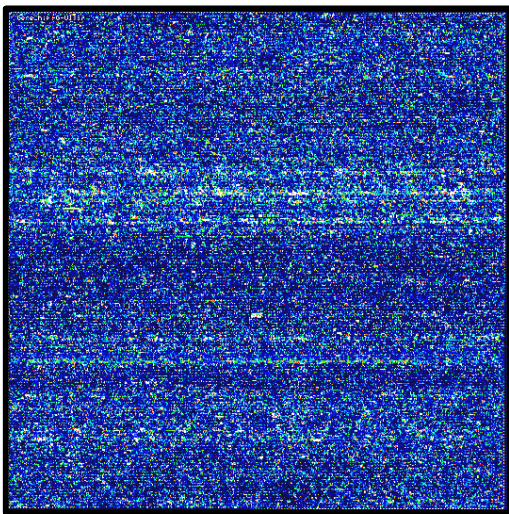


Figure 2. **Fluorescence image of a microarray (Affymetrix U133A).** The microarray contains more than 500,000 different 25-mer oligonucleotide probes in an area of 1.28 x 1.28 cm. The represented probe sets interrogate more than 22,000 human transcripts. The image of the global expression profile was obtained after overnight hybridization of an amplified and labeled human mRNA. After the washing and staining procedures, the microarray was scanned with a laser. The amount of light emitted at 570 nm is proportional to the bound target at each location on the probe array.

The mRNA abundance of a gene of interest is interrogated by a combination of a pair of 25-mer probes that span specific parts of the gene, mostly located at the 3' end (Figure 3). A first group of 25-mer oligonucleotides are called perfect match oligonucleotides (PM). In addition to these perfect match oligonucleotides, each 25-mer comes with a negative control oligonucleotide that contains a mismatch at central position (MM). This single base mismatch is sufficient to destabilize the hybridization. The MM probes are effective internal controls. They will hybridize to non-specific sequences as effectively as their counterpart PM probes. As a result, unpredictable background signal variations associated with samples from different sources as well as from cross-hybridization can be quantified and subtracted (Hubbell et al., 2002). This probe strategy addresses the issue to discern between specific and non-specific binding and offers the balance of high sensitivity and specificity in the presence of a complex background (Liu et al., 2002). The integration of the expression intensities for each of the PM-MM sets generates a value for the expression of a particular gene (Hubbell et al., 2002). Various types for probe level analyses exist. Both simple statistics as well as more sophisticated model-based approaches have successfully been applied to extract signals from the raw data (Schadt et al., 2000; Li and Wong, 2001; Irizarry et al., 2003).

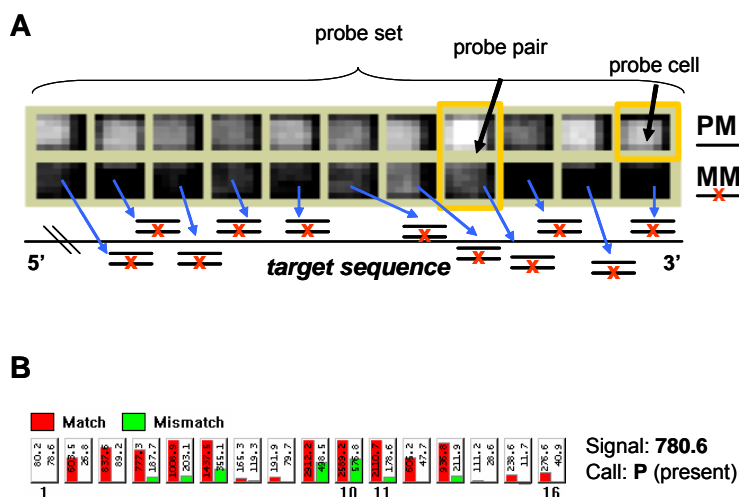


Figure 3. **Affymetrix chip design.** (A) Typical U133 chip design probe sets contain 11 probe pairs designed to detect a specific target sequence. Probe pairs comprise two probe cells, designed as perfect match (PM) and its corresponding mismatch control (MM). (B) Intensity bar graphs for the calculated signals for each probe cell. Using statistical algorithms a signal intensity and detection call for each probe set is provided.

Comparable to the glass slide microarrays, mRNA from a given sample is reverse transcribed into cDNA, which is subsequently used as a template in an *in vitro* transcription reaction which incorporates biotinylated ribonucleotides into the cRNA. The cRNA, referred to as the target, is hybridized to the 25-mer oligonucleotides on the GeneChip and is subsequently stained with streptavidin-phycoerythrin (SAPE). Thus, the major difference between the two types of DNA microarrays lies in the method to assess the transcript levels: quantitation via pairwise comparisons (ratios) for glass slides, or quantitations in arbitrary (but well-defined) expression units in the case of Affymetrix microarrays (Lockhart and Winzeler, 2000). Besides its high technical reproducibility, the *in situ* synthesized oligonucleotide technology offers several advantages over glass slide technology. It is well suited for comparisons of multiple samples because no ratios are used, making it a suitable platform for large series of clinical samples without the need of pairwise analyses. In addition, for most applications glass slides require more input RNA than Affymetrix microarrays, which can be problematic, particularly for clinical research with patient samples.

2.2 Leukemia

Malignant diseases that arise in cells of the hematopoietic system are as varied as the individual lineages that comprise this tissue, and can be broadly categorized into leukemias, myelodysplastic and myeloproliferative syndromes, Hodgkin's disease, and the non-Hodgkin's lymphomas (Downing and Shannon, 2002). Leukemias are generally classified into four different groups or types: acute myeloid (AML), acute lymphoblastic (ALL), chronic myeloid (CML) and chronic lymphatic leukemia (CLL). Acute leukemias are a heterogeneous group of malignant diseases of hematopoietic progenitor cells with different molecular genetic abnormalities, clinical characteristics, and variable outcomes with currently available treatments. As a result of recent advances in understanding of both normal hematopoietic development and the molecular pathology of hematopoietic malignancies, significant improvements have occurred in the ability to accurately diagnose, subclassify, and treat these cancers (Gilliland and Tallman, 2002). Especially cloning of recurring chromosomal translocation breakpoints has provided valuable insights into disease mechanisms, as well as identification of therapeutic targets (Rowley et al., 1977; Rowley, 1990; Rowley, 2001). These genetic alterations contribute to the leukemic transformation of hematopoietic stem cells or their committed progenitors by changing cellular functions (Gilliland, 1998; Ferrando and Look, 2000). They alter key regulatory processes by maintaining or enhancing an unlimited capacity for self-renewal, subverting the controls of normal proliferation, blocking differentiation, and promoting resistance to death signals (Pui et al., 2004).

Diagnosis and classification

Different classification schemes have been proposed over the years to assist in accurately diagnosing clinically relevant leukemia subtypes (Bennett et al., 1976; Bene et al., 1995; Jaffe et al., 2001). A comprehensive and standardized algorithm for a diagnostic workflow and an effective and carefully designed combination of methods is essential to guarantee that all of the required diagnostic information is obtained (Haferlach and Schoch, 2002).

Initially, the diagnosis of acute leukemias requires the preparation and interpretation of peripheral blood smears, accompanied by bone marrow cytology (Löffler et al., 2004; Theml et al., 2004). The morphologic evaluation is based on the FAB classification, which was proposed by the French-American-British co-operative group in 1976 (Bennett et al., 1976). The FAB classification is based on cytomorphology and cytochemistry to separate leukemia subgroups (e.g., M0 – M7 in AML) according to the morphological appearance of blasts. In certain instances, leukemia subtypes can be diagnosed by cytomorphology alone, but this typically requires that an expert reviews the smears. Often, cytomorphology is combined with cytochemistry and multiparameter flow cytometry in order to ascertain the correct entity (Bennett et al., 1985). The latter is particularly important in the subclassification of patients with ALL and to separate very undifferentiated AML from ALL (Bene et al., 1995; Campana and Behm, 2000). Using these techniques in combination, leukemias can be stratified in a first approach into CML, CLL, ALL, and AML. Within the latter three disease entities, several prognostically relevant subtypes have been identified (Lowenberg et al., 1999; Dohner et al., 2000; Pui et al., 2004). This further subclassification is based mainly on genetic abnormalities of the leukemic cells. Especially in AML, cytogenetic aberrations are the most important independent prognostic factors regarding response to therapy, as well as survival (Grimwade et al., 1998).

As a consequence, the new World Health Organization (WHO) classification of hematological malignancies, established in 2001, incorporated cytogenetics, molecular genetics, as well as morphologic and immunophenotypic findings not previously described (Jaffe et al., 2001). The diagnosis of AML is now established when at least 20% of the cells identified in the blood or bone marrow are a clonal expansion of blasts of myeloid origin (Smith et al., 2004). With respect to the classification of AML, the current WHO proposal encompasses four major categories in order to define biologically homogeneous entities which have clinical relevance. The first category is described as AML with recurring genetic abnormalities, including the following subcategories: i) AML with t(8;21)(q22;q22); fusion transcript *AML1/ETO*, ii) AML with abnormal bone marrow eosinophils inv(16)(p13q22) or t(16;16)(p13;q22); fusion transcript *CBFB/MYH11*, iii) AML with t(15;17)(q22;q12); fusion transcript *PML/RARA* and variants, so-called acute promyelocytic leukemia (APL) and iv) AML with t(11q23)/*MLL* abnormalities; various fusion transcripts. The other three categories are described as AML with multilineage dysplasia, therapy-related AML, and AML not otherwise categorized, respectively.

With respect to the classification of ALL, the immunophenotypic determination of surface antigens expressed on leukemic blast cells has important implications for treatment and prognosis of T- and B-lineage subtypes. But also recurrent chromosomal translocations and imbalances are defining molecular features of ALL and these oncogenic events identify clinically distinct subgroups of patients (Staudt, 2002). Although the frequency of particular genetic subtypes differs in children and adults (Downing and Shannon, 2002), the general mechanisms underlying the induction of ALL are similar. They include the aberrant expression of proto-oncogenes (*MYC*, *TAL1*, *LYL1*, and *HOX11*), chromosomal translocations that create fusion genes

encoding active kinases and altered transcription factors (*BCR/ABL*, *TEL/AML1*, *E2A/PBX1*, and *MLL* gene fusions), and hyperdiploidy involving more than 50 chromosomes (Pui et al., 2004).

Given the various types of leukemia-specific fusion genes, RT-PCR is the method of choice in detecting the aberrant transcripts. RT-PCR not only confirms the diagnosis, but is also used for therapy stratification. Moreover, minimal residual disease (MRD) monitoring using sensitive RT-PCR-based amplification and real time quantification of specific fusion gene transcripts has led to the development of a new powerful prognostic score predicting relapse (Schnittger et al., 2003). Recently, new techniques have begun to enter the field of diagnosis and classification of leukemias (Mathew and Raimondi, 2003): Fluorescence in situ hybridization (FISH) allows for rapid testing for specific chromosomal translocations in both metaphase and interphase cells. Spectral karyotyping (SKY) and multiplex-FISH (M-FISH) both are using 24 different fluorescently labeled chromosome painting probes to generate an automated color display of all chromosomes, enhancing accuracy and sensitivity of cytogenetic analysis, especially with complex karyotypes in myeloid leukemias (Schrock et al., 1996; Speicher et al., 1996). Comparative genomic hybridization (CGH) provides a sensitive method for identification of regions of genomic deletion or amplification and may identify new disease genes at these loci (Gilliland and Tallman, 2002). However, a drawback of many of the methods that are used today is the requirement of viable cells. For example, the cells used for genetic analyses need to divide in vitro in order to obtain metaphases. Another problem is the long lag period (>72 hours) that typically occurs between the receipt of the specimens to be analyzed in the laboratory and the generation of results. Also, a great experience in preparing chromosomes and analyzing karyotypes is needed to obtain correct results.

Therapeutic consequences

This complex workflow for subclassification of leukemias is not only necessary to correctly diagnose and stratify leukemia samples, but also results in major clinically relevant treatment decisions (Grimwade et al., 2001; Haferlach et al., 2004). The importance of this highly specific disease classification may be illustrated for AML as a very heterogeneous group of malignancies. Patients with AML whose leukemic cells have translocations t(15;17), t(8;21), or inv(16) have a favorable outcome with induction chemotherapy and intensive postremission consolidation chemotherapy (Schoch et al., 2003; Smith et al., 2004). In contrast, patients with abnormalities of chromosomes 5, 7, 11q23 or complex karyotypes have a very poor outcome with currently available induction and postremission chemotherapy (Schoch et al., 2003). Patients with a normal karyotype or with trisomy 8 have an intermediate prognosis (Schoch et al., 1997).

The prime example for this strong link between a comprehensive diagnostic algorithm and a consequential disease-specific treatment approach has been the use of all-trans retinoic acid (ATRA) in patients with acute promyelocytic leukemia (APL). APL represents one subtype with specific morphology and with a characteristic cytogenetic aberration, namely the translocation t(15;17)(q22;q12), which fuses the *PML* gene to the retinoic acid receptor alpha gene (*RARA*) (Reiter et al., 2004). According to the FAB

classification, APL can be separated into two distinct subtypes based solely on morphology (Bennett et al., 1976; Bennett et al., 1980a; Bennett et al., 1980b): AML M3 and AML M3 variant (M3v). The latter is also called microgranular APL in the new WHO classification (Jaffe et al., 2001). Both the correct diagnosis and the efficacy of the specific anti-leukemia treatment are based on the presence of the translocation t(15;17) and of the corresponding *PML/RARA* fusion gene (Warrell, Jr. et al., 1991; Warrell, Jr. et al., 1993; Tallman et al., 1997). The introduction of all-trans retinoic acid (ATRA) has improved the outcome in this subgroup of patient from about 50% to 85% long-term survivors (Lengfelder et al., 2000; Degos and Wang, 2001). In both APL subtypes the fusion protein PML/RARA induces an arrest on different stages of granulocytic differentiation. In the presence of high concentrations of all-trans retinoic acid the differentiation stop is overcome leading to maturation of the abnormal promyelocytic blasts to polymorphonuclear cells and finally inducing apoptosis (Tallman, 2004a).

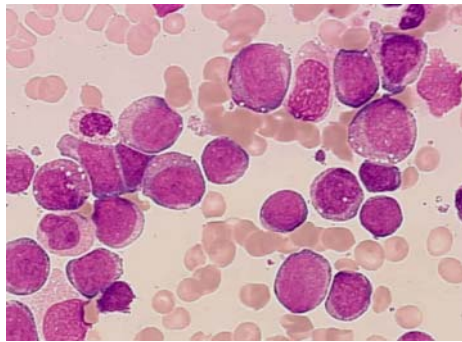
Although it did not yet result in the development of a targeted drug therapy the assured diagnosis of AML with a complex aberrant karyotype is highly relevant for the management of the patient. Depending on the age of the patient, this very dismal diagnosis is the basis for the decision to apply allogeneic stem cell transplantation very early or to even withhold any anti-leukemic therapy (Grimwade et al., 1998; Lowenberg et al., 1999; Schoch et al., 2001; Grimwade et al., 2001).

Similarly, the recent introduction of the therapeutic drug Imatinib (Glivec) into the therapeutic management of patients with CML has revolutionized the treatment strategies in this disease and may change therapeutic concepts also for *BCR/ABL*-positive ALL in the near future (Druker et al., 2001; Kantarjian et al., 2002; Goldman and Melo, 2003; Hughes et al., 2003; O'Brien et al., 2003; Pui et al., 2004). Repeatedly, the basis for both the correct diagnosis and the specifically targeted therapy is the presence of a specific genetic alteration, translocation t(9;22). In patients treated with this new drug, the therapy response is dramatically higher as compared to all other drugs that had been previously used. In addition, quantification of the *BCR/ABL* fusion gene transcripts at diagnosis and during treatment is increasingly used to sensitively assess response to therapy (Scheuring et al., 2003).

Reproducibility of methods for the diagnosis of leukemias

The methods that are used today for the diagnosis of leukemias would benefit from standardized operating procedures. In 2001, a German network of experts in cytomorphology performed interlaboratory tests to assess the reproducibility of morphological classifications in AML. As exemplarily demonstrated in Figure 4, video prints were sent to 13 experts. However, a disagreement in defining percentages of blasts was observed. This is in line with previous interlaboratory tests, where even experts from the FAB group itself observed a low inter-observer concordance in their evaluations of bone marrow smears from patients with different AML subtypes (Bennett and Begg, 1981; Argyle et al., 1989). This disagreement appeared to be based on the subjectiveness of the interpretation and also on the variability in determining percentages of cell types present (Dick et al., 1982).

AML M2 bone marrow smear



Percentage of blasts

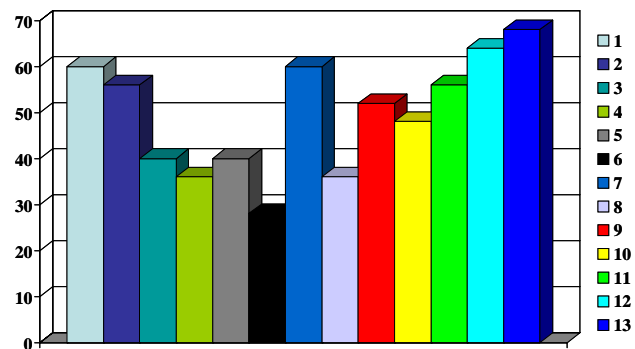


Figure 4. **Interlaboratory tests in cytomorphology.** In the German network “Akute und chronische Leukämien“ 13 experts evaluated the percentage of blasts on given video prints (left). As represented by bar graphs for each individual reviewing hematologist, the percentage of designated leukemic blast cells differ significantly between the experts (right). More information can be found online (<http://leukaemie.krebsinfo.de/>).

Also in flow cytometry variations between results from different laboratories are observed. As demonstrated for the assessment of CD34+ stem cells absolute counts, the European Working Group on Clinical Cell Analysis has attempted to standardize the flow cytometry protocol across 24 clinical sites. However, despite a reduction of the interlaboratory variation from 23.3% in trial 1 to 10.8% in trial 3, after the use of a common standardized protocol and targeted training, still large variations CD34+ cell count enumeration exist (Barnett et al., 2000). In another study including 35 laboratories performing CD4 or CD8 counts, it was shown that laboratories which do not use standardized gating strategies (CD45+ leukocytes) are more likely to return an unacceptable result. After laboratories had switched from a non-CD45 gating technique to the use of CD45 gating, their results significantly improved (Gelman and Wilkening, 2000).

With respect to cytogenetics, one has to consider that the percentages of evaluable cases in clinical studies are varying drastically. Often, up to 20% of all entered cases can not be evaluated and large discrepancies can be observed in the detection of cases with a normal karyotype (Grimwade et al., 1998; Slovak et al., 2000; Grimwade et al., 2001). Mainly, karyotypes are not available because cytogenetic analyses were either not performed, failed, were yielding no analyzable mitoses, or were deemed inadequate because the quality of banded chromosomes was poor (Byrd et al., 2002). However, the performance of cytogenetic analyses in a centralized laboratory accounted for reference protocols, such as the Laboratory for Leukemia Diagnostics, Munich, Germany, can help in increasing the percentage of evaluable cases up to 98.2% (Schoch et al., 2003).

For the detection of the *BCR/ABL* fusion gene, detailed interlaboratory tests have been performed. A first series of analyses addressed the quality and sensitivity of RT-PCR reactions in 27 different laboratories from Germany, mainly departments of hematology of university hospitals (Burmeister et al., 2000). The three most prevalent *BCR/ABL* transcripts were cloned from patient material and diluted in genomic DNA prepared from healthy donors (six defined plasmid concentrations). Of 594 samples analyzed, both false negative (n=10)

and false positive (n=11) results were observed. Also, in 11 cases wrong transcripts were detected. In summary, 14.8% of the participants had false negative results, 29.6% had false positive results, 18.5% had detected wrong transcripts (Burmeister et al., 2000). In a second series of analyses a defined amount of *BCR/ABL*-positive cells from cell lines were diluted in leukocytes from healthy donors and samples with four defined cell counts as well as negative controls were shipped to the participants on dry ice. Again, a large number of false negative results (14.2%) and false positive results (6.3%) were obtained. The discrepancies in these interlaboratory tests can be explained by contaminations of the PCR reaction mix, the use of inappropriate primers, or lack of efficiency in RNA isolation protocols (Burmeister et al., 2000). In Spain, an interlaboratory program was performed to compare the results in detecting the *PML/RARA* fusion gene transcript in patients with APL (Bolufer et al., 1998). Here, cDNA samples obtained by reverse transcription of RNA from bone marrow samples from patients with APL were sent to 12 participating laboratories. Only in 83% of the analyses concordance between laboratories was obtained. The discrepancies in 17% of the analyses were attributable to low sensitivity or inadequacy of the procedures that were used (Bolufer et al., 1998). Thus, despite the widespread use of RT-PCR in molecular laboratories most methods are not yet standardized. The implementation of an external quality assessment scheme with regular participation would ensure the accuracy of results. Taken together, given the properties of the oligonucleotide microarray technology like the high reproducibility and quality of the manufacturing process, the existing standardization of laboratory protocols, and the objectiveness of the results, it may very well be applicable for usage in clinical diagnostic procedures.

2.3 Gene expression profiling in the field of hematology

Global gene expression analyses have become an important part of biomedical basic and clinical-orientated research. The joint collaboration of biologists, physicians, and statisticians has created a fertile intellectual environment for the development of genomic approaches to questions of biological and clinical relevance. Over the past years especially hematologic malignancies have been an attractive field for a genomic approach to a heterogeneous disease (Ebert and Golub, 2004).

It all began with a study demonstrating that AML can be separated from ALL based on distinct gene expression signatures (Golub et al., 1999). The distinction of ALL and AML is routine daily practice and necessary for therapeutic decisions. Golub and colleagues showed for the first time that this distinction is also possible solely on the basis of gene expression profiles. In bone marrow samples from 27 patients with ALL and 11 patients with AML a group of only 50 discriminatory genes were presented to allow the separation of these heterogeneous entities from each other. In 36 out of 38 cases the molecular diagnosis of leukemia was made correctly based on the gene expression profile that was analyzed using a microarray representing ~6,000 transcripts. In a further set of 34 unknown samples, which had not been used for the training of the classification model, the prediction was made correctly in

29 cases. These analyses represented the first and major step towards a molecular classification of acute leukemias.

Many studies followed the pivotal work of Golub and colleagues. These analyses provided not only a “class prediction”, i.e., the prediction of a tumor entity based on specific gene expression patterns, but demonstrated also the feasibility of “class discovery”, i.e., the discovery of new subentities within groups formerly regarded as homogeneous entities. This discovery often is not limited to the pure identification of new biological tumor entities, but also includes the definition of prognostically different groups which is anticipated to influence future therapeutic strategies.

Consequently, gene expression signatures were evaluated for the correlation with cytogenetics. Virtaneva and colleagues had compared the expression status of 6,606 genes of AML blasts with normal cytogenetics and trisomy 8 as the sole abnormality (Virtaneva et al., 2001). In their study normal CD34+ cells clustered into a distinct group, whereas AML with trisomy 8 and AML with normal karyotype intercalated with each other. The microarray analyses further showed an overall increased expression of genes located on chromosome 8, suggesting a gene-dosage effect. In pediatric ALL, samples with *MLL* gene translocations were demonstrated to be distinct from other precursor B-ALL cases or AML (Armstrong et al., 2002).

The feasibility of class discovery has been impressively demonstrated for diffuse large B cell lymphoma (DLBCL). Based on distinct gene expression signatures Alizadeh and colleagues had subdivided an entity previously considered homogeneous by various pathological methods into two, not only new, but also prognostically highly relevant subgroups (Alizadeh et al., 2000). The distinctive gene expression signatures were further postulated to be able to formulate a molecular predictor of survival after chemotherapy for DLBCL (Rosenwald et al., 2002).

In a cohort of 360 pediatric ALL patients the ground-breaking study from the St. Jude Children’s Research Hospital, Memphis, TN, USA identified each of the prognostically important ALL subtypes, including precursor T-ALL, t(1;19)(q23;p13.3) (*E2A/PBX1*), t(12;21)(p13;q22) (*TEL/AML1*), rearrangements in the *MLL* gene on chromosome 11, band q23, t(9;22)(q34;q11) (*BCR/ABL*), and hyperdiploid karyotypes (i.e., >50 chromosomes). A closer examination of the distinct gene expression signatures led also to the identification of a novel ALL subgroup. Moreover, within some genetic subgroups, expression profiles identified those patients that would eventually fail therapy (Yeoh et al., 2002).

2.4 Questions addressed in this work

In the present work gene expression profiles were generated from a comprehensive cohort of leukemia patients and healthy donors referred to and diagnosed in the Laboratory for Leukemia Diagnostics, Munich, Germany. Thoroughly characterized clinical samples were analyzed by high-density microarrays interrogating the expression status of more than 33,000 transcripts. The application of global gene expression profiling allows to obtain molecular fingerprints of underlying gene expression in distinct leukemia types and gives new insights into the biology of this heterogeneous disease. Moreover, this technology possibly leads to the identification of novel diagnostic markers.

Gene expression profiling in AML

Initial experiments were related to distinct prognostical and therapeutical relevant AML subtypes with the specific genetic alterations t(15;17), t(8;21), and inv(16). Further analyses were performed to elucidating the underlying biology in the two APL subtypes FAB M3 and its variant FAB M3v.

Gene expression profiling in ALL

In ALL, a cohort of patients was analyzed to further obtain new insights into four distinct subtypes frequently occurring in adults, namely t(9;22), t(8;14), t(11q23)/*MLL*, and T-ALL. Furthermore, as a previous study reported difficulties in separating precursor B-ALL with t(9;22) from precursor B-ALL without t(9;22), a series of detailed analyses addressed the discovery of similarities or differences in these precursor B-ALL subtypes.

Gene expression profiling in t(11q23)/*MLL* leukemias

Four types of analyses may help in obtaining new insights into the underlying biology of acute leukemias with *MLL* gene rearrangements: (1) Identification of t(11q23)/*MLL* leukemia signatures compared to numerous specific subtypes of other acute leukemias, (2) discrimination of t(11q23)/*MLL*-positive AML from t(11q23)/*MLL*-positive ALL, (3) investigation of signatures correlated with *MLL/AF9* and other *MLL* partner genes, and (4) deciphering common biological networks. It is of specific interest to address the question how the differing *MLL* partner genes influence the gene expression signatures and whether pathways could be identified to explain the molecular determination of *MLL* leukemias.

Gene expression profiling as a potential diagnostic platform

To investigate whether distinct expression signatures also correlate with standard diagnostic methods a comparison to data on cytomorphology and immunophenotyping was performed. Also, the gene expression signatures of an adult cohort of patients were compared to published results on pediatric patients. Similarly, various parameters that can potentially influence the pattern of a diagnostic gene expression signature were evaluated. As a final aim of this work, a multi-class situation was tested where expression signatures of 12 different leukemia subtypes and from a control group of healthy donors were evaluated to perform the diagnosis of leukemia solely on the basis of gene expression data as assessed by microarrays.

3. Methods and Protocols

3.1 Description of patient samples

All leukemia patient samples included in this study were referred to the Laboratory for Leukemia Diagnostics, Munich, Germany, between December 1998 and February 2004. As a nation-wide reference center for the diagnosis of hematologic malignancies, the laboratory received patient samples from all over Germany, either from local hospitals or via express mail. At the time point of diagnosis the patients provided bone marrow aspirates or peripheral blood samples. In addition, bone marrow aspirates provided from healthy control subjects were included. Prior to therapy, all patients gave their informed consent for participation in the current evaluation after having been advised about the purpose and investigational nature of the study as well as of potential risks. The studies were conducted according to the rules of the local internal review board and the tenets of the revised Helsinki protocol. All samples underwent a standardized diagnostic processing (Haferlach and Schoch, 2002). All relevant clinical parameters, as well as detailed diagnostic reports, were entered in a specific leukemia database (Dugas et al., 2001). During the process of diagnosis mononuclear cells from the biopsy were purified by Ficoll-Hypaque density centrifugation. Aliquots of 5×10^6 cells were subsequently lysed using a guanidine isothiocyanate buffer (Qiagen, Hilden, Germany). The stabilized lysates were stored at -80°C until preparation for microarray analyses.

3.2 Diagnostic procedures

Following a strict algorithm (Haferlach and Schoch, 2002), the routine diagnostic procedure was performed using an individual combination of cytomorphology, cytogenetics, fluorescence in situ hybridization (FISH), immunophenotyping and molecular genetics:

Cytomorphology

The routine diagnostic cytomorphology procedure included May-Grünwald-Giemsa (MGG) staining, myeloperoxidase reaction, and non-specific esterase reaction using alpha-naphthyl-acetate. The staining was routinely performed according to standard procedures (Löffler et al., 2004). The cytomorphologic diagnosis followed the criteria of the FAB classification and the new World Health Organization classification (Bennett et al., 1976; Bennett et al., 1985; Jaffe et al., 2001).

Cytogenetics

Chromosome analyses were performed on bone marrow and/or peripheral blood samples. Cells were cultured in RPMI 1640 medium (Gibco, Gaithersburg, MD, USA) with 20% fetal calf serum and the addition of antibiotics and antimycotics. Four cultures were set up in parallel for each patient: two cultures without further supplements and two cultures with the addition of a cytokine cocktail (CC) containing erythropoietin, G-CSF, GM-CSF, SCF and IL-3. One plain culture (R24) and one stimulated culture (R24+CC) were cultivated for 24 h, colcemid was added for 2 h followed by standard slide

preparation. The other two cultures were cultivated for 24 h without colcemid and then another 24 h after the addition of colcemid (R24 HMF 24, R24+CC HMF 24) followed by standard slide preparation (Schoch et al., 2002b). Metaphases were analyzed for G-bands using a modified GAG-banding technique as described elsewhere (Fonatsch et al., 1980). A median of twenty metaphases were analyzed. The procedure was judged as not evaluable if less than 10 metaphases without clonal karyotype abnormalities were available for analysis. The chromosomes were interpreted according to the International System for Human Cytogenetic Nomenclature (ISCN) (Mitelman, 1995).

Fluorescence in situ hybridization (FISH)

FISH was performed on interphase nuclei and/or metaphases depending on the diagnostic algorithm. For interphase-FISH bone marrow and/or peripheral blood smears were processed. Metaphase-FISH was carried out on slides prepared for chromosome analysis. For interphase-FISH at least 100 interphase nuclei were evaluated (Schoch et al., 2002b). For metaphase-FISH an area of 18 x 18 mm was hybridized. FISH was performed using commercially available loci-specific probes (Vysis, Downers Grove, IL, USA) and whole chromosome painting probes (MetaSystems, Altlußheim, Germany). The signals were viewed with a Zeiss Axioskop microscope (Zeiss, Jena, Germany). The results were documented using the ISIS analyzing software (MetaSystems).

Multiparameter-immunophenotyping

Flow cytometry analyses were performed on cells isolated from bone marrow by Ficoll-Hypaque density gradient centrifugation as described (Kern et al., 2003b; Kern et al., 2004). Triple stainings, isotype controls, and monoclonal antibodies against 39 antigens were used in the following combinations as designed for diagnostic purposes and monitoring of MRD.

Antibody combinations for diagnostic antigens (triple stainings)

CD34/CD2/CD33	CD7/CD33/CD34	CD34/CD56/CD33	CD11b/CD117/CD34
CD64/CD4/CD45	CD15/CD13/CD33	HLA-DR/CD33/CD34	CD65/CD87/CD34
CD34/CD135/CD33	CD34/CD116/CD33	CD34/NG2/CD33	CD38/CD133/CD34
CD90/CD117/CD34	CD61/CD14/CD41	CD36/CD235a/CD45	CD9/CD33/CD34
CD97/CD33/CD34	CD34/CD10/CD19	CD5/CD19/CD20	CD2/CD1a/CD3
CD3/CD4/CD8	MPO/LF/cyCD15 †	TdT/cyCD22/cyCD3 †	TdT/cyCD79a/cyCD3 †

† cy: cytoplasmic antigen

All antibodies conjugated with the fluorochromes fluorescein isothiocyanate (FITC), phycoerythrin (PE), and phycoerythrin cyanine 5 (PC-5), respectively, were purchased from Immunotech (Marseilles, France), except for CD64 and CD15 (Medarex, Annandale, NJ, USA), CD133 (Milteny Biotech, Bergisch Gladbach, Germany), and MPO and LF (Caltag, Burlingame, CA, USA). The respective combinations of antibodies were added to 1×10^6 cells (volume, 100 µl) and incubated for 10 min at room temperature. The samples then were washed twice in phosphate buffered saline (PBS) and resuspended in 0.5 ml PBS. For the analysis of cytoplasmic antigens cells were fixed and permeabilized with Fix & Perm reagent (Caltag). Data acquisition was performed on a FACSCalibur four-color, dual-laser, flow cytometer (Becton

Dickinson, San Jose, CA, USA). List-mode data files were analyzed using the CellQuest Pro software, Version (Becton Dickinson).

In order to acquire data on the same cells for both flow cytometry and microarray analysis, i.e., all nucleated cells of each sample, the analysis gate was set in a forward-scatter/side-scatter plot and included lymphocyte, blast, monocyte, and granulocyte populations. Antigen expression was rated positive at a cut-off level of 20% of the cells within the mononuclear gate for membrane proteins and at a cut-off level of 10% for cytoplasmic antigens, as compared to isotype controls (in patients with analysis of isotype controls). Mean fluorescence intensity values were calculated for all events with fluorescence values higher than isotype controls. In 117 samples, a total of 39 genes/antigens were analyzed in parallel. The congruence of positivity and negativity of the expression of the respective genes as determined by flow cytometry and microarray analysis was analyzed for each gene in each individual patient. Comparisons of microarray hybridization signals with flow cytometry intensities were performed by Mann-Whitney U-test. Analyses for bivariate correlations of mRNA and protein expression levels were performed by Pearson's correlation using SPSS, Version 10.0.7 (Chicago, IL, USA).

Reverse transcriptase-polymerase chain reaction (RT-PCR)

In the years 1998 – 2000 total RNA was extracted from 1×10^7 mononuclear cells, purified by Ficoll-Hypaque density gradient centrifugation, using the RNeasy Mini kit protocol (Qiagen, Hilden, Germany). Since January 2001, mRNA was extracted from 5×10^6 mononuclear cells with the MagnaPureLC mRNA kit I (Roche Applied Science, Mannheim, Germany). The cDNA synthesis of 1-2 μg total RNA or mRNA from an equivalent of 5×10^5 cells was performed in a 50 μl reaction using 300 U Superscript II enzyme (Invitrogen, Karlsruhe, Germany) and random hexamer oligonucleotide primers (Pharmacia, Freiburg, Germany). In all cases with balanced translocations the corresponding fusion transcript was verified as described, i.e., *PML/RARA* for t(15;17), *AML1/ETO* for t(8;21), *CBFB/MYH11* for inv(16)/t(16;16) (Schnittger et al., 2003). *MLL* fusion transcripts were amplified and further verified by sequencing as previously described (Schoch et al., 2003). Detection of specific BCR/ABL fusion genes was performed as described (Maurer et al., 1991). For each sample a cABL-specific RT-PCR was performed to control the integrity of RNA (Schoch et al., 2002a). Strict precautions were taken to prevent contamination. Water instead of cDNA was included as a blank sample in each experiment. Amplification products were analyzed on 1.5% agarose gels stained with ethidium bromide according to standard protocols (Sambrook et al., 1989).

Quantification of fusion gene transcripts by quantitative RT-PCR

Each quantitative RT-PCR was carried out in a 20 μl reaction volume with 0.5 μM of forward and reverse primer, 0.25 μM Hyb-Probes, 4 mM MgCl_2 , and 2 μl LightCycler-FastStart DNA Master Hybridization Probes (Roche Applied Science, Mannheim, Germany) (Emig et al., 1999; Schnittger et al., 2003). Each 20 μl reaction contains 2 μl cDNA, which corresponds to an equivalent of about 30,000 cells at diagnosis. LightCycler data were analyzed using the LightCycler 3.0 software and the second derivative maximum method (Roche Applied Science).

3.3 Microarray target preparation

Between June 2001 and February 2004 gene expression analyses using microarrays were successfully performed in patients with newly diagnosed leukemia and normal bone marrow. Figure 5 outlines the major steps of the procedure for gene expression profiling analyses as performed in this work.

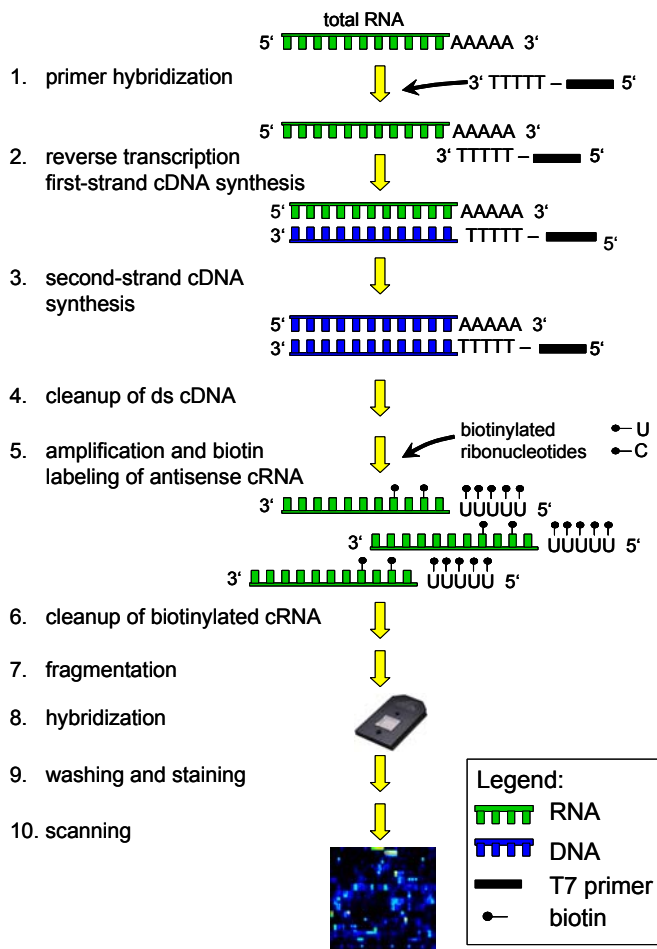


Figure 5. **Gene expression analysis overview.** The gene expression profiling analysis starts with the sample target preparation. The target is the labeled nucleic acid that is being interrogated. It is hybridized to the probes on the array. For the respective samples, double-stranded (ds) cDNA is synthesized from total RNA isolated from mononuclear cells. An in vitro transcription (IVT) reaction is then done to produce biotin-labeled cRNA from the cDNA. After fragmentation a hybridization cocktail is prepared, including the fragmented target, probe array controls, bovine serum albumin, and herring sperm DNA. The cocktail is hybridized to the probe array during a 16-hour incubation. Immediately following hybridization, the probe array undergoes an automated washing and staining protocol on the fluidics station. After scanning the array the raw data is analyzed for probe signal intensities and all results are reported in tabular and graphical formats. Then the data set is prepared for detailed statistical analyses.

Notes:

- Throughout all steps powder-free gloves were worn. All steps to minimize the introduction of exogenous nucleases were taken. Water used in the protocols is molecular biology-grade. Proper storage and handling of all reagents was done according to the manufacturer's recommendations. All steps were performed in nuclease-free 1.5 ml reaction tubes.
- The whole sample target preparation procedure was performed in two working days taking the assay's safe stopping points into account. Day 1 included isolation of total RNA, synthesis of ds cDNA, cleanup of ds cDNA, and ethanol precipitation over night. The IVT reaction, cRNA cleanup, quantification, and fragmentation were performed on the second day. After a hybridization cocktail had been prepared, it was either subsequently hybridized to a probe array, or stored at -20°C for later use.

3.3.1 Isolation of total RNA

Isolation of total RNA from frozen lysates of mononuclear cells was performed according to the RNeasy Mini Kit protocol (Qiagen, Hilden, Germany) including an initial homogenization step. In this protocol, a specialized high-salt buffer system allows up to 100 µg of RNA longer than 200 bases to bind to the RNeasy silica-gel membrane. The biological samples were first lysed and homogenized in the presence of a highly denaturing guanidine isothiocyanate (GITC)-containing buffer, which immediately inactivates RNases to ensure isolation of intact RNA. Then ethanol was added to provide appropriate binding conditions and the sample was applied to a RNeasy mini column where the total RNA binds to the membrane and contaminants are efficiently washed away. The RNA is subsequently eluted in 40 µl of nuclease-free water. Normally, eight individual samples were processed in parallel. All steps of the protocol were quickly performed at room temperature. All centrifugation steps were performed in a standard microcentrifuge (Eppendorf, Hamburg, Germany). Wash buffer RPE is supplied as a concentrate. Before using it for the first time, four volumes of absolute ethanol (Roth, Karlsruhe, Germany) were added to obtain a working solution. A 70% ethanol solution was prepared in 2.0 ml caps using absolute ethanol and nuclease-free water.

Equipment and solutions:

- RNeasy Mini Kit (Qiagen)
- QIAshredder columns (Qiagen)
- Nuclease-free water (Ambion)
- Ethanol (Roth)
- Heat block, 45°C

Method:

1. Thaw frozen cell lysates of individual patient samples (stored at -80°C) on ice. Then incubate samples for 4 min at 45°C.
2. To homogenize the sample, pipet the lysate directly onto a QIAshredder spin column, placed in a 2 ml collection tube, and centrifuge for 2 min at maximum speed.
3. Add 1 volume (usually 350 µl) of 70% ethanol to the homogenized lysate in the collection tube and mix well by pipetting. Do not centrifuge. Apply the sample, including any precipitate that may have formed, to a RNeasy mini column placed in a 2 ml collection tube. Close the tube gently and centrifuge for 15 s at 8000 x *g* (10,000 rpm). Discard the flow-through. Transfer the column into a new 2 ml collection tube.
4. Add 700 µl washing buffer RW1 to the column. Close the tube gently, and centrifuge for 15 s at 8000 x *g* (10,000 rpm). Discard the flow-through and collection tube. Transfer the column into a new 2 ml collection tube.

5. Pipet 500 μ l washing buffer RPE onto the column. Close the tube gently, and centrifuge for 15 s at $\geq 8000 \times g$ ($\geq 10,000$ rpm). Discard the flow-through. Transfer the column into a new 2 ml collection tube.
6. Add another 500 μ l washing buffer RPE to the column. Close the tube gently, and centrifuge for 2 min at $\geq 8000 \times g$ ($\geq 10,000$ rpm) to dry the membrane. Subsequently, to eliminate any chance of possible washing buffer RPE carryover, place the column in a new 2 ml collection tube, and discard the old collection tube with the flow-through. Centrifuge in a microcentrifuge at full speed for 1 min.
7. Remove the column from the collection tube carefully so the column does not contact the flow-through as this will result in carryover of ethanol. Transfer the column to a new 1.5 ml collection tube and proceed with elution of total RNA.
8. Pipet 40 μ l nuclease-free water directly onto the membrane. Close the tube gently, incubate for 1 min and centrifuge for 1 min at $8000 \times g$ (10,000 rpm) to elute.

Store the isolated total RNA on ice while aliquots are pipetted for quantification and the subsequent cDNA synthesis protocol. The concentration of RNA was determined by measuring the absorbance at 260 nm (A_{260}) in a Ultrospec 3000 spectrophotometer (Amersham Biosciences, Freiburg, Germany) using UVette cuvettes (Eppendorf, Hamburg, Germany). In general, to ensure significance, readings should be between 0.10 and 1.0. An absorbance of 1 unit at 260 nm corresponds to 40 μ g of RNA per ml. For the measurement the isolated total RNA was diluted 1:50 in nuclease-free water (2 μ l total RNA, 98 μ l water).

Notes:

- The initial sample homogenization is necessary to reduce the viscosity of the cell lysates. Homogenization shears the high-molecular-weight genomic DNA and other high-molecular-weight cellular components to create a homogeneous lysate. Incomplete homogenization results in inefficient binding of RNA to the silica-gel membrane, and therefore significantly reduced yields.
- It is important to completely dry the silica-gel membrane before the elution step since residual ethanol may interfere with downstream enzymatic reactions.

3.3.2 Synthesis of ds cDNA

For the synthesis of ds cDNA the one-tube double-stranded cDNA Synthesis System (Roche Applied Science, Mannheim, Germany) has been used. This system has been designed according to the method of Gubler and Hoffmann (1983) and is optimized to reduce manipulation steps allowing the rapid and reliable synthesis of full length cDNAs, especially from total RNA. During the first-strand reaction AMV reverse transcriptase is used. The initiation of the first-strand synthesis depends upon hybridization of an oligo [(dT)₂₄ T7promotor]₆₅ primer to the mRNA, usually at the poly(A) tail. This primer also contains a promoter for the T7 RNA polymerase, which enables a subsequent in vitro transcription reaction. The first and second-strand syntheses are performed in the same tube which speeds the synthesis procedure and maximizes recovery of cDNA. Synthesis for the second-strand takes place using the DNA/RNA hybrid as substrate. Mild treatment with RNase H inserts nicks into the RNA, providing 3' OH-primers for DNA polymerase I present in the second-strand enzyme cocktail. The 5' - 3' exonuclease activity of DNA polymerase I removes the primer stretches in the direction of synthesis, which are then replaced with new nucleotides by the polymerase activity. *E. coli* ligase links the gaps to a complete ds cDNA strand. The last step in the cDNA synthesis is to ensure that the termini of the cDNA are blunt. This is done by adding T4 DNA polymerase which does remove any remaining overhanging 3' ends on the ds cDNAs.

Equipment and solutions:

- cDNA Synthesis System Kit (Roche Applied Science)
- Nuclease-free water (Ambion)
- EDTA, 0.5 M (Sigma)
- Heat block, various temperatures (Eppendorf)

Method:

1. Thaw all necessary components and place them on ice. Pipet the following components in a sterile 1.5 ml reaction tube (40 µl total RT reaction volume):

First-strand cDNA synthesis initiation

Component	Volume	Final concentration
total RNA	variable	1 – 10 µg
oligo[(dT) ₂₄ T7 promotor] ₆₅ primer	2 µl	200 pmol
water	add to 21 µl	
final volume	21 µl	

2. Incubate 10 min at 70°C (Eppendorf Thermostat Plus; also used for all following downstream incubations), then place the tube immediately on ice. Add the following components, mix gently, and incubate 60 min at 42°C. In the meantime thaw all required components for the second-strand synthesis reaction, mix them and place on ice.

First-strand cDNA synthesis reaction

Component	Volume	Final concentration
RT-buffer, 5X concentrated	8 μ l	1X
DTT, 0.1 M	4 μ l	10 mM
AMV, 25 U/ μ l	2 μ l	50 U
RNase inhibitor, 25 U/ μ l	1 μ l	25 U
dNTP-mix, 10 mM each	4 μ l	1 mM each
total final volume	40 μ l	

3. After 60 minutes place the tube 5 min on ice to terminate the reaction. Continue immediately with the second-strand reaction. Pipet directly into the first-strand reaction tube the following components, mix gently, and incubate 2 h at 16°C.

Second-strand cDNA synthesis reaction

Component	Volume	Final concentration
2nd strand buffer, 5X concentrated	30 μ l	1X
dNTP-mix, 10 mM each	1.5 μ l	1 mM each
2nd strand enzyme blend	6.5 μ l	
water	72 μ l	
total final volume	150 μ l	

4. After 2 hours incubation, add 20 μ l (20 U) T4 DNA polymerase and incubate 5 min at 16°C. Then stop the reaction by adding 6.8 μ l EDTA (0.5 M, pH 8.0).
5. Subsequently, digest residual total RNA. Add 1.5 μ l (15 U) RNase I and incubate 30 minutes at 37°C. Add 5 μ l (3 U) proteinase K to the reaction and incubate another 30 minutes at 37°C.
6. Add 153.5 μ l water to the cDNA. The final volume now is 330 μ l and the cDNA is ready for the subsequent cleanup step.

Note:

- In order to obtain sufficient quantity of labeled cRNA for target assessment and hybridization to GeneChip probe arrays, Affymetrix recommends starting the cDNA synthesis protocol with a minimum of 5 μ g of total RNA at a minimum concentration of 0.5 μ g/ μ l.

3.3.3 Cleanup of ds cDNA

The cDNA cleanup step was performed using 1.5 ml Phase Lock Gel (PLG) technology caps (Eppendorf). PLG is a product which eliminates interface-protein contamination during the phenol extraction. Upon centrifugation, the gel migrates to form a tight seal between the phases of an aqueous/organic extraction. The organic phase and the interface material are effectively trapped in or below the barrier. This allows the complete and easy transfer of the entire aqueous phase containing the cDNA species by simply pipetting. The risk of contaminating the sample with interface material is eliminated.

Equipment and solutions:

- Phase Lock Gel light (Eppendorf)
- Nuclease-free water (Ambion)
- Ammonium Acetate, 7.5 M (Sigma)
- Glycogen (20 mg/ml) (Roche Applied Science)
- Ethanol, absolute (stored at -20°C) (Roth)
- Ethanol, 80% solution (stored at -20°C)
- Phenol/Chloroform/Isoamylalcohol (25:24:1) (Ambion)

Method:

1. Add 330 μ l phenol/chloroform/isoamylalcohol (25:24:1) to the cDNA solution, vortex 10 s and transfer the supernatant to a 1.5 ml PLG tube. Centrifuge 2 min at maximum speed. Transfer supernatant to a new tube.
2. Repeat cleanup but now add 310 μ l phenol/chloroform/isoamylalcohol (25:24:1), vortex 10 s and transfer supernatant to a 1.5 ml PLG tube. Centrifuge 2 min at maximum speed. Transfer supernatant to a new tube.
3. Repeat cleanup but now add 290 μ l phenol/chloroform/isoamylalcohol (25:24:1), vortex 10 s and transfer supernatant to a 1.5 ml PLG tube. Centrifuge 2 min at maximum speed. Transfer supernatant to a new tube.
4. In this new tube, now containing the purified cDNA, precipitate the ds cDNA by adding 175 μ l ammonium acetate (7.5 M), 0.5 μ l glycogen (20 mg/ml) and 1000 μ l of absolute ethanol. Store over night or longer at -20°C.
5. Pellet the ds cDNA by centrifugation at maximum speed for 30 min, discard the supernatant carefully. Wash the pellet by overlaying with 500 μ l 80% ethanol. Centrifuge at maximum speed for 15 min. Then discard the supernatant carefully.
6. Wash the ds cDNA pellet by overlaying with 500 μ l 80% ethanol. Centrifuge at maximum speed for 15 min. Then discard the supernatant carefully.
7. Wash the ds cDNA pellet by overlaying with 500 μ l 100% ethanol. Centrifuge at maximum speed for 15 min. Then discard the supernatant carefully.

8. Air dry the pellet by evaporating residual ethanol. This takes approximately 5 – 10 min.
9. Dissolve the cDNA pellet in 22 μ l nuclease-free water and vortex 10 s. Continue immediately with the in vitro transcription procedure.

Notes:

- It is important to use phenol for the cleaning procedure, i.e., to safely eliminate the RNase I and proteinase K used in the cDNA synthesis method.
- An addition of a carrier, e.g., in this work 0.5 μ l glycogen (20 mg/ml), to nucleic acid precipitations aids in visualization of the pellet and may increase recovery.

3.3.4 Synthesis of biotin-labeled cRNA

After the ds cDNA has been purified, it is transcribed *in vitro* to generate more than 400 biotinylated cRNA molecules for each ds cDNA molecule. Adequately intact input RNA should result in an expected yield of biotinylated cRNA of between 4- and 10-fold greater than the total RNA input (Hoffmann, 2004).

Equipment and solutions:

- Enzo BioArray HighYield RNA Transcript Labeling Kit (Affymetrix)
- Nuclease-free water (Ambion)
- 1.5 ml Safe-Lock tubes (Eppendorf)
- Heat block, 37°C (Eppendorf)

Method:

1. Pipette the template cDNA and reaction components from the RNA transcript labeling kit to RNase-free microcentrifuge tubes. Perform all steps at room temperature to avoid precipitation of DTT.

In vitro transcription reaction

Component	Volume
reaction buffer, 10X concentrated	4 μ l
DTT, 10X concentrated	4 μ l
RNase inhibitor mix, 10X concentrated	4 μ l
biotin-labeled ribonucleotides, 10X concentrated	4 μ l
T7 RNA polymerase, 20X concentrated	2 μ l
template ds cDNA	variable
water	variable (to give a final volume of 40 μ l)
final volume	40 μ l

2. Carefully mix the reagents and collect the mixture in the bottom of the tube by brief centrifugation (5 seconds). Then place the reaction tube in a 37°C incubator and incubate for 5 hours. After the IVT immediately proceed with the purification of the biotin-labeled cRNA.

Notes:

- Depending on the input total RNA used for cDNA synthesis, the amount of template cDNA used for each IVT reaction was determined as follows:

Template cDNA used for each IVT reaction

μ g total RNA	Volume cDNA	Volume H ₂ O
5 μ g or less	22 μ l	-
6 μ g	20 μ l	2 μ l
7 μ g	18 μ l	4 μ l
8 μ g	16 μ l	6 μ l
9 μ g	13 μ l	9 μ l
10 μ g	11 μ l	11 μ l
final volume	22 μ l	

3.3.5 Cleanup of biotin-labeled cRNA

After the IVT reaction, cleanup of biotinylated cRNA was performed according to the RNeasy Mini Kit protocol (Qiagen). GITC-containing lysis buffer and ethanol were added to the sample to create conditions that promote selective binding of the cRNA to the silica-gel membrane in the RNeasy mini column. The cRNA binds to the membrane, contaminants are efficiently washed away, and purified cRNA is eluted in water. Normally, eight individual samples were processed in parallel. All steps of the RNeasy protocol were quickly performed at room temperature. All centrifugation steps were performed in a standard microcentrifuge. Wash buffer RPE is supplied as a concentrate. Before using it for the first time, 4 volumes of absolute ethanol were added to obtain a working solution. According to the manufacturer's recommendation, buffer RLT was prepared freshly for each clean up procedure (10 μ l 2-mercaptoethanol per 1 ml buffer RLT; mixed in a 15 ml Falcon tube).

Equipment and solutions:

- RNeasy Mini Kit (Qiagen)
- Nuclease-free water (Ambion)
- Ethanol (Roth)

Method:

1. Adjust the sample to a volume of 100 μ l with water. Therefore, add 60 μ l water to the 40 μ l cRNA reaction volume.
2. Add 350 μ l buffer RLT and mix thoroughly. The total volume now is 450 μ l.
3. Add 250 μ l absolute ethanol to the diluted cRNA, and mix thoroughly by pipetting. Do not centrifuge. The total volume now is 700 μ l.
4. Continue immediately to apply the sample to an RNeasy mini column placed in a 2 ml collection tube. Close the tube gently, and centrifuge for 15 s at 8000 \times g (10,000 rpm).
5. Apply the flow-through again to the same column placed in a new 2 ml collection tube. Close the tube gently, and centrifuge for 15 s at 8000 \times g (10,000 rpm). Now discard the flow-through. Transfer the RNeasy column into a new 2 ml collection tube.
6. Pipet 500 μ l Buffer RPE onto the column. Close the tube gently, and centrifuge for 15 s at 8000 \times g (10,000 rpm) to wash the column. Discard the flow-through. Transfer the column into a new 2 ml collection tube.
7. Add another 500 μ l Buffer RPE to the column. Close the tube gently, and centrifuge for 2 min at \geq 8000 \times g (\geq 10,000 rpm) to dry the membrane. Place the column in a new 2 ml collection tube, and discard the old collection tube with the flow-through. Centrifuge in a microcentrifuge at full speed for 1 min.

8. To elute, transfer the column to a new 1.5 ml collection tube (Eppendorf). Pipet 40 μ l nuclease-free water directly onto the membrane and incubate for 1 minute. Close the tube gently, and centrifuge for 1 min at 8000 x *g* (10,000 rpm) to elute.

Store the isolated cRNA on ice while aliquots are pipetted for downstream applications. The concentration of cRNA was determined by measuring the absorbance at 260 nm (A_{260}) in an Ultrospec 3000 spectrophotometer (Amersham Biosciences) using UVette cuvettes (Eppendorf). In general, to ensure significance, readings should be between 0.10 and 1.0. An absorbance of 1 unit at 260 nm corresponds to 40 μ g of RNA per ml. For the measurement the isolated cRNA was diluted 1:50 in nuclease-free water (2 μ l total RNA, 98 μ l water). The A_{260}/A_{280} ratio should be close to 2.0 (ratios between 1.9 and 2.1 are acceptable).

3.3.6 Fragmenting the cRNA

After elution and quantification of the biotinylated cRNA, an aliquot of 15 µg is fragmented. The full-length cRNA is broken down to 35 – 200 base fragments by metal-induced hydrolysis. The final cRNA concentration in the fragmentation mix was usually adjusted to 0.5 µg/µl. The following procedure gives an example of a fragmentation reaction for 15 µg cRNA at a final concentration of 0.5 µg/µl.

Equipment and solutions:

- Biotinylated cRNA
- Fragmentation buffer, 5X concentrated
- Nuclease-free water (Ambion)
- Heat block, 94°C

Method:

1. Add 2 µl of 5X fragmentation buffer for every 8 µl of cRNA plus water. The cRNA is fragmented in the same tube which is later used for preparation and storage of the hybridization cocktail.

Fragmentation reaction

Component	Volume
15 µg cRNA	up to 24 µl
5X fragmentation buffer	6 µl
water	to 30 µl
final volume	30 µl (0.5 µg/µl cRNA)

2. Incubate at 94°C for 35 minutes.
3. Cool the fragmented cRNA on ice. Immediately proceed with the completion of the hybridization cocktail.

Notes:

- Fragmenting the cRNA target before hybridization to GeneChip probe arrays has been shown to be critical in obtaining optimal assay sensitivity. Affymetrix recommends that the cRNA used in the fragmentation procedure should be sufficiently concentrated to maintain a small volume during the procedure. This will minimize the amount of magnesium in the final hybridization cocktail. Thus, the cRNA should reach a minimum concentration of 0.6 µg/µl.
- Typically, an IVT reaction starting with 5.0 µg of total RNA input for cDNA synthesis yielded between 35 and 50 µg biotinylated cRNA. Then, remaining undiluted and not fragmented cRNA was deposited for long-term storage at -80°C.

3.3.7 Target hybridization

After fragmenting the cRNA, a hybridization cocktail is prepared, including the fragmented target, probe array controls, acetylated bovine serum albumin (BSA), and herring sperm DNA. It is then hybridized to the probe array during a 16-hour incubation. A GeneChip probe array chip comes mounted in a plastic package to form a cartridge. The chip contains a collection of oligonucleotide probes that have been arrayed on the inner glass surface. A chamber in the plastic package directly under the chip acts as a reservoir where hybridization and subsequent washing and staining steps occur.

Equipment and solutions:

- Eukaryotic Hybridization Control Kit (20X stock solution) (Affymetrix)
- Control oligonucleotide B2 (3 nM) (Affymetrix)
- Herring sperm DNA (10 mg/ml) (Sigma)
- Acetylated BSA (50 mg/ml) (Sigma)
- Hybridization buffer, 2X concentrated
- Hybridization buffer, 1X concentrated
- Nuclease-free water (Ambion)
- Heat block, 45°C
- Heat block, 99°C
- Hybridization oven, 45°C (Affymetrix)

Method:

1. Mix the following components for each target cRNA as given below. Standard format microarrays require a 300 μ l volume cocktail preparation. Hybridization cocktails can be stored at -20°C for later use or subsequently be hybridized.

Components for the hybridization cocktail

Component	Volume	Final concentration
fragmented cRNA	15 μ g	0.05 μ g/ μ l
control oligonucleotide B2 (3 nM)	5 μ l	50 pM
eukaryotic hybridization controls, 20X	15 μ l	1.5, 5, 25, 100 pM, respectively
herring sperm DNA (10 mg/ml)	3 μ l	0.1 mg/ml
acetylated BSA (50 mg/ml)	3 μ l	0.5 mg/ml
hybridization buffer, 2X concentrated	150 μ l	1X
water	add to 300 μ l	
final volume	300 μ l	

2. Equilibrate the microarray to room temperature.
3. Heat the hybridization cocktail for 5 min to 99°C. Then incubate it for 5 min at 45°C. Subsequently, spin hybridization cocktail 5 min at maximum speed in a microcentrifuge to pellet any insoluble material from the hybridization mixture.

4. Meanwhile, wet the microarray by filling it through one of the septa with 200 μ l 1X hybridization buffer using a micropipettor and appropriate tips (Rainin). Incubate the filled microarray in the hybridization oven for 15 min at 45°C with constant rotation (60 rpm).
5. After 15 minutes, remove the buffer solution from the microarray cartridge and fill with 200 μ l of the clarified hybridization cocktail, avoiding any pelleted, insoluble matter at the bottom of the tube.
6. Place the microarray into the hybridization oven and incubate for 16 hours at 45°C with constant rotation (60 rpm).

Notes:

- Each eukaryotic GeneChip microarray contains probe sets for several prokaryotic genes as controls. Biotinylated hybridization control nucleic acids, *bioB*, *bioC*, *bioD*, and *cre* are provided in the “GeneChip Eukaryotic Hybridization Control Kit” that contains a 20X concentrated, pre-mixed control reagent. *BioB*, *bioC*, and *bioD* are genes of the biotin synthesis pathway from the bacteria *E. coli*, and *cre* is the recombinase gene from the P1 bacteriophage. A ready-prepared mixture of these biotinylated controls at staggered concentrations is added with the labeled target cRNA to hybridize to the microarray. Signal intensities obtained on these transcripts provide information on how well the hybridization, washing, and staining procedures have performed.
- The control oligonucleotide B2 hybridizes to features along the outer edge of all expression microarrays and to the checkerboard pattern in each corner. These predefined patterns provide signals for the analysis software to perform automatic grid alignment during image analysis. If required, they can also be used by the operator to align the grid manually.

3.3.8 Microarrays

Two types of gene expression microarrays were used in this study, the HG-U95Av2 microarray and its successor, the U133 set (HG-U133A and HG-U133B). A more detailed description on microarray design, especially sequence and probe selection is available as technical note from the manufacturer (www.affymetrix.com).

HG-U95Av2

The human genome U95Av2 microarray, the first array in the set of 5 arrays (U95A-E), contains primarily full-length genes. It represents ~12,000 sequences previously characterized in terms of function or disease association. The represented sequences are derived from sequence clusters in Build 95 of the UniGene database (sequences in UniGene Build 95 are from GenBank 113 and dbEST, October 2, 1999). UniGene clusters are represented by one or more consensus sequences derived directly from cluster members. The probe selection strategy was based on heuristic rules. It is manufactured as standard format array with a feature size of 20 μm and uses 16 probe pairs per sequence. The oligonucleotide length is 25-mer.

HG-U133A and HG-U133B

The U133 two-array set provides comprehensive coverage of well-substantiated genes in the human genome. It can be used to analyze the expression level of 39,000 transcripts and variants. The two arrays comprise more than 45,000 probe sets and 1,000,000 distinct oligonucleotide features. The sequences from which these probe sets were derived were selected from GenBank, dbEST, and RefSeq. The sequence clusters were created from the UniGene database (Build 133, April 20, 2001) and then refined by analysis and comparison with a number of other publicly available databases, including the Washington University EST trace repository and the University of California, Santa Cruz Golden-Path human genome database (April 2001 release). In addition, an advanced understanding of probe uniqueness and hybridization characteristics allowed an improved selection of probes based on predicted behavior. The U133 chip design uses a multiple linear regression model that was derived from a thermodynamic model of nucleic acid duplex formation (Mei et al., 2003). This model predicts probe binding affinity and linearity of signal changes in response to varying target concentrations. The two arrays are manufactured as standard format arrays with a feature size of 18 μm and use 11 probe pairs per sequence. The oligonucleotide length is 25-mer.

Notes:

- As in the HG-U95 Set, the A array of the HG-U133 Set was designed to contain probe sets for the well-annotated genes. The vast majority of full-length mRNA sequences are contained on the HG-U133A array. In contrast, the majority of the EST-only clusters are represented by probe sets found on the HG-U133B array.

- GeneChip human genome microarrays include a set of 100 human maintenance genes to facilitate the normalization and scaling of array experiments. These probe sets are identical on all human genome arrays and serve as a tool to normalize and scale the raw expression data prior to performing interarray comparisons. These maintenance genes show consistent levels of expression over a diverse set of tissues (Warrington et al., 2000).
- A major advance in the HG-U133 design is the use of genomic sequences to verify sequence selection, sequence orientation, and the quality of sequence clustering. All input sequences were aligned to the draft assembly of the human genome (April 2001 release). Only high quality regions of genome alignment were used to annotate and analyze the input sequences. In addition, the portion of a mRNA sequence adjacent to a poly(A) site is most efficiently converted into labeled target. Great care was therefore taken to identify polyadenylation sites, since optimal probes are generally located within 600 bp upstream of the site.
- An advantage of the U133 chip design model-based probe selection system is that it provides a physical and mathematical foundation for systematic and large-scale probe selection. It utilizes both sequence and empirical information to predict optimal probes for array-based gene expression analysis. A second advantage is that the system allows simultaneous optimization of probe selection for a number of parameters, such as linear response to target concentration, independence of probes within a set, and probe sequence uniqueness.
- Due to the dynamic nature of the public databases and improvement of probe selection for the array design, probe sets between different versions of a product family, such as the human genome U95A and U133A arrays are not identical. In some cases the same sequences will be represented by completely different probe sets, creating a challenge when comparing data sets generated on different generations of a product family or in different laboratories. However, despite changes in sequence and probe selection methods for the HG-U133 set, there remains a relatively high level of concordance to its predecessor, the HG-U95 set. For example, a total number of 10,507 probe sets found on the HG-U95Av2 array have a corresponding probe set represented on the HG-U133A array. In order to search for the identifier of the probe sets that are most closely related to another Affymetrix has made comparison spreadsheets available. These spreadsheets allow some level of data comparison as the product line evolves. The respective comparison spreadsheets are available as downloads from the Affymetrix website. In this work, the stringent “Human Genome U95 to Human Genome U133 Best Match comparison spreadsheet” was used to determine the best corresponding U133 design counterparts for the given U95Av2 probe sets.

3.3.9 Microarray washing and staining

After hybridizing for 16 hours at 45°C, the microarray is ready for washing and staining. GeneChip probe arrays are processed by the Fluidics Station 400 instrument, which contains four modules with each module processing one microarray cartridge.

Equipment and solutions:

- Streptavidin-Phycoerythrin (SAPE) staining solution
- Antibody staining solution
- Non-stringent washing buffer
- Stringent washing buffer
- Sodium hypochlorite solution (0.525%)

Method:

1. Use the Microarray Suite software and define an experiment for each array to be processed (*.exp extension). Perform a priming protocol to ensure that the wash lines are full of the appropriate buffer and that the fluidics station is ready to process a cartridge.
2. In the meantime, after 16 hours of hybridization, remove the hybridization cocktail from the probe array and fill the probe array completely with non-stringent wash buffer.
3. Insert the probe array into the designated module of the fluidics station, select the correct experiment name in the drop-down experiment list, and start the protocol for washing and staining of expression microarrays. Standard format microarrays were processed using the EukGE-WS2v4 signal amplification protocol.

Fluidics protocol for antibody amplification for eukaryotic targets

Step	Details
Post Hyb Wash #1	10 cycles of 2 mixes/cycle with non-stringent wash buffer A at 25°C
Post Hyb Wash #2	4 cycles of 15 mixes/cycle with wash buffer B
1 st Stain	Stain the probe array for 10 minutes in SAPE solution at 25°C
Post stain wash	10 cycles of 4 mixes/cycle with wash buffer A at 25°C
2 nd stain	Stain the probe array for 10 minutes in antibody solution at 25°C
3 rd stain	Stain the probe array for 10 minutes in SAPE solution at 25°C
Final wash	15 cycles of 4 mixes/cycle with wash buffer A at 30°C.
Protocol	EukGE-WS2v4

4. When the LCD window indicates, place the microcentrifuge vial containing 600 µl of the respective staining solution into the sample holder. Verify that the metal sampling needle is in the vial with its tip near the bottom.

5. At the end of the run, remove the probe arrays from the fluidics station modules and check the probe array window for large bubbles or air pockets. If the probe array has no large bubbles, it is ready to be scanned. Otherwise fill the array manually with non-stringent wash buffer.

Notes:

- Streptavidin-Phycoerythrin (SAPE) should be stored in the dark at 4°C. The SAPE stain solution has always to be prepared immediately before use.
- As recommended by the manufacturer, to ensure proper functioning of the fluidics station, shutdown protocols and periodic maintenance protocols were performed. The shutdown protocol will prevent salt crystals from forming within the fluidics system. Weekly and monthly bleach protocols with a sodium hypochlorite solution eliminate any residual SAPE-antibody complex that may be present in the fluidics station tubing and needles.
- Labeled cRNA targets can be reused. The same hybridization cocktail can be hybridized to a new probe array up to 5 times. In this work, most of the targets were hybridized first to U133A and then to U133B arrays. Some of the cocktails had previously also been hybridized to U95Av2 microarrays. To prevent leaking of fluids from the cartridge during hybridization and scanning, glue dots were applied to each of the two septa on the cartridge.

3.3.10 Microarray scanning and image analysis

After the wash and staining protocols are complete, the probe array was scanned using the Agilent GeneArray scanner. The laser excitation enters through the back of the glass support and focuses at the interface of the array surface and the target solution. Then, fluorescence emission is collected by a lens and passes through a series of optical filters to a sensitive detector. This results in a quantitative two-dimensional fluorescence image of hybridization intensity. Each completed probe array image is stored in a separate image data file identified by the experiment name (*.dat extension). Then, the software defines the probe cells by grid alignment and computes an intensity for each probe cell (*.cel extension). After the raw image is obtained, the algorithms in the Microarray Suite software were applied to process the raw probe set data to generate expression values (signal intensities), detection calls (absent, marginal, present), and associated p-values for every transcript, represented on the arrays (*.chp extension). These files are used to generate detailed reports on the sample quality and technical parameters (*.rpt extension).

Method:

1. In the Microarray Suite software select the experiment name that corresponds to the probe array to be scanned. A dialog box appears prompting to load an array into the scanner. Use default settings for pixel values and wavelength of the laser beam (pixel value = 3 μm , and laser wavelength = 570 nm).
2. The scanner begins scanning the probe array and acquiring data. After the scan has been completed an image file containing the raw expression data in an uncompressed format is stored, i.e., individual pixels per probe cells.

Notes:

- Make sure the laser is warmed up prior to scanning by turning the laser on at least 15 minutes before use.
- Although the inner glass surface is protected, any contamination or scratches on the outer surface of the glass can compromise the integrity of the scan. It should be avoided to touch the surface of the chip with a bare hand as skin oils and other substances, such as lotions or ink, can fluoresce. If the surface of the probe array chip is noticeably dirty, it should carefully be cleaned with a nonabrasive laboratory tissue.

3.3.11 Quality assessment

Quality assessment is critical in obtaining reproducible microarray results. Series of quality control (QC) procedures were performed at various key checkpoints during the gene expression profile analysis and included both monitoring of sample-related parameters and technical features.

- In a selected set of samples gel electrophoresis according to standard protocols (Sambrook et al., 1989) has been performed to detect any degradation of input total RNA.
- After the IVT and cleanup of the cRNA the ratio of 260/280 absorbance values was assessed by spectrophotometer measurements. Good quality cRNA should demonstrate ratios of 1.9 to 2.1. Low cRNA yield can be a sensitive indicator of problematic labeling procedures and/or starting material.
- Basic microarray image analyses included visual array inspections (*.dat file) and check for correct grid alignment at each of the four corners and the center of the array.
- Basic raw data analyses included parameters to monitor the overall background intensity, scaling factor, percentage of present called genes (%P), and 3'/5' ratio for the *GAPD* gene.

In this work, a technically acceptable gene expression profile is defined according to the following characteristics: ≥ 1.0 μg of input total RNA resulted in sufficient cRNA yield (≥ 20.0 μg), concentration (≥ 0.6 $\mu\text{g}/\mu\text{l}$), and ratio of absorbance at 260 nm/280 nm (~ 2.0). The scanned array image should not show largely visible artifacts and have a correct grid aligned for feature extraction. After adjusting the scanned image to common target intensity, the scaling factor within a project should lie within two standard deviations of the mean. When analyzing Affymetrix A-series microarrays the %P called probe sets should be $\geq 30.0\%$. The 3'/5' ratio for *GAPD* should be ≤ 3.0 . Although, if the 3'/5' ratio is >3.0 , but still $>30.0\%$ of the genes were called present, the profile may be rated as acceptable. But, in this work, in most cases with 3'/5' ratio >3.0 , also the %P was $<30.0\%$. Then, also the data had to be normalized with higher scaling factors outside of an acceptable range. As a consequence, a sample failed if, in combination, a low 3'/5' ratio, high percentage of %P probe sets, and comparable range of scaling factors was missed. Accordingly, these gene expression profiles should not be used for gene selection or training of a classification engine. Most of these metrics directly follow the recommendations of the "Tumor Analysis Best Practices Working Group" for Affymetrix MAS 5.0 probe set algorithms and data analyses. This working group has recently been established to develop recommendations for experimental design, data analysis algorithms, signal-to-noise assessments, and biostatistical methods (Hoffmann, 2004).

Notes:

- In addition to the conventional probe sets designed to be within the most 3' end (~ 600 bases of a transcript), additional probe sets in the 5' region and

middle portion (M) of the transcript are also represented for certain housekeeping genes, including *GAPD*. The signal intensity ratio of the 3' probe set over the 5' probe set is often referred to as the 3'/5' ratio. This ratio gives an indication of the integrity of the starting RNA, efficiency of first-strand cDNA synthesis, and/or in vitro transcription of cRNA. As recommended by the manufacturer there is no single threshold cutoff to assess sample quality. Routinely, most users refer to a threshold ratio of less than 3.0 for the most common tissues.

- A high background implies that impurities, such as cell debris and salts, are binding to the microarray in a nonspecific manner, and that these substances are fluorescing at the scanning wavelength. This nonspecific binding causes a low signal-to-noise ratio (SNR), meaning that genes for transcripts present at very low levels in the sample may be incorrectly called as absent transcripts. Thus, high background creates an overall loss of sensitivity in the experiment.
- Scaling factors, i.e., the multiplication factor applied to each signal value on an array, will vary across different samples and there are no set guidelines for any particular sample type. However, if they differ by too much within a set of experiments, this indicates wide variation in the underlying image files and, therefore, the analyzed data should be treated with caution.

3.3.12 Data sets and scaling procedure

For all patient gene expression profiles master data tables were maintained. In these tables rows represent all genes for which data has been collected, and columns represent microarray experiments from individual patients. Each cell represents the measured fluorescence intensity from the corresponding target probe set on the microarray. If not indicated otherwise, each patient has been measured once. In addition, due to the dynamic nature of public databases probe set annotations were frequently updated using the NetAffx analysis center (Liu et al., 2003b). Before analyzing the data it is a routine procedure to normalize the data (Quackenbush, 2002). This is a mandatory step in the data mining process in order to appropriately compare the measured gene expression levels.

U95Av2 microarray raw expression intensities were scaled using the Affymetrix Microarray Suite 5.0 software global scaling parameter. With the global scaling method an arbitrary target intensity is selected and the average intensity of all genes (minus the highest 2% and lowest 2% signal intensity values) on each array within a data set is scaled to that number. This enables to comparing multiple arrays within a complex data set. Here, the selected global target intensity was 50.

U133 set microarray signal intensity values were calculated by scaling the raw data intensities to a common target intensity using a recommended mask file (U133A/B mask file; selected global target intensity value: 5,000).

Notes:

- As an alternative means to relate signal values between arrays, a set of 100 maintenance genes were represented on recent expression microarrays (probe set identifiers from 200000_s_at to 200099_s_at). These normalization controls were originally identified from a data set of HG-U95Av2 hybridizations representing a large number of different tissues and cell lines. The data on these probe sets shared the common characteristic of consistently being called present (P) while exhibiting relatively low signal variation over different sample types (Warrington et al., 2000). Therefore, when scaling data between the HG-U133A and B arrays, an algorithm against these normalization controls, which are represented on both arrays, avoids a skewing of the data and provides an improved alternative tool to global scaling. Specific mask files for these probe sets are available online (www.affymetrix.com).
- Probe sets representing well-annotated genes are found primarily on the HG-U133A array, and as such, tend to produce higher signal values on average when compared to the HG-U133B array. Therefore, strategies to normalize array data, such as global scaling, are not always appropriate. In some instances these methods may artificially increase the actual signal values of probe sets if a common global scaling value is used, especially if overall intensities of the arrays being normalized are quite different.

3.4 Microarray data analysis

A wide range of approaches are available for gleaning insights from the data obtained from transcriptional profiling (Slonim, 2002). In this work, data analyses were performed by two different approaches, i.e., the supervised approach and the unsupervised approach (Figure 6). Unsupervised analyses were used to test the hypothesis whether specific characteristics, e.g., genetic aberrations, would also be reflected at the level of gene expression signatures. Supervised analyses were used to identify a minimal set of genes which could be used to stratify those patients after a training of classification engines. The gene lists from supervised analyses were also further interpreted in terms of biology.

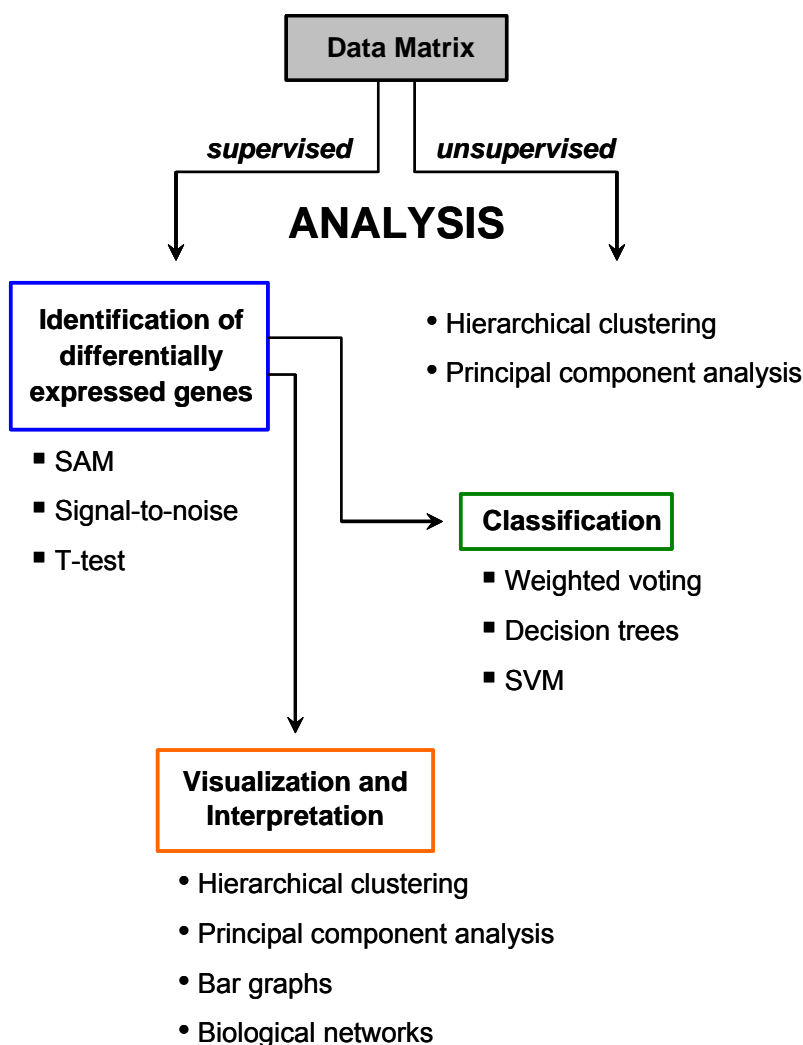


Figure 6. **Overview about the data analysis workflow.** After preparation of corresponding data sets from the main master table the data was analyzed either unsupervised or supervised. Unsupervised analyses were performed by hierarchical clustering or principal component analysis. In the supervised analyses, differentially expressed genes were identified by various methods and selected for further interpretations, e.g., visualization by hierarchical clustering, principal component analysis, plotting as bar graphs, or generation of biological networks. In addition, differentially expressed genes were selected for classification tasks where several different machine-learning approaches were applied.

3.4.1 Identification of differentially expressed genes

In microarray experiments a common goal is to detect genes that show differential expression across two or more biological conditions. Therefore, multiple hypothesis testing algorithms were performed on all genes simultaneously to determine whether each one is differentially expressed. The null hypothesis is that there is no change in expression levels between various leukemia subclasses. The alternative hypothesis is that there is significant differential gene expression (Tusher et al., 2001). The analyses were performed either between two distinct classes (pairwise comparisons; subtype A vs. subtype B), or between one distinct class and all other remaining classes in a one-versus-all (OVA) approach.

Weighted voting algorithm

This algorithm identifies differentially expressed genes following the supervised class prediction methodology using a modified t-test-statistic as described by Golub and colleagues (Golub et al., 1999; Pomeroy et al., 2002). When comparing two groups of microarray experiments, this method sorts the genes with respect to the signal-to-noise ratio of gene x : $S_x = (\mu_1 - \mu_2) / (\sigma_1 + \sigma_2)$, where μ_k and σ_k denote the mean expression and standard deviation of gene x in group k . According to a specified number of "informative" genes the best discriminating genes are selected. Because the number of informative genes, which are required to discriminate between samples, is unknown, this method was applied for different numbers of informative genes (range: 2 to 200).

For each informative gene a decision limit is calculated as $b_x = (\mu_1 + \mu_2) / 2$. To classify a new sample, the gene expression levels of informative genes are taken and for each gene x and sample y a so-called vote is calculated as $V_x = S_x (g_{xy} - b_x)$, where g_{xy} denotes expression level of gene x in sample y . The votes of all informative genes are summed up (weighted voting), and depending upon the sign of this sum the new sample is classified as group 1 or group 2. The confidence in the prediction is calculated as $|\sum V_x / \sum |V_x|$. Prediction strength values range between 0 and 1 and values >0.45 demonstrated statistical significance. To assess the significance of each gene, a permutation-based neighborhood analysis is performed, which determines signal-to-noise ratios when class labels are permuted randomly (100 cycles). Only those genes that were contained in all cross-validation (CV) classifiers were considered important. For each selected gene, the significance level p was 1% ($p \leq 0.01$), and only when comparing small groups ($n_1 + n_2 \leq 15$) and very small groups ($n_1 + n_2 \leq 10$) a significance level of 2% ($p \leq 0.02$) and 5% ($p \leq 0.05$), respectively, was chosen.

However, when the standard deviation of expression levels within the two groups are very different the decision limit is biased towards the group with the higher standard deviation. By systematically determining classification accuracies for a set of possible decision limits, an optimal decision limit can be calculated. Thus, an optimal decision limit was selected from the following set of decision limits L_x : $L_x = \{(g_{xy} + g_{xy-1}) / 2 \mid 1 < y \leq n\}$ where g_{xy} denotes expression level of gene x in sample y , n denotes the total number of samples in the training set. As a consequence, a further improved algorithm consists of the following steps: (i) Calculate the top 20 discriminating genes according to the signal-to-noise ratio (both pairwise and OVA). (ii) Calculate classification

accuracy and confidence based on optimal decision limits for each of the top 20 genes. (iii) Select the gene which provides best classification accuracy and confidence out of step 2. (iv) Test for each of the remaining 19 genes, whether adding this gene to the model improves accuracy and confidence. If the gene improves accuracy and confidence, it is added to the weighted voting model, otherwise it is discarded. To assess the robustness of the classifier, a leave-one-out cross-validation (LOOCV) is performed. The resulting accuracy is the rate of correctly classified test samples.

Significance Analysis of Microarrays (SAM)

Additionally, supervised data analyses were performed using the SAM software. SAM is a statistical technique for finding significant genes in large-scale microarray-based gene expression profiles and correlates gene expression data with an external variable, e.g., the leukemia subclass or karyotype information. The SAM software is an Add-in package for Microsoft Excel and analyzes statistical significance of the changes in gene expression from repeated permutations. It was proposed by Tusher and colleagues (Tusher et al., 2001). SAM identifies genes with statistically significant changes in expression by assimilating a set of gene-specific t-tests. Each gene is assigned a score on the basis of its change in gene expression relative to the standard deviation of repeated measurements for that gene. Genes with scores greater than an adjustable threshold are deemed potentially significant. The cutoff for significance is determined by the tuning parameter delta, chosen by the user based on the false discovery rate (FDR). The FDR, i.e., the percentage of genes identified by chance, is estimated by analyzing repeated permutations of the data.

Two-sample t-test for equal means

As a second supervised approach, differentially expressed genes were identified by means of the t-test-statistic. In all possible combinations of one-versus-all and pairwise comparisons the two-sample t-statistic score with correction for unequal variances was performed (Altman, 2004). The analysis was programmed using R (version 1.7.1; www.r-project.org/).

$$\text{score } t_i = \frac{\bar{x}_{i2} - \bar{x}_{i1}}{\sqrt{\frac{s_{i1}^2}{n_1} + \frac{s_{i2}^2}{n_2}}}$$

$$\text{where } \bar{X}_{ik} = \frac{1}{n_k} \sum_{j \in C_k} x_{ij} \text{ and } s_{ik}^2 = \frac{1}{n_k - 1} \sum_{j \in C_k} (x_{ij} - \bar{x}_{ik})^2 \text{ (for } k = 1, 2)$$

Statistical significance

Microarrays can measure the expression of thousands of genes to identify expression changes between different biological states. Methods based on conventional t-tests provide the probability (P) that a difference in gene expression occurred by chance. Although $P < 0.01$ is significant in the context of experiments designed to evaluate small numbers, a microarray experiment for more 10,000 genes would identify 100 genes by chance (Tusher et al., 2001). Thus, methods are needed to determine the significance of these changes while accounting for the enormous number of genes.

In this work to address the multiple testing problem, false discovery rates (FDR) of genes were calculated according to a statistical method adapted specifically for microarrays (Storey and Tibshirani, 2003). As it takes automatically the fact into account that thousands of genes are simultaneously being tested the concept of the FDR is a widely accepted method to measure statistical significance in genome-wide studies. A measure of statistical significance called the q-value is associated with each tested feature. Similarly to the p-value, the q-value gives each measured gene its own individual measure of significance. Whereas the p-value is a measure of significance in terms of the false positive rate, the q-value is a measure in terms of the false discovery rate (FDR). In a microarray data set the q-value of a particular feature is the expected proportion of false positives incurred when calling that feature significant (Storey and Tibshirani, 2003). In this work q-values were used as an exploratory guide for which features to investigate further, e.g., through the use of pathway applications or classification engines.

Note:

- When calling features significant, the false positive rate is the rate that truly null features are called significant. That means, that for a false positive rate of 5%, on average 5% of the truly null features in the data set will be called significant. The false discovery rate (FDR) is the rate that significant features are truly null. A FDR of 5% means that among all features called significant, 5% of these are truly null on average.

3.4.2 Estimation of prediction performance

The generalization performance of the different algorithms was estimated by performing cross-validation methods (CV). These methods are based on the idea that the most unbiased test of the predictive error is by applying it to data that was not used in the building of the initial predictive model. A common application is to partition a dataset into two parts, to fit the model on the first part, and to assess the predictive capability of that model on the second part. Depending on the CV method, the complete data set is split into different proportions of a training set and a test set. Each approach is performed to determine the accuracy, i.e., the probability of correct classification of a previously unknown sample.

Leave-one-out cross-validation

The leave-one-out cross-validation (LOOCV) method is one of several approaches to estimating how well a model that was trained on training data is going to perform on future as-yet-unseen data. LOOCV was used to evaluate the prediction performance of algorithms used for the U95Av2 data sets. LOOCV implies that one sample is excluded from the complete data set n and the remaining samples are used for training. This training and prediction process is repeated n times to include predictions for each sample (so that each sample is classified once in the n iterations).

10-fold CV

10-fold CV was the second method used to estimating the apparent accuracy, i.e., the overall rate of correct predictions of the complete data set. This classification task means that the data set was divided into 10 equally sized subsets, balanced for the respective subclasses of the data. Then, differentially expressed genes were identified in the training set (9 subsets) and a model was trained based on the top genes that demonstrate differential expression between each of the respective subclasses in the training set. This model was used to generate predictions for the remaining subset. This training and prediction process was repeated 10 times to include predictions for each subset (so that each sample is classified once in the 10 iterations).

Resampling analysis

The resampling approach was performed to assess the robustness of class predictions of U133 set profiles. Here, the data set again was randomly, but balanced for the respective subtypes, split into a training set, consisting of two thirds of samples, and an independent test set with the remaining one third. Differentially expressed genes were identified in the training set, an SVM-model was built from the training set, and predictions were made in the test set. This complete process was repeated 100 times. By this means, also 95% confidence intervals for accuracy, sensitivity and specificity were estimated. Sensitivity and specificity were calculated as follows:

Sensitivity = (number of positive samples predicted)/(number of true positives)
Specificity = (number of negative samples predicted)/(number of true negatives)

3.4.3 Hierarchical clustering

Two-dimensional hierarchical cluster analysis is a popular method of organizing expression data, i.e., arranging genes and patients according to similarity in pattern of gene expression (Figure 7). This method helps to organize but not to alter tables containing the primary expression data. The output format is a graphic display which allows to conveying the clustering and the underlying expression data in an intuitive form to biologists (Eisen et al., 1998). By adopting a mathematical description of similarity the object of this algorithm is to compute a dendrogram that assembles all elements into a single tree. In this work, for any set of n genes, an upper-diagonal similarity matrix is computed by the Euclidean distance metric, which contains similarity scores for all pairs of genes. The matrix is scanned to identify the highest value which represents the most similar pair of genes. Then a node is created joining these two genes, and a gene expression profile is computed for the node by averaging observation for the joined elements. The similarity matrix is updated with this new node replacing the two joined elements, and the process is repeated $n-1$ times until only a single element remains.

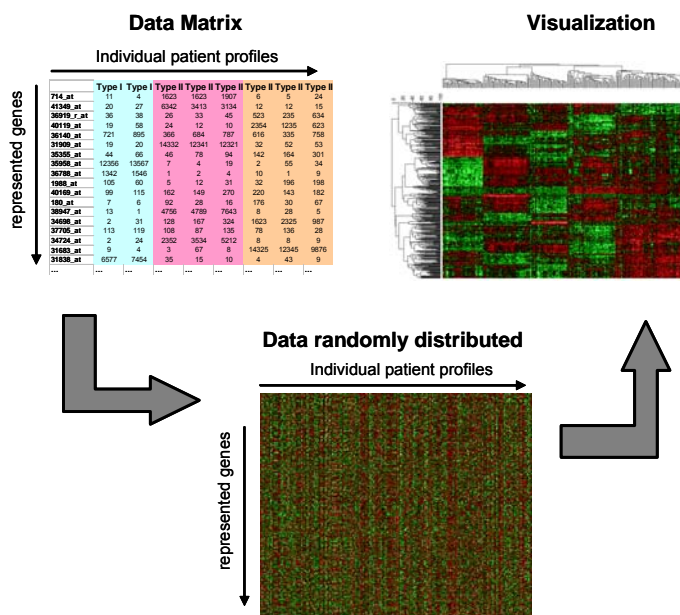


Figure 7. **Hierarchical cluster analysis workflow.** The primary expression data is graphically represented. Each data point is represented with a color that quantitatively and qualitatively reflects the original measured fluorescence intensity. One can look at such images, identify patterns or branches of the dendrogram of interest, and readily zoom in on the detailed expression patterns and identities of the genes contributing to these patterns (Eisen et al., 1998).

Any unsupervised gene expression analysis begins with a definition of similarity between expression patterns, but with no prior knowledge of the true functional classes of the genes, or patients, respectively. For visualization of unsupervised data analyses a variation filter was applied. This filter aimed at removing probe sets that demonstrated minimal variation across the complete data set. Practically, for each gene the standard variance was calculated across all samples. Then the data matrix was sorted according to the standard variances and probes demonstrating a low variance were excluded from the subsequent analysis. This is the method of choice when one has no or little a priori knowledge of the complete repertoire of expected gene expression patterns. However, no information about the statistical significance is provided. In contrast, using hierarchical clustering in a supervised approach helps to visualize differential gene expression of an already preselected set of genes.

3.4.4 Principal component analysis

The need to visualize large amounts of data in many dimensions occurs frequently in bioinformatics. Commonly, principal component analysis (PCA) is used in statistics to extract the main relations in data of high dimensionality (Jolliffe, 2002). It is a useful tool for categorization of multidimensional data such as gene expression studies, since it separates the dominating features in the data set. The background mathematical technique used in PCA is called eigen analysis. PCA reduces the dimensionality of the data set while retaining most of the information contained therein via the construction of a linear transformation matrix. This transformation matrix is composed of the most significant eigenvectors of the covariance matrix of the input matrix of feature vectors. The principal components (PC) are the projections of the data on the eigenvectors. These vectors give the directions in which the data cloud is stretched most. The significance of an eigenvector is defined by its variance, which is equivalent to its corresponding eigenvalue. Eigenvalues give an indication of the amount of information the respective PC represent. PCs corresponding to large eigenvalues represent much information in the data set and thus can tell much about the relations between the data points (Jolliffe, 2002). Since the original data's variation can be retained and explained by a smaller number of transformed variables, a PCA projects the data into a new two- or three-dimensional space and may provide valuable insight into the data (Figure 8). In this work, PCA was applied to visualize large data sets from leukemia types and subclasses. The PCA plots were generated through the use of the GeneMaths XT software (Applied Maths, Belgium).

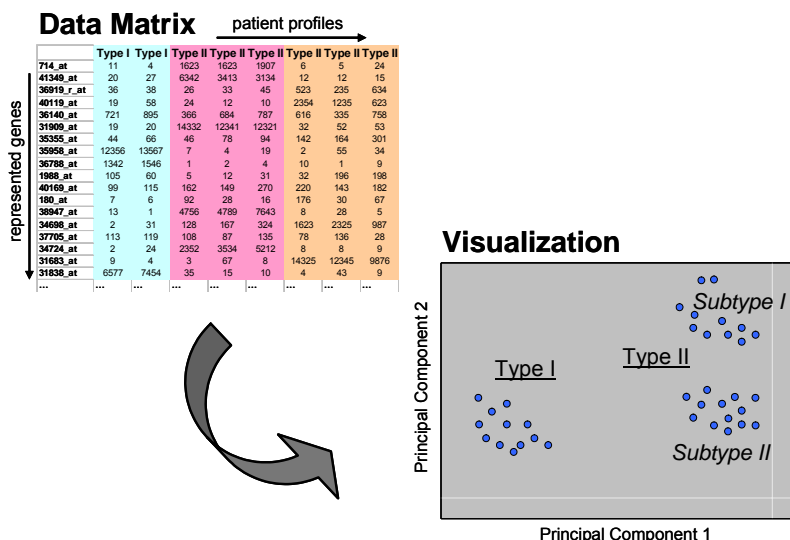


Figure 8. **Principal component analysis workflow.** The multi-dimensional data is reduced by transformation to a new set of variables, the principle components (PCs). The traditional is to use the first few PCs since they capture most of the variation in the original data. In the final graph, data points with similar characteristics will cluster together. Each patient's expression pattern is represented by a color-coded sphere.

Notes:

- It has to be emphasized that PCA is not a learning algorithm. The classifications of the samples (e.g., according to leukemia subclasses) does not affect their location in two- or three-dimensional space. A respective coloring of the spheres by classification is done after the samples are plotted and is therefore somewhat arbitrary.

3.4.5 Classification of samples based on gene expression patterns

For class prediction, the weighted voting procedure (see 3.4.1), multiple-tree models, and support vector machines (SVM) were used.

Multiple decision trees

Multiple-tree models were computed to discriminate between three different AML subclasses in the initial U95Av2 data ($n=37$ samples). To avoid overfitting of a singular tree model, a multiple-tree model was developed using an iteratively reduced set of genes. The trees were restricted to contain no more than $k-1$ nodes to discriminate between k classes. Genes whose expression values were selected for the nodes of the tree were then eliminated from the original data set, and a new tree was calculated based on the truncated data set. This was iterated until a predetermined number of trees were reached. To determine how many trees should be incorporated in the model misclassification rates were calculated for models containing 1 to 25 trees. The data set was randomly split into a training set ($n=24$) and a test set ($n=8$). Within the range tested, 15 trees were calculated to be optimal, both avoiding overfitting and reduced classification accuracy. The final class assignment was decided by applying a vote-by-majority rule to the outputs of the 15 single trees. Equal votes for two of the three classes are counted as misclassification. The generalization properties of the classifier are judged by 10-fold CV and by a test set of 5 samples that were not used for classification training. Multiple-tree models for classification were developed at the Intelligent Bioinformatics Systems division at the German Cancer Research Center (DKFZ), Heidelberg and were calculated using the C5.0 algorithm as implemented in SPSS (Quinlan, 1993). A schematic summary is given in Figure 9.

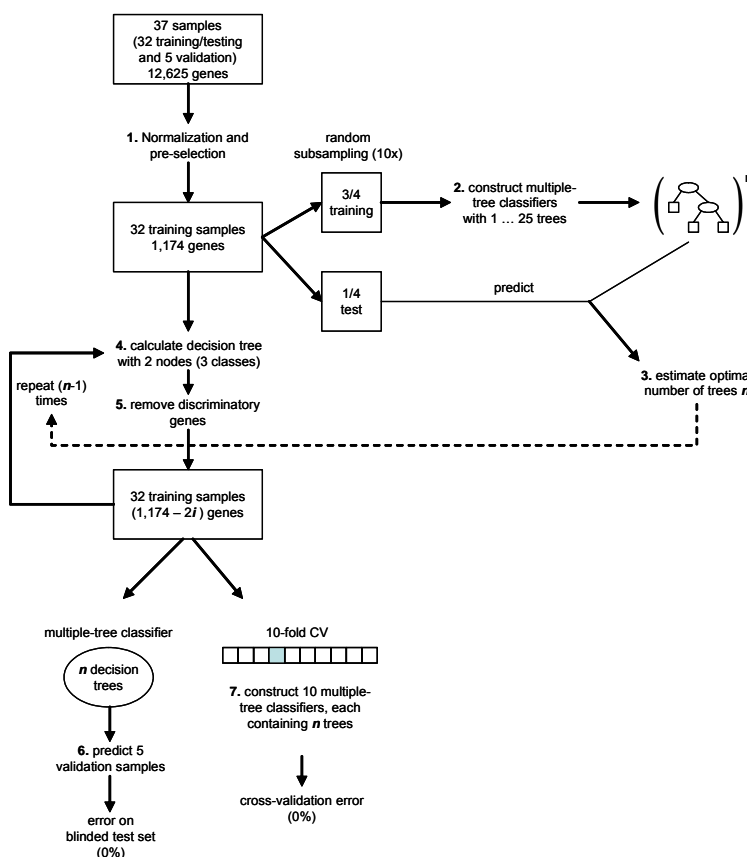


Figure 9. **Multiple-tree model computation.** The entire data set was normalized and differentially expressed genes were identified (1). A blinded validation set of five samples was excluded from further analysis for final evaluation of the constructed classifier. The remaining samples were then randomly split into training and test sets (2), and the optimal number of trees was determined (3). Then, the final classifier was built using this number through an iterative process (4) to construct the multiple-tree model (5). The independent test set error was calculated on the initially excluded 5 samples (6). Independently, the prediction error has been estimated by 10-fold CV (7).

SVM-based classification

For classification of U133 set microarray data the support vector machine (SVM) algorithm was used. SVMs are learning machines that can perform binary classification tasks (Vapnik, 1998; Guyon et al., 2002; Schölkopf and Smola, 2002). In this work, a classification task involves training and testing gene expression profiles which consist of some data instances. Each instance in the training set contains “target values” (class labels, i.e., leukemia classes) and several “attributes” (features, i.e., genes). The goal of this approach is to produce a model which predicts target values of data instances in the testing set which are only given the attributes. Applied to gene expression data, an SVM would begin with a set of genes that have a common function, e.g., genes that demonstrate differential expression between distinct leukemia subtypes. After non-linearly mapping the n-dimensional input space into a high dimensional feature space a linear classifier is constructed in this high dimensional feature space (Figure 10).

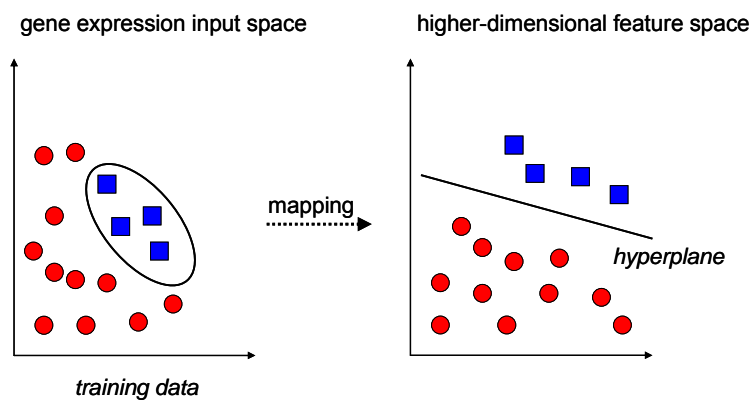


Figure 10. **Concept of SVM-based classification.** The SVM operates by mapping the given training set into a possibly high-dimensional feature space and by attempting to locate in that space a plane that separates positive from negative samples. The hyperplane, a plane in a space with more than 3 dimensions, corresponds to a non-linear decision boundary in the input space.

Using this training set, an SVM would learn to discriminate between the types and subtypes of leukemias based on expression data. Having found such a plane, the SVM can then predict the classification of an unlabeled new sample by mapping it into the feature space and asking on which side of the separating plane the example lies (Figure 11). Then a label is assigned according to its relationship with the decision boundary. In this work, multi-class SVM classifiers were built with linear kernels using the library LIBSVM version 2.36 (www.csie.ntu.edu.tw/~cjlin/libsvm/) (Chang and Lin, 2001).

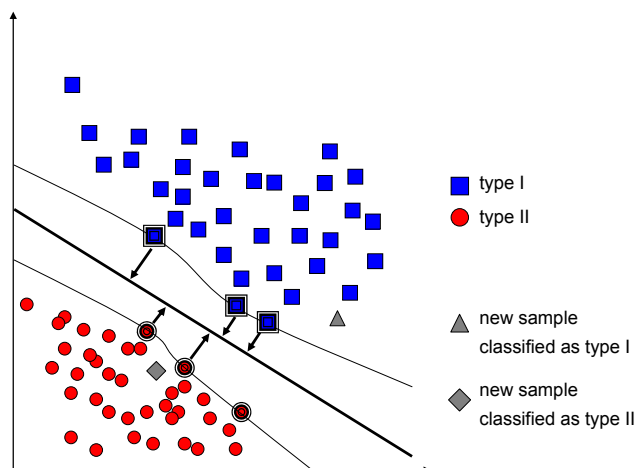


Figure 11. **Classification task.** The SVM separates a given set of binary labeled training data with a hyperplane that is maximally distant from them (maximal margin). The middle black line is the decision surface defining the borderline between the area of prediction of type I samples (red) and type II samples (blue). The outer lines precisely meet the constraint. Support vectors marked to be critical for the classification task are the points that lie closest to the separating hyperplane (Schölkopf and Smola, 2002).

3.4.6 Functional gene annotation

NetAffx database

In this work the NetAffx database was used to functionally annotate the probe sets represented on the corresponding microarrays. The NetAffx Analysis Center (www.affymetrix.com/analysis/) is an integrated, freely available online resource created by Affymetrix (Liu et al., 2003b). This web-based application enables researchers to correlate results from experiments with array design and annotation information. It is a dynamic tool and provides access underlying to array content and the design of GeneChip probe arrays, including probe sequences and extensive gene annotations from both Affymetrix and the public domain. As such, it allows the user to search array contents for sequences of interest, review gene and protein characterizations for represented probe sets and sort transcripts by functional group, metabolic pathway, or disease association. For each cataloged Affymetrix GeneChip microarray, an anchoring databank summarizes all the annotations for the probe sets. The information provided for each probe set falls into two categories: sequence annotations and static information. Sequence annotations refer to the information about the representative sequence for a probe set including functional annotations for gene title, gene symbol and cytogenetic bands. The static information for each probe set details the probe sequences, accession numbers, textual description and describes what the probes were designed to interrogate. The static probe set data is also depicted graphically (Liu et al., 2003b).

Gene Ontology annotation

The Gene Ontology (GO) project (www.geneontology.org/) provides structured, controlled vocabularies and classifications that cover several domains of molecular and cellular biology and are freely available for community use in the annotation of genes, gene products and sequences (Ashburner et al., 2000). This vocabulary that can be applied to all organisms even as knowledge of gene and protein roles in cells is accumulating and changing. GO provides three non-overlapping structured networks of defined terms, the ontologies, to describe gene product attributes (Harris et al., 2004). The three principles of organization and possibilities for the annotation are based on the description of the molecular function of the gene product (e.g., carbohydrate binding or ATPase activity), of the biologic process in which one or more molecular functions are involved (e.g., mitosis or purine metabolism), and on an assignment of the cellular component (e.g., nucleus or integral membrane protein). Within each ontology, terms have free text definitions and stable unique identifiers. In addition, detailed hierarchical models are provided, e.g., the metabolism of DNA is further separated into replication and repair of DNA.

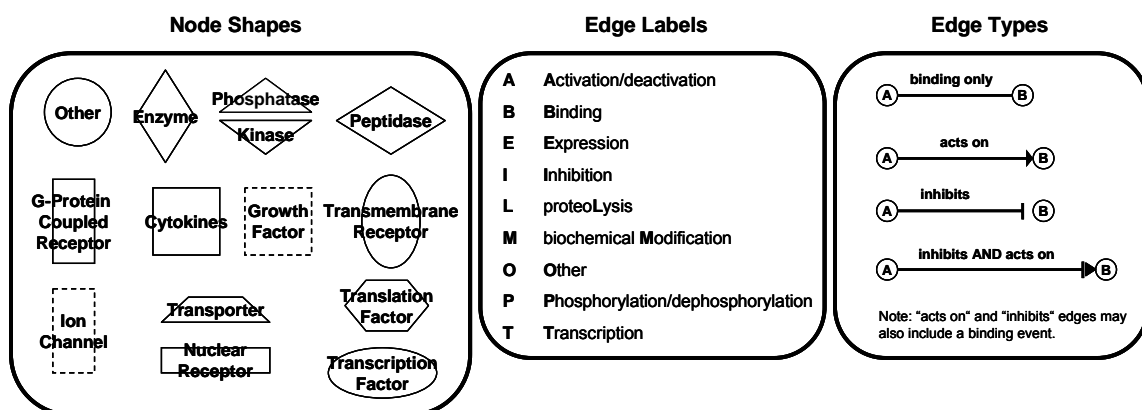
3.4.7 Network analysis

Biological networks have been generated through the use of Ingenuity Pathways Analysis, a web-delivered application that enables biologists to discover, visualize and explore networks significant to experimental results.

Firstly, genes were identified whose expression was significantly differentially regulated between the respective leukemia subtypes of interest. Next, a data set containing those gene identifiers in probe set format and their corresponding statistical parameters, e.g., p-value or fold change, was uploaded as a tab-delimited text file into the Ingenuity Pathways Knowledge Base. Then each probe set was automatically mapped by the application to its corresponding database gene object to designate the so-called focus genes. Focus genes are genes from the analysis input data file that meet both of the following criteria: These genes have been designated as being of interest, i.e., a level of significance at a certain FDR. Additionally, they directly interact with other genes in the Ingenuity global molecular network, which consists of direct physical, enzymatic, and transcriptional interactions between mammalian orthologs from the published, peer-reviewed content in Ingenuity's Pathways database. To start building the networks, the application queries the Ingenuity Pathways database for interactions between focus genes and all other gene objects stored in the knowledge base, and generates a set of networks with a network size of 35 genes. The application then computes a score for each network according to the fit of the user's set of significant genes. The score is derived from a p-value and indicates the likelihood of the focus genes in a network being found together due to random chance. A score of 2 indicates that there is a 1 in 100 chance that the focus genes are together in a network due to random chance. Therefore, scores of 2 or higher have at least a 99% confidence of not being generated by random chance alone. Biological functions are then calculated and assigned to each network.

The networks are displayed graphically as nodes using various shapes that represent the functional class of the gene product. Edges are displayed with various labels that describe the nature of the relationship between the nodes (Figure 12). The length of an edge reflects the evidence supporting that node-to-node relationship, in that edges supported by more articles from the literature are shorter.

Figure 12. Network details on node shapes, edge labels, and types.



3.4.8 Software

Software packages from Affymetrix were used for principal data acquisition (MAS5), storage (MicroDB), and analysis (DMT). Individual gene expression profiles were further prepared as Microsoft Excel tables.

Software	Source	Internet
MAS5	Affymetrix, Inc.	www.affymetrix.com/support/
MicroDB	Affymetrix, Inc.	www.affymetrix.com/support/
DMT	Affymetrix, Inc.	www.affymetrix.com/support/

The following packages were applied for identification of differentially expressed genes and classification:

Software	Source	Internet
SAM	Stanford University	www-stat.stanford.edu/~tibs/SAM/index.html
Bioconductor	open source	www.bioconductor.org
q-value	University of Washington	faculty.washington.edu/~jstorey/qvalue/
LIBSVM	National Taiwan University	www.csie.ntu.edu.tw/~cjlin/libsvm/

With the exception of SAM, which is available as Microsoft Excel Add-in, all other applications were integrated into the Gene Analysis Management System (GAMS), developed by PD Dr. Martin Dugas, Department of Medical Informatics, Biometrics and Epidemiology, Ludwig Maximilians-University, Munich, Germany. GAMS is a generic concept for large-scale microarray experiments dedicated to medical diagnostics. This system is capable of handling several 1000 microarrays per analysis and more than 100 clinical response variables and was designed to use a standardized workflow for quality control, data calibration, identification of differentially expressed genes, and estimation of classification accuracy. It is based on MySQL for data storage, R/Bioconductor for data analysis and scripting language PHP for a web-based front-end for the exploration of microarray data and analysis results. Bioconductor is an open source and open development software project for the analysis and comprehension of genomic data (Dudoit et al., 2003). The Bioconductor packages used in this work provided statistical and graphical methodologies for analyzing genomic data. LIBSVM (Version 2.6) is a software solution for SVM-based classification. The q-value software takes a list of p-values resulting from the simultaneous testing of many hypotheses and estimates their q-values (Storey and Tibshirani, 2003).

In addition, further 3rd party software packages were used for statistical analyses and data visualization:

Software	Source	Internet
SPSS	SPSS Inc.	www.spss.com/
Pathways Analysis	Ingenuity Systems	www.ingenuity.com
GeneMaths	Applied Maths, Inc	www.applied-maths.com
J-Express	MolMine AS	www.molmine.com/

4. Results

4.1 Gene expression profiling in AML

An initial investigation was to answer the question whether a leukemia-specific genotype is associated with a distinct gene expression profile.

Unsupervised analysis of AML with recurring genetic abnormalities

Initially, from the first WHO category 37 AML patient samples with thorough diagnostic documentation were selected: Cases with AML and t(8;21) had AML FAB M2 and all cases with AML and inv(16) had AML FAB M4eo. The cases with AML and t(15;17) showed FAB M3 as well as M3v characteristics. All patients showed these balanced abnormalities as the sole karyotype change. Firstly, the question whether recurrent chromosomal aberrations can be correlated with specific gene expression signatures was addressed using hierarchical clustering, a useful exploratory technique for an unsupervised analysis of the data. Global gene expression signatures from 37 patients were analyzed using U95Av2 microarrays. Figure 13 is a graphic display from an unsupervised hierarchical clustering. Each data point is represented by a color that quantitatively reflects the original experimental observations. It is clear that when the algorithm orders genes and patients according to similarity in patterns of gene expression three major branches can be observed. The dendrograms reflect underlying biology. Each one of the three branches from the top dendrogram contains exclusively samples of the specific AML subtypes t(15;17), t(8;21), or inv(16), respectively. Therefore, an unsupervised analysis algorithm correctly identifies biologically distinct AML subtypes. Specific chromosomal rearrangements translate into dramatic changes on the gene expression level. As represented in the left dendrogram, a large number of genes are differentially expressed between these three AML subclasses. It is not simply a list of genes and their associated expression signature, but rather it represents a comprehensive view of the state of the cell, its molecular fingerprint.

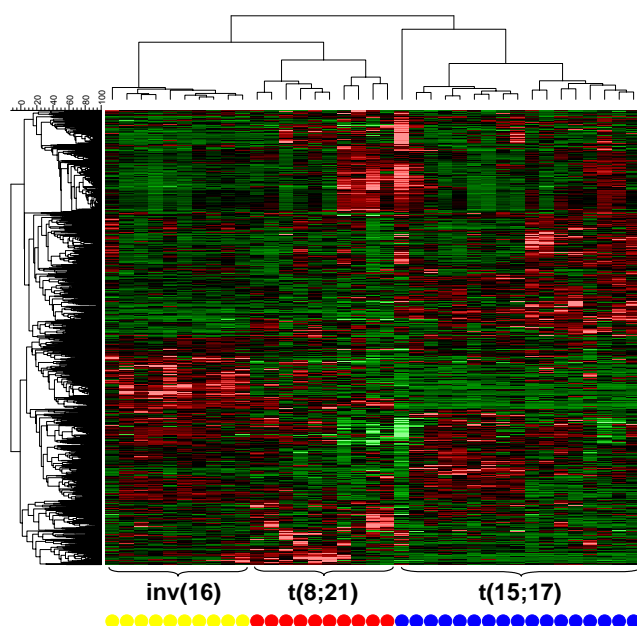


Figure 13. **Unsupervised hierarchical clustering of AML with t(15;17), t(8;21), and inv(16).** The unsupervised hierarchical cluster analysis is based on U95Av2 microarray expression data of 37 adult AML samples (columns) and a subset of 2,000 genes (rows) which showed the largest variance across all patients. The normalized expression value for each gene is coded by color (standard deviation from mean). Red cells indicate high expression and green cells indicate low expression. AML patients with t(15;17) (n=17) are colored blue, t(8;21) (n=10) red, and inv(16) (n=10) yellow, respectively.

As visualized in Figure 14 an additional unsupervised method called Principal Component Analysis (PCA) was applied to confirm the previous finding. The t(15;17) patient samples clearly cluster distinct from AML with t(8;21) or inv(16). The three cytogenetically defined AML subtypes can repeatedly be separated based on their underlying differing gene expression profiles. In conclusion, two different approaches of unsupervised data analysis methods separated biologically distinct AML subtypes based on underlying differing gene expression signatures.

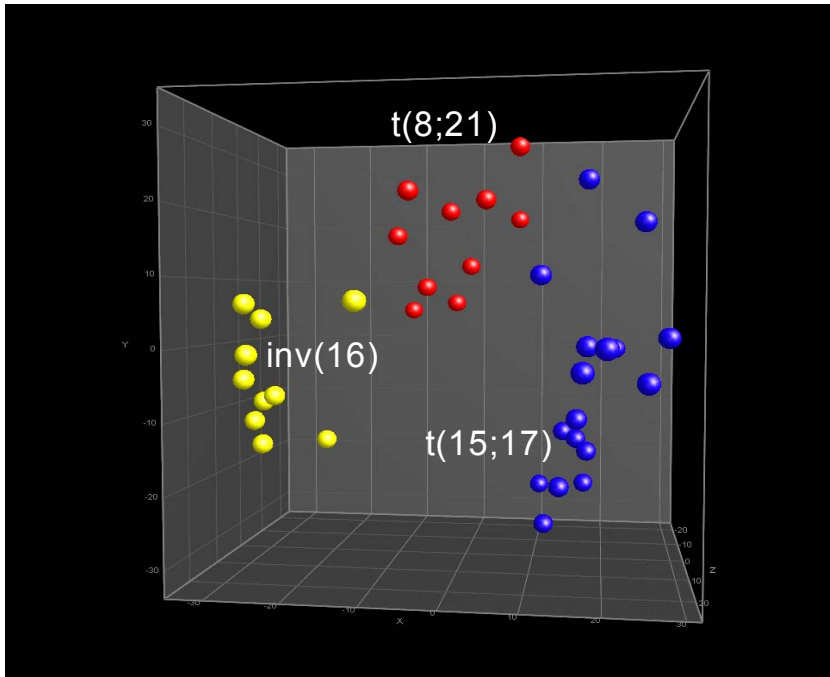


Figure 14. **Unsupervised PCA of AML with t(15;17), t(8;21), and inv(16).** This unsupervised analysis is based on U95Av2 microarray expression data of 37 adult AML samples and a set of 2,000 genes which showed the largest variance across all patients. AML patients with t(15;17) (n=17) are colored blue, t(8;21) (n=10) red, and inv(16) (n=10) yellow, respectively.

Supervised analysis of AML with recurring genetic abnormalities

Firstly, the supervised analyses were performed with the SAM software. SAM is an application for finding significant genes in a set of microarray experiments. In this application gene expression data was correlated with an external variable, i.e., the AML subtype karyotype information. A statistic for each gene was computed, measuring the strength of the relationship between the gene expression and a response variable, i.e., the respective chromosomal aberration. At a tuning parameter delta of 0.47254 n=1,004 probe sets were called significant (Figure 15A). The median number of false significant called probe sets was n=4. This set of significant genes was further evaluated. As visualized in Figure 15B, when analyzing the gene expression space of these top 1,000 differentially expressed genes, they clearly discriminate the three AML subtypes. In the top dendrogram three distinct groups of patient samples can be observed, each corresponding to the different cytogenetic AML classes.

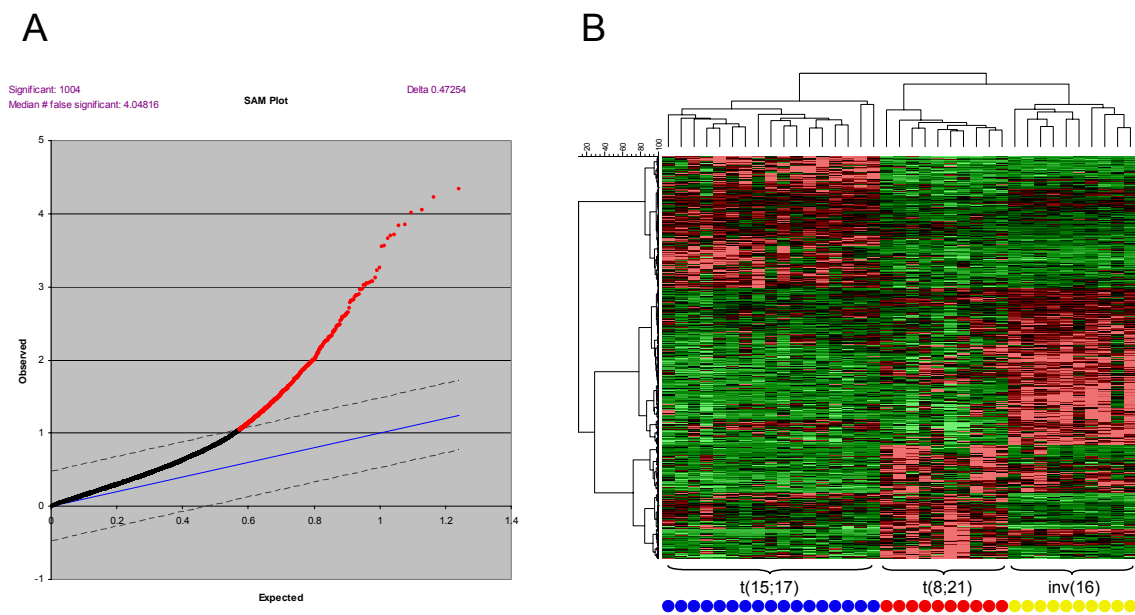


Figure 15. **Supervised analysis of AML with t(15;17), t(8;21), and inv(16).** The three AML subtypes were analyzed in a supervised way by the multiclass parameter of the SAM software. (A) The SAM plot represents a display of observed significant U95Av2 probe sets ($n=1,004$), given as red dots, and informs about the median number of false significant calls ($n=4$). (B) Hierarchical clustering visualizing the top 1,000 probe sets from the supervised analysis. AML patients with t(15;17) ($n=17$) are represented by blue, t(8;21) ($n=10$) by red, and inv(16) ($n=10$) by yellow dots, respectively.

Minimal set of genes for classification

In total, gene expression profiles from 37 AML samples were evaluated. Thirty-two hybridization cocktails with optimal cRNA quality (3'/5' ratio of *GAPD* probe sets less than 3.0) were chosen for training of the class prediction model: t(8;21) ($n=7$), t(15;17) ($n=16$), and inv(16) ($n=9$). Five cases were excluded from the training set (3'/5' *GAPD* ratios ranging between 3.9 and 5.4) and were used for a subsequent validation of the prediction models: t(8;21) ($n=2$), t(15;17) ($n=2$), and inv(16) ($n=1$).

Thirteen genes were sufficient to separate these AML subtypes with optimal classification accuracy and highest prediction strength (Table 1). All samples from the training cohort were successfully assigned to their corresponding cytogenetic subtype (accuracy estimated by leave-one-out cross-validation). The prediction strength values ranged from 0.91 to 0.98. Subsequently, the 5 primarily excluded samples were tested. Despite their non-optimal cRNA quality, all five cases were correctly classified with high prediction strength values (0.76, 1.00, 1.00, 1.00, and 1.00). This finding may indicate that the 3.0 cutoff for the 3'/5' ratio of *GAPD* probe sets is somewhat arbitrary.

Table 1. **Minimal set of 13 genes sufficient for accurate class prediction.** As calculated from pairwise comparisons, for each gene positive P(g,c) values indicate a higher expression in the first class listed, negative P(g,c) values indicate a higher expression in the second class listed, respectively.

Classes		t(15;17) vs. t(8;21)	t(15;17) vs. inv(16)	inv(16) vs. t(8;21)	inv(16) vs. remainder	t(8;21) vs. remainder	t(15;17) vs. remainder
Accuracy		1.00	1.00	1.00	1.00	1.00	1.00
Prediction strength		0.91	0.96	0.93	0.95	0.98	0.91
Symbol	Public ID	P(g,c)	P(g,c)	P(g,c)	P(g,c)	P(g,c)	P(g,c)
<i>PRKAR1B</i>	M65066				-1.52		
<i>GNAI1</i>	AL049933						-2.12
<i>PRODH</i>	AF010310						1.89
<i>CDW52</i>	N90866						-2.34
<i>KRT18</i>	M26326	2.85				-2.56	
<i>CLIPR-59</i>	N99340			8.43			
<i>CLU</i>	M25915						1.63
<i>MYH11</i>	AF013570		-6.84	7.78	6.99		
<i>PTGDS</i>	AI207842	3.08	3.08				3.08
<i>HOXB2</i>	X16665			6.56	6.56		
<i>CLECSF2</i>	X96719						-2.36
<i>CTSW</i>	AF013611	2.68					
<i>S100A9</i>	W72424						-2.05

A PCA further illustrates these results. The three-dimensional plot given in Figure 16 clearly demonstrates the capacity of this subset of 13 genes to separate the AML cases according to their cytogenetic abnormality. This finding underlines that class prediction of a chromosomal aberration in AML is feasible solely based on gene expression data of a very low number of candidate genes.

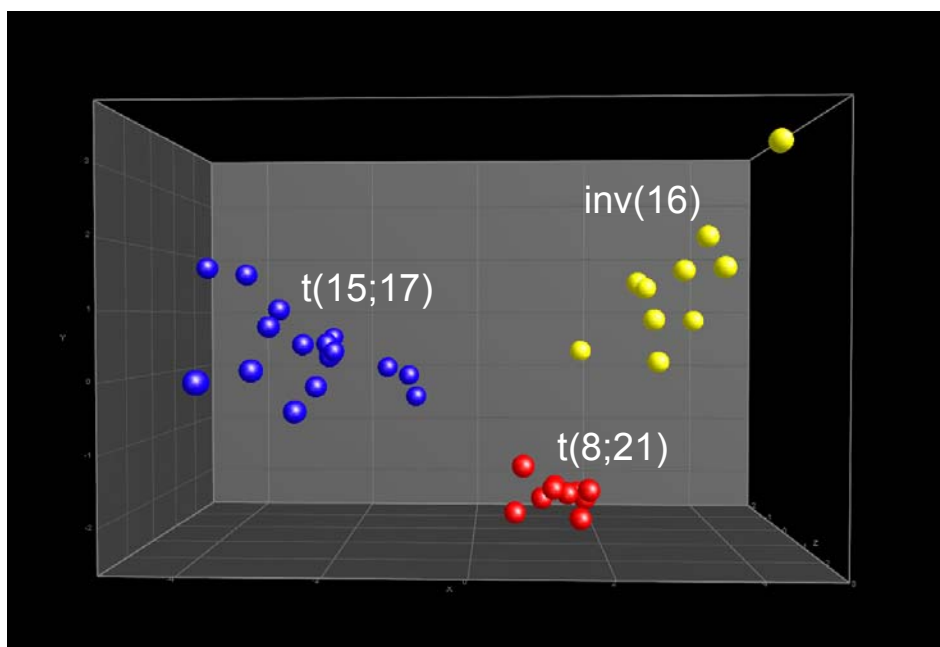


Figure 16. **PCA of three AML subtypes based on 13 genes.** The PCA visualizes U95Av2 microarray expression data of 37 adult AML samples. This analysis is based on a subset of 13 genes which were identified through the weighted voting algorithm. AML patients with t(15;17) (n=17) are colored blue, t(8;21) (n=10) red, and inv(16) (n=10) yellow, respectively.

Discrimination by decision trees

The weighted voting algorithm indicated that expression signatures would allow a discrimination of AML subtypes based on only 13 genes. In order to confirm this finding a multiple-tree model for classification was computed as a second and independent methodological approach to discriminate between the different AML subclasses. As demonstrated in Figure 17 the classifier used the expression values of 29 genes to discriminate between $t(15;17)$, $t(8;21)$, and $inv(16)$ (Table 2). The prediction accuracy for both the training set (32 samples) and the independent test set (5 samples) was 100%. The average accuracy assessed by 10-fold CV also was 100%. Thus, each patient sample was accurately given the correct cytogenetic label.

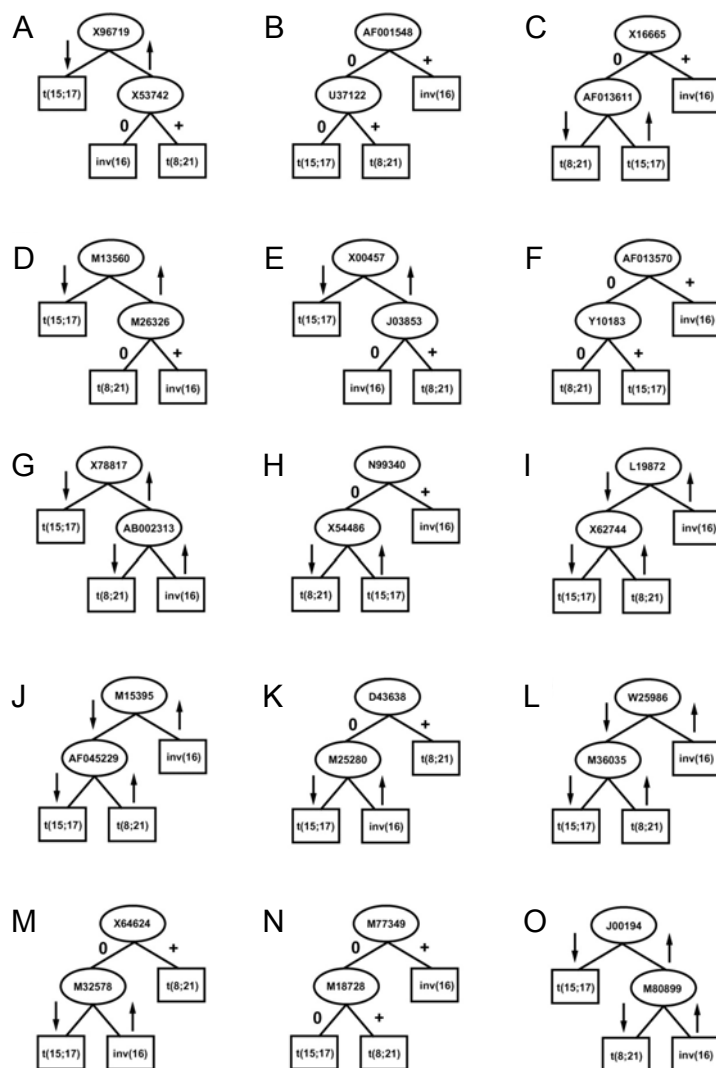


Figure 17. Multiple-tree classifier for AML with $t(15;17)$, $t(8;21)$, and $inv(16)$. Schematic representation of the 15 decision trees (A through O) used in the multiple-tree classifier for U95Av2 data. Arrows indicate high (arrow up) or low (arrow down) expression, 0 and + denote absence or presence of a gene (represented by public accession numbers). As an example, in tree A, the low expression of X96719 (*CLECSF2*) indicates AML with $t(15;17)$, whereas the high expression of X96719 (*CLECSF2*) indicates AML with $inv(16)$ or AML with $t(8;21)$. The latter two entities are distinguished by X53742 (*FBLN1*): lack of expression identifies AML with $inv(16)$ and positive expression predicts AML with $t(8;21)$. Nodes are represented as ovals and leaves as rectangles. Classes are referred to as $t(15;17)$, $t(8;21)$, or $inv(16)$.

In conclusion, this section demonstrates that cytogenetically defined AML subtypes can adequately be classified on the basis of gene expression signatures. In summary, 36 genes were specified by two independent class prediction methodologies (Table 2). Six genes were overlapping in both approaches, seven were found exclusively in the minimal set according to the weighted voting algorithm, and another 23 genes through the use of multiple-tree classifiers.

Table 2. Identified genes for the classification of AML with t(15;17), t(8;21), and inv(16).

Symbol & Accession number		Description	Weighted voting	Multiple-trees
<i>PRKAR1B</i>	M65066	protein kinase, cAMP-dependent, regulatory, type I, beta	X	
<i>GNAI1</i>	AL049933	guanine nucleotide binding protein (G protein), alpha inhibiting activity polypeptide 1	X	
<i>PRODH</i>	AF010310	proline dehydrogenase (oxidase) 1	X	
<i>CDW52</i>	N90866	CDW52 antigen (CAMPATH-1 antigen)	X	
<i>KRT18</i>	M26326	keratin 18	X	X
<i>CLIPR-59</i>	N99340	CLIP-170-related protein	X	X
<i>CLU</i>	M25915	clusterin (complement lysis inhibitor)	X	
<i>PTGDS</i>	AI207842	prostaglandin D2 synthase 21kDa (brain)	X	
<i>HOXB2</i>	X16665	homeo box B2	X	X
<i>CLECSF2</i>	X96719	C-type lectin (calcium dependent, carbohydrate-recognition domain), superfamily member 2 (activation-induced)	X	X
<i>CTSW</i>	AF013611	cathepsin W (lymphopain)	X	X
<i>S100A9</i>	W72424	S100 calcium binding protein A9 (calgranulin B)	X	
<i>MYH11</i>	AF013570	smooth muscle myosin, heavy polypeptide 11,	X	X
<i>MYH11</i>	AF001548	smooth muscle myosin, heavy polypeptide 11,		X
<i>FBLN1</i>	X53742	fibulin 1		X
<i>ADD3</i>	U37122	adducin 3 (gamma)		X
<i>ADRA2C</i>	J03853	adrenergic receptor alpha-2C		X
<i>ALCAM</i>	Y10183	CD166, activated leukocyte cell adhesion molecule		X
<i>PLXNB2</i>	AB002313	plexin B2		X
<i>ARHGAP4</i>	X78817	Rho GTPase activating protein 4		X
<i>SERPING1</i>	X54486	serine (or cysteine) proteinase inhibitor, clade G (C1 inhibitor), member 1		X
<i>AHR</i>	L19872	aryl hydrocarbon receptor		X
<i>ITGB2</i>	M15395	integrin, beta 2 (antigen CD18 (p95), lymphocyte function-associated antigen 1; macrophage antigen 1 (mac-1) beta subunit)		X
<i>RGS10</i>	AF045229	regulator of G-protein signalling 10		X
<i>CBFA2T1</i>	D43638	ETO, core-binding factor, runt domain, alpha subunit 2; translocated to, 1; cyclin D-related		X
<i>SELL</i>	M25280	selectin L (lymphocyte adhesion molecule 1)		X
<i>DKFZP564K0822</i>	W25986	hypothetical protein DKFZp564K0822		X
<i>BZRP</i>	M36035	Benzodiazepine receptor, peripheral type		X
<i>POU4F1</i>	X64624	POU domain, class 4, transcription factor 1		X
<i>CEACAM6</i>	M18728	carcinoembryonic antigen-related cell adhesion molecule 6 (non-specific cross reacting antigen)		X
<i>TGFBI</i>	M77349	transforming growth factor, beta-induced, 68kDa		X
<i>AHNAK</i>	M80899	AHNAK nucleoprotein (desmoyokin)		X
<i>CD74</i>	M13560	CD74 antigen		X
<i>HLA-DMA</i>	X62744	major histocompatibility complex, class II, DM alpha		X
<i>HLA-DRB1</i>	M32578	major histocompatibility complex, class II, DR beta 1		X
<i>HLA-DPA1</i>	X00457	major histocompatibility complex, class II, DP alpha 1		X
<i>HLA-DRA</i>	J00194	major histocompatibility complex, class II, DR alpha		X

These 36 genes are further visualized in a hierarchical cluster representation in Figure 18A. Intriguingly, the classifiers contained genes already known to be primarily involved in the pathogenesis of the respective entities, namely *MYH11* and *ETO* (*CBFA2T1*) (Look, 1997). The other genes identified belong to various functional categories (Table 2). Their potential pathogenic significance in AML has yet to be clarified. Moreover, it is interesting to note that for most of these candidates the pattern is almost like an on/off situation. In one cytogenetic subtype the gene is not expressed or demonstrates very low signal intensity while in other subtypes the gene is calculated as present with very high signal intensity. The genes *CTSW*, *MYH11*, and *POU4F1* are given as bar graphs to illustrate that finding (Figure 18B). This further supports the idea of a possible application of these candidates for a diagnostic usage.

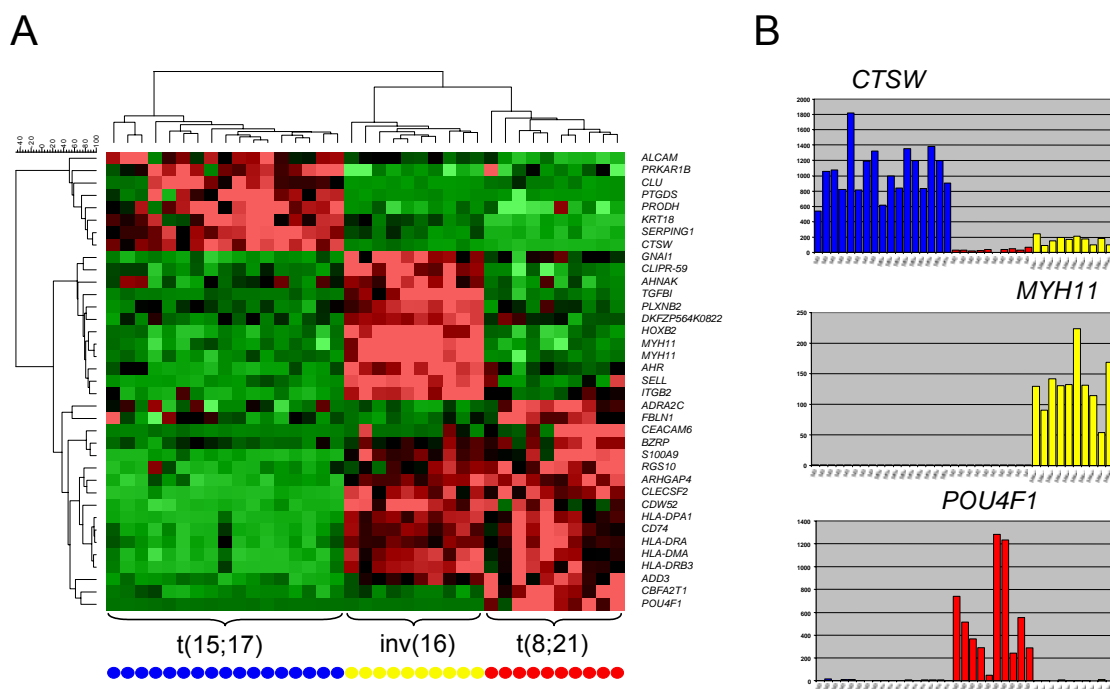


Figure 18. **Hierarchical clustering using 36 genes from both classifiers.** (A) The hierarchical cluster analysis is based on U95Av2 microarray expression data of 37 adult AML samples (columns) and 36 genes (rows) which were identified by using two independent methodologies for class prediction in cytogenetic AML subtypes. The normalized expression value for each gene is coded by color (standard deviation from mean). Red cells indicate high expression and green cells indicate low expression. AML patients with t(15;17) (n=17) are colored blue, t(8;21) (n=10) red, and inv(16) (n=10) yellow, respectively. (B) Bar graphs for three differentially expressed genes: *CTSW*, *MYH11*, and *POU4F1*.

Transition from U95Av2 microarrays to the U133 chip design

Firstly, the question was addressed whether differentially expressed genes from the previous U95Av2 analyses would also allow an accurate separation of the patients when measured with U133 design microarrays. The search for corresponding probe sets representing the genes correlated with the AML subtypes $t(15;17)$, $t(8;21)$, or $inv(16)$ resulted in a total number of 59 best match U133A counterparts for the 37 designated U95Av2 probe sets. Secondly, the genes could also be validated on new, independent patient samples which had not been used in the previous gene identification study. Thus, all previously used hybridization cocktails and additional samples for each leukemic subgroup, respectively, were hybridized to the newly designed and improved U133 microarrays. As shown in Figure 19, based on the U133 microarray expression data and also including new samples of each of the distinct AML subgroups, all 129 cases were repeatedly separated according to their underlying chromosomal aberration. In conclusion, the previously identified genes had been successfully validated on a different microarray design. Moreover, when additional patient samples were included in the analysis these new samples were also accurately assigned. Therefore, this work proceeded with the transition from U95Av2 arrays to the U133 set of microarrays.

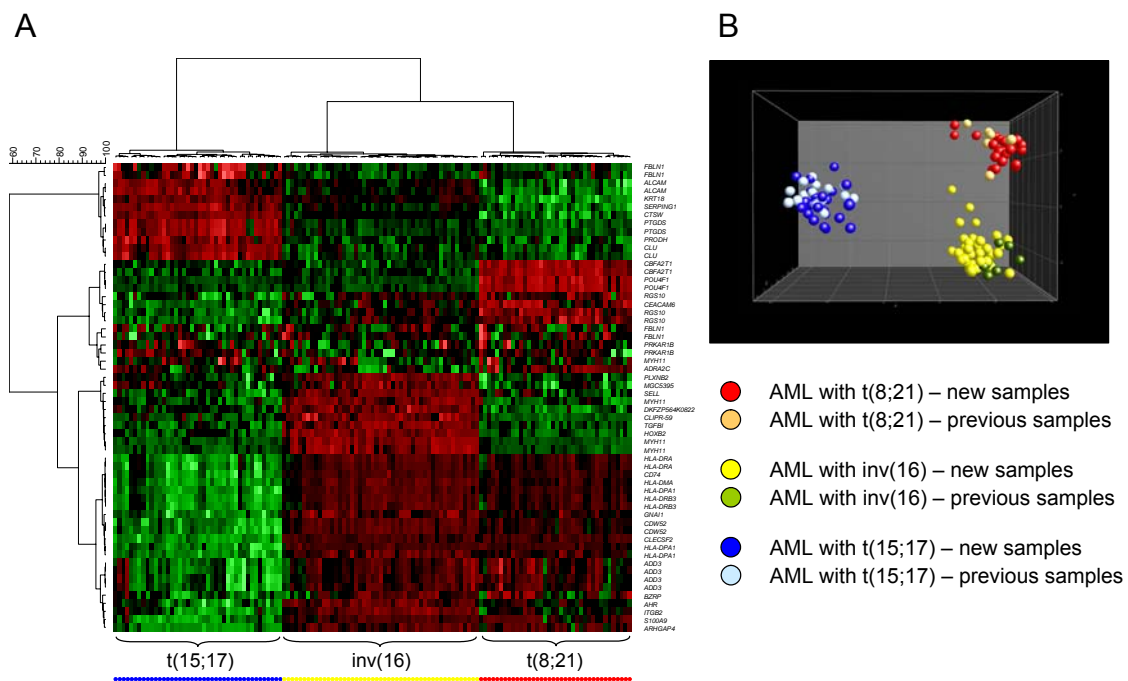


Figure 19. **Transition from U95Av2 arrays to the U133 array design.** Analysis of 42 AML with $t(15;17)$ (blue), 38 $t(8;21)$ (red), and 49 $inv(16)$ (yellow), respectively. This analysis is based on U133A gene expression data and includes patients that had been hybridized to U95Av2 arrays in a previous analysis and were rehybridized to U133A microarrays, as well as new patient samples that were directly hybridized to U133A microarrays. (A) Hierarchical clustering using only the significant minimal set of genes that was identified using the previous cohort of patients and U95Av2 microarrays. (B) Also in the PCA genes corresponding to probe sets from the U95Av2 study were selected and used to project the samples into a three-dimensional space based on U133A microarray data. New and previous patient samples for each of the three AML subtypes are accordingly indicated by different colors.

Gene expression profiling and morphology in APL

So far, no single cytogenetic or molecular genetic marker has been identified to clearly distinguish between the two morphologically highly different subtypes of APL. The previous microarray analyses could demonstrate that AML with t(15;17) are clearly distinct from AML with t(8;21) or inv(16) with respect to their transcriptome. Thus, as a next step, global gene expression profiles of APL were further investigated and M3 cases were directly compared to M3v patient samples. Cytomorphology of APL blasts is obviously different in both subtypes although few patients show features in peripheral blood or bone marrow of both phenotypes. In M3 the abnormal promyelocytes show a heavy granulation and bundles of Auer rods, whereas M3v blasts have a non- or hypogranular cytoplasm or contain fine dust-like cytoplasmic granules that may be unapparent by light microscopy. Furthermore, M3v blasts show a typical bilobed nuclear configuration (Figure 20).

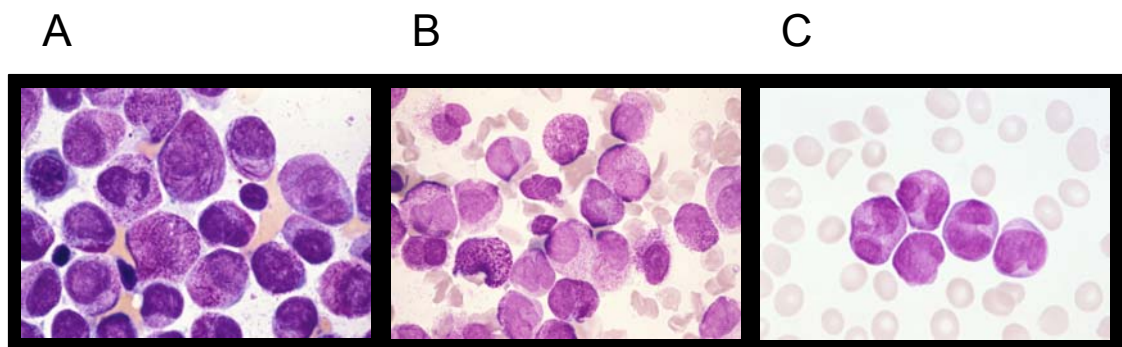


Figure 20. **Morphology of APL samples.** Three Papanheim stainings of bone marrow smears from APL patients (Figures were kindly provided by H. Löffler, St. Peter, Germany). Light microscopic view at 630-fold magnification of: (A) Typical FAB M3 case with heavy granulation and bundles of Auer rods. (B) Case demonstrating a mixture of the two morphological phenotypes. (C) Typical FAB M3v case with non- or hypogranular cytoplasm and bilobed nuclear configuration.

Discrimination of APL from other genetically defined AML subgroups

Firstly, an unsupervised class discovery approach aimed at separating patients with APL from three other AML subgroups with recurrent chromosomal aberrations, i.e., AML with t(8;21), inv(16), and t(11q23)/*MLL*. The respective global gene expression profiles derived from these samples were presented to the algorithm without any class information attached. As visualized in the PCA in Figure 21A, APL samples clearly cluster distinct from AML with t(8;21), inv(16), or t(11q23)/*MLL*. A second step was intended to investigate whether the APL patients would also be distinct from AML patients with normal karyotype. Here, an unsupervised approach demonstrated that APL profiles are clearly distinct from AML with normal karyotype (Figure 21B). Thus, these AML subclasses were discovered by analysis of their global gene expression signatures in an unsupervised way.

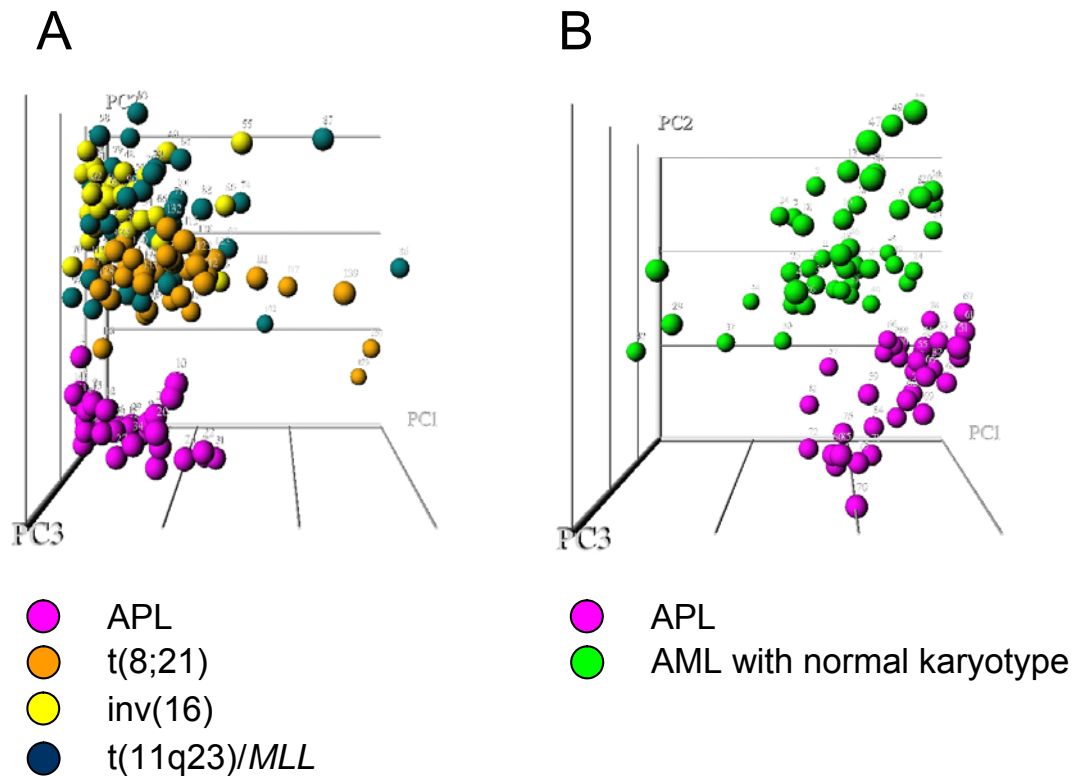


Figure 21. **Class discovery: APL vs. other AML subclasses.** Without any gene selection or filtering each patient's global gene expression pattern is represented by a single color-coded sphere. An unsupervised PCA discovers AML subclasses and segregates 35 APL samples from (A) AML with t(8;21) (n=35), inv(16) (n=35), or t(11q23)/MLL (n=35), or (B) AML with normal karyotype (n=50).

Next, a supervised algorithm was applied to identify the differentially expressed genes. The APL samples were compared to the cases with recurrent chromosomal aberrations (AML with t(8;21), inv(16), and t(11q23)/MLL), as well as to AML with normal karyotype. When both lists containing the top 1,000 differentially expressed probe sets were matched, 505 probe sets were overlapping. When this list of APL-specific genes was imputed into a network analysis software a known finding could be reproduced, i.e., that genes with functional relevance in MHC-II antigen presentation are lower expressed in APL (Figure 22) (Watts, 1997; Villadangos and Ploegh, 2000; Masternak et al., 2000; Orfao et al., 2004).

Signatures of genes with functional relevance in blood coagulation

Both APL subtypes are frequently associated with severe bleeding episodes characterized by a combination of disseminated intravascular coagulation and hyperfibrinolysis. Thus, further analyses were targeted at gene expression signatures from candidates with functional relevance in blood clotting. Using the NetAffx database the probe sets were functionally annotated and grouped according to their biological function, i.e., using the Gene Ontology process descriptions. A total number of 132 microarray probe sets, representing 61 genes, corresponded to the Biological Process GO category blood coagulation (accession number GO:0007596). When the 35 APL patients were compared to other AML subclasses with recurrent chromosomal aberrations, i.e., 35 cases each with t(8;21), inv(16), or t(11q23)/*MLL*, all APL cases can be separated based on their specific expression pattern on the basis of genes correlated with coagulation (Figure 23A). Also, when compared to 50 AML cases with normal karyotype, only on the basis of genes involved in blood coagulation, two distinct clusters were observed in the PCA (Figure 23B). Thus, in both types of comparisons, based on a preselected set of genes with functional relevance in blood clotting, all APL samples demonstrated a distinct expression pattern different from all other AML subclasses. To validate these findings AML M3 samples were compared to AML M3v samples using the same genes encoding for clotting relevant proteins. As anticipated, no clear distinction was observed between both groups as patients with both subtypes suffer from severe bleeding disorders at diagnosis (Figure 23C).

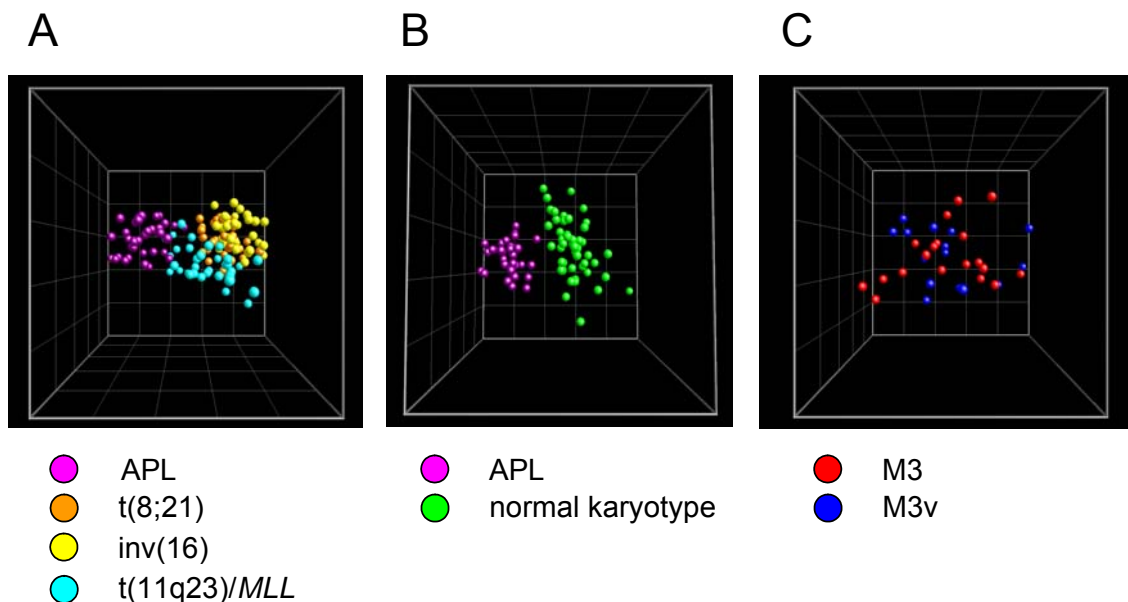


Figure 23. **PCA based on genes from the GO category blood coagulation.** The three-dimensional PCA feature space visualizes measured U133 set expression data on genes from the Gene Ontology Biological Process category blood coagulation (accession number GO:0007596). (A) Analysis of APL patients vs. AML with t(8;21), inv(16), or t(11q23)/*MLL*. (B) Analysis of APL patients vs. AML cases with normal karyotype. (C) Analysis of M3 vs. M3v samples.

Supervised comparison of FAB M3 to FAB M3v samples

Of 35 patients with t(15;17) and confirmed *PML/RARA* fusion genes detailed diagnostic reports on the morphology were available for 19 AML M3 and 16 AML M3v. Thus, it was possible to address the question whether gene expression profiling might also help to dissect this morphological phenomenon and help to increase the understanding of these two leukemia entities. In a next step, genes differentially expressed between both morphological APL subtypes were identified through a supervised data analysis approach. The morphological classification had been done in routine at diagnosis by the same expert and no further re-evaluation was performed before the samples were processed for this analysis. This was decided although some rare cases showed a mixture of the two morphological phenotypes (similar to Figure 20B). The total number of 19 AML M3 profiles were directly compared to 16 AML M3v cases and the false discovery rate (FDR) was estimated. Then several lists of differentially expressed genes were visualized.

Firstly, a FDR of 5% ($q\text{-value} < 0.05$) was chosen, i.e., among all features called significant 5% are truly null on average. A total number of 186 probe sets demonstrated this level of significance. Figure 24A shows a PCA using these 186 probe sets. The M3 samples cluster distinct from the M3v cases with few exceptions. Next, a more stringent criterion was applied, i.e., a false discovery rate of 1%. The number of significant probe sets shrunk down to 14. As given in Figure 24B now all M3 cases can be separated robustly from the M3v samples based on the expression pattern of those 14 probe sets. They were representing the genes *ANXA2*, *CAP1*, *CAPN2*, *CD97*, *GLUD1*, *LGALS1*, *LMNA*, *MMP19*, *PLXNB2*, *S100A10*, *TAGLN2*, and *TGFB1*. All genes demonstrated a higher expression in the M3v samples (Figure 24C).

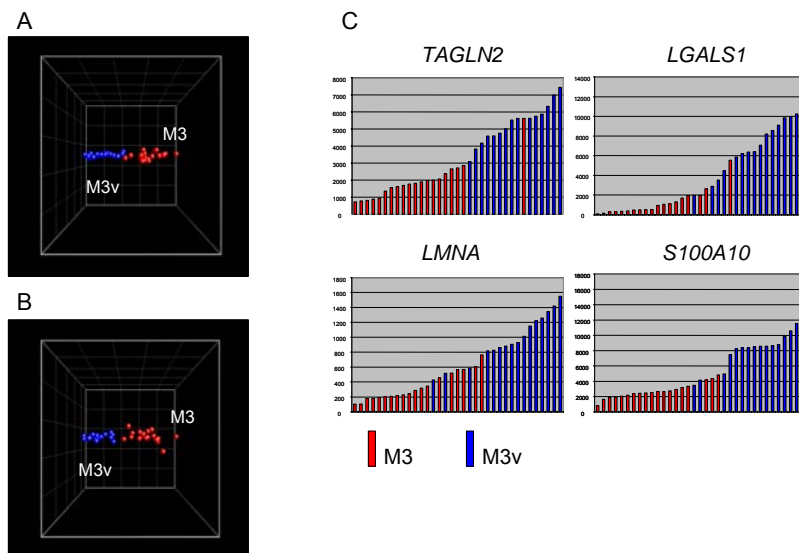


Figure 24. **Supervised analysis to discriminate APL subtypes.** After a supervised comparison of M3 vs. M3v samples (U133 set), differentially expressed genes at differing false discovery rates are visualized. (A) Visualization of data based on 186 probe sets discovered at 5% FDR. (B) Visualization of data based on 14 probe sets discovered at 1% FDR. (C) For a selection of top differentially expressed genes the absolute level of expression is represented by bar graphs. The 19 M3 cases are colored red, the 16 M3v cases are represented by blue bars, respectively.

Subsequently, a machine learning algorithm (SVM) was applied to test the accuracy when predicting the respective morphological APL subtype based on differentially expressed genes. Therefore, the complete data set was randomly, but balanced by the morphological APL subtypes split into training and independent test cohorts. Then differentially expressed genes were identified in the training set, calculated by means of t-test-statistic, and a SVM model was built based on the top 50 genes that demonstrate differential expression between FAB M3 and FAB M3v subtypes in the training set. This SVM model was used to predict samples in the test cohort. Using a 10-fold CV approach (9/10 for training and 1/10 for testing, 10 iterations) morphological APL subtypes were predicted based on their gene expression signature with a median of accuracy of 91%. In order to assess robustness of this class prediction a resampling approach was applied, i.e., the complete classification procedure was repeated for 100 times (training set: 2/3 of patients, test set 1/3). By this means 95% confidence intervals were estimated. The data demonstrate that morphological APL subtypes can be predicted based on their gene expression signature with a median of accuracy of 91% (95% confidence interval of accuracy: [73%; 100%]).

In detail, the algorithm selected the following genes in more than 90% of the runs: *S100A10*, *TAGLN2*, *LGALS1*, *CAP1*, *GLUD1*, *ANXA2*, *TGFB1*, *LMNA*, and *MMP19*. From the morphological and clinical point of view differences between typical APL and its variant are known in granulation pattern, WBC count, Auer rods, and especially the frequency of faggot cells or the detection of length mutations of the *FLT3* gene (FLT3-LM). In this respect, all AML M3 (n=118) and AML M3v cases (n=46) which were diagnosed by morphology, cytogenetics, and molecular genetic techniques in the Laboratory for Leukemia Diagnostics, Munich, Germany, between December 1998 and February 2004 were analyzed. Data of these 164 APL patients are shown in Table 3. In all cases no further mutations (i.e., *KIT* or partial tandem duplication of the *MLL* gene) were detected.

Table 3. Morphological and genetic differences in the APL cohort.

	AML M3 (n=118)	AML M3v (n=46)	p =
Age (median, range)	51.4 (17-82)	47.9 (18-83)	n.s.
Male/female	59/59	21/24	n.s.
WBC count at diagnosis (G/l)	1,400 (200-70,900)	15,300 (500-332,000)	0.000000005
Hemoglobin (g/dl)	9.4 (4-15)	9 (4.8-14.1)	n.s.
Platelets (μ l)	31,000 (7,000-187,000)	26,000 (8,000-115,000)	n.s.
Auer rods leading to faggot cells	58/66 (87.8%)	20/31 (64.5%)	0.0055
Additional chromosomal aberrations	46/118 (39%)	17/46 (37%)	n.s.
FLT3 length mutation	20/80 (25%)	34/46 (73.9%)	< 0.0001
FLT3 tyrosine kinase domain mt.	3/66 (4.5%)	4/41 (10.8%)	n.s.
NRAS mutation	3/63	0/30	n.s.

In order to prove that the genes identified to distinguish between AML M3 and AML M3v are not simply related to FLT3-LM or to the WBC count, which both are known to be different between both disease subtypes, linear regression analyses were performed for each of the top 20 genes considering AML M3v, FLT3-LM, and WBC count as covariates. The results indicate that for nearly all of the top 20 genes the relation is strongest to AML M3v (Table 4). Significant relations to FLT3-LM and WBC count were present for only two and six genes, respectively. Therefore, the identified genes not simply reflect the WBC count or the occurrence of FLT3-LM, but truly are related to the presence of AML M3 and AML M3v morphology.

Table 4. Linear regression analyses for top 20 discriminative genes (M3 vs. M3v).

Gene	Covariates		
	AML M3v	WBC count	FLT3-LM
<i>NFE2L1</i>	0.004	n.s.	n.s.
<i>S100A10</i>	0.00006	0.002	n.s.
<i>TAGLN2</i>	0.00007	n.s.	n.s.
<i>GLUD1</i>	0.0004	n.s.	n.s.
<i>LGALS1</i>	0.0001	0.005	0.034
<i>ANXA2</i>	0.00001	0.025	n.s.
<i>CD97</i>	0.00004	n.s.	n.s.
<i>TGFB1</i>	0.0001	n.s.	n.s.
<i>LMNA</i>	0.018	0.010	0.025
<i>MMP19</i>	0.00002	n.s.	n.s.
<i>CRIP1</i>	0.0003	0.00002	n.s.
<i>CAPN2</i>	0.00001	n.s.	n.s.
<i>CDC42</i>	0.0002	n.s.	n.s.
<i>PLXNB2</i>	0.00002	n.s.	n.s.
<i>ANXA2</i>	0.00006	n.s.	n.s.
<i>LMNA</i>	0.0004	0.034	n.s.
<i>ANXA2</i>	0.00002	n.s.	n.s.
<i>CAP1</i>	0.00005	n.s.	n.s.
<i>MGC10997</i>	0.0001	n.s.	n.s.
<i>CAMK1D</i>	0.001	n.s.	n.s.

(p-values are given; n.s.= not significant)

Granulation pattern and stage of maturation in APL

It has been shown that different patterns of granulation are associated with different levels of defensin and transcobalamin (Jandl, 1996). Therefore, genes were evaluated that are known to be relevant for granulation. Interestingly, higher expression levels of defensin alpha 1, *DEFA1*, were observed in M3 cases in concordance with a higher number of primary granules in these samples. On the other hand, transcobalamin II, *TCN2*, a member of cobalamin transport proteins, is found higher expressed in secondary granules. Consistent with this finding *TCN2* was detected elevated in cases with M3v morphology. In addition, genes involved in maturation were found to be differentially expressed. An elevated expression in FAB M3v cases compared to the M3 samples was

observed for *PTPRC* (CD45 antigen), *ALOX5*, involved in leukotriene pathway, and interleukin-3 receptor alpha chain, *IL3RA*. A differing gene expression was further detected for *CD2* positivity, namely being higher expressed in M3v and its intracellular binding protein 2 (*CD2BP2*). Figure 25 visualizes the absolute expression signal intensities for a selection of these genes.

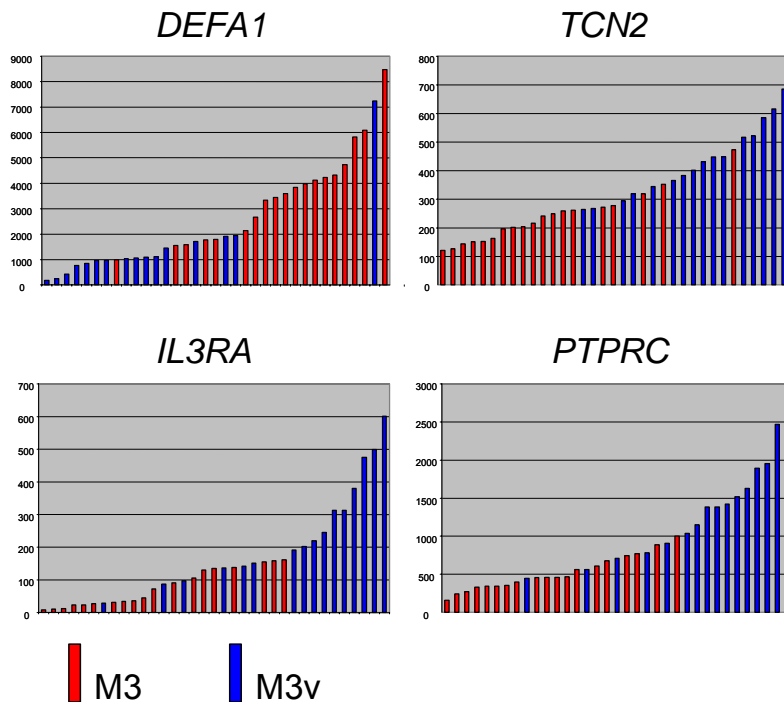


Figure 25. **Differences in expression of genes with function in granulation or maturation in APL.** For each gene the absolute level of expression is represented by bar graphs in each patient (U133 set). The 19 M3 cases are colored red, the 16 M3v cases are represented by blue bars, respectively.

4.2 Gene expression profiling in ALL

U95Av2 microarray data on four subtypes of adult ALL

Firstly, U95Av2 gene expression profiles were analyzed to accurately identify the known prognostically important adult leukemia subtypes, i.e., B-lineage leukemias that contain t(9;22), t(11q23)/*MLL* (all t(4;11)-positive), or t(8;14), as well as T-lineage leukemias, respectively. In total, ten comparisons within the four groups were performed (pairwise and OVA). Using leave-one-out cross-validation, all samples were correctly classified on the basis of 17 genes represented by 19 probe sets. The corresponding cluster dendrogram is given as Figure 26.

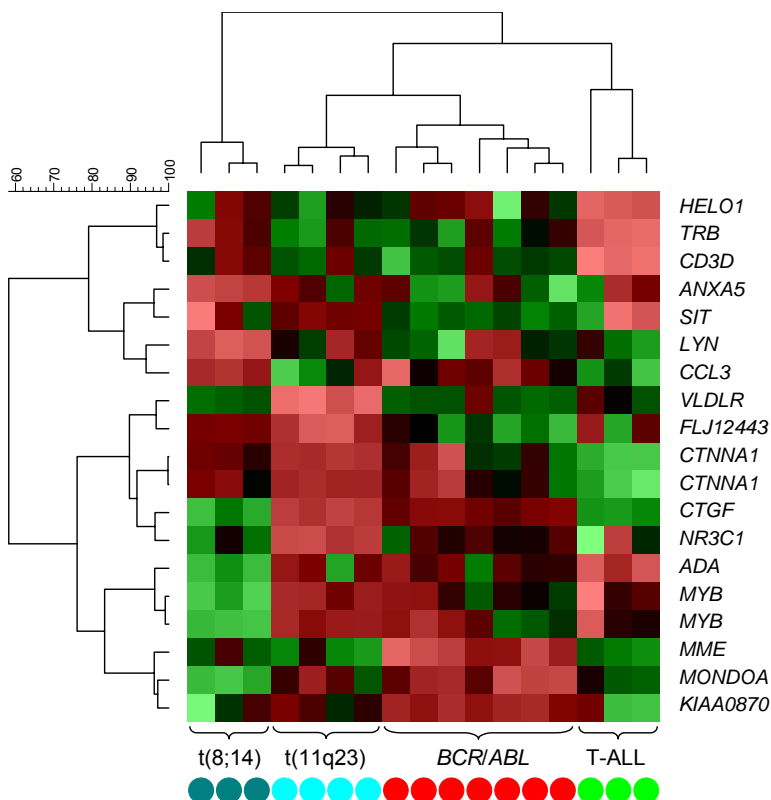


Figure 26. Analysis of adult ALL samples using U95Av2 microarrays. Hierarchical clustering based on U95Av2 expression data of 17 ALL samples (columns) from the subgroups t(11q23)/*MLL* (n=4), t(9;22) (n=7), t(8;14) (n=3), and precursor T-ALL (n=3) vs. a minimal set of 17 informative genes represented by 19 probe sets (rows). The normalized expression value for each gene is coded by color. Red cells represent high expression and green cells represent low expression.

To further demonstrate that the presented genes were characteristic for the respective leukemia subtype, also the analyses of ALL subtypes were extended to the U133A microarray. Thus, all previously used 17 hybridization cocktails and two additional samples for each subgroup, respectively, were rehybridized to the U133A microarray. Again, a stringent search determined for the presented U95Av2 probe sets their best corresponding U133A counterparts. As shown in Figure 27, now based on U133A microarray expression data and including two new samples of each of the distinct subgroups, all adult ALL cases were repeatedly separated according to their underlying chromosomal aberration or immunophenotype. Taken together, this section successfully demonstrates a subclassification of ALL samples based on gene expression profiling. It could be shown that only a small set of differentially expressed genes was necessary to correctly discriminate the different ALL subtypes. New differentially expressed genes were identified and defined as potential diagnostic markers.

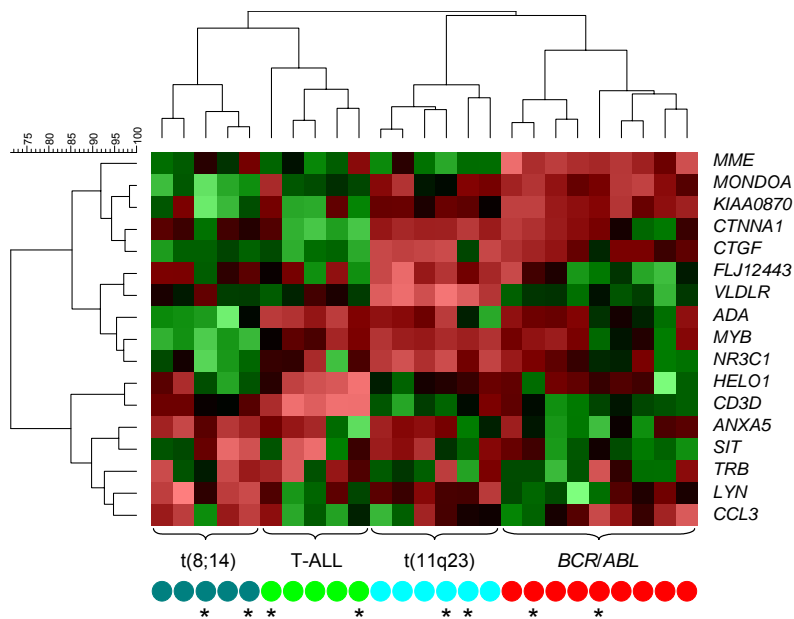


Figure 27. Analysis of adult ALL samples using U133A microarrays. Hierarchical clustering based on U133A expression data of 25 ALL samples (columns) comprising the subgroups t(11q23)/*MLL* (n=6), t(9;22) (n=9), t(8;14) (n=5), and precursor T-ALL (n=5) vs. 17 informative genes (rows). New patient samples which were not previously hybridized to U95Av2 arrays are accordingly marked (asterisks). The normalized expression value is coded by color.

Analysis of heterogeneous precursor B-ALL cases

After obtaining these results that specific signatures are also observed in adult ALL subtypes the analyses were extended to expression profiles of heterogeneous precursor B-ALL cases not positive for t(9;22) or t(11q23)/*MLL*. Therefore, in addition 7 precursor B-ALL patients (c-ALL and Pre-B-ALL) were hybridized to obtain new insights into the molecular features of these cases. This additional cohort included patients who showed a normal karyotype (n=2) or a variety of different karyotype abnormalities (n=5).

Firstly, an unsupervised analysis, i.e., hierarchical clustering and PCA of the complete data set was performed. However, this analysis did not reveal informative structures. Therefore, a supervised analysis by use of the SAM software was performed to identify differentially expressed genes correlated with T-ALL, *BCR/ABL*, and t(11q23)/*MLL* cases. A selection of the top 510 genes accurately separated the latter three ALL subtypes (Figure 28A). Next, the 7 precursor B-ALL samples without *BCR/ABL* or t(11q23)/*MLL* chromosomal aberrations were added to the data set and all cases were projected into the space of the 510 ALL subtype relevant genes. As shown in Figure 28B, the other precursor B-ALL samples (yellow spheres) intercalate with *BCR/ABL*-positive samples (red spheres).

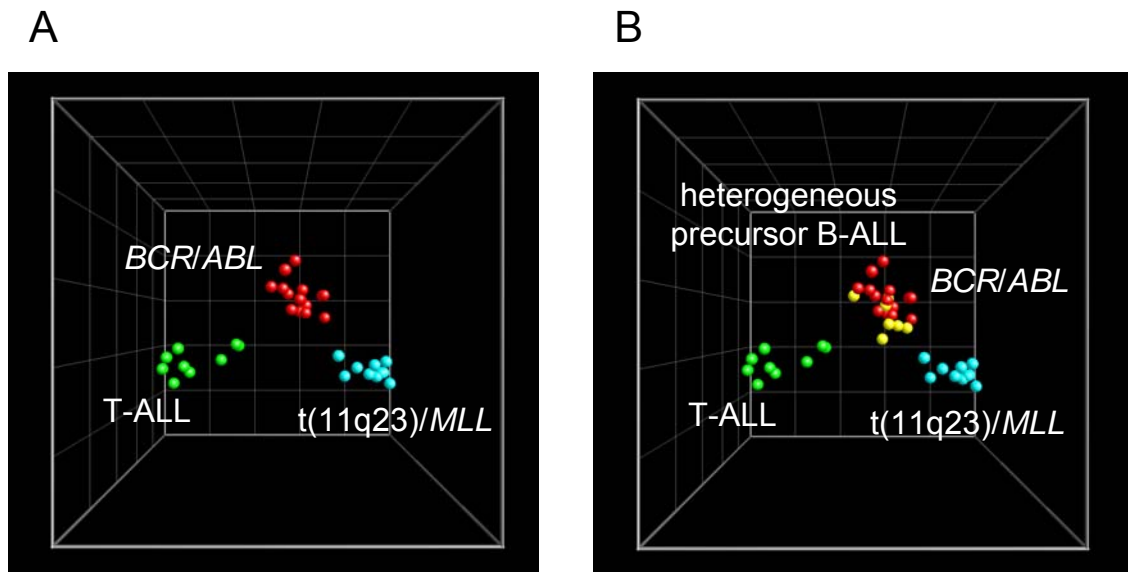
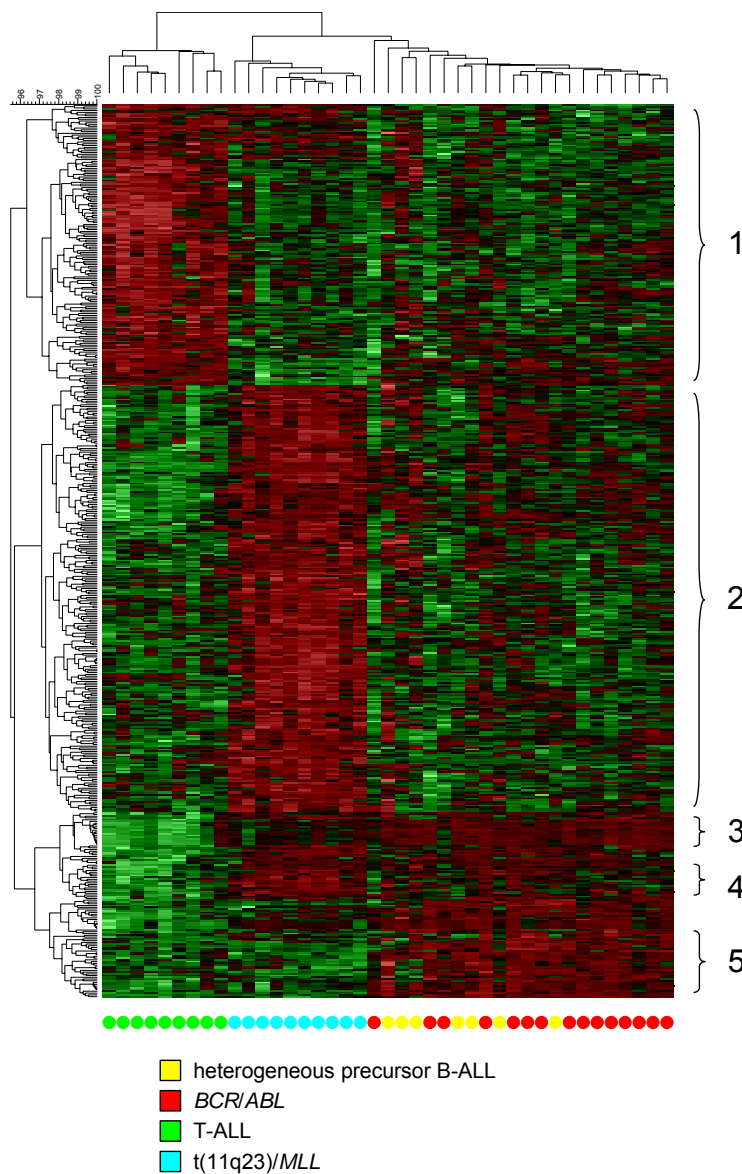


Figure 28. **PCA including heterogeneous precursor B-ALL cases.** The PCA is based on 510 differentially expressed genes that were identified by use of the SAM software to separate T-ALL ($n=9$), $t(11q23)/MLL$ ($n=10$), and BCR/ABL ($n=15$) cases (U133A). (A) T-ALL, $t(11q23)/MLL$ and BCR/ABL samples can accurately be separated using the three components capturing most of the variance in the data set. (B) When added to the data set, profiles from 7 heterogeneous precursor B-lineage ALL samples (yellow spheres) intercalate with BCR/ABL -positive samples (red spheres).

Thus, the other precursor B-ALL share similar characteristics with BCR/ABL -positive ALLs. This is in line with the definition and subclassification of precursor B-ALL according to EGIL, which is based on the immunophenotype and distinguishes Pro-B-ALL, common ALL, and Pre-B-ALL (Bene et al., 1995). Most importantly, both other ALL cases and BCR/ABL cases belong to the common ALL and Pre-B-ALL groups and are thus anticipated to have common gene expression profiles. This finding can also be visualized by use of the hierarchical clustering technique.

As shown in Figure 29, due to inherent similarities in their expression profiles three major branches of the top dendrogram can be observed. The *t(11q23)/MLL* and T-ALL samples are accurately grouped. The more heterogeneous precursor B-ALL cases are exclusively distributed in the branch containing all *BCR/ABL* patient samples. Several subtrees in the left dendrogram indicate co-expression of genes for the distinct ALL subtypes.



Subtree 1 contains genes overexpressed in T-ALL: *TRB*, *CD3D*, *CD3E*, *CD2*, *CD6*, *MAL*, *LCK*, *ITM2A*, and *SH2D1A*. A large number of these genes and additional candidates like transmembrane adapters (*LAT*, *TRIM*), further CD3 complex signal transducing members (*CD3G*, *CD3Z*), *CD8A* coreceptor, and *ZAP70* tyrosine kinase can be correlated with a functional role in the class I MHC-restricted T cell receptor signalosome (Leo et al., 2002). Subtrees 2 and 4 group genes with high expression in *MLL* gene rearranged ALL cases: *ADAM10*, *BLK*, *CD72*, *CD79A*, *CSPG4*, *HOXA9*, *HOXA10*, *IGHM*, *LGALS1*, *LMO2*, *MBNL*, *MEF2A*, *PPP2R5C*, *PTPRC*, and *VLDLR*. Subtree 3 contains

mainly genes with functional role in immune response. *BLNK*, *BRDG1*, *CD24*, *MHC2TA*, *CD74*, *HLA-DMA*, *HLA-DMB*, *HLA-DPA1*, *HLA-DRA*, *HLA-DPB1*, *HLA-DQB1*, *HLA-DRB1*, *HLA-DRB3*, *HLA-DRB4*, and *TNFRSF14* demonstrate similar patterns for *BCR/ABL*, *t(11q23)/MLL* and the more heterogeneous precursor B-ALL cases.

An interesting cluster of genes is organized in subtree 5, which is enlarged in Figure 30. Twenty-six probe sets demonstrate similar expression signatures for both *BCR/ABL*-positive and the more heterogeneous precursor B-ALL cases. All candidate genes are consistently overexpressed in these cases compared to T-ALL and *t(11q23)/MLL* samples. The probe sets represent for example *LG MN*, also called asparaginyl endopeptidase (*AEP*), a receptor tyrosine kinase activated by collagen (*DDR1*), *CD52*, an excellent target for complement-mediated lysis and antibody-dependent cellular cytotoxicity, a cytokine-like protein (*C17*), a retinoic acid induced gene (*RAI14*), or the hypothetical protein *LOC54103*.

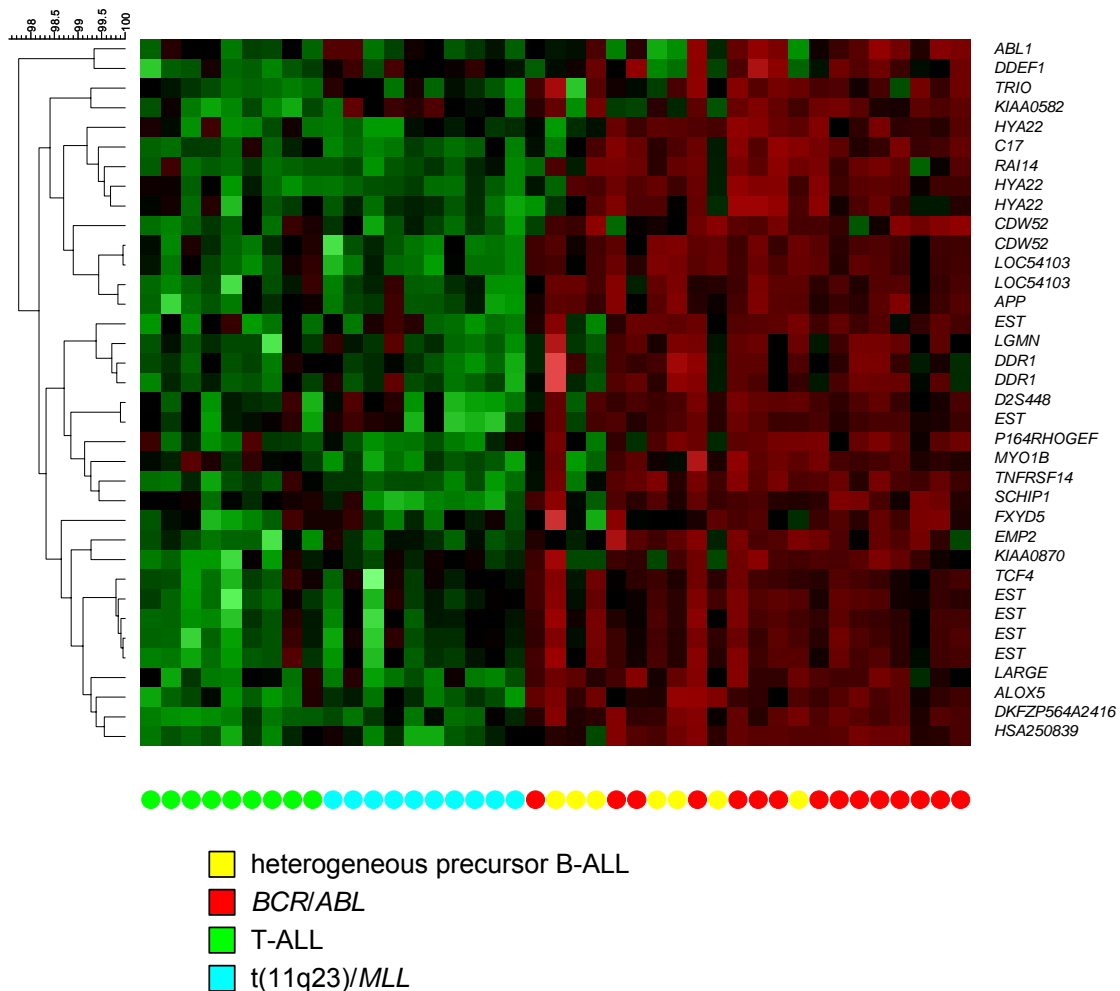


Figure 30. **Zoomed image of subtree 5 out of Figure 29.** Heterogeneous precursor B-ALL share similar expression patterns with *BCR/ABL*-positive ALLs. In this subtree, 26 probe sets were consistently overexpressed compared to both T-ALL and *t(11q23)/MLL*. The normalized expression value for each gene is coded by color. Red cells indicate high expression and green cells indicate low expression.

A similar distribution of the adult ALL samples can be observed when these cases were projected into the gene expression space of markers previously reported from Yeoh et al. to discriminate six distinct pediatric ALL subtypes, i.e., T-ALL, *E2A/PBX1*, *BCR/ABL*, *TEL/AML1*, *t(11q23)/MLL*, and hyperdiploid leukemias (Yeoh et al., 2002). As anticipated, genetically heterogeneous precursor B-ALL samples again cluster together with *BCR/ABL* cases confirming the previous observation. They do not show up as an independent fourth distinct cluster separated from adult T-ALL, *t(11q23)/MLL*, and *BCR/ABL*-positive leukemias. Figure 31 visualizes the observed dendrogram structure of a hierarchical cluster analysis as well as a three-dimensional plot from a PCA. Thus, signatures, previously reported to correlate with *E2A/PBX1*, *TEL/AML1*, and hyperdiploid childhood leukemias could not separate these two groups. This is not unexpected as none of the heterogeneous precursor B-ALL showed one of these genetic characteristics.

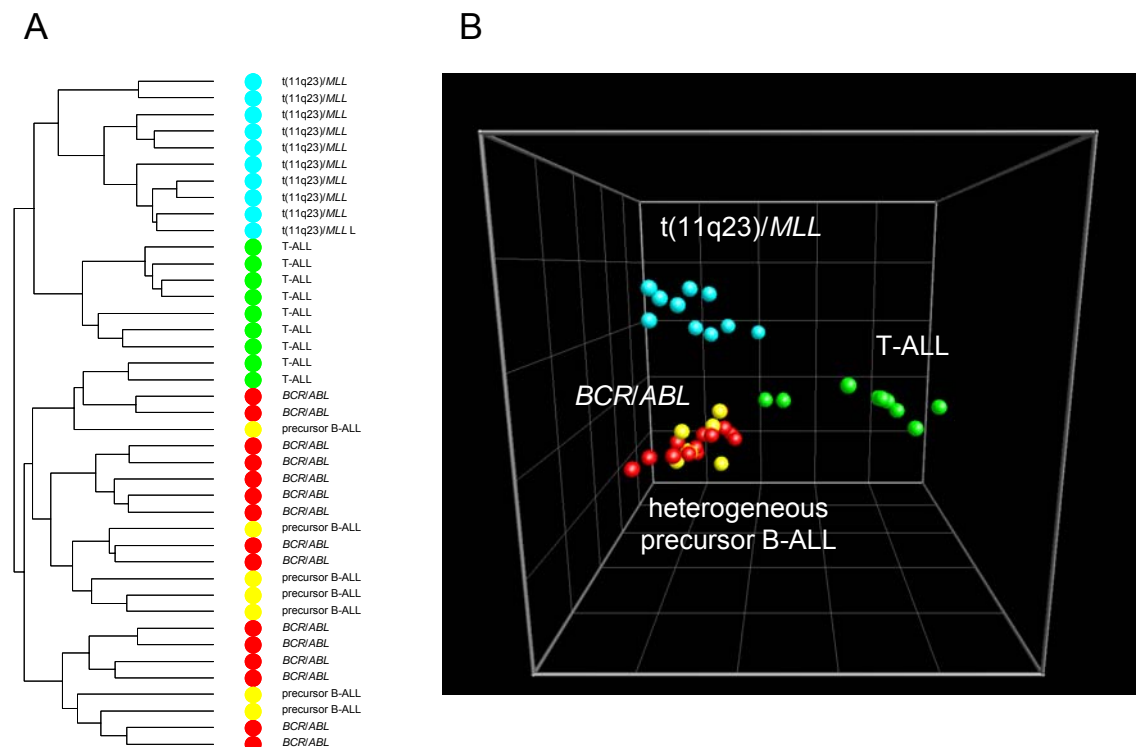


Figure 31. Heterogeneous precursor B-ALL in the context of pediatric markers. The analyses are based on reported differentially expressed genes to distinguish pediatric T-ALL, *E2A/PBX1*, *BCR/ABL*, *TEL/AML1*, *t(11q23)/MLL* and hyperdiploid leukemias (Yeoh et al., 2002). (A) Hierarchical clustering and (B) PCA of adult T-ALL (n=9), *t(11q23)/MLL* (n=10), *BCR/ABL* (n=15), and heterogeneous precursor B-lineage ALL (n=7) patients (U133A). Each patient sample is represented by a color-coded sphere. Heterogeneous precursor B-lineage ALL samples (yellow spheres) cluster together with *BCR/ABL*-positive samples (red spheres) when projected in this specific gene space.

4.3 Gene expression profiling in t(11q23)/*MLL* leukemias

*Distinct gene expression signatures in t(11q23)/*MLL* leukemias*

Firstly, the question was addressed whether t(11q23)/*MLL*-positive samples share also a characteristic gene expression pattern and are clearly distinct from other samples. Thus, the gene expression profiles of 73 adult t(11q23)/*MLL*-positive samples (n=25 ALL and n=48 AML with t(11q23)/*MLL*) were compared to 204 adult myeloid and 86 lymphoblastic leukemia samples with other defined genetic aberrations. In a supervised data analysis approach a robust set of differentially expressed genes was identified which accurately stratified the samples according to their underlying cytogenetic and immunophenotypic characteristics, i.e., myeloid subclasses, precursor B-lineage, or precursor T-lineage ALL. In detail, for lymphoblastic leukemias, t(11q23)/*MLL* samples (n=25) were accurately separated from precursor B-ALL cases with t(9;22) (n=42), t(8;14) (n=12), and precursor T-ALL (n=32). Figure 32A displays a PCA of the 111 ALL samples based on the differential expression of 262 genes. When projected into the expression space of these informative genes, the four distinct ALL subclasses accurately cluster together.

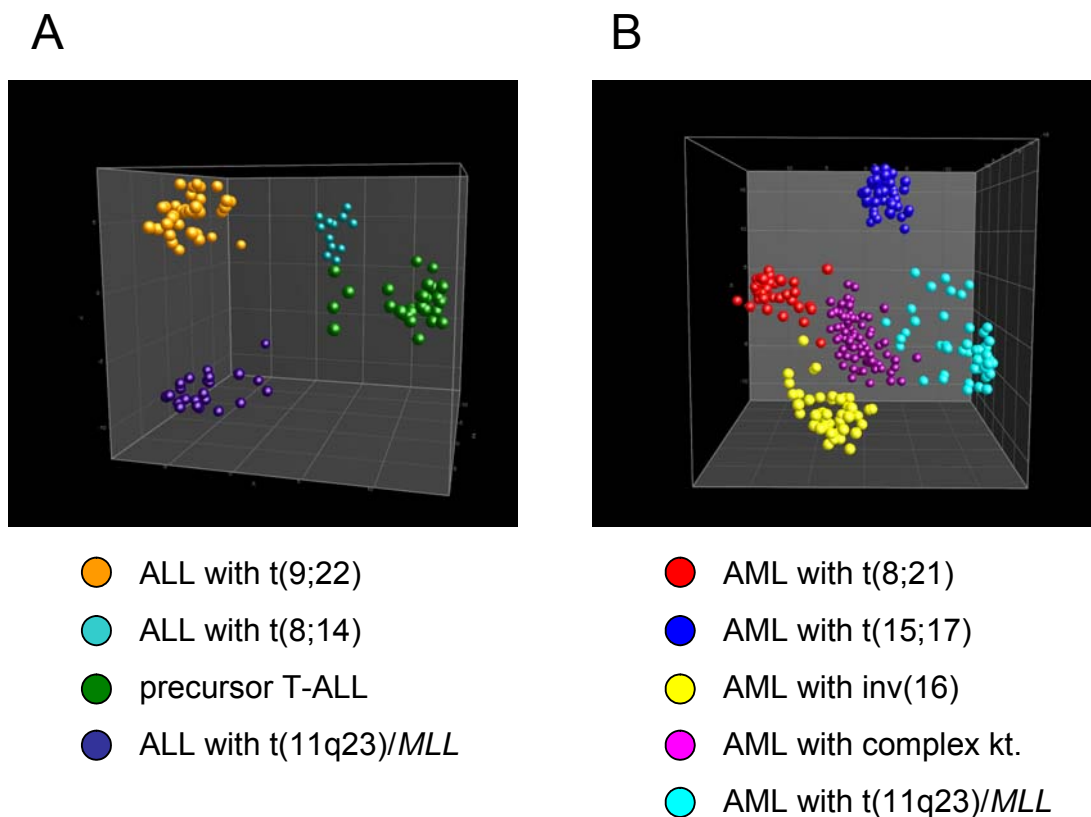


Figure 32. **PCA including various acute leukemia subtypes.** The leukemia samples are plotted in a three-dimensional space using the three components capturing most of the variance in the original data set (U133 set). (A) Adult ALL of the four subcategories precursor B-ALL samples comprising t(11q23)/*MLL* (n=25), t(9;22) (n=42), t(8;14) (n=12), and precursor T-ALL (n=32) are accurately separated based on 262 differentially expressed genes. (B) Adult AML samples including t(11q23)/*MLL* (n=48), t(8;21) (n=38), t(15;17) (n=42), inv(16) (n=49), and complex aberrant karyotypes (n=75) are accurately separated based on 416 differentially expressed genes.

Likewise, by use of the differential expression of 416 genes, the 252 AML samples could accurately be stratified. Specific patterns in gene expression were correlated with $t(11q23)/MLL$ ($n=48$), $t(8;21)$ ($n=38$), $t(15;17)$ ($n=42$), $inv(16)$ ($n=49$), and AML samples with complex aberrant karyotypes ($n=75$). This finding is also visualized by a principal component analysis (Figure 32B). Therefore, in both types of acute leukemias, $t(11q23)/MLL$ -positive samples are clearly distinct from other subtypes of same cell lineage, i.e., myeloid or lymphoblastic. They have a characteristic underlying expression signature compared to other distinct acute leukemia subclasses.

Subsequently, all samples were included into one comprehensive analysis. A supervised data analysis algorithm was applied to identify genes that separate each of the nine subtypes from the remaining classes. As shown in Figure 33, the nine distinct acute leukemia subtypes can accordingly be separated. The hierarchical clustering algorithm identified common expression signatures and orders the patient samples accurately by similarities. Interestingly, $t(11q23)/MLL$ -positive samples are not found to cluster together, but rather according to the lineage they are derived from, i.e., a lymphoblastic $t(11q23)/MLL$ cluster and a myeloid $t(11q23)/MLL$ cluster can be observed. In the top dendrogram ALL samples with $t(11q23)/MLL$ are grouped next to ALL with $t(9;22)$ and $t(8;14)$, and AML with $t(11q23)/MLL$ are grouped next to AML with $t(15;17)$ or AML with $t(8;21)$ cases.

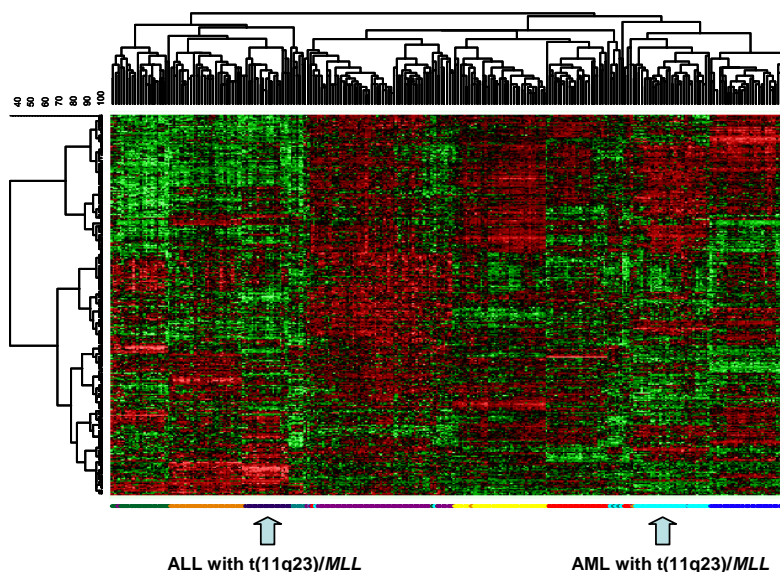


Figure 33. **Hierarchical clustering of 363 ALL and AML samples.** The normalized expression value for each gene (given in rows) is coded by color (U133 set). Red cells indicate high expression and green cells indicate low expression. The coloring is identical to Figure 32. Arrows highlight $t(11q23)/MLL$ leukemias.

Common *MLL* target genes

In order to identify common *MLL* target genes both types of $t(11q23)/MLL$ leukemias were grouped together and were compared to the various types of precursor B- and T-lineage ALLs as well as to other cytogenetically defined AML subtypes. In doing so, a set of differentially expressed genes specifically associated with $t(11q23)/MLL$ leukemias was specified. Relationships between these genes were further examined using a network analysis application. As given in Figure 34 *HOXA9* as well as *MEIS1* show up as genes with higher expression in both $t(11q23)/MLL$ leukemias. Other genes with higher expression in this network included *NICAL* and chromatin remodeling actor *RUNX2*.

Downregulated genes included for example TNF-receptor superfamily members *TNFRSF10A* and *TNFRSF10D*, or *MADH1*, functioning downstream of TGF-beta receptor serine/threonine kinases. Additional networks contain further genes with known relationship with t(11q23)/*MLL* leukemias, e.g., *HOX-A* cluster genes (*HOXA5*, *HOXA10*), as well as the Hox co-regulator *PBX3*, or the tyrosine kinase *FLT3*. Other target genes with higher expression in t(11q23)/*MLL* leukemias included *HIP1*, so far associated with prostate cancer progression, proto-oncogene *FRAT1*, *TAF1B*, playing a role in the tumorigenesis of colorectal carcinomas, and *ZFH1B*, a transcriptional corepressor.

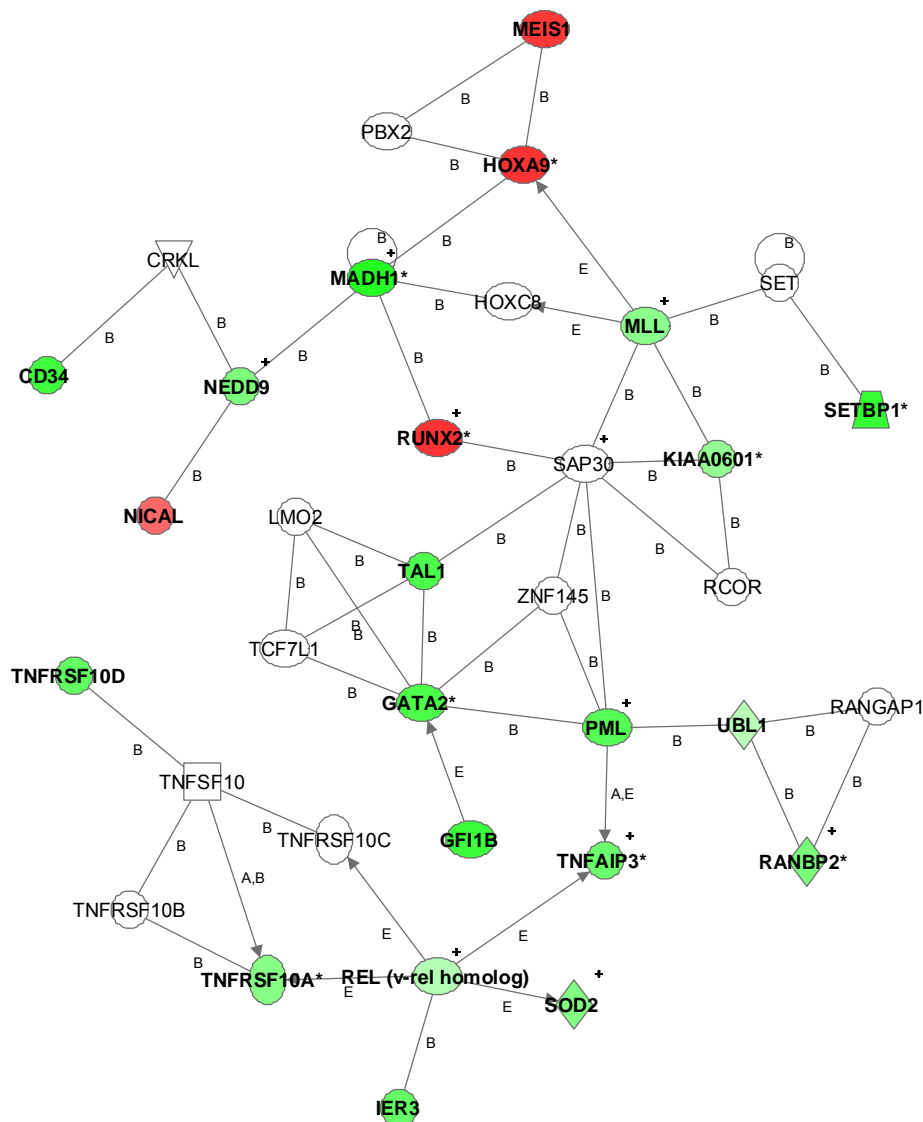


Figure 34. **Network distinguishing t(11q23)/*MLL* leukemias from other acute leukemia subtypes.** The network with a score of 18 is graphically displayed with genes/gene products as nodes and the biological relationship between the nodes as edges. The intensity of the node color indicates the degree of differential gene expression. Green intensities correspond to a lower expression (downregulated) in t(11q23)/*MLL* cases compared to AML subtypes (inv(16), t(8;21), t(15;17), complex karyotypes) or ALL subtypes (t(9;22), t(8;14), T-ALL), respectively. Red intensities correspond to a higher expression in t(11q23)/*MLL* cases (upregulated).

Unsupervised hierarchical clustering of t(11q23)/MLL leukemias

Next, the question was addressed whether an unsupervised analysis including exclusively *MLL* gene rearranged leukemias was also able to distinguish between the different lineages. Both a PCA and a two-dimensional hierarchical cluster analysis of 25 ALL and 48 AML with *MLL* gene translocation were performed. As demonstrated in Figure 35, although both types of acute leukemias are characterized by *MLL* gene rearrangements, an unsupervised data analysis approach clearly separates the samples according to their hematopoietic lineage, i.e., myeloid or lymphoblastic origin.

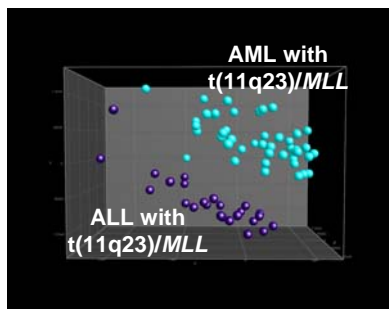


Figure 35. **Unsupervised PCA of adult ALL and AML with t(11q23)/MLL.** An unsupervised analysis is based on a selection of 5,000 genes that showed the largest variance across all samples (U133 set). In the three-dimensional PCA plot ALL with t(11q23)/MLL samples (labeled mauve) are distinct from AML with t(11q23)/MLL (turquoise).

Moreover, given the dendrogram from the unsupervised hierarchical cluster analysis no clear subclustering of cases with identical *MLL* partner genes can be observed (Figure 36). In ALL with t(11q23)/MLL the *MLL/ENL* cases intercalate with the *MLL/AF4* samples. In AML with t(11q23)/MLL no obvious structure, neither according to FAB criteria, nor to the different *MLL* partner genes can be observed. The *MLL/AF6*, *MLL/AF10*, *MLL/ELL* samples, as well as rare cases (*MLL/p300*, *MLL/AF17*, *MLL/SMAP1*, and *MLL/X*) are intercalated between the *MLL/AF9* samples. Thus, two independent unsupervised algorithms consistently separate *MLL* gene rearranged leukemias into ALL and AML subgroups, but not with respect to the partner genes.

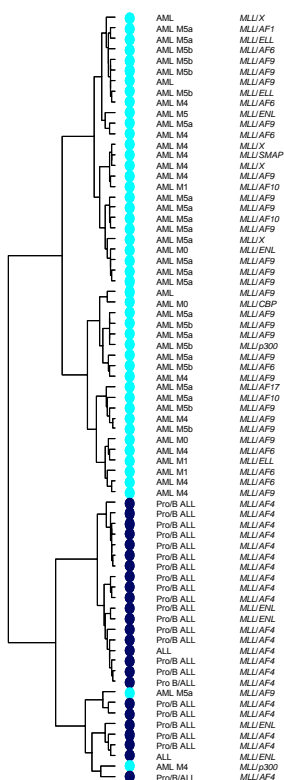


Figure 36. **Unsupervised hierarchical clustering of adult ALL and AML with t(11q23)/MLL.** The similarity dendrogram of an unsupervised hierarchical cluster analysis is based on a selection of 5,000 genes that showed the largest variance across all samples (U133 set). For each sample the respective immunophenotype, FAB subtype, and *MLL* fusion partner gene as confirmed by FISH and/or RT-PCR-based molecular analyses is given. *MLL/X* indicates samples with unknown partner genes. Two of the 48 *MLL* gene rearranged AML are contained in the ALL branch of the dendrogram.

Supervised analysis to discriminate t(11q23)/MLL leukemias

Next, gene expression signatures of ALL with t(11q23)/MLL were directly compared to AML with t(11q23)/MLL using a supervised algorithm. Among the differentially expressed genes, upregulated candidates in lymphoblastic t(11q23)/MLL leukemias demonstrated a dominant pattern according to B-lineage commitment. *PAX5*, the B cell lineage specific activator was designated as one of the top-ranked differentially expressed genes. In line with this finding, *PAX5* target genes *BLK* and *CD19* could also be confirmed upregulated in ALL with t(11q23)/MLL by microarray analysis. An upregulated expression of *IGHM* (encoding the IgM heavy chain), *VPREB1* (surrogate light-chain, important for forming the pre-B cell receptor), and *CD22* or *CD79A* further elucidates the B-lineage commitment of ALL with t(11q23)/MLL.

In addition, the list of differentially expressed genes was also imputed into a pathway analysis application. Various networks of functionally related genes were obtained. In Figure 37, a biological network is represented. In this network, *LEF1*, a transcriptional regulator is connected to *PAX5* and its target *CD79A*, which is included in the B cell antigen receptor. These genes, as well as the transcriptional regulators *MEF2A* and *TCF3* demonstrated a higher expression in ALL with t(11q23)/MLL profiles compared to AML with t(11q23)/MLL cases. In other networks, further interesting differentially expressed genes with higher expression in t(11q23)/MLL-positive ALL include *BCL11A*, also involved in lymphoid malignancies, transcription regulator *ETS2*, chromatin binding proteins *CBX2* and *CBX4*, and early B cell factor *EBF*, who can restrict lymphopoiesis to the B cell lineage and works in concert with *PAX5* to activate genes required for B cell differentiation.

Reversely, genes with higher expression in t(11q23)/MLL-positive AML included the transcriptional activator *CEBPB*, protein tyrosine kinase *KIT*, *MADH2*, a transcription factor binding protein and *MITF*, a transcriptional regulator (Figure 37). Also, as obtained in additional networks a myeloid commitment through higher expression in AML with t(11q23)/MLL could be demonstrated by differential expression of *CEBPA* (CCAAT/enhancer binding protein-alpha), a transcription factor required for differentiation of myeloid progenitors, as well as *SPI1* (*PU.1*), a critical player in myeloid development, or *GM-CSFR*, and *G-CSFR* genes. Other candidates with significantly higher expression in t(11q23)/MLL-positive AML are *FES*, a tyrosine kinase oncogene, *MNDA*, encoding the myeloid cell nuclear differentiation antigen, or *CITED4*, a CBP/p300-interacting transcriptional transactivator. Also, a different repertoire of expression of suppressors of cytokine signaling (SOCS) family members as well as members of the tumor necrosis factor superfamily could be observed.

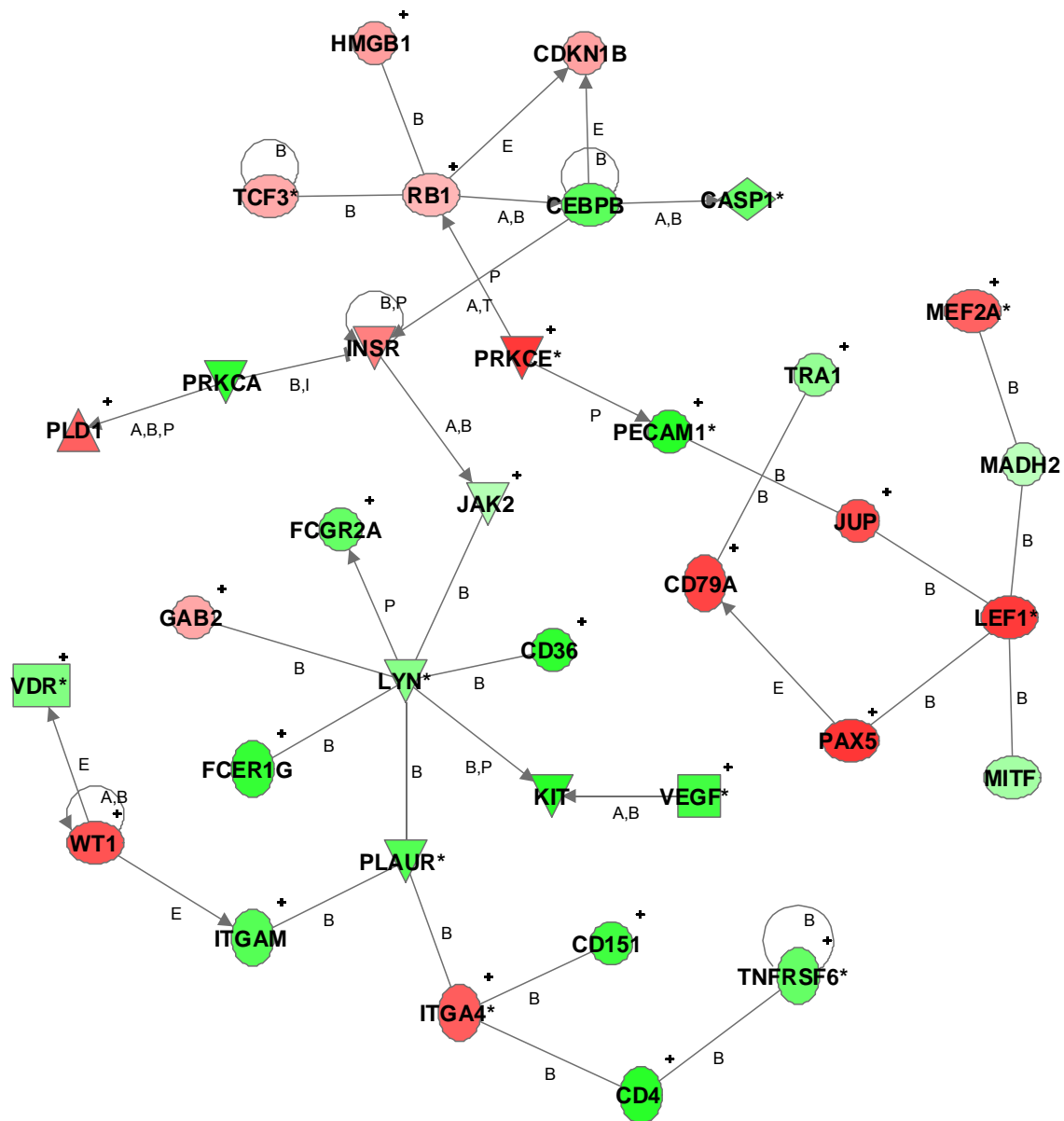


Figure 37. **Differentially expressed genes between ALL and AML with t(11q23)/MLL.** The biological network with a score of 42 is displayed graphically. Green intensities correspond to a lower expression in ALL with t(11q23)/MLL cases compared to AML with t(11q23)/MLL samples (downregulated). Red intensities correspond to a higher expression in ALL with t(11q23)/MLL cases compared to AML with t(11q23)/MLL samples (upregulated).

Influence of MLL translocation partners on gene expression signatures

A following series of analyses was performed to investigate the influence of different *MLL* gene translocation partners. Firstly, within the cohort of AML with *t(11q23)/MLL*, the group of *t(9;11)*-positive cases ($n=23$) was compared to *t(9;11)*-negative samples ($n=25$). Neither supervised nor unsupervised analyses revealed a specific expression signature associated with the *MLL* translocation partner *AF9*. In Figure 38 SAM plots demonstrate that, compared to the previous analysis of ALL with *t(11q23)/MLL* vs. AML with *t(11q23)/MLL*, no significantly differentially expressed genes clearly correlate with *t(9;11)* (left plot). The *q*-values of the top differentially expressed genes ranged between 0.75 and 0.82, i.e., calling this set of genes significant would result in a false discovery rate (FDR) of $>75\%$. For comparison, a very high number of differentially expressed genes can be identified when comparing ALL with *t(11q23)/MLL* vs. AML with *t(11q23)/MLL* (right plot).

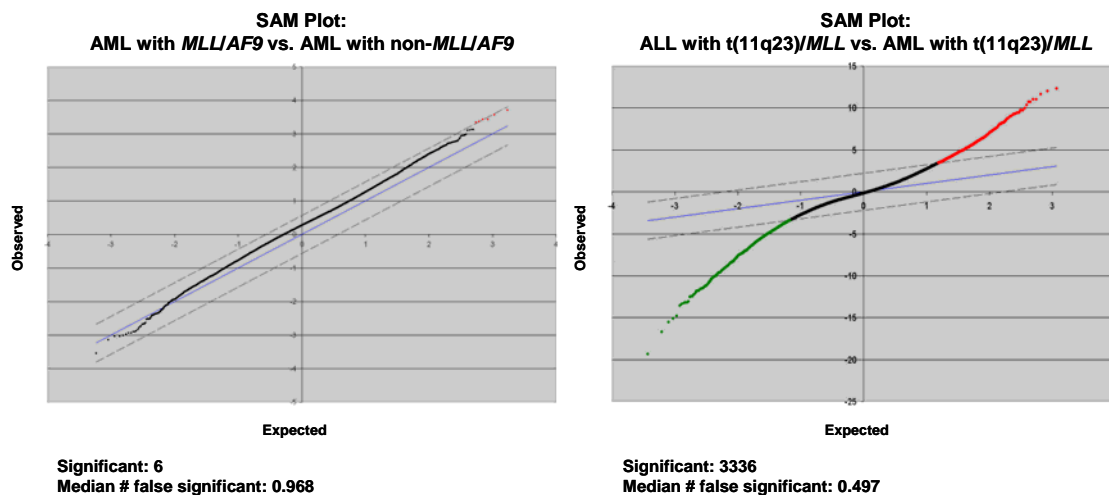
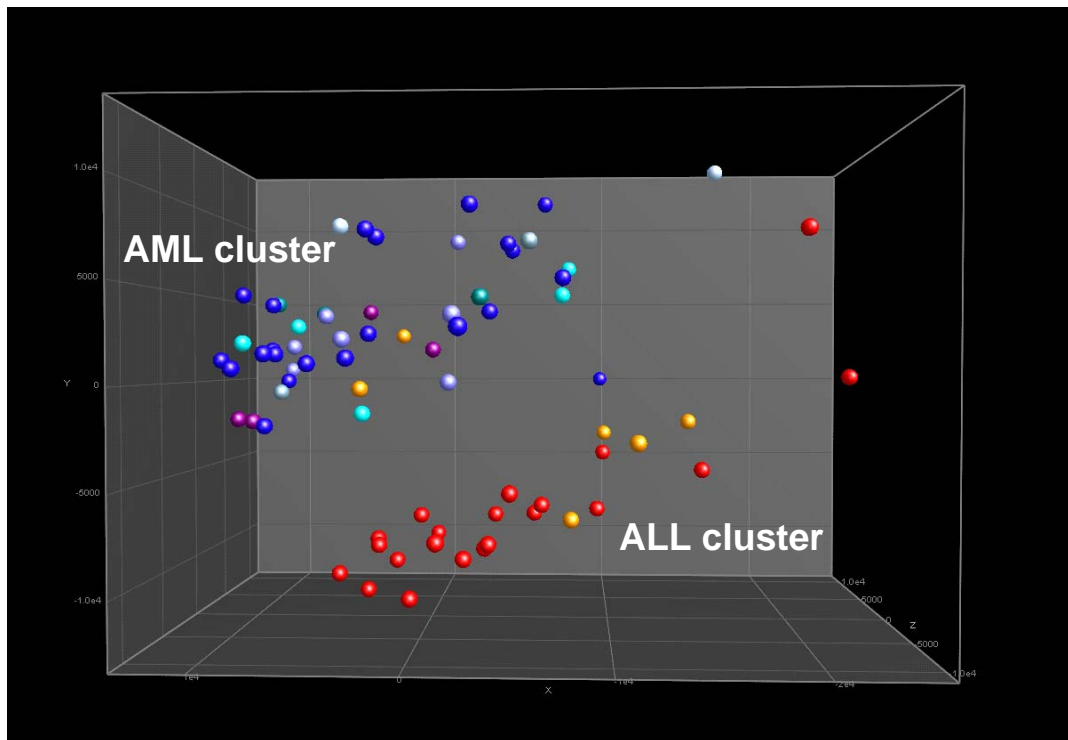


Figure 38. **Supervised identification of differentially expressed genes in *t(11q23)/MLL* leukemias.** The left plot shows a supervised analysis of AML samples comparing a group of *t(9;11)*-positive cases ($n=23$) to non-*t(9;11)*-positive samples ($n=25$) (U133 set). Here, no statistically significant differentially expressed genes were identified. The right plot shows a supervised comparison of ALL with *t(11q23)/MLL* vs. AML with *t(11q23)/MLL*. Red dots indicate genes with statistically significant higher expression in AML with *t(11q23)/MLL* and green dots indicate higher expressed genes in ALL with *t(11q23)/MLL*.

Furthermore, as demonstrated in Figure 39, the unsupervised data analysis approach including all *t(11q23)/MLL* samples did also not reveal any specific patterns associated with distinct *MLL* partner genes. It is interesting to note that *MLL/ENL* samples, included both in the AML and ALL patient cohorts are separated. Four ALL cases with *MLL/ENL* intercalate with the *MLL/AF4* samples, two AML with *MLL/ENL* samples are distributed between the various cases in the AML cluster.



- | | |
|----------------------------|-----------------------------|
| ● ALL with <i>MLL/AF4</i> | ● AML with <i>MLL/ENL</i> |
| ● ALL with <i>MLL/ENL</i> | ● AML with <i>MLL/p300</i> |
| ● AML with <i>MLL/AF10</i> | ● AML with <i>MLL/SMAP1</i> |
| ● AML with <i>MLL/AF6</i> | ● AML with <i>MLL/CBP</i> |
| ● AML with <i>MLL/AF9</i> | ● AML with <i>MLL/X</i> |
| ● AML with <i>MLL/AF17</i> | ● AML with <i>MLL/ELL</i> |

Figure 39. **Unsupervised analysis of t(11q23)/*MLL* samples with various partner genes.** The unsupervised analysis is based on 5,000 genes that showed the largest variance across all samples (U133 set). For each sample the *MLL* fusion partner gene as confirmed by FISH and/or RT-PCR-based molecular analyses is given. *MLL/X* indicates samples with unknown partner genes.

A more detailed analysis then aimed at mining the data supervised for differential gene expression between various *MLL* partner genes. Here, six groups of t(11q23)/*MLL* patient samples were included: 23 AML cases with t(9;11) (*MLL/AF9*), 7 t(6;11) (*MLL/AF6*), 4 t(10;11) (*MLL/AF10*), and 3 t(11;19) (*MLL/ELL*) cases, as well as 21 ALL samples with t(4;11) (*MLL/AF4*) and 4 t(11;19) (*MLL/ENL*). In this data set no statistically significant expression signatures were found to be specifically correlated with one of the distinct partner genes. Table 5 represents a confusion matrix of t(11q23) leukemia subgroup predictions based on the top 100 genes that demonstrate differential expression between the respective subclasses (10-fold CV approach). It can be

observed that the classifier is good at predicting the *MLL* partner genes *AF9* and *AF4*, the two major groups in the AML and ALL patient cohorts, respectively. Other partner genes are not accurately identified. The misclassifications mainly occur in the corresponding myeloid or lymphoblastic compartment. Thus, there is only a strong correlation with the lineage the *t(11q23)/MLL* leukemias are derived from. The gene expression profile does not support the hypothesis of a clear distinct signature associated with one of the various partner genes that can interact with the *MLL* gene.

Table 5. ***MLL* partner gene confusion matrix determined by 10-fold CV.** The matrix shows the predicted *MLL* fusion partner gene. Misclassified samples are given by bold red letters. For example, of 21 *MLL/AF4* samples, 20 are accurately identified and one sample is classified as *MLL/ENL*. Likewise, *MLL/AF10* or *MLL/AF6* samples are classified as *MLL/AF9* samples.

		real					
		<i>MLL/AF10</i>	<i>MLL/AF6</i>	<i>MLL/AF9</i>	<i>MLL/ELL</i>	<i>MLL/AF4</i>	<i>MLL/ENL</i>
predicted	<i>MLL/AF10</i>			1			
	<i>MLL/AF6</i>			1	1		
	<i>MLL/AF9</i>	4	7	20	2		
	<i>MLL/ELL</i>						
	<i>MLL/AF4</i>			1		20	4
	<i>MLL/ENL</i>					1	

In order to assess the robustness of partner gene prediction a resampling approach was applied, i.e., the complete SVM classification procedure was repeated for 100 times. The training set included 2/3 of patients and the test set 1/3. Here, the test set for each of the 100 runs included 20 samples which were randomly chosen from the total patient cohort to include 1 *MLL/AF10*, 2 *MLL/AF6*, 8 *MLL/AF9*, 1 *MLL/ELL*, 7 *MLL/AF4*, and 1 *MLL/ENL* sample. Given the differential gene expression mainly the *MLL* partner genes *AF9* and *AF4*, dominating the patient cohort, are given correct class labels by the classification algorithm (Table 6).

Table 6. ***MLL* partner gene confusion matrix determined by resampling.** The matrix shows the predicted *MLL* fusion partner gene as determined after 100 runs of SVM-based classifications. Misclassified samples are given by bold red letters. Average numbers of predictions per run are given. For example, 7 *MLL/AF4* samples have been predicted by the algorithm 700 times (each sample 100 times). Of the 700 predictions the class label *MLL/AF4* has been given correctly 659 times, i.e., on average 6.59 per run. In 9 individual predictions, a *MLL/AF4* sample has been predicted as *MLL/AF9*, in 1 prediction as *MLL/ELL*, and in 31 predictions as *MLL/ENL*, respectively.

		real					
		<i>MLL/AF10</i>	<i>MLL/AF6</i>	<i>MLL/AF9</i>	<i>MLL/ELL</i>	<i>MLL/AF4</i>	<i>MLL/ENL</i>
predicted	<i>MLL/AF10</i>	0.05		0.27			
	<i>MLL/AF6</i>		0.44	0.47	0.2		
	<i>MLL/AF9</i>	0.95	1.55	7.09	0.8	0.09	
	<i>MLL/ELL</i>			0.1		0.01	
	<i>MLL/AF4</i>		0.01	0.07		6.59	0.84
	<i>MLL/ENL</i>					0.31	0.16

4.4 Gene expression profiling as potential diagnostic method

Pattern Robustness

The robustness of diagnostic gene expression patterns was approached by visualizing gene signatures according to various parameters. Samples from 240 untreated adult leukemia patients at diagnosis were analyzed. The diagnostic subclasses can be categorized as follows: AML with t(15;17) (n=42), t(8;21) (n=40), inv(16) (n=49), t(11q23)/*MLL* (n=51), inv(3) (n=22), as well as CML (n=36).

Firstly, an analysis included AML cases with t(15;17), t(8;21), inv(16), and t(11q23)/*MLL*. Six different parameters were analyzed and for each condition, the total group of 182 patient profiles was splitted into an ideal group and a non-ideal group using the following criteria: (A) Duration of sample shipment: Samples with shipment time of ≤ 24 h were grouped as ideal cohort. Non-ideal patients had a shipment time of >24 h (up to four days). (B) 3'/5' ratio of *GAPD* hybridization signals: Samples with a 3'/5' ratio of the *GAPD* gene ≤ 3.0 were grouped as ideal cohort. In non-ideal patients the 3'/5' ratio was >3.0 (up to 10.3). (C) Duration of sample storage time until microarray target preparation: Samples with <2.5 years storage time of the frozen cell lysate at -80°C since the individual time point of diagnosis were grouped as ideal cohort. Samples that were frozen for ≥ 2.5 years (up to 4.5 years) were designated as non-ideal cohort. (D) Date of sample target preparation: This work was conducted between June 2001 and February 2004. In order to monitor differences in the process that might be related to target preparation, array lots, and technical equipment, samples that were prepared within the first 2/3 of the study were arbitrarily grouped as "ideal" cohort. Expression profiles that were generated in the last third of the study were grouped as "non-ideal" cohort. (E) Type of specimen: The ideal cohort included gene expression profiles from bone marrow specimens. Peripheral blood samples were considered as non-ideal cohort. (F) Age of the leukemia patient at diagnosis: With respect to stratifying the patients into two age groups current therapy protocols were followed which apply different treatment approaches in younger and elderly patients (Schoch et al., 2004a). Accordingly, the "ideal" cohort included patients <60 years. Patients ≥ 60 years were grouped as "non-ideal" cohort.

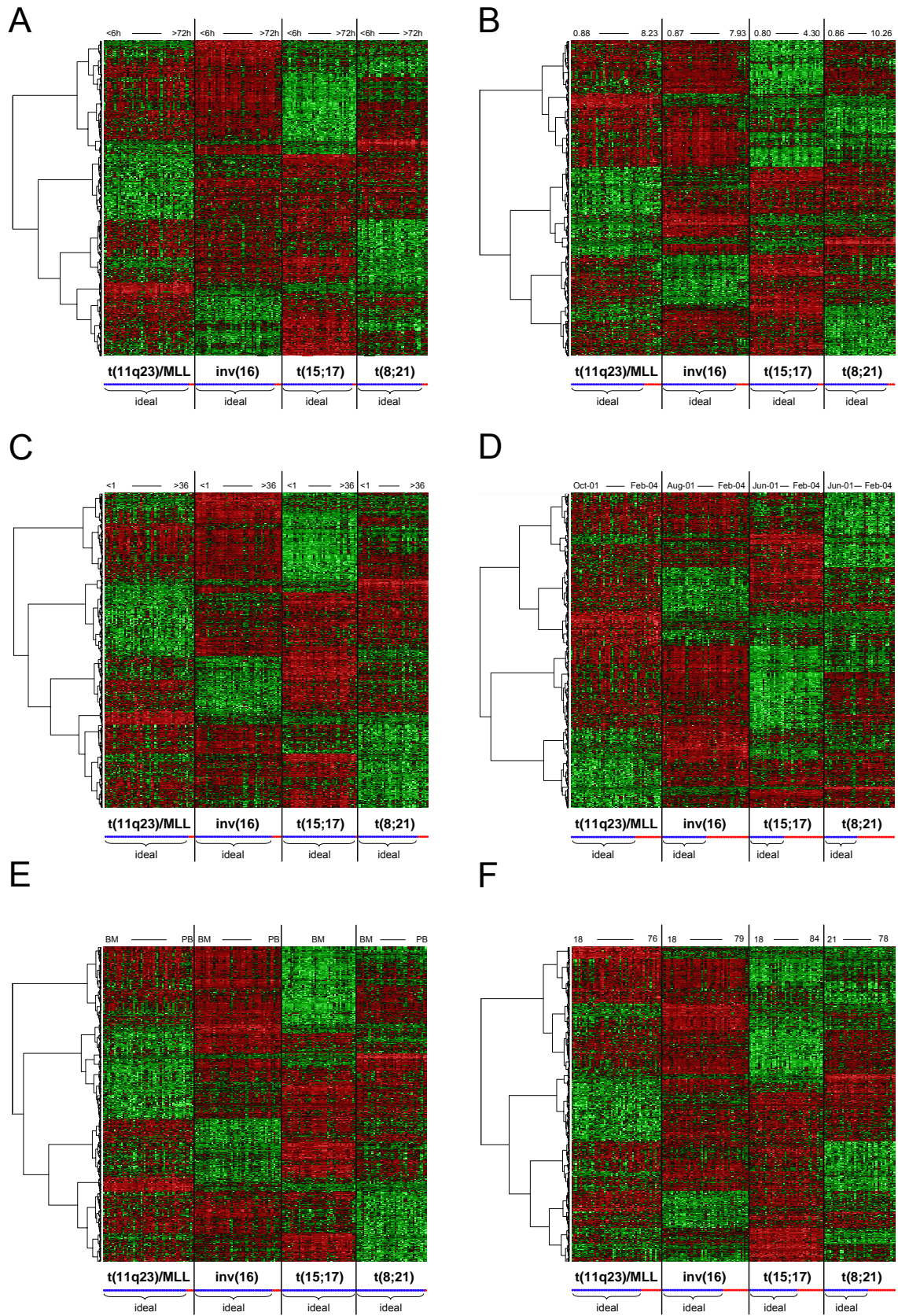
As demonstrated in Table 7 gene sets identified from ideal cohorts also accurately classify patients from non-ideal cohorts. Each ideal group was split into a training set and a test set. Then, each training set was used to perform the gene selection (top 200 genes for each subtype) and training of the classification engine for each of the parameters, and the test set was used to assess the predictive power of the diagnostic signature, respectively. Then, the six SVM models (referring to parameters A through F), were also tested on the non-ideal group for their prediction accuracy. Thus, the respective signatures indeed were robust. The table represents a prediction matrix of AML subtypes based on their gene expression signatures of an ideal patient cohort using a 10-fold CV (left column) and resampling approach (middle column), as well as the predictions of the non-ideal cohort (right column).

Table 7. **Classification accuracies for various parameters.** Distribution of the different ideal cohorts and non-ideal cohorts for the total group of 182 profiles of AML patients with t(15;17), t(8;21), inv(16), and t(11q23)/MLL. In the ideal cohort, the percentage of the classification accuracy is given by 10-fold CV and median accuracy and 95% confidence interval for the resampling analysis. In the non-ideal cohort the subtype prediction of the samples is given after using a classification engine which was trained on the profiles from each ideal cohort. Individual numbers of patients for each cohort are given in parentheses.

	<i>parameter</i>	ideal cohort		non-ideal cohort
		<i>10-fold CV accuracy</i>	<i>resampling accuracy</i>	<i>prediction</i>
A	shipment time	98% (166/170)	98% [96%; 100%]	100%(12/12)
B	<i>GAPD</i> 3'/5' ratio	99% (157/158)	100% [98%; 100%]	96% (23/24)
C	storage time	98% (161/165)	98% [95%; 100%]	100% (17/17)
D	preparation period	99% (99/100)	100% [94%; 100%]	99% (81/82)
E	specimen type	99% (171/172)	100% [97%; 100%]	100% (10/10)
F	age of the patient	99% (124/125)	100% [95%; 100%]	100% (57/57)

These results can also be visualized in the gene expression clustering (Figure 40A through F). No glaring changes occurred for the various conditions when a significant set of differentially expressed genes was used. The hierarchical cluster dendrograms group significant genes of the diagnostic signatures that were identified in the corresponding ideal patient cohorts. In all samples, both from ideal and non-ideal cohorts, AML subtypes with recurrent chromosomal aberrations showed homogeneous signatures for each parameter, which enabled an accurate prediction of the respective leukemia subtype.

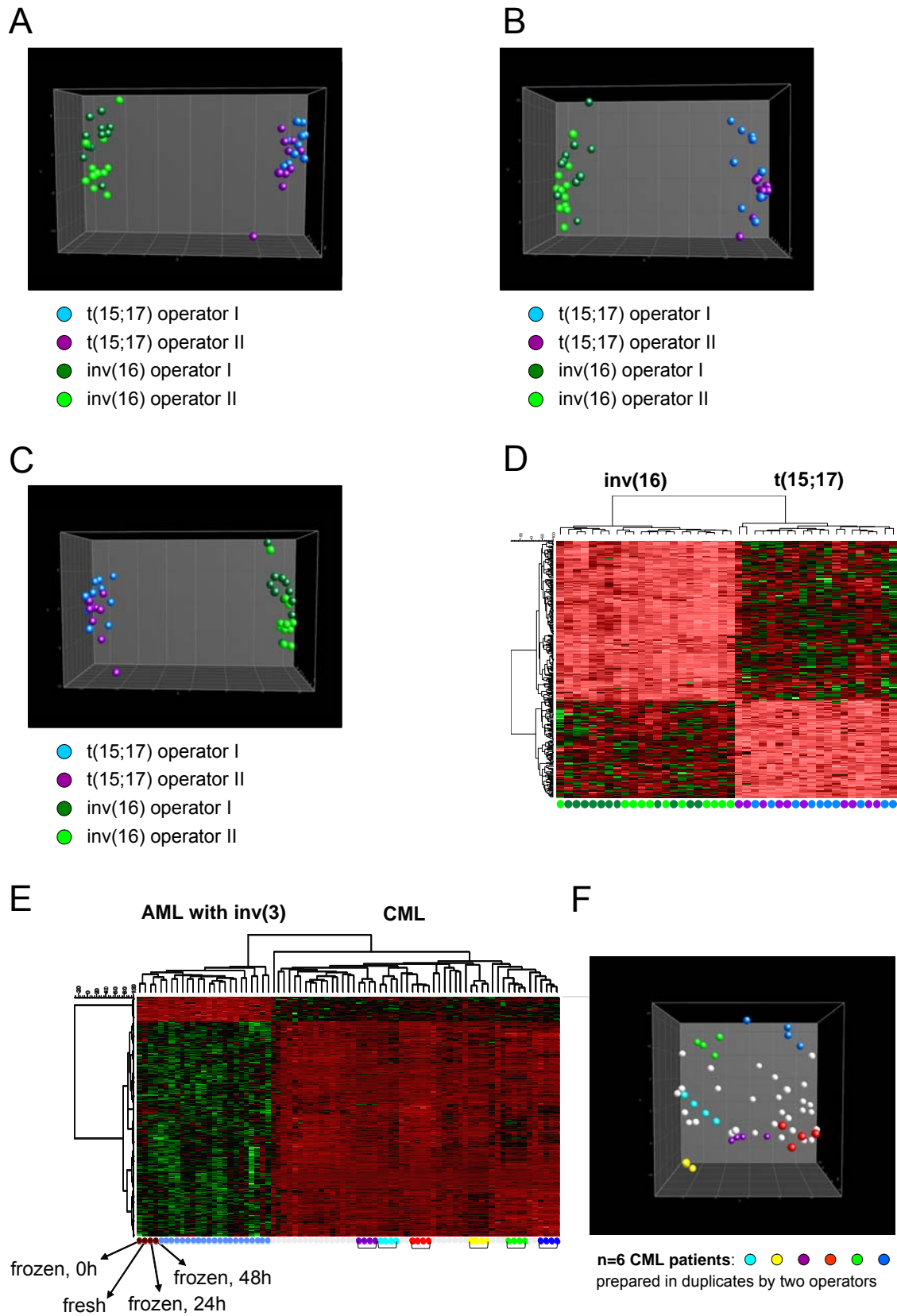
Figure 40. **Pattern robustness in AML with recurrent chromosomal aberrations.** Hierarchical cluster analyses of adult AML samples with recurrent chromosomal aberrations. The analyses visualize six different subsets of probe sets which were identified to be differentially expressed when analyzing AML samples with t(15;17), t(8;21), inv(16), and t(11q23)/MLL. For parameter (A) through (F) the total group of 182 patient profiles was splitted into respective ideal cohorts, used to identify the differentially expressed genes, and non-ideal cohorts. Only the genes (rows) were clustered by the algorithm. For each AML subtype, the samples (columns) are given in ascending order according to the various parameters: (A) Duration of sample shipment, (B) 3'/5' ratio of *GAPD* signals, (C) duration of sample storage time until microarray target preparation, (D) date of sample target preparation within our study, (E) type of specimen, and (F) age of the leukemia patient at diagnosis. The normalized expression value for each gene is coded by color (standard deviation from mean). Red cells indicate high expression and green cells indicate low expression.



Within a larger gene expression profiling study, the handling of the samples, e.g., freezing of cell preparations vs. freshly prepared samples, and storage time of the samples at -80°C may vary. Also, differences between operators for sample target preparation and microarray washing and scanning procedures might represent interfering factors. As given in detail in Figure 41 some of the samples had been transferred to another laboratory in order to assess the influence of sample preparation operators. A different operator prepared the samples according to the recommended protocol and subsequently measured the gene expression profile. Firstly, two different patient cohorts were analyzed, i.e., AML with $t(15;17)$ and $inv(16)$. Differentially expressed genes between these two entities were identified based on the expression profiles according to the preparation of operator 1, operator 2, or including all samples from both operators, respectively (Figure 41A,B,C,D). No influence on the robustness of the signature is seen. Moreover, also expression profiles generated from a freshly prepared sample vs. samples which had been frozen as cell lysates for several days at -80°C were analyzed. Figure 41E shows that the different storage times also had no impact on the diagnostic signature.

This analysis did also include sample preparations at three different time points from one patient with AML and $inv(3)$, i.e., an immediate target preparation after the sample was obtained, and preparations after 24h and 48h storage of the sample at room temperature, respectively. A final step focused on an analysis of six CML samples which had been prepared in duplicates by the two operators working in different laboratories. As demonstrated in Figures 41E,F for each sample the four individual profiles, two for each operator, cluster near to each other indicating the robustness of the sample preparation protocol, microarray platform, and resulting gene expression signature.

Figure 41. **Analysis of varying sample handling and operator parameters.** Two different operators prepared samples of AML patients with $t(15;17)$ and $inv(16)$. Principal component analyses (PCA) visualize the separation of AML with $t(15;17)$ and $inv(16)$ using (A) the top 300 probe sets from the data set generated by operator 1, or (B) the top 300 probe sets from the data set generated by operator 2. In the three-dimensional PCA plot, data points with similar characteristics will cluster together. Each patient's expression pattern is represented by a single color-coded sphere. The labels and coloring of the classes were added after the analysis for means for better visualization. (C) PCA based on the top 300 probe sets from a combined data set containing the matrices of both operators. (D) Hierarchical clustering based on the top 300 probe sets from a combined data set containing the matrices of both operators. (E) Differentially expressed genes between AML with $inv(3)$ and CML. This analysis includes freshly prepared versus frozen AML with $inv(3)$ samples. The frozen samples had been prepared after various storage times at room temperature. (F) Visualization of the CML samples from the previous analysis by PCA. Six patient samples were prepared in replicates by two different operators in different laboratories.



Correlation of microarray analysis and cytomorphology

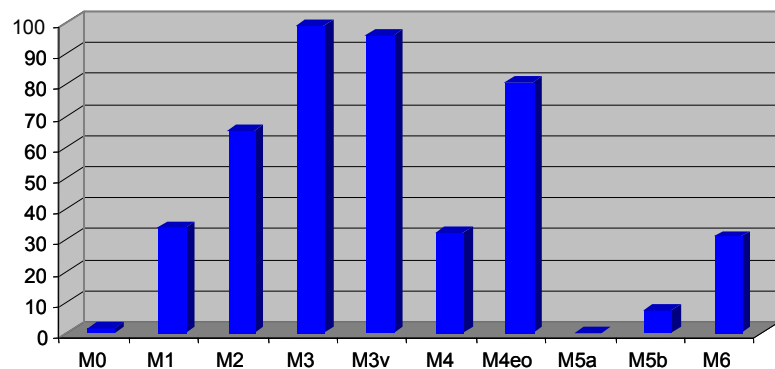
In order to assess the correlation of the microarray technology with a current diagnostic method a cohort of 130 patients representing different FAB subtypes was included in this analysis. All cases were characterized by cytomorphology and cytogenetics. As shown in Figure 42 the percentage of myeloperoxidase positive cells as measured by cytochemistry highly correlates to *MPO* microarray signal intensities across the different FAB subtypes (Spearman rank correlation $r=0.803$; $p < 0.001$).

Cytochemistry

MPO

mean positivity (%)

n=130



Microarray

MPO

mean signal intensity

n=130

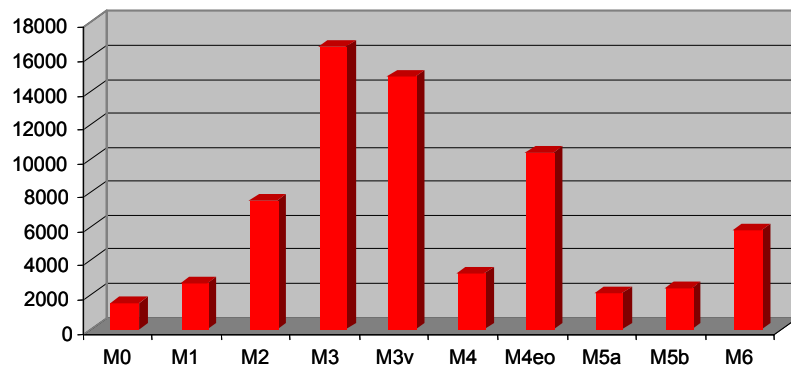


Figure 42. **Concordance between cytochemistry and gene expression.** In 130 AML samples the percentage of myeloperoxidase positive cells as determined by standard cytochemistry on bone marrow smears in different FAB subtypes is shown. The following FAB subtypes were evaluated: M0 (n=8), M1 (n=23), M2 (n=28), M3 (n=10), M3v (n=9), M4 (n=13), M4eo (n=11), M5a (n=10), M5b (n=12), and M6 (n=6). The same patients were also analyzed using U133A microarrays. The mean signal intensity for the *MPO* (myeloperoxidase) gene is given for the different FAB subtypes.

Correlation of microarray analysis and flow cytometry

For comparison of methods, flow cytometry and microarray analyses were performed in parallel in 113 patients with newly diagnosed AML, ALL, and 4 normal bone marrow samples from healthy donors (Table 8). Protein expression levels of 39 relevant antigens were correlated with the mRNA abundance of the corresponding probes represented on the microarray.

Table 8. Patients for comparison of flow cytometry and microarray analyses.

Parameter	Number of samples
AML (total)	85
t(8;21)	5
t(15;17)	5
inv(16)	4
trisomy 8	2
normal karyotype	54
complex aberrant karyotype	11
other abnormalities	4
ALL (total)	28
t(9;22)	14
other precursor B-ALL	9
precursor T-ALL	5
Normal bone marrow	4
Percentage of blasts in bone marrow samples	
median, range	90%, 10-100%

Firstly, the 2,187 comparisons of individual expression data obtained by both methods were analyzed with regard to positivity. As demonstrated in Table 9, of these comparisons, 1,512 (69.1%) revealed congruent results for positivity of protein expression and mRNA abundance (881 cases (40.3%) with positive expression and 631 cases (28.9%) with negative expression, respectively). In 509 comparisons (23.3%) microarray analysis detected positivity for mRNA expression (call: present) while the results of flow cytometry indicated negativity. In 166 cases (7.6%) protein expression was demonstrated by flow cytometry while no mRNA expression was detected by microarray analysis (call: absent).

Next, the degree of correlation between protein expression and mRNA abundance within specific leukemia subtypes, i.e., AML, precursor B-ALL, and precursor T-ALL, was determined. Thus, a first analysis focused on the genes most specific for the diagnosis of AML. In the AML cases a high correlation between protein expression and mRNA abundance was observed (Table 10).

In detail, the congruence assessed was 76% for MPO, 88% for CD13, and 76% for CD33. However, these three genes were rated positive by microarray analysis and negative by flow cytometry in 24%, 10%, and 2%, respectively. In only 1%, 2%, and 12%, respectively, MPO, CD13, and CD33 were rated positive by flow cytometry and negative by microarray analysis. Furthermore, the data are similar for most other AML-specific antigens and for the antigens necessary to subclassify AML. Thus, the percentages of congruent cases, microarray analysis positive and flow cytometry negative cases, and flow cytometry positive and microarray analysis negative cases are 75%, 23%, and

2% for CD117; 59%, 41%, and 0% for CD11b; 80%, 17%, and 3% for CD133; 65%, 35%, and 0% for CD14; 56%, 42%, and 2% for CD15; 46%, 51%, and 3% for CD235a; and 67%, 33%, and 0% for CD36.

With respect to precursor B-ALL the overall percentage of congruent cases was 69.8% (Table 11). It was even higher for the antigens most relevant for establishing the diagnosis and for subclassification of ALL. In detail the congruence assessed was 89% for CD22, 75% for CD79A, 100% for CD19, 83% for CD10, and 86% for TdT.

Similar data were obtained for precursor T-ALL, although the total number of patients analyzed was relatively small (Table 12). The highest congruence was observed for CD3 and TdT (100% each).

Importantly, the high correlations between protein expression and mRNA abundance were not limited to congruence in positivity but were significantly correlated also quantitatively. When protein expression levels and mRNA abundance were compared by Pearson's correlation (Table 9), these comparisons revealed significant although in many cases rather low correlations for the fluorescence intensities for many of the analyzed genes. Figure 43 further underlines the high coherence of expression patterns for both protein and mRNA of important antigens for the diagnosis of leukemias.

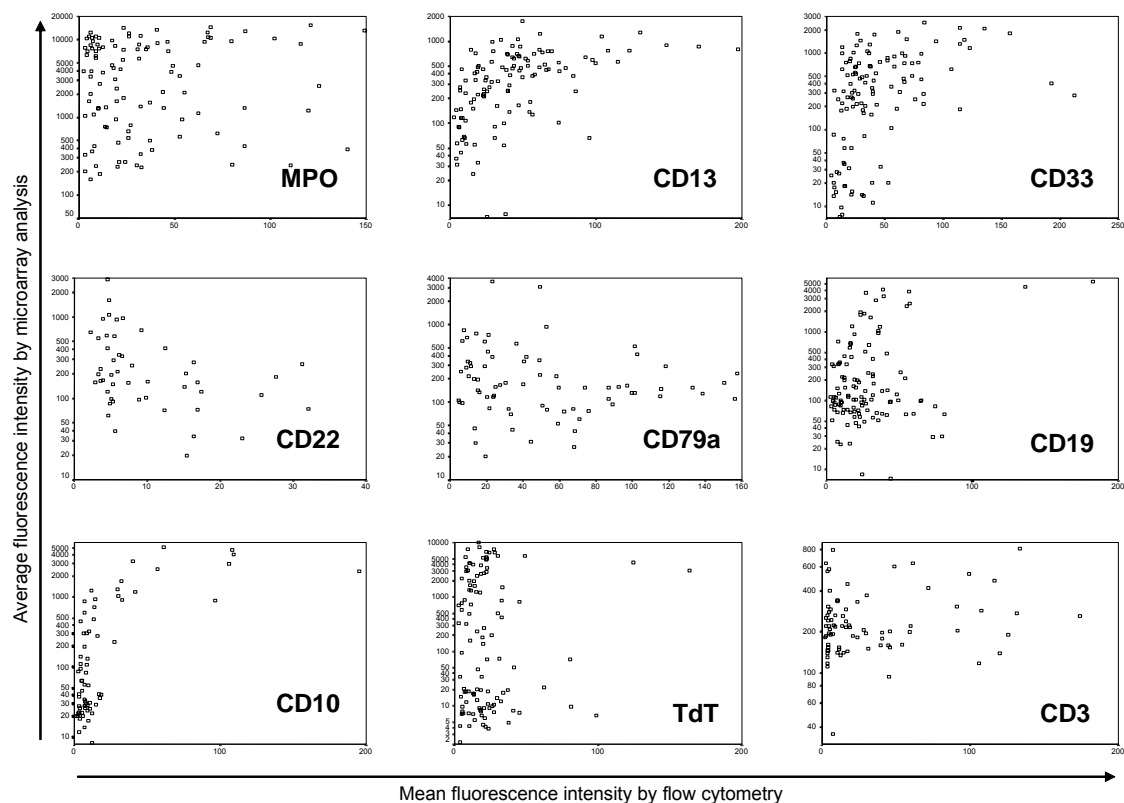


Figure 43. **Protein expression and mRNA abundance in a subset of diagnostic antigens.** Comparison of protein expression levels and mRNA abundance of 9 markers with significant correlations (Pearson's correlation). Mean fluorescence intensity values obtained by flow cytometry were calculated for all events with fluorescence values higher than isotype controls using the CellQuest Pro software (Becton Dickinson) and are given on the x-axis. Average fluorescence intensity values obtained by U133A microarray analyses were calculated by using Microarray Suite software (Affymetrix) and are given on the y-axis.

Table 9. Comparisons of protein expression and mRNA abundance in acute leukemia.

Antigen	Number of comparisons	Both FC and MA positive*	Both FC and MA negative*	MA positive and FC negative*	FC positive and MA negative*	Correlation of mean fluorescence intensity by flow cytometry and average fluorescence intensity by microarray analysis	
						Coefficient of correlation (Spearman)	Significance of correlation (Spearman)
CD10	33	17	12	0	4	0.608	0.000
CD116	65	29	0	35	1	0.159	0.166
CD117	73	28	23	21	1	0.378	0.000
CD11b	61	33	2	26	0	0.607	0.000
CD13	75	58	5	11	1	0.590	0.000
CD133	45	21	13	10	1	-0.135	0.272
CD135	65	42	2	21	0	0.102	0.367
CD14	72	17	27	28	0	0.585	0.000
CD15	68	30	5	31	2	-0.014	0.888
CD19	74	27	43	3	1	0.106	0.253
CD1a	23	0	16	7	0	0.208	0.319
CD2	73	13	9	51	0	0.109	0.248
CD20	3	0	2	0	1	-0.500	0.391
CD22	63	20	26	0	17	-0.379	0.007
CD235a	61	4	24	30	3	0.092	0.358
CD33	75	43	14	2	16	0.494	0.000
CD34	72	45	9	17	1	0.545	0.000
CD36	56	27	9	18	2	0.703	0.000
CD38	60	52	1	1	6	0.612	0.000
CD3e	69	19	20	11	19	0.119	0.296
CD4	67	10	37	8	12	-0.196	0.040
CD41	5	0	0	5	0	0.298	0.050
CD45	71	71	0	0	0	0.276	0.004
CD5	2	0	1	0	1	-0.100	0.873
CD56	73	0	60	1	12	0.126	0.180
CD61	63	0	56	0	7	0.041	0.679
CD64	68	17	16	33	2	0.524	0.000
CD7	72	12	54	0	6	0.144	0.132
CD79a	22	6	1	0	15	-0.196	0.094
CD87	66	15	1	50	0	0.422	0.028
CD8a	5	0	3	2	0	0.182	0.572
CD9	40	26	5	6	3	0.369	0.002
CD90	60	3	42	7	8	0.029	0.842
CD97	38	35	0	2	1	-0.253	0.041
HLA-DR	73	63	1	9	0	0.322	0.059
Lactoferrin	63	15	14	31	3	0.209	0.027
MPO	74	43	2	29	0	0.057	0.558
NG2	70	1	63	1	5	0.359	0.044
TdT	69	39	13	2	15	0.026	0.790
Total	2187 (100.0%)	881 (40.3%)	631 (28.9%)	509 (23.3%)	166 (7.6%)		
		1512 (69.1%) congruent		675 (30.9%) not congruent			

* FC= flow cytometry, MA= microarray analysis

Table 10. Comparisons of protein expression and mRNA abundance in AML.

Antigen	Number of comparisons	Both FC and MA positive*	Both FC and MA negative*	MA positive and FC negative*	FC positive and MA negative*
CD10	12	3	8	0	1
CD116	46	25	0	21	0
CD117	48	28	8	11	1
CD11b	41	23	1	17	0
CD13	50	44	0	5	1
CD133	30	15	9	5	1
CD135	45	29	1	15	0
CD14	49	15	17	17	0
CD15	48	26	1	20	1
CD19	50	6	40	3	1
CD1a	8	0	6	2	0
CD2	49	9	6	34	0
CD20	0	0	0	0	0
CD22	43	5	24	0	14
CD235a	39	4	14	20	1
CD33	50	36	2	1	11
CD34	47	24	9	13	1
CD36	39	22	4	13	0
CD38	41	35	0	1	5
CD3e	47	11	14	7	15
CD4	47	10	22	6	9
CD41	5	0	0	5	0
CD45	48	48	0	0	0
CD5	0	0	0	0	0
CD56	49	0	38	1	10
CD61	42	0	38	0	4
CD64	49	15	7	25	2
CD7	48	10	35	0	3
CD79a	13	0	1	0	12
CD87	47	13	0	34	0
CD8a	3	0	3	0	0
CD9	27	14	5	6	2
CD90	41	2	29	6	4
CD97	25	23	0	2	0
HLA-DR	48	39	1	8	0
Lactoferrin	44	12	12	17	3
MPO	50	38	0	12	0
NG2	46	0	41	1	4
TdT	45	18	13	1	13
Total	1459 (100.0%)	602 (41.3%)	409 (28.0%)	329 (22.5%)	119 (8.2%)
		1011 (69.3%) congruent		448 (30.7%) not congruent	

* FC= flow cytometry, MA= microarray analysis

Table 11. Comparisons of protein expression and mRNA abundance in precursor B-ALL.

Antigen	Number of comparisons	Both FC and MA positive*	Both FC and MA negative*	MA positive and FC negative*	FC positive and MA negative*
CD10	18	13	2	0	3
CD116	17	4	0	12	1
CD117	21	0	15	6	0
CD11b	18	8	1	9	0
CD13	21	11	5	5	0
CD133	13	4	4	5	0
CD135	18	11	1	6	0
CD14	19	1	8	10	0
CD15	17	4	2	10	1
CD19	20	20	0	0	0
CD1a	13	0	8	5	0
CD2	21	2	3	16	0
CD20	2	0	1	0	1
CD22	19	15	2	0	2
CD235a	18	0	8	8	2
CD33	21	6	11	0	4
CD34	21	18	0	3	0
CD36	15	5	5	4	1
CD38	17	15	1	0	1
CD3e	19	5	6	4	4
CD4	17	0	14	2	1
CD41	0	0	0	0	0
CD45	19	19	0	0	0
CD5	1	0	1	0	0
CD56	20	0	20	0	0
CD61	17	0	16	0	1
CD64	17	2	8	7	0
CD7	20	0	19	0	1
CD79a	8	6	0	0	2
CD87	17	2	1	14	0
CD8a	0	0	0	0	0
CD9	11	10	0	0	1
CD90	17	1	12	1	3
CD97	11	10	0	0	1
HLA-DR	21	21	0	0	0
Lactoferrin	17	3	2	12	0
MPO	20	4	1	15	0
NG2	20	1	18	0	1
TdT	21	18	0	1	2
Total	622 (100%)	239 (38.4%)	195 (31.4%)	155 (24.9%)	33 (5.3%)
		434 (69.8%) congruent		188 (30.2%) not congruent	

* FC= flow cytometry, MA= microarray analysis

Table 12. Comparisons of protein expression and mRNA abundance in precursor T-ALL.

Antigen	Number of comparisons	Both FC and MA positive*	Both FC and MA negative*	MA positive and FC negative*	FC positive and MA negative*
CD10	2	1	1	0	0
CD116	2	0	0	2	0
CD117	3	0	0	3	0
CD11b	2	2	0	0	0
CD13	3	3	0	0	0
CD133	2	2	0	0	0
CD135	2	2	0	0	0
CD14	3	0	2	1	0
CD15	3	0	2	1	0
CD19	3	0	3	0	0
CD1a	2	0	2	0	0
CD2	3	2	0	1	0
CD20	1	0	1	0	0
CD22	1	0	0	0	1
CD235a	3	0	2	1	0
CD33	3	1	1	0	1
CD34	3	3	0	0	0
CD36	2	0	0	1	1
CD38	2	2	0	0	0
CD3e	3	3	0	0	0
CD4	3	0	1	0	2
CD41	0	0	0	0	0
CD45	3	3	0	0	0
CD5	1	0	0	0	1
CD56	3	0	2	0	1
CD61	3	0	1	0	2
CD64	2	0	1	1	0
CD7	3	1	0	0	2
CD79a	1	0	0	0	1
CD87	2	0	0	2	0
CD8a	2	0	0	2	0
CD9	2	2	0	0	0
CD90	2	0	1	0	1
CD97	2	2	0	0	0
HLA-DR	3	2	0	1	0
Lactoferrin	2	0	0	2	0
MPO	3	0	1	2	0
NG2	3	0	3	0	0
TdT	3	3	0	0	0
Total	91 (100%)	34 (37.4%)	24 (26.4%)	20 (22.0%)	13 (14.3%)
		58 (63.8%) congruent		33 (36.3%) not congruent	

* FC= flow cytometry, MA= microarray analysis

Application of pediatric expression patterns to classify adult patients

Here, the gene expression patterns of a cohort of 100 adult ALL patients comprising 26 precursor B-ALLs with *MLL* gene rearrangements and 42 translocation t(9;22)-positive cases, as well as 32 precursor T-ALLs were analyzed. The diagnostic compositions of candidate genes as reported in microarray studies by Yeoh and colleagues and by Armstrong and colleagues, respectively, were used to stratify these cases (Yeoh et al., 2002; Armstrong et al., 2002). The genes identified by Yeoh et al. and Armstrong et al. were represented on recent Affymetrix HG-U95 chip design microarrays. In this work, the newly designed HG-U133 array set was used. In order to achieve comparability of differing sets of microarray expression data the different Affymetrix U95A chip design and U133A chip design probe set information had to be compared. Briefly, as depicted in the respective original publications, the significant U95Av2 probe sets of interest, i.e., genes to discriminate ALL with t(11q23)/*MLL*, *BCR/ABL*, and T-ALL, were extracted. Unique U95Av2 probe sets then were functionally annotated using the NetAffx database descriptions. Next, for those unique U95Av2 probe sets their corresponding U133A counterparts were determined using the “Human Genome U95 to Human Genome U133 Best Match comparison spreadsheet” (www.affymetrix.com). This search resulted in best match U133 design counterparts for the U95Av2 probe sets which were chosen for subsequent statistical analyses, i.e., predicting the ALL subtype in the independent cohort of adult ALL patients.

Firstly, the gene expression data was compared to available expression signatures of the St. Jude Children’s Research Hospital childhood ALL samples (<http://www.stjudechildrens.org/data/ALL1>). Yeoh et al. had used Affymetrix U95Av2 oligonucleotide microarrays to analyze the pattern of genes expressed in leukemic blasts from 360 pediatric ALL patients. Distinct expression profiles identified each of the prognostically important leukemia subtypes, including T-ALL, *E2A/PBX1*, *BCR/ABL*, *TEL/AML1*, t(11q23)/*MLL*, and hyperdiploid karyotypes (i.e., >50 chromosomes). They selected discriminating genes for the various ALL subtypes using a variety of statistical metrics. In this work, all significant U95Av2 probe sets specific for t(11q23)/*MLL*, *BCR/ABL*, and T-ALL subtypes were extracted from their publication, combined, and their corresponding U133A counterparts used to stratify the adult patients. The data presented here indicates that the genes reported by Yeoh et al. can also separate an independent cohort of adult ALL patient samples. Subgroup prediction using SVM classification algorithms demonstrated the discriminative properties of those candidate genes specific for T-ALL, *BCR/ABL*, and t(11q23)/*MLL* in adult ALL (Table 13).

Table 13. **Classification of three adult ALL subtypes based on pediatric markers.**

	SVM based on 312 probe sets according to Yeoh et al.	
<i>Adult ALL subtype</i>	<i>10-fold CV accuracy</i>	<i>resampling accuracy</i>
T-ALL	100% (32/32)	100% [97%; 100%]
<i>BCR/ABL</i>	100% (42/42)	
t(11q23)/ <i>MLL</i>	100% (26/26)	

A hierarchical cluster analysis and PCA of adult ALL samples using the preselected subset of genes specific for T-ALL, *BCR/ABL*, and *t(11q23)/MLL* confirms the capability of separating three ALL subtypes based on distinct expression signatures. As visualized in Figure 44, samples of each of the three distinct ALL subtypes cluster together. Based on the given preselected gene expression data, both algorithms accurately assign the ALL samples according to their underlying genetic aberration and immunophenotype, respectively.

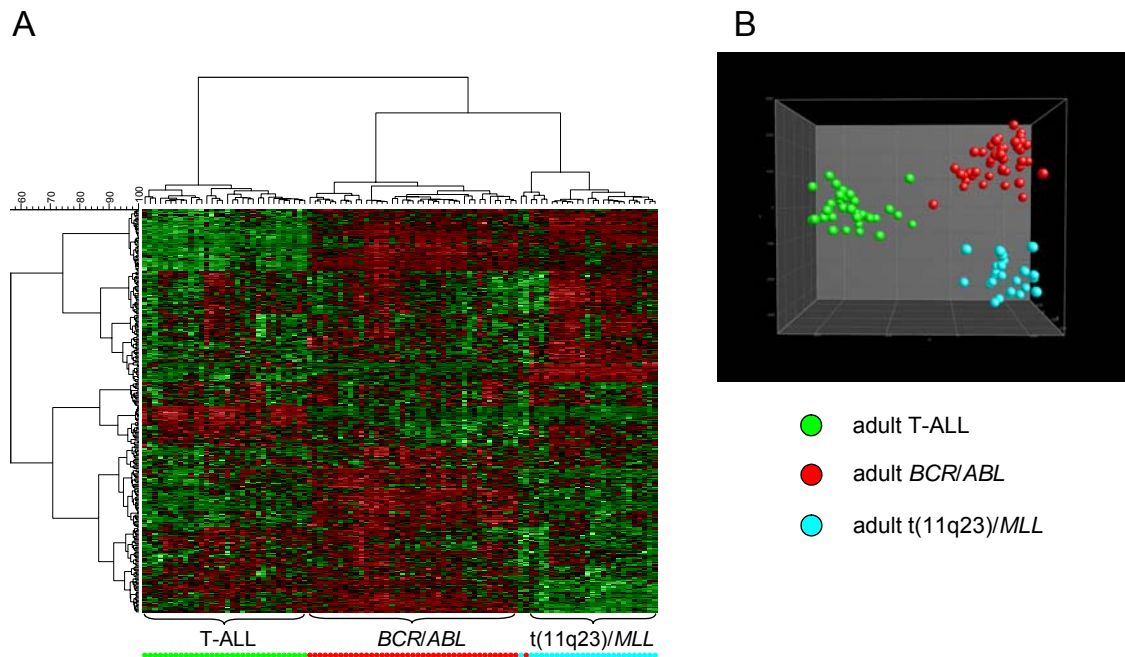


Figure 44. **Pediatric markers according to Yeoh et al. can classify adult patients.** The analysis is based on U133A microarray expression data of adult ALL samples from the Laboratory for Leukemia Diagnostics, Munich, using a published subset of genes identified to classify pediatric ALL samples from the St. Jude Children's Research Hospital, Memphis, TN, USA (Yeoh et al., 2002). 312 unique best match U133A probe sets were identified to represent the 364 unique U95Av2 probe sets according to Yeoh and colleagues for the distinction of *t(11q23)/MLL*, *BCR/ABL* and T-ALL leukemias. (A) In the hierarchical clustering the normalized expression value for each gene is coded by color. Red cells indicate high expression and green cells indicate low expression. (B) In the PCA adult ALL samples of the three subtypes T-ALL (n=32), *BCR/ABL* (n=42) and *t(11q23)/MLL* (n=26) are accordingly distinguished.

Secondly, the expression data on adult ALL was compared to available expression profiles of Dana-Farber Cancer Institute childhood ALL samples (<http://research.dfc.harvard.edu/korsmeyer/MLL.htm>). Armstrong et al. had compared the gene expression profiles of leukemic cells from individuals diagnosed with precursor B-ALL bearing *MLL* gene rearrangements to those from patients diagnosed with conventional precursor B-ALL that lack this translocation (n=44 pediatric ALL patients). They had determined whether there were genes correlated with the presence of a *MLL* translocation. That set of published genes was applied to distinguish between *t(11q23)/MLL*-positive and *t(11q23)/MLL*-negative cases in the independent cohort. By applying this preselected set of marker genes it is possible to robustly distinguish between

t(11q23)/*MLL*-positive and t(11q23)/*MLL*-negative cases in the independent cohort of adult patients with high accuracy (Table 14).

Table 14. Prediction of t(11q23)/*MLL* aberrations in adult ALL using pediatric markers.

	SVM based on 182 probe sets according to Armstrong et al.	
Adult ALL subtype	10-fold CV accuracy	resampling accuracy
t(11q23)/ <i>MLL</i>	100% (26/26)	100% [97%; 100%]
non-t(11q23)/ <i>MLL</i>	100% (74/74)	

As visualized in Figure 45, based on the given preselected U133 chip design gene expression data, two analysis algorithms accurately group the ALL samples into *MLL* gene rearrangement positive and *MLL* gene rearrangement negative cases.

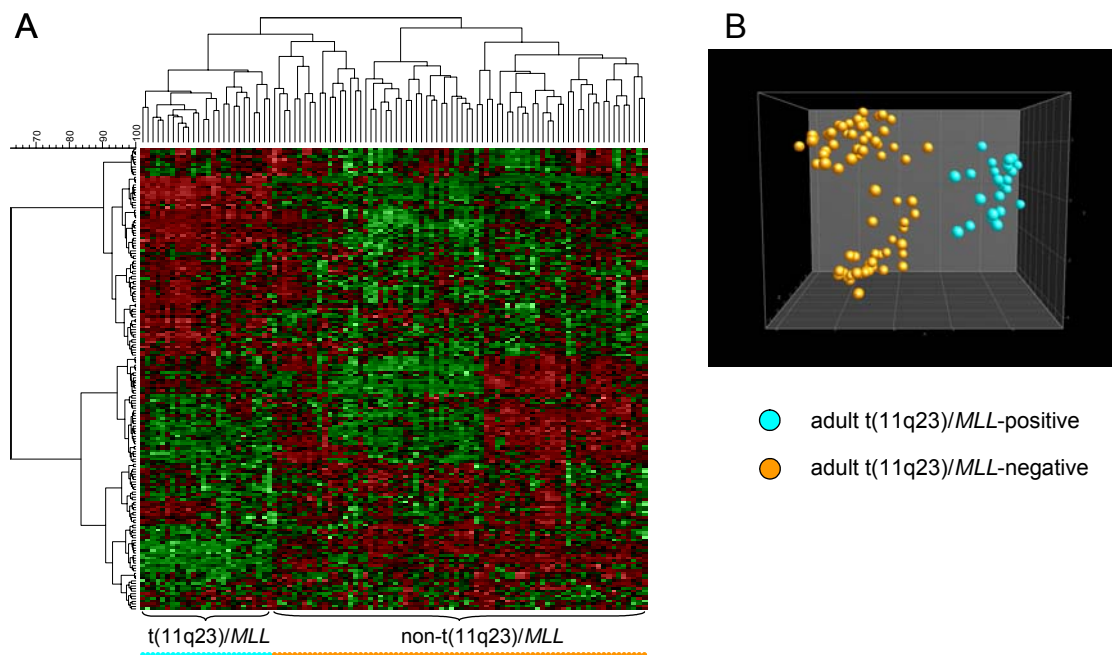


Figure 45. **Pediatric markers according to Armstrong et al. can classify adult patients.** The analysis is based on U133A microarray expression data of adult ALL samples from the Laboratory for Leukemia Diagnostics, Munich, using a published subset of genes identified to classify pediatric ALL samples from the Dana-Farber Cancer Institute, Boston, MA, USA (Armstrong et al., 2002). 182 unique best match U133A probe sets corresponded to 217 identified U95A chip design probe sets for the distinction of t(11q23)/*MLL*-positive and t(11q23)/*MLL*-negative samples according to Armstrong and colleagues. (A) In the hierarchical clustering the normalized expression value for each gene is coded by color. Red cells indicate high expression and green cells indicate low expression. (B) In the PCA adult ALL samples of the subtypes t(11q23)/*MLL* (n=26) and non-t(11q23)/*MLL* (n=74) are accordingly distinguished.

Finally, it is possible to identify overlapping genes specific for t(11q23)/*MLL* and non-t(11q23)/*MLL* cases in both published data sets and apply this stringent marker selection to stratify adult patient samples. A substantial number of genes characterizing t(11q23)/*MLL*-positive patient samples are overlapping between the Yeoh et al. and Armstrong et al. gene lists. When tested on the

adult ALL microarray expression data set, the SVM classification engine demonstrates the accurate discriminative properties of those *MLL* gene translocation specific candidate genes (Table 15).

Table 15. Prediction of *MLL* aberrations using overlapping t(11q23)/*MLL*-specific genes.

	SVM based on 55 overlapping probe sets according to both Yeoh et al. and Armstrong et al.	
Adult ALL subtype	10-fold CV accuracy	resampling accuracy
t(11q23)/ <i>MLL</i>	96% (25/26)	97% [97%; 100%]
non-t(11q23)/ <i>MLL</i>	99% (73/74)	

Again, based on the given preselected gene expression data, analysis algorithms accurately separate the adult ALL samples into t(11q23)/*MLL*-positive and t(11q23)/*MLL*-negative cases (Figure 46). In conclusion, in both pediatric and adult ALL patient cohorts, *MLL* gene rearrangement positive and *MLL* gene rearrangement negative cases can robustly be predicted.

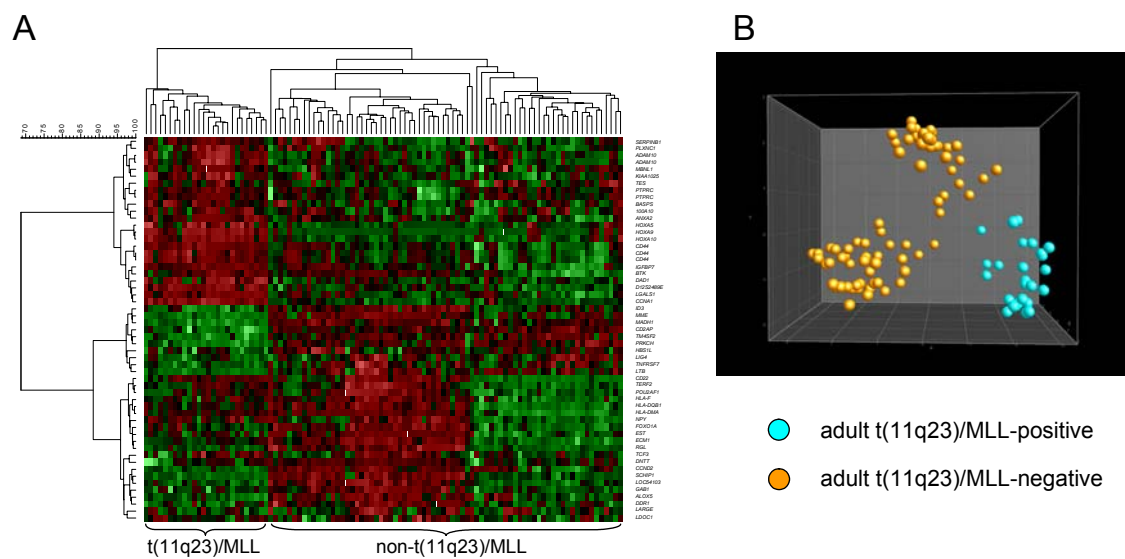


Figure 46. **Overlapping t(11q23)/*MLL* markers from two pediatric cohorts classify adult patients.** The analysis is based on U133A microarray expression data of adult ALL samples from the Laboratory for Leukemia Diagnostics, Munich, using an overlapping subset of genes identified to classify pediatric ALL with and without *MLL* gene rearrangement. A comparison of both Yeoh et al. and Armstrong et al. published gene lists resulted in a number of 57 overlapping U95Av2 chip design probe sets reported to be correlated with pediatric ALL carrying *MLL* gene aberrations (Yeoh et al., 2002; Armstrong et al., 2002). 55 unique best match U133A probe sets corresponded to those 57 identified U95 microarray design probe sets. (A) In the hierarchical clustering the normalized expression value for each gene is coded by color. Red cells indicate high expression and green cells indicate low expression. (B) In the PCA adult ALL samples of the subtypes t(11q23)/*MLL* (n=26) and non-t(11q23)/*MLL* (n=74) are accordingly distinguished.

Taken together, the data presented in this section provide evidence that genes reported to classify and predict childhood ALL are also capable of distinguishing the respective adult ALL subentities. Thus, the gene expression signatures are validated and also confirmed on a truly independent cohort of patients.

Gene expression profiling as a novel diagnostic method

Between June 2001 and February 2004 a total of 965 target preparations for gene expression profiling were performed yielding sufficient cRNA for hybridization to microarrays, i.e., $\geq 20 \mu\text{g}$ after the in vitro transcription. These samples were hybridized to U133A and U133B microarrays between March 2002 and February 2004. Each scan was visually inspected. In 28 (2.9%) cases samples were excluded that did not meet a combination of the following stringent criteria: (i) %P called probe sets of the U133A array $\geq 30\%$, (ii) low 3'/5' ratio of *GAPD* probe sets (normally less than 3.0), and (iii) no scan artifacts detected, i.e., bubbles, scratches, high background, or comparable range of scaling factors. For the remaining 937 (97.1%) samples included in this analysis, the median value of the percentage of present called genes was 46.3% (U133A) and 31.3% (U133B), respectively, the median 3'/5' ratio of *GAPD* probe sets was 1.65 (U133A) and 1.87 (U133B), respectively. Table 16 gives an overview about the samples included in this analysis.

Table 16. Number of samples and patient characteristics.

	Number of patients (%)	median	range
Shipment time (days)		1	0-3
Storage time at -80°C (months)		13	0-67
Patient age (years)		57	16-90
AML patients		61	18-90
ALL patients		46	16-86
CML patients		49	21-82
CLL patients		63	36-84
non-leukemia cases		45	18-83
Sex (male/female)	53%/47%		
WBC count at diagnosis (G/l)		28.8	0.4-514
Bone marrow blasts (acute leukemias only)*		85%	10%-100%
AML	total	620 (66%)	
	t(15;17)	42 (4%)	
	t(8;21)	38 (4%)	
	inv(16)	49 (5%)	
	t(11q23)/ <i>MLL</i>	47 (5%)	
	complex aberrant karyotype	75 (8%)	
	other abnormalities	176 (19%)	
	normal karyotype	193 (21%)	
ALL	total	152 (16%)	
	Pro-B-ALL/t(11q23)/ <i>MLL</i>	26 (3%)	
	c-ALL/Pre-B-ALL with t(9;22)	42 (4%)	
	c-ALL/Pre-B-ALL without t(9;22)	40 (4%)	
	mature B-ALL/t(8;14)	12 (1%)	
	cortical T-ALL	20 (2%)	
	immature T-ALL	12 (1%)	
CML, chronic phase	75 (8%)		
CLL	45 (5%)		
Non-leukemia	45 (5%)		

*Threshold for definition of AML according to the WHO classification is a bone marrow blast count of at least 20% (which may be even lower by definition, however, if recurrent balanced translocations are present)

Besides the distinction between the four main categories of leukemia, i.e., AML, ALL, CML, and CLL, the acute leukemias also comprise specific subentities. Thus, the following 12 clinically relevant subgroups were analyzed: AML with t(15;17), AML with t(8;21), AML with inv(16), AML with normal karyotype or so-called "other" cytogenetic abnormalities, AML with t(11q23)/*MLL* rearrangement, AML with complex aberrant karyotype, Pro-B-ALL/t(11q23)/*MLL*, mature B-ALL/t(8;14), c-ALL/Pre-B-ALL with or without t(9;22), T-ALL, CML, CLL. Additionally, a group designated "non-leukemia" was included. These were samples obtained from healthy bone marrow donors or patients with reactive

bone marrow conditions, vitamin B12 or iron deficiency, or idiopathic thrombocytopenic purpura, respectively.

The separation of samples with AML and normal karyotypes from those with AML and “other” cytogenetic aberrations was not done since the prognosis of both subgroups is identical. This is clearly demonstrated in Figure 47A showing that the overall survival is identical for these two subgroups when applying a standardized treatment approach (Buchner et al., 2003; Kern et al., 2003a; Haferlach et al., 2003b). This is also true when the cohort of patients that were hybridized to the microarrays were compared to a control group of patients not included in this work (Figure 47B). Thus, at present there is no clinical relevance or need for the distinction between these two groups in this analysis.

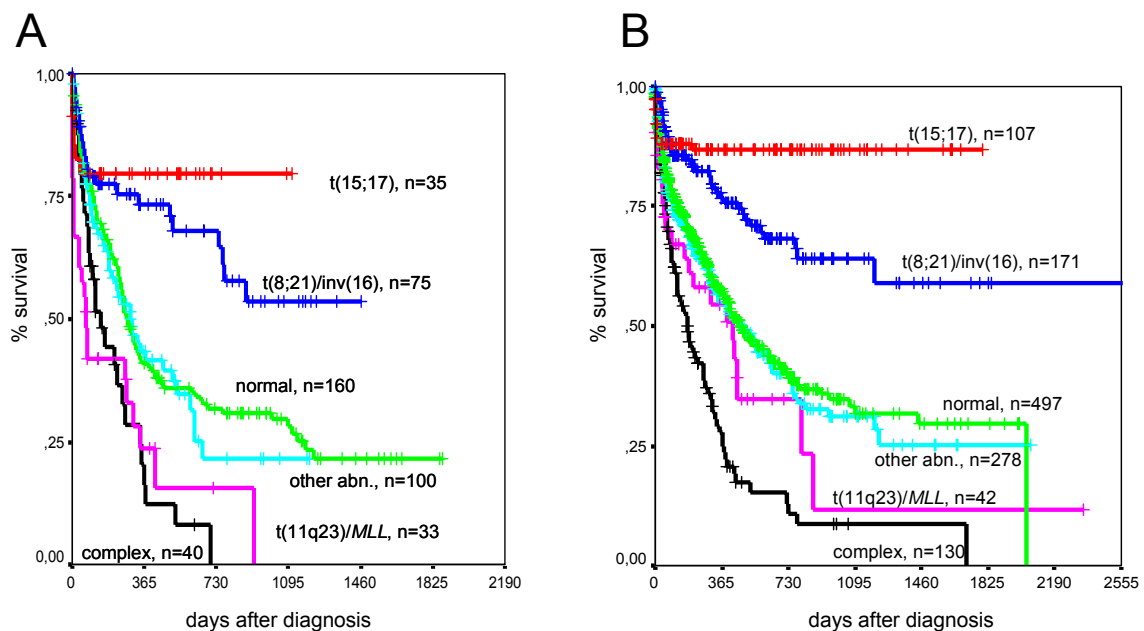


Figure 47. **Overall survival in cytogenetically defined AML subgroups.** Patients with complex aberrant karyotypes and those with AML and t(11q23)/MLL have the worst prognosis, patients with AML and t(15;17), t(8;21), or inv(16) have a relatively good prognosis. Importantly, there is no difference with regard to prognosis between patients with a normal karyotype and those with other karyotype abnormalities, i.e., those not in the before-mentioned subgroups. (A) Representation of patients analyzed in this work with available follow-up data (days after diagnosis). (B) Representation of unselected 1,225 patients (total cohort) where follow-up data were available in the database from the Laboratory for Leukemia Diagnostics.

Prediction of 13 subgroups

The prediction of the respective leukemia type or subtype was approached using Support Vector Machines (SVM). Therefore, the complete data set was randomly, but balanced by the subtypes split into training and independent test cohorts for the 13 different subgroups. Then differentially expressed genes were identified in the training set and a SVM model was built based on the genes that demonstrated differential expression between the respective subclasses in the training set. This SVM model was used to predict samples in the test cohort. The use of the top 100 genes per group resulted in best prediction accuracies

(superior to top 20, 50, 150, 200, 250, and 300 genes, respectively). Table 17 represents a confusion matrix of subgroup predictions based on their gene expression signature using a 10-fold CV approach. Overall, a 95.1% accuracy of subgroup predictions has been achieved analyzing the 13 classes. Specifically, the highest accuracy was achieved for seven of the 13 classes, i.e., AML with t(15;17), 100% accurate predictions; AML with inv(16), 98.0%; CLL, 97.8%; CML, 97.3%; AML normal/other, 97.3%; Pro-B-ALL/t(11q23), 96.2%; AML with t(8;21), 94.7%. For the other six subgroups the percentage of accurate predictions ranged between 83.3% and 93.3%. Most of the misclassifications occurred in subgroups that either had relatively low sample numbers, or which are characterized by a high intra-subgroup biologic heterogeneity. The first aspect clearly applies to mature B-ALL with t(8;14) with a sample number of 12 and 83.3% accurate predictions. The latter aspect is reflected in AML with t(11q23)/*MLL* (89.4% accurate predictions) with balanced translocations involving the *MLL* gene and different fusion partner genes. Another example of biologic heterogeneity is AML with complex aberrant karyotype (88.0% accurate predictions). Samples in this group demonstrated a wide range of three to 30 chromosomal abnormalities (median, 9). As anticipated, most of the misclassifications of these groups (4 out of 5 for AML with t(11q23)/*MLL* and 8 out of 9 for AML with complex aberrant karyotype) were due to a prediction of the samples as class AML normal/other. A third aspect to consider is the relative similarity of distinct subgroups with regard to specific characteristics, e.g., the detected expression of myeloid antigens on immature T-ALL cases by flow cytometry (Onciu et al., 2002). Probably due to these complexities, 4 out of 32 cases with T-ALL were classified as AML normal/other.

Table 17. Confusion matrix for prediction of 13 groups as determined by 10-fold CV.

Confusion matrix	real												
	c-ALL/Pre-B-ALL	Pro-B-ALL/t(11q23)	mature B-ALL with t(8;14)	T-ALL	AML with t(15;17)	AML with t(8;21)	AML with inv(16)	AML with t(11q23)	AML with complex karyotype	AML normal/other	CLL	CML	non-leukemia
c-ALL/Pre-B-ALL	76												
Pro-B-ALL/t(11q23)		25											
mature B-ALL with t(8;14)	1		10							1			
T-ALL				28					1				
AML with t(15;17)					42								
AML with t(8;21)						36	1						
AML with inv(16)							48						
AML with t(11q23)								42		4			1
AML with complex kt.						1			66	4			
AML normal/other	4	1	2	4		1		4	8	359	1	2	2
CLL											44		
CML								1				73	
non-leukemia	1									1			42
Sum (n=937)	82	26	12	32	42	38	49	47	75	369	45	75	45

In order to assess the robustness of these predictions a resampling approach was applied, i.e., the complete SVM classification procedure was repeated 100 times. For each of the 100 runs all samples were randomly, but balanced by the subtypes divided into a training set (2/3 of all samples, n=625) and a test set (1/3 of all samples, n=312). Thus, the test set for each run contained 28 c-ALL/Pre-B-ALL, 9 Pro-B-ALL/t(11q23), 4 mature B-ALL/t(8;14), 10 T-ALL, 14 AML with t(15;17), 12 AML with t(8;21), 16 AML with inv(16), 16 AML with t(11q23), 25 AML with complex karyotype, 123 AML with normal karyotype or other aberrations, 15 CLL, 25 CML, and 15 non-leukemia samples, respectively. Table 18 gives the average number of class predictions as determined after 100 runs of classifications. For example, 9 Pro-B-ALL/t(11q23) samples were predicted by the algorithm 900 times (each sample 100 times). Of the 900 predictions the class label Pro-B-ALL/t(11q23) was assigned correctly 854 times, i.e., on average 8.54 per run. In 2 individual predictions, Pro-B-ALL/t(11q23) samples were predicted as c-ALL/Pre-B-ALL, and in 44 predictions as AML with normal karyotype or other aberrations, respectively.

Table 18. Confusion matrix for prediction of 13 groups as determined by resampling.

Confusion matrix	real												
	c-ALL/Pre-B-ALL	Pro-B-ALL/t(11q23)	mature B-ALL with t(8;14)	T-ALL	AML with t(15;17)	AML with t(8;21)	AML with inv(16)	AML with t(11q23)	AML with complex karyotype	AML normal/other	CLL	CML	non-leukemia
c-ALL/Pre-B-ALL	25.77	0.02	0.85							0.27		0.07	0.14
Pro-B-ALL/t(11q23)		8.54											
mature B-ALL with t(8;14)	0.15		2.57							0.11	0.02		0.04
T-ALL				9.23					0.36	0.04			
AML with t(15;17)					14								
AML with t(8;21)						11.43	0.04						
AML with inv(16)							15.7						
AML with t(11q23)								13.05	0.01	1.23			0.04
AML with complex kt.						0.11			21.38	1.36		0.02	0.09
AML normal/other	1.43	0.44	0.36	0.77		0.46	0.26	2.71	3.14	119.1	0.36	0.8	1.02
CLL											14.62		
CML	0.09							0.18		0.48		23.82	0.44
non-leukemia	0.56		0.22					0.06	0.11	0.41		0.29	13.23
Sum (n=312)	28	9	4	10	14	12	16	16	25	123	15	25	15

Confirming the previous data obtained by 10-fold CV, the overall median accuracy amounts to 93.8% (95% confidence interval: [91.4%; 95.8%]). In particular and similar to the 10-fold CV approach, a very high degree of accurate predictions was achieved in seven of the 13 subgroups, i.e., AML with t(15;17), 100% median accuracy; AML with inv(16), 98.1%; CLL, 97.5%; CML, 95.3%; AML normal/other, 96.8%; Pro-B-ALL/t(11q23), 94.9%; AML with t(8;21), 95.3%. For the other six subgroups the median prediction accuracies ranged between 64.3% and 92.3%. Thus, the results obtained for the subgroups by applying the resampling approach are highly consistent with those obtained by 10-fold CV and strongly confirm the capability of gene expression profiling to predict distinct leukemia subtypes. The reasons for the misclassifications are most likely the same as those described above, in particular the relatively low number of cases with mature B-ALL with t(8;14).

The sensitivities and specificities of the predictions for each of the 13 subclasses are given in Table 19. According to the accuracy data given above, the specificity overall is very high, more than 99% for all but one subgroup. Since most misclassified samples were classified as AML normal/other, the specificity of this subgroup was slightly lower than for other subgroups and amounted to 93.7%. The median sensitivity ranged between 75% and 100% for all subgroups.

Table 19. **Sensitivities and specificities for leukemia classification in 13 subgroups.**

Leukemia class	Number of cases (n=937)	Sensitivity		Specificity	
		Median	95% confidence interval	Median	95% confidence interval
c-ALL/Pre-B-ALL	82	92.9%	[82.1%; 100%]	99.7%	[98.6%; 100%]
Pro-B-ALL/t(11q23)	26	100%	[77.8%; 100%]	100%	[100%; 100%]
mature B-ALL/t(8;14)	12	75.0%	[25.0%; 100%]	100%	[99.4%; 100%]
T-ALL	32	90.0%	[70.0%; 100%]	100%	[99.7%; 100%]
AML with t(15;17)	42	100%	[100%; 100%]	100%	[100%; 100%]
AML with t(8;21)	38	100%	[83.3%; 100%]	100%	[99.7%; 100%]
AML with inv(16)	49	100%	[87.5%; 100%]	100%	[100%; 100%]
AML with t(11q23)	47	81.3%	[62.5%; 100%]	99.7%	[99.0%; 100%]
AML with complex kt.	75	86.0%	[72.0%; 96.0%]	99.7%	[98.6%; 100%]
AML normal/other	369	96.8%	[94.3%; 99.2%]	93.7%	[90.2%; 96.6%]
CLL	45	100%	[93.3%; 100%]	100%	[100%; 100%]
CML	75	96.0%	[84.0%; 100%]	99.7%	[98.6%; 100%]
non-leukemia	45	90.0%	[66.3%; 100%]	99.7%	[98.3%; 100%]

Cluster analysis of 13 subgroups

To further validate the findings described above cluster analyses were performed for the 13 groups analyzed as well as for paired comparisons of selected groups. Firstly, a hierarchical clustering of all of the analyzed samples reflects the clearly differing gene expression patterns of the 13 groups resulting in a highly accurate separation of this large and comprehensive series of 937 samples (Figure 48).

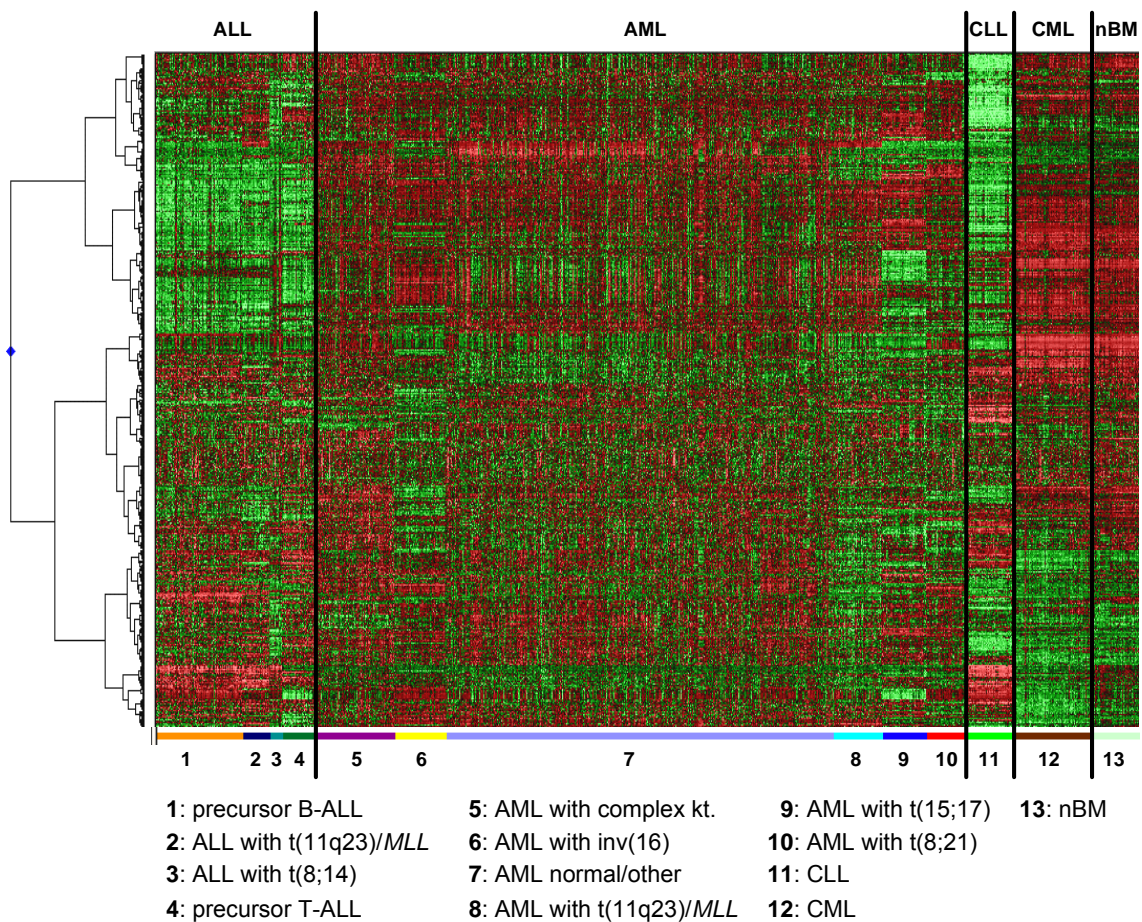


Figure 48. **Hierarchical cluster analysis of 937 samples representing 13 classes.** Analysis of 937 samples (columns) using a set of 1,019 differentially expressed genes (rows) (U133 set). The normalized expression value for each gene is coded by color (standard deviation from mean). Red cells indicate high expression and green cells indicate low expression. The major leukemia types are separated by bars. For each of the 13 classes the top 100 differentially expressed genes, according to t-test-statistic, were used. Of the 1,300 genes, 281 were repeatedly identified as important diagnostic markers and were overlapping between the respective top 100 gene lists. Thus, this results in a list of 1,019 non-overlapping genes.

When a three-dimensional PCA was performed, the power of the gene expression profile-based leukemia classification can be demonstrated by the clear separation of precursor T-ALL from c-ALL/Pre-B-ALL (with or without t(9;22)) (Figure 49A). Similarly, three-dimensional PCA provides a clear distinction between both t(9;22)-positive entities, CML and c-ALL/Pre-B-ALL (Figure 49B). Interestingly, the one sample of t(9;22)-positive c-ALL/Pre-B-ALL shown in the proximity of the CML samples is characterized by only 50% leukemic bone marrow infiltration. Thus, the normal hematopoiesis present in this sample, which is largely myelomonocytic, and the forced assignment to either of the two groups are the likely reasons for this result.

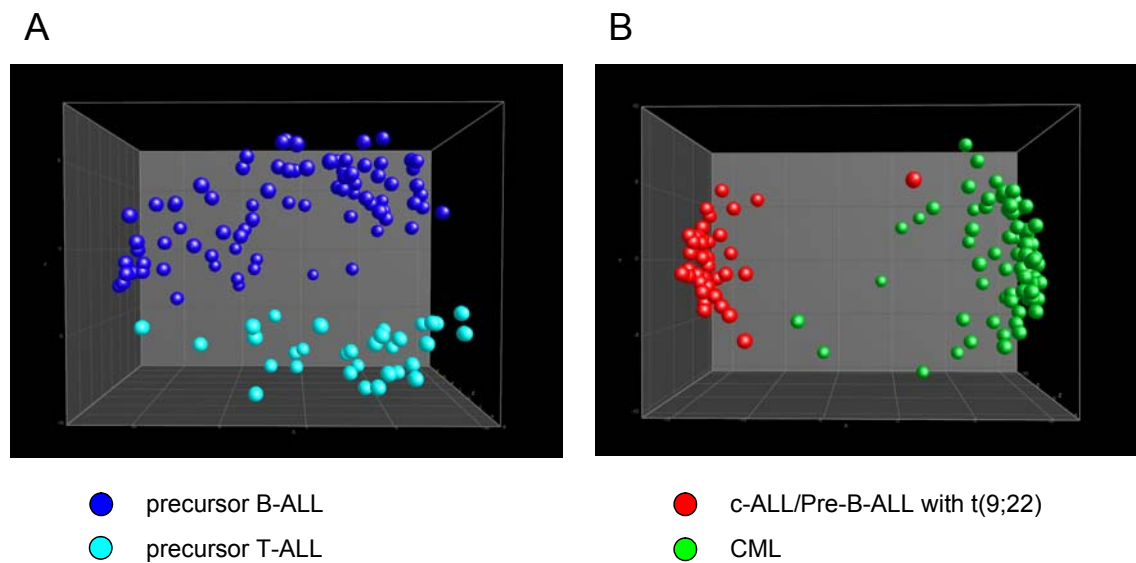


Figure 49. **Three-dimensional PCA visualizing distinctions of leukemia subtypes.** (A) Distinction between precursor B-ALL and T-ALL (U133 set). The 114 ALL samples were projected into the feature space consisting of a combination of the top 100 differentially expressed genes when comparing precursor B-ALL vs. the other 12 classes or T-ALL vs. the other 12 classes. The 82 precursor B-ALL samples are colored blue and include 42 c-ALL/Pre-B-ALL with t(9;22) and 40 c-ALL/Pre-B-ALL without t(9;22). The 32 T-ALL samples are colored turquoise. (B) Distinction between c-ALL/Pre-B-ALL with t(9;22) and CML. The 117 samples were projected into the feature space consisting of a combination of the top 100 differentially expressed genes when comparing c-ALL/Pre-B-ALL with or without t(9;22) samples vs. the other 12 classes and CML vs. the other 12 classes. The 42 c-ALL/Pre-B-ALL with t(9;22) samples are colored red, the 75 CML samples are colored green, respectively.

Identification of cortical T-ALL and precursor B-ALL with t(9;22)

In order to further refine the classification capabilities of this approach an analysis aimed at identifying the clinically distinct entities c-ALL/Pre-B-ALL with t(9;22) and cortical T-ALL out of the groups classified as c-ALL/Pre-B-ALL and T-ALL, respectively.

In Figure 50A a cluster analysis shows that the majority of the cases fall either into the branch of c-ALL/Pre-B-ALL without t(9;22), or into the branch of c-ALL/Pre-B-ALL with t(9;22). The remaining 21 samples (26%) fall into a third branch characterized by a gene expression profile clearly differing from the other two groups. Accordingly, the 10-fold CV analysis, allowing the separation into two groups only, reveals an accuracy of 82.9%. Importantly, misclassifications occurred in both directions, i.e., cases with t(9;22) were classified as without it and vice versa. Resampling of the training and test sets resulted in a median accuracy of 77.8% (95% confidence interval: [61.0%; 90.8%]) and indicated that these misclassifications are not limited to distinct samples, i.e., the percentages of misclassifications per sample range from 3.1% to 88.1%, probably reflecting a significant overlap of gene expression signatures between both groups (Figure 50B), or being due to the presence of a clinically not yet identified third group of c-ALL/Pre-B-ALL.

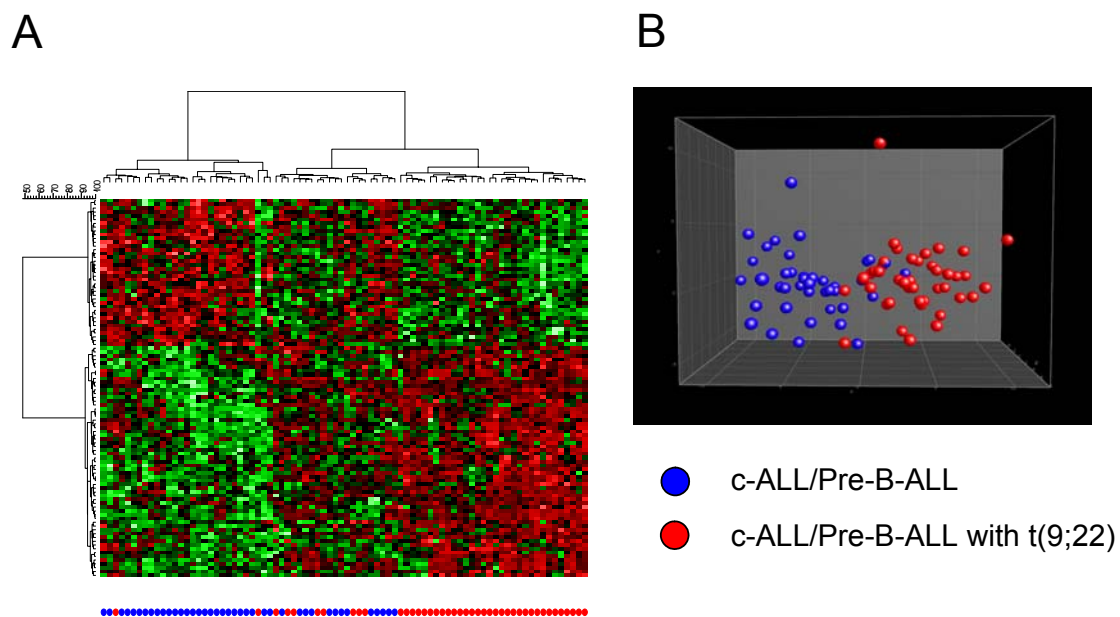


Figure 50. **Identification of c-ALL/Pre-B-ALL samples with or without t(9;22).** Analysis of 82 c-ALL/Pre-B-ALL samples based on a supervised identification of differentially expressed genes between 42 cases demonstrating a t(9;22), colored in red, and 40 cases without t(9;22), colored in blue, respectively (U133 set). (A) In the hierarchical cluster analysis the normalized expression value for each gene (given in rows) is coded by color (standard deviation from mean). Red cells indicate high expression and green cells indicate low expression. (B) In the three-dimensional PCA the c-ALL/Pre-B-ALL samples were projected into the feature space consisting of the top 100 differentially expressed genes when comparing t(9;22)-positive vs. t(9;22)-negative cases.

The separation of cortical T-ALL samples from immature T-ALL samples is shown in the corresponding cluster analysis (Figure 51A). Interestingly, two samples of immature T-ALL show a gene expression profile slightly different from the other immature T-ALL cases. In fact, these two samples are the ones lying nearest to the cortical T-ALL samples in the PCA (Figure 51B). According to the relative vicinity of these two samples to samples of cortical T-ALL, the accuracy of the 10-fold CV is 84% and resampling results in a median accuracy of 80% (95% confidence interval: [60%; 100%]).

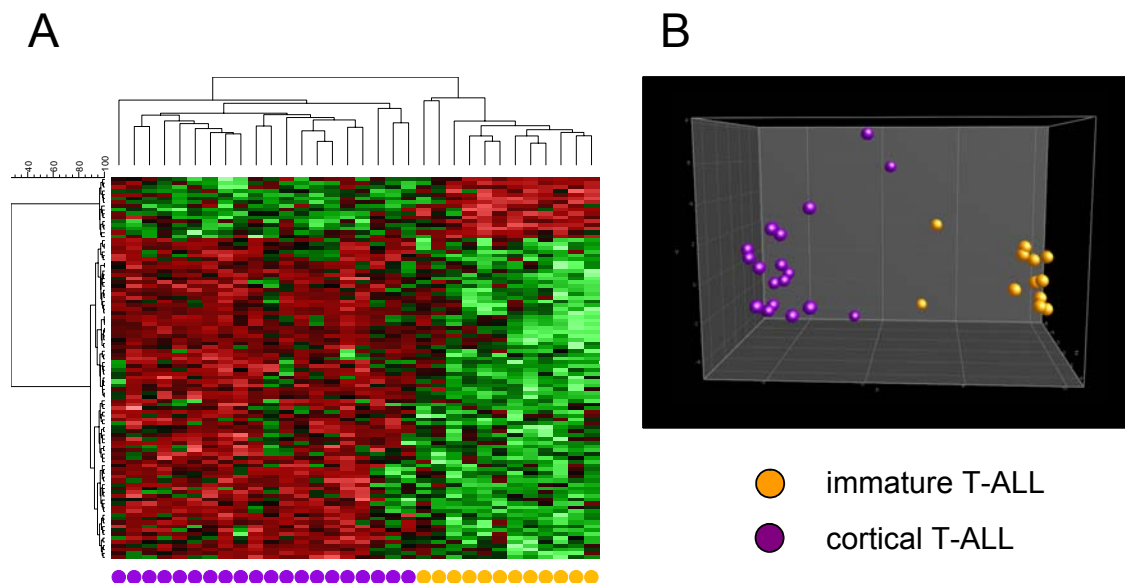


Figure 51. **Distinction between immature and cortical T-ALL samples.** The analysis of 32 T-ALL samples is based on a supervised identification of differentially expressed genes between 12 immature T-ALL samples (orange) and 20 cortical T-ALL samples (purple) (U133 set). (A) In the hierarchical cluster analysis the normalized expression value for each gene (given in rows) is coded by color (standard deviation from mean). Red cells indicate high expression and green cells indicate low expression. (B) In the three-dimensional PCA the T-ALL samples were projected into the feature space consisting of the top 100 differentially expressed genes when comparing immature vs. cortical T-ALL cases.

Taken together, it was successfully shown in an extensive analysis of leukemia samples that a one-step diagnostic approach for the diagnosis of leukemias is feasible. In 937 samples from patients with newly diagnosed leukemia and normal bone marrow from healthy donors all leukemic subentities which are clinically relevant with respect to specific treatment approaches and prognostication were assessed. Thus, the diagnostic accuracy and efficiency of current methods may be improved by the use of microarrays.

5. Discussion

Three major questions were addressed in this thesis. Firstly, is there a specific gene expression signature associated with distinct leukemia types and subtypes? Secondly, if that is the case, can these gene expression patterns give new insights into the biology of the different forms of leukemia? Thirdly, are these signatures robust enough for diagnostic usage? To answer these questions samples obtained from leukemia patients, diagnosed and characterized in the Laboratory for Leukemia Diagnostics, Munich, Germany, were analyzed using high-density oligonucleotide microarrays. Various microarray data analysis algorithms were applied to identify minimal sets of genes and existing data analysis methods were adapted to assess diagnostic accuracies and enable a comparison to both available published microarray data and conventional methods used for the diagnosis of leukemias.

5.1 Specific patterns in AML with reciprocal rearrangements

The main focus of the initial analyses was the assessment of the differences between three highly characterized subgroups of AML defined by specific primary chromosome aberrations. By applying different independent approaches for the analysis of microarray data, it was demonstrated that AML samples from previously defined subtypes can be adequately classified on the basis of gene expression profiles. It is intriguing that there is both sufficient coherence in gene expression within and difference between these subtypes to classify them with high accuracy even though the samples derive from the same myeloid cell lineage.

Firstly, unsupervised algorithms were applied and revealed that AML with $t(15;17)$, $t(8;21)$, and $inv(16)$ are characterized by different transcriptomes. Unsupervised algorithms are the method of choice when one has no or little a priori knowledge of the complete repertoire of expected gene expression signatures. Cluster analyses represented complex gene expression data that, however, through statistical organization and graphical display, allow to explore the data in a natural intuitive manner. As anticipated, it was further shown that AML with $t(8;21)$ and AML with $inv(16)$, which both involve alterations of the core binding factor complex (Friedman, 1999), are more related to each other as compared to AML with $t(15;17)$. Recently, detailed analyses have confirmed this finding (Ross et al., 2004). The two phenotypically different subtypes of AML with $t(15;17)$, i.e., AML M3 and AML M3v, clustered within one area and therefore demonstrate similarities in their underlying transcriptome.

So far, several studies confirmed that gene expression profiles can be used for class prediction. This has been shown for acute leukemias, round blue cell tumors, and malignant melanomas (Golub et al., 1999; Bittner et al., 2000; Khan et al., 2001), as well as for different types of solid tumors by using multiclass cancer classification (Ramaswamy et al., 2001). Whereas the selection of different subgroups in these studies was performed by using exclusively phenotypic criteria, other studies were based on genetically defined entities (Perou et al., 2000; Hedenfalk et al., 2001). In this work, for the first time the discrimination of three genetically defined AML subgroups was

accomplished. Thus, a second step of the initial analyses was to search for minimal gene sets using supervised algorithms and to test the possibility of predicting AML subtypes solely based on gene expression signatures. Two classifiers were developed using two independent approaches. Both classifiers accurately predicted the AML subtypes t(15;17), t(8;21), and inv(16). However, they differed in the number of genes needed for the classification task. Whereas classification by the weighted voting algorithm according to Golub and colleagues (Golub et al., 1999) allowed the discrimination between the three classes based on a minimal set of 13 genes, the multiple-tree classifier was based on 29 genes. As indicated by cross-validation, generalization properties are excellent for the multiple-tree classifier, i.e., it is likely to perform equally well on new, unseen samples. Interestingly, the classifiers contained genes already known to be primarily involved in the pathogenesis of the respective entities, namely *MYH11* in AML with inv(16) (Shigesada et al., 2004) and *ETO* (*CBFA2T1*) in AML with t(8;21) (Peterson and Zhang, 2004). Presumably, the detection of overexpression of *MYH11* in inv(16) cases and *ETO* in t(8;21) cases relates to the detection of the fusion gene transcripts rather than of the wild-type transcripts. The other genes identified belong to various functional categories and their potential pathogenetic significance in AML has yet to be clarified.

In 2002, the U133 two-array set replaced the U95 array design and provided a comprehensive coverage of well-substantiated genes in the human genome. As the next step forward the analyses then were extended to the U133 microarray design. Firstly, the question was addressed whether differentially expressed genes from the U95A study would also allow an accurate separation of the patients when measured with U133 design microarrays. Secondly, the genes were also validated on new, independent patient samples which had not been used in the initial gene identification study. Therefore, all previously used hybridization cocktails utilized in the initial profiling study and additional patient samples were hybridized to the improved U133A microarray. Repeatedly, the presented diagnostic composition of genes accurately separated the three AML subtypes in all 129 cases. Taken together, both the genes were successfully confirmed on an updated chip design, but also novel candidates which had not been represented on the U95Av2 microarray were identified in this analysis. As a consequence, further investigations proceeded with the transition from U95Av2 arrays to the U133 set of microarrays.

As a first conclusion, an unequivocal association between disease-specific genetic alterations and distinct gene expression profiles in AML was shown. For each of the three analyzed clearly defined subtypes of AML, i.e., t(15;17), t(8;21), and inv(16), signatures of gene expression were identified that were homogeneous within all samples of the respective subgroups, but clearly differed between these three subgroups. The analyzed samples represent disease subtypes that are defined specifically on the genetic and the phenotypic level by conventional diagnostics including cytomorphology, cytogenetics, and molecular genetics. Thus, it was expected that the extension of the gene expression analyses to currently less well-defined leukemia entities would reveal new insights into the underlying biology.

Reproducibility of results between laboratories

In several laboratories, where gene expression profiles had been generated, distinct AML subtypes were correctly identified based on different gene expression patterns. It is therefore of interest to ask the question to which extent the genes described in this work to discriminate between AML with t(15;17), t(8;21), or inv(16) can also be found in other reports. Consequently, the reported list of 36 genes to stratify the AML subtypes t(15;17), t(8;21), and inv(16) was further examined. This list of genes is disclosed in the initial gene expression profiling analysis and was based on Affymetrix U95A microarrays (Table 2). It could be demonstrated that, using both independent patients and a new microarray with higher density (U133A), genes from that list were still excellent diagnostic markers (Kohlmann et al., 2003; Haferlach et al., 2003a). Moreover, genes from that list were also reported and confirmed by other major European and USA leukemia laboratories. In 2003, Debernardi and colleagues from the Barts and the Royal London School of Medicine and Dentistry, London, UK, presented data on AML subtypes with recurrent translocations (U95Av2 microarray). Several of the markers from this work are also contained in their report (Debernardi et al., 2003). In 2004, some of the genes were confirmed on both pediatric and adult cohorts. Ross et al., from the St Jude Children's Research Hospital had generated profiles from pediatric AML patients using U133A microarrays (Ross et al., 2004). Genes depicted in their manuscript and supplemental data have also been part of the list in this work. Moreover, as shown in the publication by Bullinger and colleagues from Stanford University, Stanford, CA, USA, unsupervised analyses accurately separated AML with t(15;17), t(8;21), and inv(16) (Bullinger et al., 2004). Signatures correlated with this separation also contained genes depicted in this work. Interestingly, this study was based on cDNA microarrays, an alternative gene expression profiling platform. Lastly, some of the predictors to stratify AML with specific translocations were also reported by Valk and colleagues from the Erasmus University Medical Center, Rotterdam, The Netherlands, though using a completely unsupervised analysis approach for their U133A microarray data (Valk et al., 2004). Detailed information on the genes that were confirmed is given in the table below (Table 20).

Some of the genes were not contained in the reported lists from other groups. But, for a number of reasons, it is actually expected that gene lists from the numerous publications contain some discrepancies. This is due to several parameters that can influence gene expression profiling studies: (A) The studies on gene expression profiles of acute leukemias differ with respect to the microarray platform used and types of microarrays, i.e., the content of represented genes. This also may include differences in sample preprocessing and variations in target preparation for microarray analysis. (B) Additionally, the studies differ in patient cohorts. (C) Moreover, in each of the studies acute leukemias were compared to a variety of different leukemia types. Thus, the pattern of specific genes is dependent on the constellation of the data based on the experimental design. (D) Lastly, one can also expect to observe variances due to different algorithms used for data analysis.

Table 20. Confirmation of genes correlated with AML with t(15;17), t(8;21), and inv(16).

Genes from Schoch et al., 2002		Debernardi et al., 2003 ^a	Ross et al., 2004 ^b	Kohlmann et al., 2003 ^c	Bullinger et al., 2004 ^d	Valk et al., 2004 ^e
<i>ADD3</i>	U37122				X	
<i>ADRA2C</i>	J03853					X
<i>AHNAK</i>	M80899					
<i>AHR</i>	L19872					
<i>ALCAM</i>	Y10183		X			
<i>ARHGAP4</i>	X78817	X	X	X		X
<i>BZRP</i>	M36035					
<i>CBFA2T1</i>	D43638	X	X	X	X	X
<i>CD74</i>	M13560					
<i>CDW52</i>	N90866		X		X	
<i>CEACAM6</i>	M18728					
<i>CLECSF2</i>	X96719	X			X	
<i>CLU</i>	M25915					
<i>CTSW</i>	AF013611		X	X	X	
<i>DKFZP564K0822</i>	W25986		X			X
<i>DKFZP586N1922</i>	N99340					
<i>FBLN1</i>	X53742					
<i>GNAI1</i>	AL049933					
<i>HLA-DMA</i>	X62744				X	
<i>HLA-DPA1</i>	X00457			X	X	
<i>HLA-DRA</i>	J00194					
<i>HLA-DRB1</i>	M32578					
<i>HOXB2</i>	X16665					
<i>ITGB2</i>	M15395					
<i>KRT18</i>	M26326		X			
<i>MYH11</i>	AF013570	X	X	X	X	X
<i>PIG6</i>	AF010310					
<i>PLXNB2</i>	AB002313		X		X	
<i>POU4F1</i>	X64624	X	X	X		X
<i>PRKAR1B</i>	M65066					
<i>PTGDS</i>	AI207842		X			X
<i>RGS10</i>	AF045229	X	X	X		
<i>S100A9</i>	W72424		X			
<i>SELL</i>	M25280			X		
<i>SERPING1</i>	X54486		X		X	
<i>TGFBI</i>	M77349	X	X			X

^a Compared to the 43 genes correlated with t(15;17), t(8;21), or inv(16) as disclosed in Table 2 of their manuscript.

^b Compared to the top 100 probes correlated with t(15;17), t(8;21), or inv(16) as disclosed in Supplemental Tables S7 - S9 of their manuscript.

^c Compared to the 17 genes correlated with t(15;17), t(8;21), or inv(16) as disclosed in Table 2 of the publication.

^d Compared to the top 50 up- and downregulated probes correlated with t(15;17), t(8;21), or inv(16) as listed in Supplementary Table 5 of their manuscript.

^e Compared to the top 40 genes correlated with t(15;17), t(8;21), or inv(16) clusters, given as Supplemental Table I1, Table L1, or Table M1, respectively.

Gene expression signatures and morphology in APL

A next series of analyses then focused on the investigation of the transcriptome of APL in more detail. It could be confirmed that APL has a specific gene expression signature, which is shared by AML M3 and its morphological variant M3v, distinguishing both APL subtypes from other genetically defined AML. An unsupervised data analysis approach discriminated APL (FAB M3 and M3v combined) from AML with t(8;21), or inv(16), or t(11q23)/*MLL* aberrations and also from AML with a normal karyotype. Thus, it could be proven repeatedly that *PML/RARA* fusion transcripts lead to a unique and highly reproducible gene expression signature. The differentially expressed genes from a supervised

analysis comparing APL to AML with t(8;21), or inv(16), or t(11q23)/*MLL* aberrations as well as to AML with normal karyotype were further examined in more detail. Through the use of a pathway analysis application, a phenomenon known from immunophenotyping of APL was visualized in a biological network, i.e., that genes with functional relevance in MHC-II antigen presentation are lower expressed in APL (Orfao et al., 2004). Other overlapping probe sets that were found to be consistently expressed higher in APL in these two analyses encoded for genes like *AGRN*, *ANXA8*, *CTSW*, *HGF*, *LAMC1*, *LGALS12*, *MST1*, *PTGDS*, *SERPING1*, *SLC24A3*, *STAB1*, or *TPM4*. Some of these genes were also listed as highly correlated with a t(15;17)-specific gene signature in a recent study (Valk et al., 2004). Similarly, consistently lower expressed genes in APL included the genes *CD86*, *CDW52*, *CSPG2*, *CTSS*, *DEFA4*, *HOXA9*, *HOXA10*, *MEIS1*, *MARCKS*, *MS4A6A*, *S100A9*, *SCAP2*. This confirms recent data regarding a global downregulation of *HOX* gene expression in APL (Thompson et al., 2003).

Patients with APL suffer from severe bleeding episodes at diagnosis and had an early death rate of up to 30% before the ATRA era (Haferlach et al., 1993) and up to 10% after ATRA was introduced into induction therapy protocols (Sanz et al., 1999; Fenaux et al., 2000; Lengfelder et al., 2000; Degos and Wang, 2001; Tallman et al., 2002). Therefore, through the use of the Gene Ontology annotation a supervised analysis was performed including genes known to be involved in blood clotting. Intriguingly, several genes such as *ANXA5*, *CD59*, *THBS1*, *SERPINE1*, *LMAN1*, and *THBD* were found to be expressed higher when comparing APL against other AML subtypes. This confirms a previous finding in patients with disseminated intravascular coagulation where elevated plasma levels of *SERPINE1*, also known as the plasminogen activator inhibitor-I (*PAI1*), have been reported (Watanabe et al., 2001).

In 56% of AML patients the WBC count at diagnosis is >10,000/ μ l, in 15% it is within normal ranges, and in 29% leukocyte counts <4,000/ μ l were measured (data on 1,155 unselected AML patients). However, a striking difference is observed with respect to the WBC count in patients with t(15;17) and AML M3 vs. M3v showing leukopenia mostly in M3 and normal or elevated WBC count in M3v patients. This is surprising as the bone marrow also in AML M3 cases is mostly packed and does not demonstrate a pattern different from other AML subtypes or AML M3v, respectively. The phenotype in M3 demonstrates a heavy granulation of promyelocytic blasts even in the peripheral blood. But the picture is much more distinct in the bone marrow with abnormal promyelocytes having primary granules bigger than in normal promyelocytes. In contrast, the granulation in the M3v cases is mostly invisible in the MGG or Pappenheim stain. Only in the myeloperoxidase reaction both APL subtypes are strongly positive. This makes it obvious that granules in M3v cases are so-called secondary granules that can be found in more mature cells of granulocytic differentiation. Thus, one can speculate that both subtypes of APL arise on different levels of immature stem cells leading to individual programming and maturation controls and stops (Grimwade and Enver, 2004).

Therefore, several genes were evaluated with respect to different stages of differentiation. For example, interleukin-3 receptor alpha chain, *IL3RA*, was expressed higher in M3v cases. Abnormalities of *IL3RA* are frequently observed

in AML and may contribute to the proliferative advantage of leukemic blasts (Testa et al., 2002; Testa et al., 2004). In another study it was demonstrated that activation of human interleukin-3 receptor stimulates self-renewal or myeloid differentiation, respectively (Evans et al., 2002). It can be hypothesized that, as it was observed, a reduced expression of *IL3RA* might therefore contribute to a block in M3 differentiation and a deregulated overexpression in M3v might lead to a more mature form of APL. Also, M3 and M3v cases might differ in their leukotriene pathway due to changes in *ALOX5* expression and thereby represent different stages of myeloid differentiation (Scoggan et al., 1996). It has also been shown that isoforms of *PTPRC* (CD45 antigen) play an important role in the proliferation and differentiation of hematopoietic cells (Craig et al., 1994). In AML, CD45 isoform expression characterized differential stages both in myelocytic and monocytic lineages (Miyachi et al., 1999). In this work, *PTPRC* demonstrated an elevated expression in M3v cases compared to M3 samples. In addition, differing gene expression was observed with respect to CD2 positivity as has been suggested by Grimwade et al. being higher expressed in M3v (Mistry et al., 2003; Grimwade and Enver, 2004). A similar pattern of expression was also detected for *CD2BP2*, which binds to a site within the cytoplasmic region of CD2 (Nishizawa et al., 1998).

Next, the phenotypical findings were correlated with the expression levels of candidates that are known to be present in primary and/or in secondary granules. Highly significant correlations between phenotype and gene expression profiles were found irrespective of the shared cytogenetic genotype. As Auer rods are known to be fused, cylindrical stacks of abnormal primary granules and accordingly stain strongly positive for myeloperoxidase they are a hallmark for AML and are especially frequent in AML M3. It is well known that the overwhelming number of primary granules in this APL subtype in most cases leads to bundles of Auer rods in one cell, so-called faggot cells. It was possible to confirm this in the analyzed cohort of AML M3 cases (87.8% with faggot cells). This was significantly different as compared to the M3v cases, mostly occurring with secondary granules and faggot cells found in only 64.5%. Myeloperoxidase (*MPO*) was seen highly elevated in both subtypes, but differences were detected for defensin alpha 1, *DEFA1*, (known to be higher expressed in primary granules) and for transcobalamin II, *TCN2*, (higher in secondary granules) with respect to their gene expression in M3 or M3v cells. This demonstrates the concordance of morphology and gene expression with respect to phenotypical differences in APL. It also further supports the hypothesis that the M3v form of APL is the more mature subtype and has its maturation stop at a later stage in differentiation of granulopoiesis compared to M3.

Another very important phenotypical difference in M3 vs. M3v is the shape of the nucleus. This led to the speculation that genes encoding for nuclear envelope proteins might be differentially expressed in the two morphological APL subtypes. Indeed, a close examination of an APL-specific biological network revealed that *LMNA*, a member of the intermediate filament family, is upregulated in M3v compared to M3 cases. Lamins are components of the nuclear lamina, a fibrous layer on the nucleoplasmic side of the inner nuclear membrane, which is thought to provide a framework for the nuclear envelope (McKeon et al., 1986). The fact that lamins A and C are lacking from

some undifferentiated cells might also point FAB M3v towards the more mature APL subtype (Wydner et al., 1996).

It has been shown in animal models that the expression of *PML/RARA* alone is not sufficient to induce APL. Therefore, additional molecular genetic mechanisms have to be proposed for full-blown leukemia (Gilliland and Griffin, 2002; Kelly et al., 2002). Recently, a first hint of additional molecular mutations in APL and also for molecular differences between both subtypes has been identified. In comparison to classical APL, a higher frequency of *FLT3* gene length mutations (FLT3-LM) was observed in M3v patients (75% vs. 23%) (Schnittger et al., 2002; Mistry et al., 2003; Grimwade and Enver, 2004). However, the FLT3-LM was not detected in all AML M3v cases and was also observed in M3. Thus, further components in a currently unknown molecular network have to be identified. In this work, a highly significant correlation between morphology, WBC count, and FLT3-LM in AML M3v and vice versa in AML M3 was observed. With respect to FLT3-LM a highly significant difference between M3 and M3v was confirmed. In order to test the independency of the genes identified by microarray analysis from these different aspects a linear regression analysis was performed and included the 20 most differentiating genes between M3 and M3v as well as level of WBC count and FLT3-LM status. Only six genes were found to be dependent on the other two parameters, again showing the multifactorial background of M3 and M3v subtypes in APL.

In conclusion, patients with APL and t(15;17) show in comparison to other AML subgroups distinct gene expression signatures. Some of these APL-specific genes can be correlated with the clotting disorder that is known to be highly affected in APL. Through supervised approaches AML M3 was discriminated from M3v with a very high accuracy based in some parts on genes responsible for maturation, granulation and nucleus configuration. These genes may therefore explain the known differences between these leukemia entities. Furthermore, these different expression profiles in AML M3 and M3v may hint to different levels of stem cells from which the two subtypes of APL are arising (Gilliland and Griffin, 2002; Grimwade and Enver, 2004).

5.2 Molecular characterization of ALL using microarrays

With respect to ALL, initially four differing adult ALL subtypes were analyzed. Precursor B-ALL with t(11q23)/*MLL*, *BCR/ABL*, or t(8;14), and precursor T-ALL all formed distinct clusters in various data analysis approaches which reflect their highly differing underlying gene expression profiles. This is in line with previous reports showing that pediatric ALL with t(11q23)/*MLL*, *BCR/ABL*, or precursor T-ALL samples, respectively, can be separated and also predicted with high accuracies using microarray technology (Yeoh et al., 2002; Ross et al., 2003). The report from Yeoh and colleagues has been a milestone in microarray data analysis with respect to class discovery, class prediction, and prediction of outcome. Their data on 360 childhood ALL analyzed by Affymetrix U95A arrays revealed distinct signatures for each of the prognostically important ALL subtypes, including T-ALL, *E2A/PBX1*, *BCR/ABL*, *TEL/AML1*, t(11q23)/*MLL*, and hyperdiploid karyotypes (i.e., >50 chromosomes). This has been confirmed in a follow-up study by Ross and colleagues using a selection

of the initial cohort of patients that were rehybridized to U133 set microarrays. Most surprisingly, however, Yeoh et al. not only predicted the therapeutic outcome in most children with ALL, but astoundingly also found specific genes in the ALL blasts at diagnosis that indicate an increased risk of developing a therapy-induced AML after successful treatment of ALL, which was considered a provocative observation by the authors themselves.

In this work, using both U95A and U133A microarrays genes differentially expressed in precursor B-ALL with t(11q23)/*MLL*, *BCR/ABL*, or t(8;14), and precursor T-ALL contained for example candidates encoding for the T cell receptor beta subunit and T cell surface CD3 delta chain (*TRB*, *CD3D*). *TRB* and *CD3D* were identified as highly indicative for T-ALL as compared to both ALL with t(9;22) and all other ALL subtypes. This is in line with standard diagnostics of T-ALL by immunophenotyping where these antigens include the most specific ones (Campana and Behm, 2000). Most of the other genes discovered to be overexpressed in T-ALL were mainly related to a functional role in the class I MHC-restricted T cell receptor signalosome (Leo et al., 2002). Several candidates have also recently been reported by other microarray studies: *TRB*, *CD3D*, *CD3E*, *CD2*, *CD6*, *MAL*, *LCK*, *ITM2A*, *SH2D1A* (Yeoh et al., 2002; Ferrando et al., 2002). As such, the identification of these overexpressed T-ALL associated genes illustrates the power of gene expression profiling to elucidate complex pathways in a highly parallel manner. *MME* (formerly *CD10*) was highly expressed in ALL with t(9;22) only. This may reflect that the translocation t(9;22) is observed in common-ALL and in pre-B ALL only. On the other hand, these data again demonstrate that the gene used for diagnostic purposes in flow cytometry, *MME*, is highly indicative of these ALL subtypes in comparison to the more immature B-lineage ALL, i.e., pro-B ALL, as well as the mature B-ALL and the T-ALL. Furthermore, the identification of connective tissue growth factor (*CTGF*) as a specific marker for ALL with t(11q23)/*MLL* adds to previous data demonstrating its increased gene expression in malignant lymphoblasts of B cell origin (Vorwerk et al., 2002). Other genes with high expression in t(11q23)/*MLL*-positive ALLs and also recently reported by other microarray studies were: *ADAM10*, *BLK*, *CD72*, *CD79A*, *CSPG4*, *HOXA9*, *HOXA10*, *IGHM*, *LGALS1*, *LMO2*, *MBNL*, *MEF2A*, *PPP2R5C*, *PTPRC*, *VLDLR* (Yeoh et al., 2002; Armstrong et al., 2002; Rozovskaia et al., 2003). Candidate genes like *IGHM*, *BLK*, or *CD79A* illustrate the B-lineage characteristic of these cases, and an observed overexpression of *HOX-A* cluster members illustrates important components of leukemogenesis driven by *MLL* gene rearrangements (Kawagoe et al., 1999; Armstrong et al., 2002). In addition, similar patterns were observed for all precursor B-ALL samples. Here, the gene cluster included candidates mainly with a functional role in immune response: *BLNK*, *BRDG1*, *CD24*, *MHC2TA*, *CD74*, *HLA-DMA*, *HLA-DMB*, *HLA-DPA1*, *HLA-DRA*, *HLA-DPB1*, *HLA-DQB1*, *HLA-DRB1*, *HLA-DRB3*, *HLA-DRB4*, and *TNFRSF14*. In detail, major components of the class II MHC restricted antigen presentation machinery are consistently overexpressed compared to the T-ALL samples: *MHC2TA*, interacting with MHC class II as well as *HLA-DM* and *CD74* promoters, is a highly regulated transactivator governing all spatial, temporal and quantitative aspects of MHC class II expression (Masternak et al., 2000). The chaperone *CD74* (invariant chain) blocks the peptide binding site of newly synthesized MHC class II molecules by its so-

called CLIP fragment (Villadangos and Ploegh, 2000). *HLA-DM* molecules catalyze the exchange of CLIP for antigenic peptides derived from endosomal compartments.

Secondly, a series of analyses was then targeted to obtain new insights into the underlying biology in heterogeneous B-lineage leukemias not positive for *BCR/ABL* or *t(11q23)/MLL*. In order to obtain information on the similarity of the heterogeneous B-lineage leukemias to any of the other analyzed ALL subtypes an approach was chosen which has been proposed by Ferrando and colleagues for discovering novel oncogenes in T-ALL (Ferrando et al., 2002). Following this strategy, in this work the heterogeneous precursor B-ALL samples were projected into an ALL subtype relevant gene space. This gene space was defined to include genes differentially expressed between *t(11q23)/MLL*, *BCR/ABL*, or precursor T-ALL. The resulting hierarchical cluster and principal component analyses demonstrated that the genetically more heterogeneous precursor B-ALL samples intercalate with *BCR/ABL*-positive cases, but were clearly distinct from T-ALL and *t(11q23)/MLL* profiles. Thus, similar expression signatures were observed for both heterogeneous precursor B-ALL and for *BCR/ABL*-positive cases. All genes in this signature were consistently overexpressed in both *BCR/ABL*-positive and the more heterogeneous precursor B-ALL cases compared to T-ALL and *t(11q23)/MLL* samples. In detail, this signature included *LGMN* (legumain), also called asparaginyl endopeptidase (*AEP*). *LGMN* has been reported to be critically involved in the processing of antigens for MHC class II presentation (Schwarz et al., 2002). More recently, a prodrug strategy incorporating a legumain-cleavable peptide substrate onto doxorubicin was developed (Liu et al., 2003a). A receptor tyrosine kinase activated by collagen, *DDR1* (discoidin domain receptor 1), is represented by three probe sets. In a recent report, high-grade primary brain and metastatic brain tumors showed unequivocal, intense *DDR1* expression within the majority of tumor cells (Weiner et al., 2000). *CDW52*, an excellent target for complement-mediated lysis and antibody-dependent cellular cytotoxicity, has been identified by two probe sets. Several clinical trials have already been carried out with Alemtuzumab (CAMPATH-1H), a humanized monoclonal antibody directed against the CDW52 antigen of lymphocytes (Dyer, 1999). A cytokine-like protein (*C17*), retinoic acid induced gene (*RAI14*), or hypothetical protein *LOC54103* represent further overexpressed genes. However, no functional gene annotation is available yet.

Furthermore, the similarity of genetically heterogeneous precursor B-ALL samples to *BCR/ABL* cases was also confirmed in an expanded analysis based on published genes to discriminate six distinct pediatric ALL subtypes, i.e., T-ALL, *E2A/PBX1*, *BCR/ABL*, *TEL/AML1*, *t(11q23)/MLL* and hyperdiploid leukemias (Yeoh et al., 2002). In this analysis, the genetically heterogeneous precursor B-ALL samples repeatedly clustered together and intercalated with *BCR/ABL* cases.

5.3 Novel insights into the biology of t(11q23)/*MLL* leukemias

The *MLL* gene, also termed *ALL-1*, *HRX*, and *TRX1*, located at chromosome band 11q23 is a recurrent target of chromosomal translocations in acute leukemias (Figure 52) (Huret et al., 2001). Leukemias with *MLL* gene aberrations are particularly prevalent in infant leukemias and treatment-related secondary leukemias, and are associated with dismal prognosis (Biondi et al., 2000; Schoch et al., 2003; Pui et al., 2004).

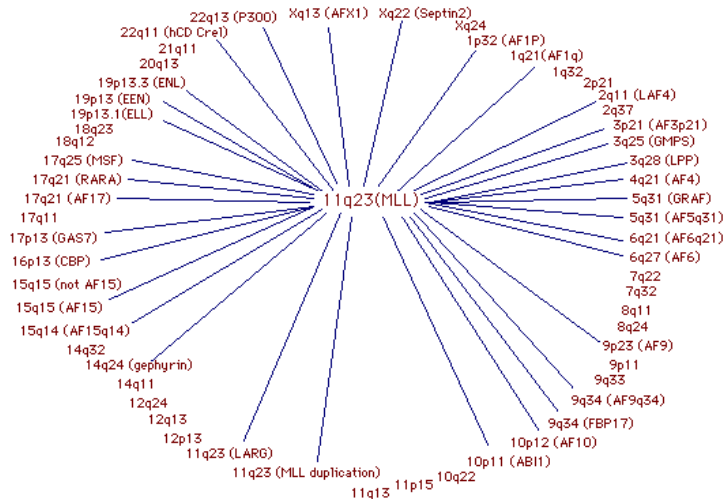


Figure 52. **Overview of *MLL* translocation partners.** For both myeloid and lymphoblastic leukemias *MLL* gene rearrangements have been described (Huret et al., 2001). Reciprocal translocations associated with the *MLL* gene result in in-frame fusion transcripts with various partner genes from at least 50 distinct gene loci.

Both in AML and ALL, a distinct gene expression profile for t(11q23)/*MLL* leukemias was observed. Thus, this work further aimed at identifying common targets of *MLL* chimeric fusion genes. In order to designate common target genes, both types of acute leukemias with *MLL* translocations were combined, and were compared to various types of other precursor B- and T-lineage ALL cases as well as to other cytogenetically defined AML subtypes. This supervised analysis resulted in a list of statistically significant differentially expressed genes irrespective of lineage. A closer examination of these genes showed that also in this data a significantly overexpressed “Hox code” was detectable, i.e., overexpression of *HOX-A* cluster gene members (Kumar et al., 2004). Other genes with higher expression in t(11q23)/*MLL* leukemias have also been previously reported to be implicated in *MLL* related leukemogenesis, i.e., *MEIS1* and *PBX3* (Rozovskaia et al., 2001; Thorsteinsdottir et al., 2001). The t(11q23)/*MLL* leukemias are generally associated with a high risk of treatment failure and therefore novel therapeutic strategies are needed to improve outcome in patients with *MLL* abnormalities. Small molecule inhibitors of FLT3, a receptor tyrosine kinase, may prove to be beneficial (Gilliland and Griffin, 2002). It can be hypothesized that, besides the known mutations affecting the juxtamembrane region and receptor activation loop, a constitutive FLT3 signaling caused by high level expression also contributes to the development and maintenance of t(11q23)/*MLL* leukemias. In recent studies high levels of *FLT3* expression in patients with *MLL* gene rearrangements have been identified and *FLT3* has been successfully validated as a therapeutic target (Armstrong et al., 2002; Armstrong et al., 2003). Also in this work, an

overexpression of *FLT3* in both t(11q23)/*MLL* leukemias compared to other acute leukemia classes was observed.

However, here it could further be demonstrated how the t(11q23)/*MLL* leukemia-associated genes are related to each other in a novel constellation. As given in biological networks consistently upregulated candidates with oncogenic potential included, for example, *RUNX2*, *HIP1*, *FRAT1*, *TAF1B*, and *ZFHX1*. *RUNX2* normally plays a key role in osteogenesis but also a direct oncogenic role had been proposed (Stewart et al., 1997; Ito, 2004). *HIP1* encodes an endocytic protein with transforming properties that is involved in a cancer-causing translocation and which is overexpressed in a variety of human cancers (Hyun and Ross, 2004). Proto-oncogene *FRAT1* represents the human homologue to mouse proto-oncogene *Frat1*, which promotes carcinogenesis through activation of the Wnt/beta-catenin/TCF signaling pathway (Saitoh et al., 2002). *TAF1B* has been identified to play a role in the tumorigenesis of colorectal carcinomas with microsatellite instability (Kim et al., 2002). *ZFHX1* encoding Smad-interacting protein 1 (SIP1), directly represses E-cadherin gene transcription and activates cancer invasion via the upregulation of the matrix metalloproteinase gene family (Miyoshi et al., 2004). Consistently downregulated genes in t(11q23)/*MLL* leukemias included TNF-receptor superfamily members required in TRAIL-mediated apoptosis, *TNFRSF10A* and *TNFRSF10D* (Almasan and Ashkenazi, 2003), or *MADH1* (*SMAD1*), functioning downstream of TGF-beta receptor serine/threonine kinases (ten Dijke et al., 2002). However, it only can be speculated whether the deregulated expression of these genes confer any resistance to apoptotic stimuli.

Novel insights into lineage commitment in t(11q23)/*MLL* leukemias

It was further demonstrated that ALL and AML cases with t(11q23)/*MLL* segregate according the lineage, i.e., myeloid or lymphoblastic, respectively. In unsupervised data analyses the cases with *MLL* gene translocations did not cluster as a unique subgroup, but instead clustered according to their lineage of origin. This leads to the proposal that *MLL* aberrations translate into specific expression signatures but that there is a clear identification of lymphoblastic lineage commitment for ALL with t(11q23)/*MLL*. This seems to be conflictive to the previously reported finding that t(11q23)/*MLL*-positive leukemias are unique and should be constituted as a distinct disease (Armstrong et al., 2002). In contrast, this work demonstrates that this cellular differentiation can be explained by a specific transcriptional program and further elucidated this through the use of biological network analysis. Among the top ranked differentially expressed genes to discriminate ALL and AML cases with t(11q23)/*MLL* *PAX5* was represented. *PAX5* restricts the developmental options of lymphoid progenitors to the B cell lineage by repressing the transcription of lineage-inappropriate genes and simultaneously activating the expression of B-lymphoid signaling molecules (Busslinger, 2004). Its influence can also be followed more downstream when focusing on *PAX5* target genes that are also included in the list of top-ranked differential genes. It is known that, e.g., *BLK* or *CD19* are controlled by *PAX5*. As visualized in the biological networks, these and other B-lineage characteristic candidates (*CD79A*, *VPREB1*, *CD22*) were grouped together, all with higher expression in *MLL* gene rearranged ALL compared to AML samples. Interestingly, not only *PAX5* but also *EBF*, a second

essential regulator of early B cell development was higher expressed in ALL with t(11q23)/*MLL*. Specific activities of these proteins include roles in chromatin remodeling and recruitment of partner proteins (Maier and Hagman, 2002). Taken together, a multitude of genes visualized a strong B-lineage commitment in lymphoblastic t(11q23)/*MLL* leukemias. With respect to AML with t(11q23)/*MLL* a transcriptional pattern for myeloid commitment was represented through the higher expression of key players in myeloid development, *CEBPA* and *SPI1*. The finding that C/EBPalpha binds and activates the endogenous *SPI1* gene in myeloid cells further contributes to the specification of myeloid progenitors (Kummalue and Friedman, 2003). Also, genes encoding the receptors for granulocyte/macrophage colony-stimulating factor (*GM-CSFR*) and granulocyte colony-stimulating factor (*G-CSFR*) clearly underline a completely differing transcriptional program since it has been suggested that G-CSFR signals may play a role in directing the commitment of primitive hematopoietic progenitors to the common myeloid lineage (Richards et al., 2003). Also, the down-regulation of *GM-CSFR* represents a critical event in producing cells with a lymphoid-restricted lineage potential (Iwasaki-Arai et al., 2003). Other differentially expressed genes with higher expression in t(11q23)/*MLL*-positive AML included for example *FES*, a tyrosine kinase oncogene, implicated in signaling downstream from hematopoietic cytokines (Sangrar et al., 2003). *FES* may be a key component of the granulocyte differentiation machinery and contributes to lineage determination at the level of multi-lineage hematopoietic progenitors as well as the more committed granulomonocytic progenitors (Kim et al., 2003). Another gene which may be involved in myeloid differentiation is *MNDA*, encoding the myeloid cell nuclear differentiation antigen (Cousar and Briggs, 1990). It is expressed exclusively in maturing myeloid cells and cell lines and is not expressed in lymphoid cells. Recent data suggest that there is a strong correlation between *MNDA* expression and myeloid differentiation (Asefa et al., 2004). In this work, *MNDA* expression further elucidates the myeloid lineage specificity in t(11q23)/*MLL*-positive AML. Lastly, *CITED4*, a CBP/p300-interacting transcriptional transactivator is significantly higher expressed in AML with t(11q23)/*MLL* (Braganca et al., 2002). It may function as a co-activator for transcription factor AP-2 and possible roles for *CITED4* in regulation of gene expression during development and differentiation of blood cells have been implied (Yahata et al., 2002). Moreover, an exploration of the differentially expressed genes identified in this work may provide new insights into the altered biology of these leukemias and may lead to useful target genes for follow-up experiments. Interesting candidates with higher expression in ALL with t(11q23)/*MLL* for subsequent experimentation include *CBX2* (the homologue of the murine polycomb-like gene M33) and *CBX4* (novel human Pc homolog, *hPc2*), both components of the chromatin-associated polycomb complex. Polycomb group proteins assemble to form large multiprotein complexes and are thought to repress their targets by modifying chromatin structure (Pirrotta, 1998). It has been suggested that interference with *CBX4* function can lead to derepression of proto-oncogene transcription and subsequently to cellular transformation (Satijn et al., 1997).

Influence of the different MLL translocation partners

Another major goal of this section was to directly assess the influence of the different *MLL* translocation partners on the transcriptional program. Thus, a supervised comparison of *MLL/AF9*-positive samples against *MLL/AF9*-negative samples in AML was performed. However, no statistically significant differences were found. Using SAM plots to visualize the degree of differences in their gene expression pattern it was clear that within AML the *MLL/AF9*-positive samples were very similar compared to the *MLL/AF9*-negative samples. Furthermore, as demonstrated by an unsupervised data analysis no clear subclustering of *MLL/AF9*-positive samples was observed. Instead of being distinct from other AML with differing *MLL* gene rearrangements global gene expression patterns of cases with *MLL/AF9* intercalated with other AML with *t(11q23)/MLL*. This transcriptional concordance is an unexpected result. However, it would correlate with the observation of comparable clinical outcome in those subset of AML patients (Schoch et al., 2003). When the algorithm was used to plot signatures of ALL with *t(11q23)/MLL* vs. AML with *t(11q23)/MLL* their completely differing underlying transcriptional profile is visible. This repeatedly reflects the previous finding from the unsupervised two-dimensional hierarchical clustering where *t(11q23)/MLL* samples segregated according to their lineage of origin. Also, it was not possible to clearly specify differentially expressed genes when six different *MLL* partner genes, i.e., *AF9*, *AF6*, *AF10*, and *ELL* in AML and *AF4* as well as *ENL* in ALL, respectively, were examined. At this step no statistically significant expression signatures were found to be correlated with one of the distinct partner genes. This also explains the failure of predicting the respective partner gene based on differential gene expression signatures using SVMs as classification algorithm. It can be observed that the classifier is good at predicting the *MLL* partners *AF9* and *AF4*. However, these sets of samples are the two major groups in the AML and ALL patient cohorts, respectively, and might mean a bias for the result. All other groups are not accurately identified. Misclassifications, on the other side, occur only in the corresponding myeloid or lymphoblastic compartment, respectively. Given the presented data the global gene expression profile analysis does not reveal a clear distinct pattern associated with one of the various partner genes in *t(11q23)/MLL* leukemias.

Taken together, further experiments are required to investigate why most of the *MLL* partner genes are strictly correlated with a specific leukemia subtype. Gene expression is determined not only by the available combination of transcription factors, but also by the structure of the local chromatin, which is the physiological substrate for all nuclear processes including transcription and recombination, and the location of a gene within a chromosome territory (Cremer and Cremer, 2001; Busslinger, 2004). Therefore, it can be speculated that at the time point of the chromosomal aberration the hematopoietic progenitor target cell already is committed to myeloid or lymphoid lineage development. Given the differing chromatin structure and its accessibility to regulatory factors thus only certain genes would be suitable as fusion partner, e.g., *AF4* in lymphoblastic, or *AF9* in myeloid leukemias. On the other hand, if the progenitor target cell is not committed to a particular lineage the fusion partner might be able to contribute to cell-fate decisions. Then the different *MLL* fusion proteins would dictate the respective differentiation pathway by facilitating the establishment of lineage-specific gene expression programs. In

the gene expression patterns described in this work a strong association of lymphoid commitment in ALL with t(11q23)/*MLL* was observed. The coexpression of *PAX5*, the critical B-lineage commitment factor that restricts the developmental options of early progenitors to the B cell pathway, and early B cell factor *EBF* in these samples suggests that the leukemogenic hit did occur in the earliest phase of B-lymphopoiesis.

Typically, the resultant t(11q23)/*MLL* leukemias display features of a maturation arrest at a later stage of differentiation. This has particularly been described by Cozzio and colleagues (Cozzio et al., 2003). In this model, purified progenitor subsets, i.e., hematopoietic stem cells (HSC), common myeloid progenitors (CMP), and the lineal descendent granulocytic/monocytic-restricted progenitors (GMP) were susceptible to *MLL* fusion protein-mediated transformation. Regardless of the initiating cell, targeted by a *MLL/ENL* construct, the resultant leukemias displayed immunophenotypes and gene expression profiles characteristic of a maturation arrest at an identical late state of myelomonocytic differentiation downstream of the GMP.

In human leukemias *MLL/ENL* occurs in both AML and ALL. Interestingly, in the cohort analyzed in this work myeloid and lymphoblastic gene expression profiles of *MLL/ENL* samples were separated. The t(11;19)(q23;p13.1) chromosomal translocation fuses the gene encoding transcriptional elongation factor *ENL* to the *MLL* gene (Rubnitz et al., 1994). Recent data indicate that neoplastic transformation by the *MLL/ENL* fusion protein is likely to result from aberrant transcriptional activation of *MLL* target genes (Zeisig et al., 2004). This finding would further support the model of “lineage promiscuity” a mechanism described for mixed lineage leukemias in the context of *MLL/GAS7* (So et al., 2003). In their study, So et al. had used a retroviral *MLL/GAS7* construct to model acute biphenotypic leukemia (ABL) in mice. Cells that were transformed in vitro were able to induce three different leukemias in vivo, i.e., AML, ALL and ABL, which also exhibited distinct gene expression profiles for a selection of transcripts. The progenitor cells affected by the *MLL* oncogene were phenotypically most comparable to the multipotent progenitor (MPP), the direct progeny of short-term HSC. When injected into sub-lethally irradiated mice the biphenotypic progenitors sequentially further differentiated along the myeloid or lymphoid lineages and induced AML or ALL, respectively.

In conclusion, these results underline that AML with t(11q23)/*MLL* and ALL with t(11q23)/*MLL* are distinct entities as proposed in the current WHO classification of hematological malignancies (Jaffe et al., 2001). Both subtypes share a distinct gene expression signature with upregulation of *HOX* genes but on the other hand vary substantially in the expression of genes determining the lymphoid or myeloid lineage. While a clear gene expression pattern with respect to the lineage was identified, a specific signature associated with the different *MLL* partner genes was not observed. Microarray technology demonstrated that based on a cohort of thoroughly characterized leukemia samples, expression signatures lead to a better understanding of biological features of these specific acute leukemia subtypes. Novel networks of candidate genes were depicted and may inspire follow-up studies to elucidate the events leading to these types of prognostically unfavorable acute leukemias and may be exploited to identify new therapeutic targets.

5.4 Microarray technology as a potential diagnostic platform

Diagnosing and classifying leukemias are clinically highly relevant tasks. In order to guarantee the appropriateness of the results a comprehensive and well-structured approach in the laboratory is required. Significant resources with regard to time, well-trained and skilled personnel, laboratory space and equipment are needed to cover this approach. Furthermore, the interlaboratory reproducibility of the currently applied diagnostic methods, i.e., cytomorphology, cytochemistry, cytogenetics, immunophenotyping, and molecular genetics, ranges only between 56% and 90%, even in experienced hands, and therefore clearly needs improvement (Bennett and Begg, 1981; Argyle et al., 1989; Grimwade et al., 1998; Lucio et al., 2001; Gleissner et al., 2001; Byrd et al., 2002). Gene expression profiling using microarray technology has the potential of optimizing leukemia diagnostics and overcoming the above mentioned shortcomings of current methods. Assumptions that leukemia-specific chromosomal aberrations translate into dramatic changes on the transcriptional level have now been confirmed by several studies from various diagnostic and research centers.

Robustness of diagnostic gene expression patterns

Before a new technology can be used in a diagnostic setting it has to be proven that the methodology can provide robust results. With respect to microarrays, various parameters can principally influence the measured gene expression. In this work it was demonstrated that for a subset of leukemias expression profiling is applicable in a diagnostic setting considering a variety of influencing parameters.

As an example an analysis assessed the impact of different variables of sample manipulation in the context of a diagnostic gene expression signature. Using a set of predefined differentially expressed genes for AML with t(15;17), t(8;21), inv(16), and t(11q23)/*MLL* it was shown that neither the varying duration of sample shipment, nor the overall RNA quality as assessed by the 3'/5' ratio of *GAPD* hybridization signals, nor the duration of sample storage time until microarray target preparation, nor the time point of the sample target preparation within the marker discovery study, nor the age of the leukemia patient at diagnosis, nor the type of specimen, i.e., bone marrow or peripheral blood impair the robustness of diagnostic gene expression patterns. The presented data further indicates that preparations from different operators, and different sample handling procedures, i.e., freezing of cell preparations vs. freshly prepared samples, and storage periods of the samples at -80°C also did not impair the robustness of diagnostic expression signatures. The results of these two analyses provided evidence that those homogeneous signatures would enable an accurate prediction when applied in a diagnostic setting. However, to finally address the robustness of these patterns and their applicability for the diagnosis of leukemias one has to enroll patients in a prospective study in which microarrays are tested as an additional routine diagnostic method in parallel to gold standard diagnostic procedures.

It has to be noted that these analyses not directly addressed the impact of each of the variables involved in sample manipulation in the global pattern of gene expression. It is clear that global gene expression patterns can

dramatically change given the technical aspects of specimen sampling and target preparation. In order to identify the real effect of the discussed variables on gene expression signatures a supervised analysis of the effects of the different manipulation variables on the global pattern of gene expression has to be performed. For example, as postulated by Debey et al. one should try to reduce the time between biopsy and RNA isolation, as within the first 24 hours after sampling changes in expression levels of genes related to hypoxia, metabolism, or apoptosis become measurable (Debey et al., 2004). On the other hand, one should also consider to further investigate the issue of tumor load and contaminating cells that potentially contribute to the gene expression profiles as differences were observed between diagnosis and relapse samples in precursor-B ALL (Staal et al., 2003). In addition, an assessment of the impact of sample origin, i.e., leukemia blast cells purified from bone marrow vs. peripheral blood samples, would also benefit from further investigations. And ideally, future studies will address this question with a larger series of paired samples.

However, it can be speculated that blast cells in the peripheral blood might very well be identical to blasts located in the bone marrow compartment and with respect to a diagnostic application a purity of approximately 80% blast cells can easily be achieved with various techniques for sample enrichment from both compartments. But how much purity is needed at all? A recent study demonstrates that for the overall gene expression profile anything above a 75% pure sample population was found to be indistinguishable from the pure sample (Szaniszlo et al., 2004).

Pediatric signatures can classify adult patients

Another aspect of this work was to test the subsets of markers from recent studies published by Yeoh et al. and Armstrong et al. for their accuracy to predict the known prognostically relevant corresponding adult ALL subclasses (Yeoh et al., 2002; Armstrong et al., 2002). Firstly, it could be demonstrated that the published expression signatures from a pediatric cohort of patients from the St Jude Children's Research Hospital, Memphis, TN, USA, identified with U95A microarrays, also accurately stratify a respective cohort of adult ALL patients with T cell ALL, *BCR/ABL*, or *t(11q23)/MLL*, analyzed with U133A microarrays. All important U95A chip design candidate genes to discriminate ALL with *MLL* gene translocation, *t(9;22)*-positive ALL, and T-ALL were matched to the corresponding U133A probe sets from the adult gene expression profiles. Then the independent cohort of adult ALL patients was accurately classified using common machine learning algorithms. In this way, the diagnostic power of previously reported gene expression signatures has been validated and confirmed on a truly independent patient cohort across different array designs and age groups of patients. Another analysis further supported this finding, i.e., the applicability of pediatric markers to classify adult patients. In a second approach, published data on pediatric ALL samples from the Armstrong et al. study (Dana-Farber Cancer Institute, Boston, MA, USA) was compared to adult patients. Repeatedly, patterns from pediatric patients are intriguingly reproducible and precisely predict *MLL* gene rearrangements in adult ALLs. Similarly, the pediatric markers had been identified with the U95A design and were validated with the U133A array design. In both of these comparisons, not

only the type of array differed, but also parameters such as technical equipment, different sample handling, routine diagnostic procedures, and target preparation protocol for expression analysis by unrelated personnel in a different laboratory. Even so, the diagnostic composition of genes demonstrates robust and reproducible signatures. Finally, both published data sets were mined for overlapping genes specific for t(11q23)/*MLL* and non-t(11q23)/*MLL* subtypes. A substantial number of genes characterizing patient samples with *MLL* rearrangements was contained in both public available data sets and subsequently was used to classify the corresponding adult cases. Again, based on the given preselected gene expression data a SVM classification engine demonstrated the accurate discriminative properties of those specific candidate genes and accordingly separated the adult ALL samples into t(11q23)/*MLL*-positive and t(11q23)/*MLL*-negative cases. Taken together, these observations now provide strong evidence that genes suitable for classification and prediction of childhood ALL are also capable of distinguishing the respective adult ALL subentities. Moreover, this is a promising finding, as new molecular targets in common genetic subtypes of acute leukemias identified by microarray technology might be common therapeutic targets for both age groups of patients.

In a recent study using U133A oligonucleotide microarrays Ross et al. from the St Jude Children's Research Hospital, Memphis, TN, USA, demonstrated that also pediatric AML share a specific gene expression signature (Ross et al., 2004). Their study included a representation of the known morphologic, genetic and prognostic subtypes of childhood AML samples, namely t(15;17), t(8;21), inv(16), *MLL* rearrangements, acute megakaryocytic morphology (FAB-M7), or samples lacking any of these features. A variety of algorithms showed that the top 50 ranked probe sets for each subtype tightly cluster those cases into the respective subgroups. Moreover, when these probe sets were used in a supervised learning algorithm to classify cases from a blinded test set, 100% diagnostic accuracies were obtained for t(15;17), t(8;21), inv(16), and FAB-M7, and 93% accuracy for cases with *MLL* rearrangement (95% confidence interval: [79%; 99%]). Optimal class assignment was achieved with as few as five probe sets, which is the smallest number they had tested, for t(15;17), t(8;21), inv(16), and FAB-M7, and 35 probe sets for cases with *MLL* rearrangements. Since the incidence of AML is significantly higher in adults than in pediatric patients, they also assessed whether the specific expression patterns from their pediatric patients could be used to accurately diagnose these specific corresponding AML subtypes in adults. When the identified discriminating probe sets were used in the supervised learning algorithm, an available cohort of 20 adult de novo AML patients was classified with an overall diagnostic accuracy of 90% (95% confidence interval: [68%; 98%]). These data suggest that also in AML class discriminating probe sets selected from a cohort of pediatric cases can be used to accurately diagnose adult cases. However, even more interesting is the fact that their adult AML samples were from a different ethnic group as the samples were all from patients diagnosed in a hospital in Taipei, Taiwan. Therefore, the classification of adult AML samples is not only possible using specific gene expression signatures previously identified in pediatric samples, but also allows to predict samples from a differing ethnic group. As indicated in their study,

gene signatures identified in Caucasians allowed the stratification of Asian patients.

Correlation of gene expression with conventional diagnostic methods

In routine clinical hematology the peroxidase test is important for the identification of AML subtypes according to the FAB classification. The determination of the mean positivity of peroxidase-positive cells results in classifying leukemias into peroxidase-positive (myeloid or monocytic) and peroxidase-negative (lymphoblastic) cases (Theml et al., 2004). In this work it was of specific interest to investigate the correlation of gene expression data with results from conventional diagnostic methods. Thus, in a first approach gene expression data was compared to data on the percentage of myeloperoxidase-positive cells as measured by a standard cytochemistry protocol on bone marrow smears in the different FAB subtypes. In 130 samples representing the subtypes M0 through M6, all measured both by cytochemistry and microarray analysis, a high correlation of the mean signal intensity for the *MPO* gene to the percentage of myeloperoxidase positive cells was observed. This underlines the fact that microarray technology can reproduce the classification of AML FAB subtypes (Haferlach et al., 2003a).

Multiparameter flow cytometry is a standard method for diagnosing and subclassifying AML and ALL. In a second aspect of this work gene expression data obtained by microarray analyses was compared to protein expression data determined by multiparameter flow cytometry. A group of 39 relevant markers in 113 patients with newly diagnosed AML and ALL and 4 normal bone marrow samples were assessed and analyzed by both methods simultaneously. A high degree of correlation between protein expression and mRNA abundance was observed with regard to both positivity/negativity and quantitative data. In 1,512 of 2,187 (69.1%) comparisons congruent results were obtained with regard to positivity or negativity of expression. Most importantly, in antigens highly relevant for diagnosing and subclassifying AML and ALL, namely CD13, CD33, MPO, CD22, CD79a, CD19, CD10, and TdT, congruent results were obtained in 75% to 100%. These data are considered as evidence that protein expression is highly correlated with mRNA abundance in AML and ALL. While the high degree of congruence of the comparisons might have been anticipated the incongruent cases need specific considerations. It has to be noted that the incongruent cases were not due to differences of cells analyzed, since both methods were applied to the same fractions of cells as obtained by Ficoll-Hypaque density gradient centrifugation.

Positive results in microarrays and at the same time negative results in flow cytometry most probably indicate that the abundance of the respective mRNA is not sufficient to result in positivity for protein expression as defined in these analyses, i.e., detection of protein by flow cytometry in $\geq 20\%$ ($\geq 10\%$ for cytoplasmic antigens) of gated cells with limit a for positivity set by 99% of cells analyzed as isotype controls. It must be taken into consideration that the analytic strategy applied for flow cytometry included gating on all cells and better sensitivity is anticipated for gating on blasts or specific subpopulations. This, however, is not possible for microarray analysis and was not the scope of the present analyses.

On the other hand, positivity in flow cytometry and at the same time negativity by microarray analysis may be due to non-specific binding of antibodies in flow cytometry or lack of sensitivity of microarray analysis which cannot be further substantiated in the present setting. In addition, it is obvious that the results that were positive in flow cytometry and negative in microarray analysis mainly involved lymphoid-associated markers while the results that were positive in microarray analysis and negative in flow cytometry typically involved myeloid-associated antigens. Thus, in the latter cases microarray analysis might have detected mRNA from residual normal hematopoietic cells which account for less than 10%-20% of all cellularity in the sample and might be related to the lower sensitivity of flow cytometry which is at least in part limited in the present analyses by the placement of arbitrary cut-off levels for positivity. Though this is not in accordance with the consensus for diagnostic purposes this strategy has provided the only possibility to directly compare results from flow cytometry and microarray analysis with regard to positivity and negativity. These shortcomings must be taken into account when speculating on a complementary role of microarray analysis in addition to flow cytometry for diagnosing acute leukemias.

However, microarray analysis may be able to detect mRNA of disease-specific genes when flow cytometry reveals negative results and may thus optimize diagnostic procedures. Moreover, one can speculate that new antigens may be identified in the gene expression profiles, which are expressed on the cell surface of AML and ALL cells and which may be promising future targets to monitoring minimal residual disease.

Global approach to the diagnosis of leukemia using expression profiling

This work further demonstrates a very high degree of accuracy for the correct assignment of patient samples to all clinically relevant subgroups of leukemia and to normal bone marrow, respectively. A cohort of 937 patients representing 13 distinct classes has been classified with an accuracy of 95.1%. An essential basis for the achievement of this accuracy was the careful and comprehensive use of standard methods to characterize all of the samples before they underwent microarray analysis. Besides the use of cytomorphology and cytochemistry, the samples were processed applying immunophenotyping, cytogenetics, and molecular genetics in order to allow the subsequent optimal supervised identification of pure subtype-specific gene expression patterns and to exclude any misclassification of samples or overlaps between the subcategories focused on in the microarray analyses. In total, 12 distinct leukemia subtypes were addressed in a multiclass classification approach. The relative distribution of the analyzed cases with regard to these subgroups reflects that there has been no selection bias. Moreover, the age distribution of the analyzed cohort is very similar to the true age distribution of patients with AML as well as with the other diseases analyzed.

With regard to AML, more than 50 different recurrent cytogenetic abnormalities have been described. However, reliable data on their prognostic impact are available only for the most frequent ones. These include t(15;17), t(8;21), and inv(16), which are associated with a favorable outcome, and complex aberrant karyotypes and t(11q23)/*MLL* carrying an unfavorable prognosis (Grimwade et al., 1998; Schoch et al., 2001; Grimwade et al., 2001;

Schoch et al., 2003; Schoch et al., 2004b). The remaining cases, i.e., normal karyotypes and so-called other cytogenetic abnormalities, have an intermediate prognosis. The separation between these subgroups results in highly differing prognoses supporting the clinical relevance of the selection of AML subgroups in the present work. There are even more subgroups, in particular in AML, which have been suggested to feature a biologically homogeneous background with potential impact on the clinical course of patients being affected by these abnormalities (Tallman, 2004b). Examples are mutations of *CEBPA* (Preudhomme et al., 2002), length mutations of *FLT3* (Schnittger et al., 2002), and partial tandem duplications of *MLL* (Schnittger et al., 2000). However, since this evidence is still under evaluation in clinical trials these subgroups have not been the focus of the present work. With regard to clinical relevance, similar characteristics apply to the different entities of ALL included in the analyses. Besides the separation of precursor T-ALL from precursor B-ALL, it is important to identify those with Pro-B-ALL and t(11q23)/*MLL*, c-ALL or Pre-B-ALL and t(9;22), as well as mature B-ALL with t(8;14). These subentities differ highly with respect to prognostic impact and require substantially differing therapies which is true for mature B-ALL in particular (Hoelzer et al., 1996; Pui et al., 2004). Because it was known that the gene expression profiles of ALL with and without t(9;22), respectively, are difficult to distinguish from other cases with t(9;22) it was not approached in the first step but in a second step of the analyses. The overall smaller numbers of cases with CLL, CML, and “non-leukemia” had been chosen because these entities are biologically and clinically more homogeneous as compared to the acute leukemia cases discussed above.

In AML, the detection of six different subgroups was approached. For the classification of AML with t(15;17), t(8;21), and inv(16), respectively, the highest degree of accuracy was achieved with 42 out of 42, 36 out of 38, and 48 out of 49 correct assignments by 10-fold CV and an average number of correct predictions of 14 out of 14, 11.4 out of 12, and 15.7 out of 16, respectively, by resampling. Accordingly, all of the median sensitivities and specificities were 100%. This is in line with previous reports describing a unique biological background for these subentities (Alcalay et al., 2001; Mecucci et al., 2002; Tenen, 2003), which is reflected in distinct gene expression profiles. However, since the latter have not yet been assessed by microarray analysis in the context of the full spectrum of AML and the other leukemias, the present study adds important information by clearly demonstrating that based on their distinct features these subentities can be accurately predicted even in the context of the very heterogeneous background of other acute and chronic leukemias. The other three subtypes AML with t(11q23)/*MLL*, AML with complex karyotype, and AML normal/other, have a more heterogeneous biology. This is reflected by different partner genes of the *MLL* gene and an overall heterogeneity with regard to cytogenetic and molecular genetic aberrations, respectively. With these complexities in mind, it was anticipated that misclassifications would occur. Importantly, however, out of the 24 misclassifications (total, 491 classifications) in these subgroups only four were misclassified into the non-AML subgroups. As a consequence, while the median specificities for AML with t(11q23)/*MLL* and for AML with complex aberrant karyotype were very high (both 99.7% and 99.7%), the median specificity for AML normal/other of 93.7% highlights the need for further improvements of the applied methodology or for

the use of supplemental analyses in these cases. In particular, this is true since a small number of samples with ALL (n=11), CLL (n=1), CML (n=2), and non-leukemia (n=2) were classified into this subgroup.

With the exception of the three samples described above there have been no misclassifications in CLL and CML in the 10-fold CV analysis. Accordingly, CLL and CML were correctly assigned in 14.62 out of 15 and 23.82 out of 25 resampling predictions, respectively. As a result, the median sensitivities (100% and 96.0%) and the clinically most important median specificities (100% and 99.7%) were very high for these distinct disease entities. In addition, all of the four subgroups of ALL analyzed in the present study could be classified with a high median accuracy (99.7% for c-ALL/Pre-B-ALL, 100% for the other subgroups). As discussed above, most of the misclassifications (11 out of 13) occurred into the group AML normal/other. Interestingly, these cases did not feature the immunophenotype of an aberrant expression of myeloid antigens which is often observed in ALL cases.

Previous studies disclosed difficulties in separating c-ALL/Pre-B-ALL cases with t(9;22) from other precursor B-ALL cases resulting in prediction accuracies of 80% (Yeoh et al., 2002). Thus, the approach in the present study was to include c-ALL/Pre-B-ALL cases combined as one class irrespective of the presence of t(9;22) into the analysis and to separate cases positive for t(9;22) from those without it in a second step. While the separation of c-ALL/Pre-B-ALL cases from the other entities has been straight forward, difficulties in separating t(9;22)-positive from t(9;22)-negative cases were observed (only 82.9% accuracy). Interestingly, the corresponding hierarchical cluster analysis demonstrates that the majority of cases are accurately grouped in one of the two categories. However, a third branch becomes evident revealing a gene expression pattern distinct from the two categories. The hypothesis that a further and not yet identified genetic lesion could be responsible for this third branch has been abandoned due to a follow-up cluster analysis and classification approach which did not reveal a reproducible gene expression pattern different from the other two groups (data not shown). Furthermore, the use of a classifier with differentially expressed genes selected based on the comparison of only the first two more homogeneous groups did not result in a more accurate assignment of samples of the third group either (data not shown). Taken together, this supports the concept that *BCR/ABL* represents a type 1 mutation (Gilliland and Griffin, 2002) and downstream pathways are shared by many other master genes. Thus, the gene expression profile of t(9;22)-positive ALL cases is not highly specific.

Another clinically relevant subgroup has also been approached in a second step. After separation of T-ALL from all other entities the subgroup of immature T-ALL has been discriminated from cortical T-ALL, which in the clinical setting is characterized by a favorable prognosis (Onciu et al., 2002). Again, the separation of both entities has been highly accurate with the exception of two samples that originally were classified by immunophenotyping as immature T-ALL. It is important to note that the definition of cortical T-ALL is based only on the positivity for antigen CD1a (Bene et al., 1995), while other T cell markers CD7, CD2, CD5, CD4, or CD8 may be positive in either subgroup. Intriguingly, while the use of CD1a is a diagnostic standard the presented analysis suggests that in the two misclassified cases the overall gene

expression profile is very similar to the cortical T-ALL signature. Thus, these two cases may be rather cortical T-ALL featuring an aberrant lack of CD1a expression than truly be immature T-ALL. As a consequence of this work, the classification of cortical T-ALL may not only be based on the positivity for CD1a, but also include other markers such as the differentially expressed gene *PAWR* (Johnstone et al., 1996). In this regard further implications may be gained from analyzing the cellular function of top differentially expressed genes when comparing immature T-ALL to cortical T-ALL. It is known that dexamethasone leads to a downregulation of *CARD4* (Galon et al., 2002) which encodes a pro-apoptotically acting protein (Bertin et al., 1999; Inohara et al., 1999). Since *CARD4* is highly expressed in cortical T-ALL corticoid therapy may be less effective in this entity as compared to immature T-ALL. However, clinical studies are needed to prove this hypothesis.

A particularly important issue which has not yet been substantially addressed in other microarray studies so far is the identification of non-leukemic bone marrow and its discrimination from all leukemia subtypes (Hofmann et al., 2002; Whitney et al., 2003; Jelinek et al., 2003). In this work, 42 out of 45 non-leukemia samples have been accurately predicted. Of the misclassifications one sample was classified as AML with t(11q23)/*MLL* and two cases as AML normal/other (10-fold CV). The median accuracy by resampling analysis has been 13.23 out of 15 independent test samples. Importantly, the median specificity for non-leukemia is 99.6% while the sensitivity is 90.0%. As a consequence, until improvements of the applied methods are achieved which better characterize the heterogeneous subgroup of AML normal/other it seems appropriate to add conventional methods, if the microarray analysis result assigns a sample to the latter subgroup. In contrast, due to its high specificity the result "non-leukemia" can be the basis to exclude the presence of leukemia in a given sample analyzed.

In general, there are two strategies to handling the occurrence of misclassifications obtained by microarray analysis. The first one is to identify the most frequent false positive result, i.e., the subgroup with the lowest specificity, and to add conventional diagnostic procedures to confirm or revise a malignant diagnosis. Clearly, this applies for AML normal/other with a median specificity of 93.7% (95% confidence interval of accuracy: [90.2%; 96.6%]). Through the use of cytochemistry, immunophenotyping, and cytogenetics the discrimination of this subgroup from c-ALL/Pre-B-ALL, AML with t(11q23)/*MLL*, and AML with complex aberrant karyotype is straight forward although obviously consuming significant resources. Another possible application for additional methods is the use of RT-PCR to identify or exclude the presence of the *BCR/ABL* fusion gene once c-ALL/Pre-B-ALL is diagnosed. The second and more promising strategy would be an improvement of the content on the microarray by taking advantage of the additional representation of oligonucleotides specific for leukemic fusion genes. Through this approach, many of the misclassifications should be avoidable, e.g., c-ALL/Pre-B-ALL with t(9;22) should be identifiable by the detection of *BCR/ABL* as should AML with t(11q23)/*MLL* by the detection of fusion genes involving *MLL* and various partners (Repp et al., 1995). This approach would potentially result in even higher accuracies in the subgroups discussed above as well as improving accuracies in other subgroups.

5.5 Concluding remarks

In conclusion, in this work a large-scale gene expression database of distinct leukemia types and subtypes has been generated, analyzed, and interpreted. It provides a valuable resource for the forthcoming post-genomic dissection of the complexities of genetic networks and the biological phenotypes emerging from them. Furthermore, it is envisioned that this data set provides significant new insights into the specific genetic alterations of distinct entities. Possibly, it will allow the discovery of novel markers which can be targeted by RT-PCR-based assays and multiparameter flow cytometry. Then, given the gene expression signatures at the time point of diagnosis, individualized for each patient, specific markers might be suitable to quantify minimal residual disease during the course of anti-leukemic treatment.

Hypotheses that leukemia-specific chromosomal aberrations translate into dramatic changes on the transcriptional level have now been confirmed by several studies from various diagnostic laboratories and research centers. Specific subtypes of acute leukemia can be classified by gene expression signatures with exceedingly high accuracies. The analyses presented in this work followed these published studies and additionally provided the opportunity, by focusing on all clinically relevant subtypes of chronic and acute leukemias in a single comprehensive approach, to build on these expression signatures and develop a highly accurate diagnostic tool. Also important is that the separation of leukemia samples from samples with non-malignant diseases and from healthy volunteers has been accomplished. A future scenario which may result from this work includes the wide-spread use of microarray technology applying a carefully designed and comprehensive leukemia diagnostic microarray which allows a significant improvement of current standard diagnostics by strengthening the diagnostic accuracy and by a more efficient allocation of resources.

What are the next steps for the development of a diagnostic tool? Firstly, the costs are no longer insurmountable. Especially, new advances in gene expression profiling, particularly with regard to instrumentation and reliability of assays for sample target preparation have paved the way to now enroll patients in prospective multi-center trials. In these studies, microarrays can be tested as an additional routine diagnostic method in parallel to gold standard procedures. Moreover, the design of a custom array will also optimize costs and needs for sample material. Thus, it is more a question of when will microarrays routinely be used for subclassification of leukemias and what methods performed today can be replaced. On the other side, with respect to the development of a clinical diagnostic test, a smaller number of genes could also be evaluated using alternative technologies such as multiplexed, quantitative RT-PCR. As such, these prospective studies might also address the question how these findings will be translated into a diagnostic test, either custom-designed microarray or multiplexed, quantitative RT-PCR.

Ultimately, new advances in genomic technologies, such as whole-genome microarrays will contribute to the central goals of parsing malignancies into specific diagnostic categories defined by recurrent molecular abnormalities, and targeting the essential oncogenic pathways with specific therapies. As has been the case to date, this molecular reformation of oncology will likely be led

by hematologic malignancies (Ebert and Golub, 2004). However, one should always consider not focusing too early on the establishment of unstable markers or finalization of the technical platform. Only without compromising existing standards of care these new advances in genomic medicine will successfully be translated from a genomic dissection of a complex disease into a novel platform to diagnose leukemias.

Besides the diagnostic aspect of distinct gene expression signatures underlying patterns in gene expression might also allow to identify new classes in categories which have not yet been further distinguished. For example, the identification of prognostic markers or marker constellations providing the opportunity to predict the response to anti-leukemic treatment is another highly relevant clinical topic which is currently evolving and will be covered by future microarray trials. Especially in AML, the current classification system does not fully reflect the molecular heterogeneity of the disease, and treatment stratification is difficult, e.g., for patients with intermediate-risk with a normal karyotype. Recently, Bullinger and colleagues had identified new molecular subtypes of AML, including two prognostically relevant subgroups in AML with a normal karyotype. Their 133-gene clinical-outcome predictor accurately predicted overall survival in their cohort of patients (Bullinger et al., 2004). Thus, the use of gene expression profiling may further result in a molecular prognostication.

However, so far those findings are based on a limited number of patient samples or training and testing sets, respectively. More importantly, discriminative genes were in most studies validated using expression profiles generated in one specific setting of an individual laboratory or diagnostic center. In order to become generally accepted, either as an additional method for diagnosis or prognostication, the robustness of subtype-specific gene expression signatures for leukemia subclassification has to be proven on large series of independent and unselected patient samples. Thus, a prospective validation of the results of recent microarray studies is a challenging aspect for the future. In this way it will be possible to define gene expression-based molecular classifiers and predictors for outcome that are accurate and reproducible.

6. References

- Alcalay M, Orleth A, Sebastiani C, Meani N, Chiaradonna F, Casciari C, Scirpi MT, Gelmetti V, Riganelli D, Minucci S et al. 2001. Common themes in the pathogenesis of acute myeloid leukemia. *Oncogene* 20:5680-5694.
- Alizadeh AA, Eisen MB, Davis RE, Ma C, Lossos IS, Rosenwald A, Boldrick JC, Sabet H, Tran T, Yu X et al. 2000. Distinct types of diffuse large B-cell lymphoma identified by gene expression profiling. *Nature* 403:503-511.
- Almasan A, Ashkenazi A. 2003. Apo2L/TRAIL: apoptosis signaling, biology, and potential for cancer therapy. *Cytokine Growth Factor Rev* 14:337-348.
- Altman DG. 2004. *Practical Statistics for Medical Research*. CRC Press: London.
- Argyle JC, Benjamin DR, Lampkin B, Hammond D. 1989. Acute nonlymphocytic leukemias of childhood. Inter-observer variability and problems in the use of the FAB classification. *Cancer* 63:295-301.
- Armstrong SA, Staunton JE, Silverman LB, Pieters R, Den Boer ML, Minden MD, Sallan SE, Lander ES, Golub TR, Korsmeyer SJ. 2002. MLL translocations specify a distinct gene expression profile that distinguishes a unique leukemia. *Nat Genet* 30:41-47.
- Armstrong SA, Kung AL, Mabon ME, Silverman LB, Stam RW, Den Boer ML, Pieters R, Kersey JH, Sallan SE, Fletcher JA et al. 2003. Inhibition of FLT3 in MLL. Validation of a therapeutic target identified by gene expression based classification. *Cancer Cell* 3:173-183.
- Asefa B, Klarmann KD, Copeland NG, Gilbert DJ, Jenkins NA, Keller JR. 2004. The interferon-inducible p200 family of proteins: a perspective on their roles in cell cycle regulation and differentiation. *Blood Cells Mol Dis* 32:155-167.
- Ashburner M, Ball CA, Blake JA, Botstein D, Butler H, Cherry JM, Davis AP, Dolinski K, Dwight SS, Eppig JT et al. 2000. Gene ontology: tool for the unification of biology. The Gene Ontology Consortium. *Nat Genet* 25:25-29.
- Barnett D, Granger V, Kraan J, Whitby L, Reilly JT, Papa S, Gratama JW. 2000. Reduction of intra- and interlaboratory variation in CD34+ stem cell enumeration using stable test material, standard protocols and targeted training. DK34 Task Force of the European Working Group of Clinical Cell Analysis (EWGCCA). *Br J Haematol* 108:784-792.
- Bene MC, Castoldi G, Knapp W, Ludwig WD, Matutes E, Orfao A, van't Veer MB. 1995. Proposals for the immunological classification of acute leukemias. European Group for the Immunological Characterization of Leukemias (EGIL). *Leukemia* 9:1783-1786.
- Bennett JM, Catovsky D, Daniel MT, Flandrin G, Galton DA, Gralnick HR, Sultan C. 1976. Proposals for the classification of the acute leukaemias. French-American-British (FAB) co-operative group. *Br J Haematol* 33:451-458.
- Bennett JM, Catovsky D, Daniel MT, Flandrin G, Galton DA, Gralnick HR, Sultan C. 1980a. A variant form of hypergranular promyelocytic leukaemia (M3). *Br J Haematol* 44:169-170.
- Bennett JM, Catovsky D, Daniel MT, Flandrin G, Galton DA, Gralnick HR, Sultan C. 1980b. A variant form of hypergranular promyelocytic leukemia (M3). *Ann Intern Med* 92:261.
- Bennett JM, Begg CB. 1981. Eastern Cooperative Oncology Group study of the cytochemistry of adult acute myeloid leukemia by correlation of subtypes with response and survival. *Cancer Res* 41:4833-4837.

- Bennett JM, Catovsky D, Daniel MT, Flandrin G, Galton DA, Gralnick HR, Sultan C. 1985. Proposed revised criteria for the classification of acute myeloid leukemia. A report of the French-American-British Cooperative Group. *Ann Intern Med* 103:620-625.
- Bertin J, Nir WJ, Fischer CM, Tayber OV, Errada PR, Grant JR, Keilty JJ, Gosselin ML, Robison KE, Wong GH et al. 1999. Human CARD4 protein is a novel CED-4/Apaf-1 cell death family member that activates NF-kappaB. *J Biol Chem* 274:12955-12958.
- Biondi A, Cimino G, Pieters R, Pui CH. 2000. Biological and therapeutic aspects of infant leukemia. *Blood* 96:24-33.
- Bittner M, Meltzer P, Chen Y, Jiang Y, Seftor E, Hendrix M, Radmacher M, Simon R, Yakhini Z, Ben Dor A et al. 2000. Molecular classification of cutaneous malignant melanoma by gene expression profiling. *Nature* 406:536-540.
- Bolufer P, Barragan E, Sanz MA, Martin G, Bornstein R, Colomer D, Delgado MD, Gonzalez M, Marugan I, Roman J et al. 1998. Preliminary experience in external quality control of RT-PCR PML-RAR alpha detection in promyelocytic leukemia. *Leukemia* 12:2024-2028.
- Bowtell DD. 1999. Options available--from start to finish--for obtaining expression data by microarray. *Nat Genet* 21:25-32.
- Braganca J, Swingler T, Marques FI, Jones T, Eloranta JJ, Hurst HC, Shioda T, Bhattacharya S. 2002. Human CREB-binding protein/p300-interacting transactivator with ED-rich tail (CITED) 4, a new member of the CITED family, functions as a co-activator for transcription factor AP-2. *J Biol Chem* 277:8559-8565.
- Buchner T, Hiddemann W, Berdel WE, Wormann B, Schoch C, Fonatsch C, Loffler H, Haferlach T, Ludwig WD, Maschmeyer G et al. 2003. 6-Thioguanine, Cytarabine, and Daunorubicin (TAD) and High-Dose Cytarabine and Mitoxantrone (HAM) for Induction, TAD for Consolidation, and Either Prolonged Maintenance by Reduced Monthly TAD or TAD-HAM-TAD and One Course of Intensive Consolidation by Sequential HAM in Adult Patients at All Ages With De Novo Acute Myeloid Leukemia (AML): A Randomized Trial of the German AML Cooperative Group. *J Clin Oncol* 21:4496-4504.
- Bullinger L, Dohner K, Bair E, Frohling S, Schlenk RF, Tibshirani R, Dohner H, Pollack JR. 2004. Use of gene-expression profiling to identify prognostic subclasses in adult acute myeloid leukemia. *N Engl J Med* 350:1605-1616.
- Burmeister T, Maurer J, Aivado M, Elmaagacli AH, Grunebach F, Held KR, Hess G, Hochhaus A, Hoppner W, Lentges KU et al. 2000. Quality assurance in RT-PCR-based BCR/ABL diagnostics--results of an interlaboratory test and a standardization approach. *Leukemia* 14:1850-1856.
- Busslinger M. 2004. Transcriptional control of early B cell development¹. *Annu Rev Immunol* 22:55-79.
- Byrd JC, Mrozek K, Dodge RK, Carroll AJ, Edwards CG, Arthur DC, Pettenati MJ, Patil SR, Rao KW, Watson MS et al. 2002. Pretreatment cytogenetic abnormalities are predictive of induction success, cumulative incidence of relapse, and overall survival in adult patients with de novo acute myeloid leukemia: results from Cancer and Leukemia Group B (CALGB 8461). *Blood* 100:4325-4336.
- Campana D, Behm FG. 2000. Immunophenotyping of leukemia. *J Immunol Methods* 243:59-75.
- Chang CC, Lin CJ. 2001. LIBSVM: a library for support vector machines. Software is available online (www.csie.ntu.edu.tw/~cjlin/libsvm/).

- Cousar JB, Briggs RC. 1990. Expression of human myeloid cell nuclear differentiation antigen (MNDA) in acute leukemias. *Leuk Res* 14:915-920.
- Cozzio A, Passegue E, Ayton PM, Karsunky H, Cleary ML, Weissman IL. 2003. Similar MLL-associated leukemias arising from self-renewing stem cells and short-lived myeloid progenitors. *Genes Dev* 17:3029-3035.
- Craig W, Poppema S, Little MT, Dragowska W, Lansdorp PM. 1994. CD45 isoform expression on human haemopoietic cells at different stages of development. *Br J Haematol* 88:24-30.
- Cremer T, Cremer C. 2001. Chromosome territories, nuclear architecture and gene regulation in mammalian cells. *Nat Rev Genet* 2:292-301.
- Debernardi S, Lillington DM, Chaplin T, Tomlinson S, Amess J, Rohatiner A, Lister TA, Young BD. 2003. Genome-wide analysis of acute myeloid leukemia with normal karyotype reveals a unique pattern of homeobox gene expression distinct from those with translocation-mediated fusion events. *Genes Chromosomes Cancer* 37:149-158.
- Debey S, Schoenbeck U, Hellmich M, Gathof BS, Pillai R, Zander T, Schultze JL. 2004. Comparison of different isolation techniques prior gene expression profiling of blood derived cells: impact on physiological responses, on overall expression and the role of different cell types. *Pharmacogenomics J* 4:193-207.
- Degos L, Wang ZY. 2001. All trans retinoic acid in acute promyelocytic leukemia. *Oncogene* 20:7140-7145.
- Dick FR, Armitage JO, Burns CP. 1982. Diagnostic concurrence in the subclassification of adult acute leukemia using French-American-British criteria. *Cancer* 49:916-920.
- Dohner H, Stilgenbauer S, Benner A, Leupolt E, Krober A, Bullinger L, Dohner K, Bentz M, Lichter P. 2000. Genomic aberrations and survival in chronic lymphocytic leukemia. *N Engl J Med* 343:1910-1916.
- Downing JR, Shannon KM. 2002. Acute leukemia: a pediatric perspective. *Cancer Cell* 2:437-445.
- Druker BJ, Sawyers CL, Kantarjian H, Resta DJ, Reese SF, Ford JM, Capdeville R, Talpaz M. 2001. Activity of a specific inhibitor of the BCR-ABL tyrosine kinase in the blast crisis of chronic myeloid leukemia and acute lymphoblastic leukemia with the Philadelphia chromosome. *N Engl J Med* 344:1038-1042.
- Dudoit S, Gentleman RC, Quackenbush J. 2003. Open source software for the analysis of microarray data. *Biotechniques Suppl*:45-51.
- Dugas M, Schoch C, Schnittger S, Haferlach T, Danhauser-Riedl S, Hiddemann W, Messerer D, Uberla K. 2001. A comprehensive leukemia database: integration of cytogenetics, molecular genetics and microarray data with clinical information, cytomorphology and immunophenotyping. *Leukemia* 15:1805-1810.
- Duggan DJ, Bittner M, Chen Y, Meltzer P, Trent JM. 1999. Expression profiling using cDNA microarrays. *Nat Genet* 21:10-14.
- Dyer MJ. 1999. The role of CAMPATH-1 antibodies in the treatment of lymphoid malignancies. *Semin Oncol* 26:52-57.
- Ebert BL, Golub TR. 2004. Genomic Approaches to Hematologic Malignancies. *Blood* 104:923-932.

- Eisen MB, Spellman PT, Brown PO, Botstein D. 1998. Cluster analysis and display of genome-wide expression patterns. *Proc Natl Acad Sci U S A* 95:14863-14868.
- Emig M, Saussele S, Wittor H, Weisser A, Reiter A, Willer A, Berger U, Hehlmann R, Cross NC, Hochhaus A. 1999. Accurate and rapid analysis of residual disease in patients with CML using specific fluorescent hybridization probes for real time quantitative RT-PCR. *Leukemia* 13:1825-1832.
- Evans CA, Ariffin S, Pierce A, Whetton AD. 2002. Identification of primary structural features that define the differential actions of IL-3 and GM-CSF receptors. *Blood* 100:3164-3174.
- Fenaux P, Chevret S, Guerci A, Fegueux N, Dombret H, Thomas X, Sanz M, Link H, Maloisel F, Gardin C et al. 2000. Long-term follow-up confirms the benefit of all-trans retinoic acid in acute promyelocytic leukemia. *European APL group. Leukemia* 14:1371-1377.
- Ferrando AA, Look AT. 2000. Clinical implications of recurring chromosomal and associated molecular abnormalities in acute lymphoblastic leukemia. *Semin Hematol* 37:381-395.
- Ferrando AA, Neuberg DS, Staunton J, Loh ML, Huard C, Raimondi SC, Behm FG, Pui CH, Downing JR, Gilliland DG et al. 2002. Gene expression signatures define novel oncogenic pathways in T cell acute lymphoblastic leukemia. *Cancer Cell* 1:75-87.
- Fields S, Kohara Y, Lockhart DJ. 1999. Functional genomics. *Proc Natl Acad Sci U S A* 96:8825-8826.
- Fonatsch C, Schaadt M, Kirchner H, Diehl V. 1980. A possible correlation between the degree of karyotype aberrations and the rate of sister chromatid exchanges in lymphoma lines. *Int J Cancer* 26:749-756.
- Friedman AD. 1999. Leukemogenesis by CBF oncoproteins. *Leukemia* 13:1932-1942.
- Galon J, Franchimont D, Hiroi N, Frey G, Boettner A, Ehrhart-Bornstein M, O'Shea JJ, Chrousos GP, Bornstein SR. 2002. Gene profiling reveals unknown enhancing and suppressive actions of glucocorticoids on immune cells. *FASEB J* 16:61-71.
- Gelman R, Wilkening C. 2000. Analyses of quality assessment studies using CD45 for gating lymphocytes for CD3(+)4(+)%. *Cytometry* 42:1-4.
- Gilliland DG. 1998. Molecular genetics of human leukemia. *Leukemia* 12 Suppl 1:S7-12.
- Gilliland DG, Griffin JD. 2002. The roles of FLT3 in hematopoiesis and leukemia. *Blood* 100:1532-1542.
- Gilliland DG, Tallman MS. 2002. Focus on acute leukemias. *Cancer Cell* 1:417-420.
- Gleissner B, Rieder H, Thiel E, Fonatsch C, Janssen LA, Heinze B, Janssen JW, Schoch C, Goekbuget N, Maurer J et al. 2001. Prospective BCR-ABL analysis by polymerase chain reaction (RT-PCR) in adult acute B-lineage lymphoblastic leukemia: reliability of RT-nested-PCR and comparison to cytogenetic data. *Leukemia* 15:1834-1840.
- Goldman JM, Melo JV. 2003. Chronic myeloid leukemia--advances in biology and new approaches to treatment. *N Engl J Med* 349:1451-1464.
- Golub TR, Slonim DK, Tamayo P, Huard C, Gaasenbeek M, Mesirov JP, Coller H, Loh ML, Downing JR, Caligiuri MA et al. 1999. Molecular classification of cancer: class discovery and class prediction by gene expression monitoring. *Science* 286:531-537.

- Grimwade D, Walker H, Oliver F, Wheatley K, Harrison C, Harrison G, Rees J, Hann I, Stevens R, Burnett A et al. 1998. The importance of diagnostic cytogenetics on outcome in AML: analysis of 1,612 patients entered into the MRC AML 10 trial. The Medical Research Council Adult and Children's Leukaemia Working Parties. *Blood* 92:2322-2333.
- Grimwade D, Walker H, Harrison G, Oliver F, Chatters S, Harrison CJ, Wheatley K, Burnett AK, Goldstone AH. 2001. The predictive value of hierarchical cytogenetic classification in older adults with acute myeloid leukemia (AML): analysis of 1065 patients entered into the United Kingdom Medical Research Council AML11 trial. *Blood* 98:1312-1320.
- Grimwade D, Enver T. 2004. Acute promyelocytic leukemia: where does it stem from? *Leukemia* 18:375-384.
- Gubler U, Hoffman BJ. 1983. A simple and very efficient method for generating cDNA libraries. *Gene* 25:263-269.
- Guyon I, Weston J, Barnhill S, Vapnik V. 2002. Gene selection for cancer classification using support vector machines. *Machine Learning* 46:389-422.
- Haferlach T, Gassmann W, Loffler H, Jurgensen C, Noak J, Ludwig WD, Thiel E, Haase D, Fonatsch C, Becher R et al. 1993. Clinical aspects of acute myeloid leukemias of the FAB types M3 and M4Eo. The AML Cooperative Group. *Ann Hematol* 66:165-170.
- Haferlach T, Schoch C. 2002. Modern techniques in leukemia diagnosis. *Internist (Berl)* 43:1190, 1193-1190, 1202.
- Haferlach T, Kohlmann A, Kern W, Hiddemann W, Schnittger S, Schoch C. 2003a. Gene expression profiling as a tool for the diagnosis of acute leukemias. *Semin Hematol* 40:281-295.
- Haferlach T, Schoch C, Loffler H, Gassmann W, Kern W, Schnittger S, Fonatsch C, Ludwig WD, Wuchter C, Schlegelberger B et al. 2003b. Morphologic dysplasia in de novo acute myeloid leukemia (AML) is related to unfavorable cytogenetics but has no independent prognostic relevance under the conditions of intensive induction therapy: results of a multiparameter analysis from the German AML Cooperative Group studies. *J Clin Oncol* 21:256-265.
- Haferlach T, Kern W, Schoch C, Schnittger S, Sauerland MC, Heinecke A, Buchner T, Hiddemann W. 2004. A new prognostic score for patients with acute myeloid leukemia based on cytogenetics and early blast clearance in trials of the German AML Cooperative Group. *Haematologica* 89:408-418.
- Halgren RG, Fielden MR, Fong CJ, Zacharewski TR. 2001. Assessment of clone identity and sequence fidelity for 1189 IMAGE cDNA clones. *Nucleic Acids Res* 29:582-588.
- Harris MA, Clark J, Ireland A, Lomax J, Ashburner M, Foulger R, Eilbeck K, Lewis S, Marshall B, Mungall C et al. 2004. The Gene Ontology (GO) database and informatics resource. *Nucleic Acids Res* 32 Database issue:D258-D261.
- Hedenfalk I, Duggan D, Chen Y, Radmacher M, Bittner M, Simon R, Meltzer P, Gusterson B, Esteller M, Kallioniemi OP et al. 2001. Gene-expression profiles in hereditary breast cancer. *N Engl J Med* 344:539-548.
- Hoelzer D, Ludwig WD, Thiel E, Gassmann W, Loffler H, Fonatsch C, Rieder H, Heil G, Heinze B, Arnold R et al. 1996. Improved outcome in adult B-cell acute lymphoblastic leukemia. *Blood* 87:495-508.
- Hoffmann EP. 2004. Expression profiling--best practices for data generation and interpretation in clinical trials. *Nat Rev Genet* 5:229-237.

- Hofmann WK, de Vos S, Komor M, Hoelzer D, Wachsmann W, Koeffler HP. 2002. Characterization of gene expression of CD34+ cells from normal and myelodysplastic bone marrow. *Blood* 100:3553-3560.
- Holloway AJ, van Laar RK, Tothill RW, Bowtell DD. 2002. Options available--from start to finish--for obtaining data from DNA microarrays II. *Nat Genet* 32 Suppl:481-489.
- Hubbell E, Liu WM, Mei R. 2002. Robust estimators for expression analysis. *Bioinformatics* 18:1585-1592.
- Hughes TP, Kaeda J, Branford S, Rudzki Z, Hochhaus A, Hensley ML, Gathmann I, Bolton AE, van Hoomissen IC, Goldman JM et al. 2003. Frequency of major molecular responses to imatinib or interferon alfa plus cytarabine in newly diagnosed chronic myeloid leukemia. *N Engl J Med* 349:1423-1432.
- Huret JL, Dessen P, Bernheim A. 2001. An atlas of chromosomes in hematological malignancies. Example: 11q23 and MLL partners. *Leukemia* 15:987-989.
- Hyun TS, Ross TS. 2004. HIP1: trafficking roles and regulation of tumorigenesis. *Trends Mol Med* 10:194-199.
- Inohara N, Koseki T, del Peso L, Hu Y, Yee C, Chen S, Carrio R, Merino J, Liu D, Ni J et al. 1999. Nod1, an Apaf-1-like activator of caspase-9 and nuclear factor-kappaB. *J Biol Chem* 274:14560-14567.
- Irizarry RA, Hobbs B, Collin F, Beazer-Barclay YD, Antonellis KJ, Scherf U, Speed TP. 2003. Exploration, normalization, and summaries of high density oligonucleotide array probe level data. *Biostatistics* 4:249-264.
- Ito Y. 2004. Oncogenic potential of the RUNX gene family: 'overview'. *Oncogene* 23:4198-4208.
- Iwasaki-Arai J, Iwasaki H, Miyamoto T, Watanabe S, Akashi K. 2003. Enforced granulocyte/macrophage colony-stimulating factor signals do not support lymphopoiesis, but instruct lymphoid to myelomonocytic lineage conversion. *J Exp Med* 197:1311-1322.
- Jaffe ES, Harris NL, Stein H, Vardiman JW. 2001. World Health Organization Classification of Tumours. Pathology and Genetics of Tumours of Haematopoietic and Lymphoid Tissues. IARC Press: Lyon.
- Jandl JH. 1996. Textbook of Hematology. Little, Brown and Company: Boston.
- Jelinek DF, Tschumper RC, Stolovitzky GA, Iturria SJ, Tu Y, Lepre J, Shah N, Kay NE. 2003. Identification of a global gene expression signature of B-chronic lymphocytic leukemia. *Mol Cancer Res* 1:346-361.
- Johnstone RW, See RH, Sells SF, Wang J, Muthukkumar S, Englert C, Haber DA, Licht JD, Sugrue SP, Roberts T et al. 1996. A novel repressor, par-4, modulates transcription and growth suppression functions of the Wilms' tumor suppressor WT1. *Mol Cell Biol* 16:6945-6956.
- Jolliffe IT. 2002. Principal Component Analysis. Springer: New York.
- Kantarjian H, Sawyers C, Hochhaus A, Guilhot F, Schiffer C, Gambacorti-Passerini C, Niederwieser D, Resta D, Capdeville R, Zoellner U et al. 2002. Hematologic and cytogenetic responses to imatinib mesylate in chronic myelogenous leukemia. *N Engl J Med* 346:645-652.
- Kawagoe H, Humphries RK, Blair A, Sutherland HJ, Hogge DE. 1999. Expression of HOX genes, HOX cofactors, and MLL in phenotypically and functionally defined subpopulations of leukemic and normal human hematopoietic cells. *Leukemia* 13:687-698.

- Kelly LM, Kutok JL, Williams IR, Boulton CL, Amaral SM, Curley DP, Ley TJ, Gilliland DG. 2002. PML/RARalpha and FLT3-ITD induce an APL-like disease in a mouse model. *Proc Natl Acad Sci U S A* 99:8283-8288.
- Kern W, Haferlach T, Schoch C, Loffler H, Gassmann W, Heinecke A, Sauerland MC, Berdel WE, Buchner T, Hiddemann W. 2003a. Early blast clearance by remission induction therapy is a major independent prognostic factor for both achievement of complete remission and long-term outcome in acute myeloid leukemia: data from the German AML Cooperative Group (AMLCG) 1992 Trial. *Blood* 101:64-70.
- Kern W, Kohlmann A, Wuchter C, Schnittger S, Schoch C, Mergenthaler S, Ratei R, Ludwig WD, Hiddemann W, Haferlach T. 2003b. Correlation of protein expression and gene expression in acute leukemia. *Cytometry* 55B:29-36.
- Kern W, Voskova D, Schoch C, Hiddemann W, Schnittger S, Haferlach T. 2004. Determination of relapse risk based on assessment of minimal residual disease during complete remission by multiparameter flow cytometry in unselected patients with acute myeloid leukemia. *Blood* 104:3078-3085.
- Khan J, Wei JS, Ringner M, Saal LH, Ladanyi M, Westermann F, Berthold F, Schwab M, Antonescu CR, Peterson C et al. 2001. Classification and diagnostic prediction of cancers using gene expression profiling and artificial neural networks. *Nat Med* 7:673-679.
- Kim J, Ogata Y, Feldman RA. 2003. Fes tyrosine kinase promotes survival and terminal granulocyte differentiation of factor-dependent myeloid progenitors (32D) and activates lineage-specific transcription factors. *J Biol Chem* 278:14978-14984.
- Kim NG, Rhee H, Li LS, Kim H, Lee JS, Kim JH, Kim NK, Kim H. 2002. Identification of MARCKS, FLJ11383 and TAF1B as putative novel target genes in colorectal carcinomas with microsatellite instability. *Oncogene* 21:5081-5087.
- Kohlmann A, Schoch C, Schnittger S, Dugas M, Hiddemann W, Kern W, Haferlach T. 2003. Molecular characterization of acute leukemias by use of microarray technology. *Genes Chromosomes Cancer* 37:396-405.
- Kumar AR, Hudson WA, Chen W, Nishiuchi R, Yao Q, Kersey JH. 2004. Hoxa9 influences the phenotype but not the incidence of Mll-AF9 fusion gene leukemia. *Blood* 103:1823-1828.
- Kummalue T, Friedman AD. 2003. Cross-talk between regulators of myeloid development: C/EBPalpha binds and activates the promoter of the PU.1 gene. *J Leukoc Biol* 74:464-470.
- Lander ES, Linton LM, Birren B, Nusbaum C, Zody MC, Baldwin J, Devon K, Dewar K, Doyle M, FitzHugh W et al. 2001. Initial sequencing and analysis of the human genome. *Nature* 409:860-921.
- Lengfelder E, Reichert A, Schoch C, Haase D, Haferlach T, Loffler H, Staib P, Heyll A, Seifarth W, Saussele S et al. 2000. Double induction strategy including high dose cytarabine in combination with all-trans retinoic acid: effects in patients with newly diagnosed acute promyelocytic leukemia. German AML Cooperative Group. *Leukemia* 14:1362-1370.
- Leo A, Wienands J, Baier G, Horejsi V, Schraven B. 2002. Adapters in lymphocyte signaling. *J Clin Invest* 109:301-309.
- Li C, Wong WH. 2001. Model-based analysis of oligonucleotide arrays: expression index computation and outlier detection. *Proc Natl Acad Sci U S A* 98:31-36.
- Lipshutz RJ, Fodor SP, Gingeras TR, Lockhart DJ. 1999. High density synthetic oligonucleotide arrays. *Nat Genet* 21:20-24.

- Liu WM, Mei R, Di X, Ryder TB, Hubbell E, Dee S, Webster TA, Harrington CA, Ho MH, Baid J et al. 2002. Analysis of high density expression microarrays with signed-rank call algorithms. *Bioinformatics* 18:1593-1599.
- Liu C, Sun C, Huang H, Janda K, Edgington T. 2003a. Overexpression of legumain in tumors is significant for invasion/metastasis and a candidate enzymatic target for prodrug therapy. *Cancer Res* 63:2957-2964.
- Liu G, Loraine AE, Shigeta R, Cline M, Cheng J, Valmeekam V, Sun S, Kulp D, Siani-Rose MA. 2003b. NetAffx: Affymetrix probesets and annotations. *Nucleic Acids Res* 31:82-86.
- Lockhart DJ, Dong H, Byrne MC, Follettie MT, Gallo MV, Chee MS, Mittmann M, Wang C, Kobayashi M, Horton H et al. 1996. Expression monitoring by hybridization to high-density oligonucleotide arrays. *Nat Biotechnol* 14:1675-1680.
- Lockhart DJ, Winzeler EA. 2000. Genomics, gene expression and DNA arrays. *Nature* 405:827-836.
- Löffler H, Rastetter J, Haferlach T. 2004. Atlas of clinical hematology. Springer: Berlin.
- Look AT. 1997. Oncogenic transcription factors in the human acute leukemias. *Science* 278:1059-1064.
- Lowenberg B, Downing JR, Burnett A. 1999. Acute myeloid leukemia. *N Engl J Med* 341:1051-1062.
- Lucio P, Gaipa G, van Lochem EG, van Wering ER, Porwit-MacDonald A, Faria T, Bjorklund E, Biondi A, van den Beemd MW, Baars E et al. 2001. BIOMED-I concerted action report: flow cytometric immunophenotyping of precursor B-ALL with standardized triple-stainings. BIOMED-1 Concerted Action Investigation of Minimal Residual Disease in Acute Leukemia: International Standardization and Clinical Evaluation. *Leukemia* 15:1185-1192.
- Maier H, Hagman J. 2002. Roles of EBF and Pax-5 in B lineage commitment and development. *Semin Immunol* 14:415-422.
- Masternak K, Muhlethaler-Mottet A, Villard J, Zufferey M, Steimle V, Reith W. 2000. CIITA is a transcriptional coactivator that is recruited to MHC class II promoters by multiple synergistic interactions with an enhanceosome complex. *Genes Dev* 14:1156-1166.
- Mathew S, Raimondi SC. 2003. FISH, CGH, and SKY in the diagnosis of childhood acute lymphoblastic leukemia. *Methods Mol Biol* 220:213-233.
- Maurer J, Janssen JW, Thiel E, van Denderen J, Ludwig WD, Aydemir U, Heinze B, Fonatsch C, Harbott J, Reiter A et al. 1991. Detection of chimeric BCR-ABL genes in acute lymphoblastic leukaemia by the polymerase chain reaction. *Lancet* 337:1055-1058.
- McKeon FD, Kirschner MW, Caput D. 1986. Homologies in both primary and secondary structure between nuclear envelope and intermediate filament proteins. *Nature* 319:463-468.
- Mecucci C, Rosati R, Starza RL. 2002. Genetic profile of acute myeloid leukemia. *Rev Clin Exp Hematol* 6:3-25.
- Mei R, Hubbell E, Bekiranov S, Mittmann M, Christians FC, Shen MM, Lu G, Fang J, Liu WM, Ryder T et al. 2003. Probe selection for high-density oligonucleotide arrays. *Proc Natl Acad Sci U S A* 100:11237-11242.

- Mistry AR, Pedersen EW, Solomon E, Grimwade D. 2003. The molecular pathogenesis of acute promyelocytic leukaemia: implications for the clinical management of the disease. *Blood Rev* 17:71-97.
- Mitelman F. 1995. Guidelines for cancer cytogenetics: An international system for human cytogenetic nomenclature. Karger: Basel.
- Miyachi H, Tanaka Y, Gondo K, Kawada T, Kato S, Sasao T, Hotta T, Oshima S, Ando Y. 1999. Altered expression of CD45 isoforms in differentiation of acute myeloid leukemia. *Am J Hematol* 62:159-164.
- Miyoshi A, Kitajima Y, Sumi K, Sato K, Hagiwara A, Koga Y, Miyazaki K. 2004. Snail and SIP1 increase cancer invasion by upregulating MMP family in hepatocellular carcinoma cells. *Br J Cancer* 90:1265-1273.
- Nishizawa K, Freund C, Li J, Wagner G, Reinherz EL. 1998. Identification of a proline-binding motif regulating CD2-triggered T lymphocyte activation. *Proc Natl Acad Sci U S A* 95:14897-14902.
- O'Brien SG, Guilhot F, Larson RA, Gathmann I, Baccarani M, Cervantes F, Cornelissen JJ, Fischer T, Hochhaus A, Hughes T et al. 2003. Imatinib compared with interferon and low-dose cytarabine for newly diagnosed chronic-phase chronic myeloid leukemia. *N Engl J Med* 348:994-1004.
- Onciu M, Lai R, Vega F, Bueso-Ramos C, Medeiros LJ. 2002. Precursor T-cell acute lymphoblastic leukemia in adults: age-related immunophenotypic, cytogenetic, and molecular subsets. *Am J Clin Pathol* 117:252-258.
- Orfao A, Ortuno F, de Santiago M, Lopez A, San Miguel J. 2004. Immunophenotyping of acute leukemias and myelodysplastic syndromes. *Cytometry* 58A:62-71.
- Perou CM, Sorlie T, Eisen MB, van de RM, Jeffrey SS, Rees CA, Pollack JR, Ross DT, Johnsen H, Akslen LA et al. 2000. Molecular portraits of human breast tumours. *Nature* 406:747-752.
- Peterson LF, Zhang DE. 2004. The 8;21 translocation in leukemogenesis. *Oncogene* 23:4255-4262.
- Pirrotta V. 1998. Polycomb the genome: PcG, trxG, and chromatin silencing. *Cell* 93:333-336.
- Pomeroy SL, Tamayo P, Gaasenbeek M, Sturla LM, Angelo M, McLaughlin ME, Kim JY, Goumnerova LC, Black PM, Lau C et al. 2002. Prediction of central nervous system embryonal tumour outcome based on gene expression. *Nature* 415:436-442.
- Preudhomme C, Sagot C, Boissel N, Cayuela JM, Tigaud I, De Botton S, Thomas X, Raffoux E, Lamandin C, Castaigne S et al. 2002. Favorable prognostic significance of CEBPA mutations in patients with de novo acute myeloid leukemia: a study from the Acute Leukemia French Association (ALFA). *Blood* 100:2717-2723.
- Pui CH, Relling MV, Downing JR. 2004. Acute lymphoblastic leukemia. *N Engl J Med* 350:1535-1548.
- Quackenbush J. 2002. Microarray data normalization and transformation. *Nat Genet* 32 Suppl:496-501.
- Quinlan JR. 1993. C4.5: Programs for machine learning. Morgan Kaufmann: San Mateo.

- Ramaswamy S, Tamayo P, Rifkin R, Mukherjee S, Yeang CH, Angelo M, Ladd C, Reich M, Latulippe E, Mesirov JP et al. 2001. Multiclass cancer diagnosis using tumor gene expression signatures. *Proc Natl Acad Sci U S A* 98:15149-15154.
- Reiter A, Lengfelder E, Grimwade D. 2004. Pathogenesis, diagnosis and monitoring of residual disease in acute promyelocytic leukaemia. *Acta Haematol* 112:55-67.
- Repp R, Borkhardt A, Haupt E, Kreuder J, Brettreich S, Hammermann J, Nishida K, Harbott J, Lampert F. 1995. Detection of four different 11q23 chromosomal abnormalities by multiplex-PCR and fluorescence-based automatic DNA-fragment analysis. *Leukemia* 9:210-215.
- Richards MK, Liu F, Iwasaki H, Akashi K, Link DC. 2003. Pivotal role of granulocyte colony-stimulating factor in the development of progenitors in the common myeloid pathway. *Blood* 102:3562-3568.
- Rickman DS, Herbert CJ, Aggerbeck LP. 2003. Optimizing spotting solutions for increased reproducibility of cDNA microarrays. *Nucleic Acids Res* 31:e109.
- Rosenwald A, Wright G, Chan WC, Connors JM, Campo E, Fisher RI, Gascoyne RD, Muller-Hermelink HK, Smeland EB, Giltnane JM et al. 2002. The use of molecular profiling to predict survival after chemotherapy for diffuse large-B-cell lymphoma. *N Engl J Med* 346:1937-1947.
- Ross ME, Zhou X, Song G, Shurtleff SA, Girtman K, Williams WK, Liu HC, Mahfouz R, Raimondi SC, Lenny N et al. 2003. Classification of pediatric acute lymphoblastic leukemia by gene expression profiling. *Blood* 102:2951-2959.
- Ross ME, Mahfouz R, Onciu M, Liu HC, Zhou X, Song G, Shurtleff SA, Pounds S, Cheng C, Ma J et al. 2004. Gene Expression Profiling of Pediatric Acute Myelogenous Leukemia. *Blood* 104:3679-3687.
- Rowley JD. 1990. The Philadelphia chromosome translocation. A paradigm for understanding leukemia. *Cancer* 65:2178-2184.
- Rowley JD. 2001. Chromosome translocations: dangerous liaisons revisited. *Nat Rev Cancer* 1:245-250.
- Rowley JD, Golomb HM, Dougherty C. 1977. 15/17 translocation, a consistent chromosomal change in acute promyelocytic leukaemia. *Lancet* 1:549-550.
- Rozovskaia T, Feinstein E, Mor O, Foa R, Blechman J, Nakamura T, Croce CM, Cimino G, Canaani E. 2001. Upregulation of Meis1 and HoxA9 in acute lymphocytic leukemias with the t(4 : 11) abnormality. *Oncogene* 20:874-878.
- Rozovskaia T, Ravid-Amir O, Tillib S, Getz G, Feinstein E, Agrawal H, Nagler A, Rappaport EF, Issaeva I, Matsuo Y et al. 2003. Expression profiles of acute lymphoblastic and myeloblastic leukemias with ALL-1 rearrangements. *Proc Natl Acad Sci U S A* 100:7853-7858.
- Rubnitz JE, Morrissey J, Savage PA, Cleary ML. 1994. ENL, the gene fused with HRX in t(11;19) leukemias, encodes a nuclear protein with transcriptional activation potential in lymphoid and myeloid cells. *Blood* 84:1747-1752.
- Saitoh T, Mine T, Katoh M. 2002. Molecular cloning and expression of proto-oncogene FRAT1 in human cancer. *Int J Oncol* 20:785-789.
- Sambrook J, Fritsch EF, Maniatis T. 1989. *Molecular cloning: a laboratory manual* (2nd edition). Cold Spring Harbor Laboratory.

- Sangrar W, Gao Y, Zirngibl RA, Scott ML, Greer PA. 2003. The *fps/fes* proto-oncogene regulates hematopoietic lineage output. *Exp Hematol* 31:1259-1267.
- Sanz MA, Martin G, Rayon C, Esteve J, Gonzalez M, Diaz-Mediavilla J, Bolufer P, Barragan E, Terol MJ, Gonzalez JD et al. 1999. A modified AIDA protocol with anthracycline-based consolidation results in high antileukemic efficacy and reduced toxicity in newly diagnosed PML/RARalpha-positive acute promyelocytic leukemia. PETHEMA group. *Blood* 94:3015-3021.
- Satijn DP, Olson DJ, van der Vlag J, Hamer KM, Lambrechts C, Masselink H, Gunster MJ, Sewalt RG, van Driel R, Otte AP. 1997. Interference with the expression of a novel human polycomb protein, hPc2, results in cellular transformation and apoptosis. *Mol Cell Biol* 17:6076-6086.
- Schadt EE, Li C, Su C, Wong WH. 2000. Analyzing high-density oligonucleotide gene expression array data. *J Cell Biochem* 80:192-202.
- Schena M, Shalon D, Davis RW, Brown PO. 1995. Quantitative monitoring of gene expression patterns with a complementary DNA microarray. *Science* 270:467-470.
- Scheuring UJ, Pfeifer H, Wassmann B, Bruck P, Atta J, Petershofen EK, Gehrke B, Gschaidmeier H, Hoelzer D, Ottmann OG. 2003. Early minimal residual disease (MRD) analysis during treatment of Philadelphia chromosome/Bcr-Abl-positive acute lymphoblastic leukemia with the Abl-tyrosine kinase inhibitor imatinib (STI571). *Blood* 101:85-90.
- Schnittger S, Kinkelin U, Schoch C, Heinecke A, Haase D, Haferlach T, Buchner T, Wormann B, Hiddemann W, Griesinger F. 2000. Screening for MLL tandem duplication in 387 unselected patients with AML identify a prognostically unfavorable subset of AML. *Leukemia* 14:796-804.
- Schnittger S, Schoch C, Dugas M, Kern W, Staib P, Wuchter C, Loffler H, Sauerland CM, Serve H, Buchner T et al. 2002. Analysis of FLT3 length mutations in 1003 patients with acute myeloid leukemia: correlation to cytogenetics, FAB subtype, and prognosis in the AMLCG study and usefulness as a marker for the detection of minimal residual disease. *Blood* 100:59-66.
- Schnittger S, Weisser M, Schoch C, Hiddemann W, Haferlach T, Kern W. 2003. New score predicting for prognosis in PML-RARA+, AML1-ETO+, or CBFMBYH11+ acute myeloid leukemia based on quantification of fusion transcripts. *Blood* 102:2746-2755.
- Schoch C, Haase D, Fonatsch C, Haferlach T, Loffler H, Schlegelberger B, Hossfeld DK, Becher R, Sauerland MC, Heinecke A et al. 1997. The significance of trisomy 8 in de novo acute myeloid leukaemia: the accompanying chromosome aberrations determine the prognosis. German AML Cooperative Study Group. *Br J Haematol* 99:605-611.
- Schoch C, Haferlach T, Haase D, Fonatsch C, Loffler H, Schlegelberger B, Staib P, Sauerland MC, Heinecke A, Buchner T et al. 2001. Patients with de novo acute myeloid leukaemia and complex karyotype aberrations show a poor prognosis despite intensive treatment: a study of 90 patients. *Br J Haematol* 112:118-126.
- Schoch C, Kohlmann A, Schnittger S, Brors B, Dugas M, Mergenthaler S, Kern W, Hiddemann W, Eils R, Haferlach T. 2002a. Acute myeloid leukemias with reciprocal rearrangements can be distinguished by specific gene expression profiles. *Proc Natl Acad Sci U S A* 99:10008-10013.
- Schoch C, Schnittger S, Bursch S, Gerstner D, Hochhaus A, Berger U, Hehlmann R, Hiddemann W, Haferlach T. 2002b. Comparison of chromosome banding analysis, interphase- and hypermetaphase-FISH, qualitative and quantitative PCR for diagnosis and for follow-up in chronic myeloid leukemia: a study on 350 cases. *Leukemia* 16:53-59.
- Schoch C, Schnittger S, Klaus M, Kern W, Hiddemann W, Haferlach T. 2003. AML with 11q23/MLL abnormalities as defined by the WHO classification: incidence, partner

chromosomes, FAB subtype, age distribution, and prognostic impact in an unselected series of 1897 cytogenetically analyzed AML cases. *Blood* 102:2395-2402.

Schoch C, Kern W, Schnittger S, Buchner T, Hiddemann W, Haferlach T. 2004a. The influence of age on prognosis of de novo acute myeloid leukemia differs according to cytogenetic subgroups. *Haematologica* 89:1082-1090.

Schoch C, Kern W, Schnittger S, Hiddemann W, Haferlach T. 2004b. Karyotype is an independent prognostic parameter in therapy-related acute myeloid leukemia (t-AML): an analysis of 93 patients with t-AML in comparison to 1091 patients with de novo AML. *Leukemia* 18:120-125.

Schölkopf B, Smola AJ. 2002. *Learning with Kernels*. MIT Press: Cambridge, MA.

Schrock E, du MS, Veldman T, Schoell B, Wienberg J, Ferguson-Smith MA, Ning Y, Ledbetter DH, Bar-Am I, Soenksen D et al. 1996. Multicolor spectral karyotyping of human chromosomes. *Science* 273:494-497.

Schwarz G, Brandenburg J, Reich M, Burster T, Driessen C, Kalbacher H. 2002. Characterization of legumain. *Biol Chem* 383:1813-1816.

Scoggan KA, Nicholson DW, Ford-Hutchinson AW. 1996. Regulation of leukotriene-biosynthetic enzymes during differentiation of myelocytic HL-60 cells to eosinophilic or neutrophilic cells. *Eur J Biochem* 239:572-578.

Shigesada K, van de SB, Liu PP. 2004. Mechanism of leukemogenesis by the inv(16) chimeric gene CFBF/PEBP2B-MHY11. *Oncogene* 23:4297-4307.

Slonim DK. 2002. From patterns to pathways: gene expression data analysis comes of age. *Nat Genet* 32 Suppl:502-508.

Slovak ML, Kopecky KJ, Cassileth PA, Harrington DH, Theil KS, Mohamed A, Paietta E, Willman CL, Head DR, Rowe JM et al. 2000. Karyotypic analysis predicts outcome of preremission and postremission therapy in adult acute myeloid leukemia: a Southwest Oncology Group/Eastern Cooperative Oncology Group Study. *Blood* 96:4075-4083.

Smith M, Barnett M, Bassan R, Gatta G, Tondini C, Kern W. 2004. Adult acute myeloid leukaemia. *Crit Rev Oncol Hematol* 50:197-222.

So CW, Karsunky H, Passegue E, Cozzio A, Weissman IL, Cleary ML. 2003. MLL-GAS7 transforms multipotent hematopoietic progenitors and induces mixed lineage leukemias in mice. *Cancer Cell* 3:161-171.

Southan C. 2004. Has the yo-yo stopped? An assessment of human protein-coding gene number. *Proteomics* 4:1712-1726.

Southern E, Mir K, Shchepinov M. 1999. Molecular interactions on microarrays. *Nat Genet* 21:5-9.

Speicher MR, Gwyn BS, Ward DC. 1996. Karyotyping human chromosomes by combinatorial multi-fluor FISH. *Nat Genet* 12:368-375.

Staal FJ, van der BM, Wessels LF, Barendregt BH, Baert MR, van den Burg CM, van Huffel C, Langerak AW, van dV, V, Reinders MJ et al. 2003. DNA microarrays for comparison of gene expression profiles between diagnosis and relapse in precursor-B acute lymphoblastic leukemia: choice of technique and purification influence the identification of potential diagnostic markers. *Leukemia* 17:1324-1332.

- Staudt LM. 2002. It's ALL in the diagnosis. *Cancer Cell* 1:109-110.
- Staudt LM. 2003. Molecular diagnosis of the hematologic cancers. *N Engl J Med* 348:1777-1785.
- Stewart M, Terry A, Hu M, O'Hara M, Blyth K, Baxter E, Cameron E, Onions DE, Neil JC. 1997. Proviral insertions induce the expression of bone-specific isoforms of PEBP2alphaA (CBFA1): evidence for a new myc collaborating oncogene. *Proc Natl Acad Sci U S A* 94:8646-8651.
- Storey JD, Tibshirani R. 2003. Statistical significance for genomewide studies. *Proc Natl Acad Sci U S A* 100:9440-9445.
- Szaniszlo P, Wang N, Sinha M, Reece LM, Van Hook JW, Luxon BA, Leary JF. 2004. Getting the right cells to the array: Gene expression microarray analysis of cell mixtures and sorted cells. *Cytometry* 59A:191-202.
- Tallman MS, Andersen JW, Schiffer CA, Appelbaum FR, Feusner JH, Ogden A, Shepherd L, Willman C, Bloomfield CD, Rowe JM et al. 1997. All-trans-retinoic acid in acute promyelocytic leukemia. *N Engl J Med* 337:1021-1028.
- Tallman MS, Andersen JW, Schiffer CA, Appelbaum FR, Feusner JH, Woods WG, Ogden A, Weinstein H, Shepherd L, Willman C et al. 2002. All-trans retinoic acid in acute promyelocytic leukemia: long-term outcome and prognostic factor analysis from the North American Intergroup protocol. *Blood* 100:4298-4302.
- Tallman MS. 2004a. Acute promyelocytic leukemia as a paradigm for targeted therapy. *Semin Hematol* 41:27-32.
- Tallman MS. 2004b. Relevance of pathologic classifications and diagnosis of acute myeloid leukemia to clinical trials and clinical practice. *Cancer Treat Res* 121:45-67.
- ten Dijke P, Goumans MJ, Itoh F, Itoh S. 2002. Regulation of cell proliferation by Smad proteins. *J Cell Physiol* 191:1-16.
- Tenen DG. 2003. Disruption of differentiation in human cancer: AML shows the way. *Nat Rev Cancer* 3:89-101.
- Testa U, Riccioni R, Mili S, Coccia E, Stellacci E, Samoggia P, Latagliata R, Mariani G, Rossini A, Battistini A et al. 2002. Elevated expression of IL-3Ralpha in acute myelogenous leukemia is associated with enhanced blast proliferation, increased cellularity, and poor prognosis. *Blood* 100:2980-2988.
- Testa U, Riccioni R, Diverio D, Rossini A, Lo CF, Peschle C. 2004. Interleukin-3 receptor in acute leukemia. *Leukemia* 18:219-226.
- Thiel H, Diem H, Haferlach T. 2004. *Hematology: Practical microscopic and clinical diagnosis*. Thieme: Stuttgart.
- Thompson A, Quinn MF, Grimwade D, O'Neill CM, Ahmed MR, Grimes S, McMullin MF, Cotter F, Lappin TR. 2003. Global down-regulation of HOX gene expression in PML-RARalpha + acute promyelocytic leukemia identified by small-array real-time PCR. *Blood* 101:1558-1565.
- Thorsteinsdottir U, Kroon E, Jerome L, Blasi F, Sauvageau G. 2001. Defining roles for HOX and MEIS1 genes in induction of acute myeloid leukemia. *Mol Cell Biol* 21:224-234.
- Tusher VG, Tibshirani R, Chu G. 2001. Significance analysis of microarrays applied to the ionizing radiation response. *Proc Natl Acad Sci U S A* 98:5116-5121.

- Valk PJ, Verhaak RG, Beijen MA, Erpelinck CA, Barjesteh van Waalwijk van Doorn-Khosrovani, Boer JM, Beverloo HB, Moorhouse MJ, van der Spek PJ, Lowenberg B et al. 2004. Prognostically useful gene-expression profiles in acute myeloid leukemia. *N Engl J Med* 350:1617-1628.
- Van Gelder RN, von Zastrow ME, Yool A, Dement WC, Barchas JD, Eberwine JH. 1990. Amplified RNA synthesized from limited quantities of heterogeneous cDNA. *Proc Natl Acad Sci U S A* 87:1663-1667.
- Vapnik V. 1998. *Statistical Learning Theory*. Wiley: New York.
- Venter JC, Adams MD, Myers EW, Li PW, Mural RJ, Sutton GG, Smith HO, Yandell M, Evans CA, Holt RA et al. 2001. The sequence of the human genome. *Science* 291:1304-1351.
- Villadangos JA, Ploegh HL. 2000. Proteolysis in MHC class II antigen presentation: who's in charge? *Immunity* 12:233-239.
- Virtaneva K, Wright FA, Tanner SM, Yuan B, Lemon WJ, Caligiuri MA, Bloomfield CD, de La CA, Krahe R. 2001. Expression profiling reveals fundamental biological differences in acute myeloid leukemia with isolated trisomy 8 and normal cytogenetics. *Proc Natl Acad Sci U S A* 98:1124-1129.
- Vorwerk P, Wex H, Hohmann B, Mohnike K, Schmidt U, Mittler U. 2002. Expression of components of the IGF signalling system in childhood acute lymphoblastic leukaemia. *Mol Pathol* 55:40-45.
- Warrell RP, Jr., Frankel SR, Miller WH, Jr., Scheinberg DA, Itri LM, Hittelman WN, Vyas R, Andreeff M, Tafuri A, Jakubowski A et al. 1991. Differentiation therapy of acute promyelocytic leukemia with tretinoin (all-trans-retinoic acid). *N Engl J Med* 324:1385-1393.
- Warrell RP, Jr., de The H, Wang ZY, Degos L. 1993. Acute promyelocytic leukemia. *N Engl J Med* 329:177-189.
- Warrington JA, Nair A, Mahadevappa M, Tsyganskaya M. 2000. Comparison of human adult and fetal expression and identification of 535 housekeeping/maintenance genes. *Physiol Genomics* 2:143-147.
- Watanabe R, Wada H, Miura Y, Murata Y, Watanabe Y, Sakakura M, Okugawa Y, Nakasaki T, Mori Y, Nishikawa M et al. 2001. Plasma levels of total plasminogen activator inhibitor-I (PAI-I) and tPA/PAI-1 complex in patients with disseminated intravascular coagulation and thrombotic thrombocytopenic purpura. *Clin Appl Thromb Hemost* 7:229-233.
- Watts C. 1997. Capture and processing of exogenous antigens for presentation on MHC molecules. *Annu Rev Immunol* 15:821-850.
- Weiner HL, Huang H, Zagzag D, Boyce H, Lichtenbaum R, Ziff EB. 2000. Consistent and selective expression of the discoidin domain receptor-1 tyrosine kinase in human brain tumors. *Neurosurgery* 47:1400-1409.
- Wheeler DL, Church DM, Edgar R, Federhen S, Helmberg W, Madden TL, Pontius JU, Schuler GD, Schriml LM, Sequeira E et al. 2004. Database resources of the National Center for Biotechnology Information: update. *Nucleic Acids Res* 32 Database issue:D35-D40.
- Whitney AR, Diehn M, Popper SJ, Alizadeh AA, Boldrick JC, Relman DA, Brown PO. 2003. Individuality and variation in gene expression patterns in human blood. *Proc Natl Acad Sci U S A* 100:1896-1901.

Wright G, Tan B, Rosenwald A, Hurt EH, Wiestner A, Staudt LM. 2003. A gene expression-based method to diagnose clinically distinct subgroups of diffuse large B cell lymphoma. *Proc Natl Acad Sci U S A* 100:9991-9996.

Wydner KL, McNeil JA, Lin F, Worman HJ, Lawrence JB. 1996. Chromosomal assignment of human nuclear envelope protein genes LMNA, LMNB1, and LBR by fluorescence in situ hybridization. *Genomics* 32:474-478.

Yahata T, Takedatsu H, Dunwoodie SL, Braganca J, Swingler T, Withington SL, Hur J, Coser KR, Isselbacher KJ, Bhattacharya S et al. 2002. Cloning of mouse Cited4, a member of the CITED family p300/CBP-binding transcriptional coactivators: induced expression in mammary epithelial cells. *Genomics* 80:601-613.

Yeoh EJ, Ross ME, Shurtleff SA, Williams WK, Patel D, Mahfouz R, Behm FG, Raimondi SC, Relling MV, Patel A et al. 2002. Classification, subtype discovery, and prediction of outcome in pediatric acute lymphoblastic leukemia by gene expression profiling. *Cancer Cell* 1:133-143.

Young RA. 2000. Biomedical discovery with DNA arrays. *Cell* 102:9-15.

Zeisig BB, Milne T, Garcia-Cuellar MP, Schreiner S, Martin ME, Fuchs U, Borkhardt A, Chanda SK, Walker J, Soden R et al. 2004. Hoxa9 and Meis1 are key targets for MLL-ENL-mediated cellular immortalization. *Mol Cell Biol* 24:617-628.

7. Appendix

Reagents, components, and instruments for microarray analysis were purchased from the following vendors:

Manufacturer	Contact information	Internet
Affymetrix	Santa Clara, CA, USA	www.affymetrix.com
Alexis	Grünberg, Germany	www.alexis-corp.com/
Ambion	Huntingdon, United Kingdom	www.ambion.com
Amersham Biosciences	Freiburg, Germany	www.amershambiosciences.com
Biozym	Hess. Oldendorf, Germany	www.biozym.com
Dianova	Hamburg, Germany	www.dianova.de
Eppendorf	Hamburg, Germany	www.eppendorf.com
Invitrogen	Karlsruhe, Germany	www.invitrogen.com
Millipore	Schwalbach, Germany	www.millipore.com
NeoLab	Heidelberg, Germany	www.neolab.de
Nunc	Wiesbaden, Germany	www.nalgenunc.com/
Pierce Chemicals	Rockford, IL, USA	www.piercenet.com
Qiagen	Hilden, Germany	www.qiagen.de
Rainin	Oakland, CA, USA	www.rainin.com
Roche Applied Science	Mannheim, Germany	www.roche-applied-science.com
Roth	Karlsruhe, Germany	www.carl-roth.de
Sigma	Munich, Germany	www.sigmaaldrich.com

7.1 Chemicals, enzymes, and reagents

Chemicals & Reagents	Manufacturer
2-Mercaptoethanol (25 ml)	Sigma
Acetic acid, glacial (100 ml)	Sigma
Ammonium acetate, 7.5 M (100 ml)	Sigma
Antifoam O-30 (100 ml)	Sigma
anti-streptavidin-PE antibody, goat, biotinylated (0.5 mg/ml)	Alexis
BSA, acetylated (50 mg/ml)	Invitrogen
DEPC-treated Water, nuclease free (10 x 50 ml)	Ambion
DEPC-treated Water, nuclease free (1000 ml)	Ambion
DEPC-treated Water, nuclease free (5 x 100 ml)	Ambion
EDTA, 0.5 M (100 ml)	Sigma
Ethanol, absolute, Rotisolv (1000 ml)	Roth
Glycogen (20 mg/ml)	Roche Applied Science
goat IgG, reagent grade (10 mg/ml)	Sigma
Herring sperm DNA (10 mg/ml)	Promega
Lauryl sulfate (100 ml)	Sigma
Magnesium acetate (100 g)	Sigma
MES, free acid monohydrate (250 g)	Sigma
MES, sodium salt (100 g)	Sigma
NaCl, 5 M (100 ml)	Ambion
PBS (1000 ml)	Invitrogen
Phenol/Chloroform/IAA, 25:24:1 (100 ml)	Ambion

Potassium acetate (100 g)	Sigma
Sodium acetate, 3 M (100 ml)	Sigma
Sodium hypochlorite, 12% (1000 ml)	Roth
SSPE, 20X (1000 ml)	Ambion
Streptavidin R-PE (1 mg/ml)	Dianova
TRIZMA base (100 g)	Sigma
Tween-20 (Surfact-Amps), 10% (10 ml)	Pierce Chemicals

Plastic ware	Manufacturer
Collection Tubes, 2 ml	Qiagen
Micro test tubes, amber, 1.6 ml	Biozym
Micro test tubes, nuclease free, 1.6 ml	Biozym
Micro test tubes, individually sealed, Biopur® Safe-Lock, 0.5 ml	Eppendorf
Micro test tubes, individually sealed, Biopur® Safe-Lock, 1.5 ml	Eppendorf
Micro test tubes, individually sealed, Biopur® Safe-Lock, 2,0 ml	Eppendorf
Pipette tips, Fine Point, aerosol resistant, 200 µl	Rainin
Pipette tips, SafeSeal, Premium, 10 µl	Biozym
Pipette tips, SafeSeal, Premium XL, 100 µl	Biozym
Pipette tips, SafeSeal, Premium, 1000 µl	Biozym
Serological pipettes, individually sealed, 10 ml	Nunc
Serological pipettes, individually sealed, 50 ml	Nunc
Stericups Filter Units, Stericup GP (1000 ml)	Millipore
UVette (80 disposable cuvettes)	Eppendorf

Kits	Manufacturer
cDNA Synthesis Kit (10 reactions)	Roche Applied Science
Control Oligonucleotide B2, 3 nM (150 reactions)	Affymetrix
BioArray HighYield RNA Transcript Labeling Kit (10 reactions)	Affymetrix
Eukaryotic Hybridization Control Kit (150 reactions)	Affymetrix
Phase Lock Gel, light (1.5 ml)	Eppendorf
QIAshredder Homogenizer (250 columns)	Qiagen
RNeasy Mini Kit (50 columns)	Qiagen

Miscellaneous	Manufacturer
Precision wipes, Kimberly-Clark Kimwipes Lite (23 x 42 cm)	Roth
RNaseZap Spray (250 ml)	Ambion
RNaseZap Wipes (100 sheets)	Ambion

7.2 Instrumentation and technical equipment

All laboratory equipment used to prepare the target for the microarray analysis was calibrated and carefully maintained to ensure accuracy. Maintenance of the UV spectrophotometer bulbs and scanner laser power settings was performed every 12 months, micropipettors were recalibrated every 9 months, respectively.

Instruments & Equipment	Manufacturer
Accu-jet pipet boy, pipettor for serological pipettes	NeoLab
GeneChip System Fluidics Station 400	Affymetrix
GeneChip System GeneArray Scanner (Agilent version)	Affymetrix
GeneChip System Hybridization Oven 640	Affymetrix
Heat block, for 24 micro test tubes (1.5 ml)	NeoLab
Microcentrifuge 5415 R	Eppendorf
Microcentrifuge rotor F-45-24-11, for 24 tubes (1.5 ml)	Eppendorf
Micropipettor Eppendorf Reference, 0.5-10 μ l	Eppendorf
Micropipettor Eppendorf Reference, 100-1000 μ l	Eppendorf
Micropipettor Eppendorf Reference, 10-100 μ l	Eppendorf
Micropipettor Eppendorf Reference, 2-20 μ l	Eppendorf
Micropipettor Gilson Pipetman P200, 10-200 μ l	NeoLab
Spectrophotometer Ultrospec 3000	Amersham Biosciences
Thermoblock ThermoStat plus, for 24 tubes (1.5 ml)	Eppendorf
Vortex-Genie 2	NeoLab

7.3 Buffers and solutions

According to the manufacturer's recommendations the following buffers and solutions were prepared with RNase-free reagents and molecular biology grade water (Expression Analysis Technical Manual; www.affymetrix.com).

12X MES stock solution

12X MES stock solution (1000 ml)

(1.22 M MES, 0.89 M [Na⁺])

Components

70.4 g MES-free acid monohydrate

193.3 g MES sodium salt

800 ml of water

Mix and adjust volume to 1000 ml.

The pH should be between 6.5 and 6.7. Filter through a 0.2 µm filter. Do not autoclave. Store at 2°C to 8°C and shield from light. Discard solution if yellow.

2X Hybridization buffer

2X Hybridization buffer (50 ml)

(Final 1X concentration is: 100 mM MES, 1 M [Na⁺], 20 mM EDTA, 0.01% Tween-20)

Components

8.3 ml of 12X MES stock solution

17.7 ml of 5 M NaCl

4.0 ml of 0.5 M EDTA

0.1 ml of 10% Tween-20

19.9 ml of water

Mix thoroughly

Store at 2°C to 8°C and shield from light.

5X RNA Fragmentation buffer

5X RNA Fragmentation buffer (20 ml)

(200 mM Tris-acetate, pH 8.2, 500 mM KOAc, 150 mM MgOAc)

Components

4.0 ml 1 M Tris acetate pH 8.1 (Trizma Base, pH adjusted with glacial acetic acid)

0.64 g MgOAc

0.98 g KOAc

Mix and adjust volume with water to 20 ml

Mix thoroughly and filter through a 0.2 µm vacuum filter unit. This reagent was aliquotted (1000 µl each) and stored at room temperature.

Non-stringent wash buffer (Wash A)

Non-stringent wash buffer (1000 ml)

(6X SSPE, 0.01% Tween-20)

Components

300 ml of 20X SSPE

1.0 ml of 10% Tween-20

699 ml of water

Mix thoroughly

Filter through a 0.2 μm filter and then add 500 μl 5% Antifoam solution. Do not autoclave. Store at 2°C to 8°C.

Stringent wash buffer (Wash B)

Stringent wash buffer (1000 ml)

(100 mM MES, 0.1 M [Na⁺], 0.01% Tween-20)

Components

83.3 ml of 12X MES stock solution

5.2 ml of 5 M NaCl

1.0 ml of 10% Tween-20

910.5 ml of water

Mix thoroughly

Filter through a 0.2 μm filter. Store at 2°C to 8°C and shield from light. Discard solution if yellow.

2X Stain buffer

2X Stain buffer (250 ml)

(Final 1X concentration: 100 mM MES, 1 M [Na⁺], 0.05% Tween-20)

Components

41.7 ml 12X MES stock solution

92.5 ml 5 M NaCl

2.5 ml 10% Tween-20

113.3 ml water

Mix thoroughly

Filter through a 0.2 μm filter and then add 500 μl 5% Antifoam solution. Do not autoclave. Store at 2°C to 8°C and shield from light. Discard solution if yellow.

SAPE stain solution

For 4 arrays that are processed in parallel prepare a 10X mastermix in a 15 ml Falcon tube.

SAPE stain solution (600 μ l)

Components

300 μ l 2X stain buffer

24 μ l acetylated BSA (50 mg/ml)

6 μ l Streptavidin-Phycoerythrin (1 mg/ml)

270 μ l water

Mix thoroughly

Method:

1. Combine all necessary components, mix well and divide into four 1.4 ml aliquots (1.5 ml amber tubes).
2. Centrifuge the aliquots for 5 min to pellet insoluble complexes (maximum speed).
3. From the supernatant carefully transfer 600 μ l staining solution into a new amber tube. Do not disturb the pelleted insoluble complexes.

Antibody solution

For 4 arrays that are processed in parallel prepare a 5X mastermix in a 15 ml Falcon tube.

Antibody solution (600 μ l)

Components

300 μ l 2X stain buffer

24 μ l acetylated BSA (50 mg/ml)

6 μ l goat IgG (10 mg/ml)

3.6 μ l biotinylated anti-streptavidin antibody (0.5 mg/ml)

266.4 μ l water

Mix thoroughly

Method:

1. Centrifuge goat IgG and biotinylated anti-streptavidin antibody solutions for 5 min to pellet insoluble complexes (maximum speed). Then combine all necessary components, mix well and divide into two 1.4 ml aliquots.
2. Centrifuge the aliquots for 5 min to pellet insoluble complexes (maximum speed).
3. From the supernatant carefully transfer 600 μ l staining solution into a new tube. Do not disturb the pelleted insoluble complexes.

Antifoam solution

5% (w/v) Antifoam solution

Components

10 g Antifoam O-30

Mix and adjust volume with water to 200 ml

10 mg/ml Goat IgG stock solution

Resuspend 50 mg goat IgG in 5 ml 150 mM NaCl. Store at 4°C.

Publications

- 1 Dugas M, Schoch C, Schnittger S, **Kohlmann A**, Kern W, Haferlach T, Uberla K. 2002. Impact of integrating clinical and genetic information. In *Silico Biol* 2:383-391.
- 2 **Kohlmann A**, Schoch C, Schnittger S, Kern W, Haferlach T. 2002. Diagnosis of leukemia using microarray technology. *Dtsch Med Wochenschr* 127:2216-2222.
- 3 Schoch C*, **Kohlmann A***, Schnittger S, Brors B, Dugas M, Mergenthaler S, Kern W, Hiddemann W, Eils R, Haferlach T. 2002. Acute myeloid leukemias with reciprocal rearrangements can be distinguished by specific gene expression profiles. *Proc Natl Acad Sci U S A* 99:10008-10013.
- 4 Elsasser A, Franzen M, **Kohlmann A**, Weisser M, Schnittger S, Schoch C, Reddy VA, Burel S, Zhang DE, Ueffing M, Tenen DG, Hiddemann W, Behre G. 2003. The fusion protein AML1-ETO in acute myeloid leukemia with translocation t(8;21) induces c-jun protein expression via the proximal AP-1 site of the c-jun promoter in an indirect, JNK-dependent manner. *Oncogene* 22:5646-5657.
- 5 Haferlach T, **Kohlmann A**, Kern W, Hiddemann W, Schnittger S, Schoch C. 2003. Gene expression profiling as a tool for the diagnosis of acute leukemias. *Semin Hematol* 40:281-295.
- 6 Kern W*, **Kohlmann A***, Wuchter C, Schnittger S, Schoch C, Mergenthaler S, Ratei R, Ludwig WD, Hiddemann W, Haferlach T. 2003. Correlation of protein expression and gene expression in acute leukemia. *Cytometry* 55B:29-36.
- 7 **Kohlmann A***, Schoch C*, Schnittger S, Dugas M, Hiddemann W, Kern W, Haferlach T. 2003. Molecular characterization of acute leukemias by use of microarray technology. *Genes Chromosomes Cancer* 37:396-405.
- 8 Rangatia J, Vangala RK, Singh S, Peer Zada A, Elsasser A, **Kohlmann A**, Haferlach T, Tenen DG, Hiddemann W, Behre G. 2003. Elevated c-Jun expression in acute myeloid leukemias inhibits C/EBPalpha DNA binding via leucine zipper domain interaction. *Oncogene* 22:4760-4764.
- 9 Tschoep K, **Kohlmann A**, Schlemmer M, Haferlach T, Issels R. 2003. Gene expression analysis using DNA microarrays in soft tissue and bone tumors. *Dtsch Med Wochenschr* 128:2030-2036.
- 10 **Kohlmann A**, Schoch C, Schnittger S, Dugas M, Hiddemann W, Kern W, Haferlach T. 2004. Pediatric acute lymphoblastic leukemia (ALL) gene expression signatures classify an independent cohort of adult ALL patients. *Leukemia* 18:63-71.

- 11 Kern W, **Kohlmann A**, Schnittger S, Hiddemann W, Schoch C, Haferlach T. 2004. Gene expression profiling as a diagnostic tool in acute myeloid leukemia. *Am J Pharmacogenomics* 4:225-237.
- 12 Xiang W, Windl O, Wunsch G, Dugas M, **Kohlmann A**, Dierkes N, Westner IM, Kretzschmar HA. 2004. Identification of differentially expressed genes in scrapie-infected mouse brains by using global gene expression technology. *J Virol* 78:11051-11060.
- 13 **Kohlmann A**, Schoch C, Dugas M, Rauhut S, Weniger F, Schnittger S, Kern W, Haferlach T. 2004. Pattern robustness of diagnostic gene expression signatures in leukemia *Genes Chromosomes Cancer*: in press.

* both authors contributed equally

Patent applications

Inventions disclosing the lists of differentially expressed genes have been filed at the European Patent Office. In the respective applications, genes identified to be differentially expressed between different types of leukemia and normal bone marrow, respectively, are given by official gene symbol, public database accession numbers, sequence, and Affymetrix probe set identifiers.

- 1 Haferlach T, **Kohlmann A**, Kern W, Schnittger S, Brors B, Mergenthaler S, Eils R, Dugas M, Schoch C. Novel genetic markers for leukemias. European Patent Application EP 1308522 A1, Date of Filing: 5.11.2001, Date of Publication: 7.5.2003
- 2 Haferlach T, **Kohlmann A**, Kern W, Schnittger S, Brors B, Mergenthaler S, Eils R, Dugas M, Schoch C. Novel genetic markers for leukemias. International Patent Application (PCT) WO 03/039433 A2, Date of Filing: 4.11.2002, Date of Publication: 15.5.2003
- 3 Haferlach T, **Kohlmann A**, Kern W, Schnittger S, Dugas M, Schoch C. Method for distinguishing WHO classified AML subtypes. European Patent Application EP 03025337.1, Date of Filing: 4.11.2003
- 4 Haferlach T, **Kohlmann A**, Kern W, Schnittger S, Dugas M, Schoch C. Method for distinguishing immunologically defined ALL subtypes. European Patent Application EP 03025340.1, Date of Filing: 4.11.2003
- 5 Haferlach T, **Kohlmann A**, Kern W, Schnittger S, Dugas M, Schoch C. Method for distinguishing t(11q23)/*MLL*-positive leukemias from t(11q23)/*MLL*-negative leukemias. European Patent Application EP 03025346.2, Date of Filing: 4.11.2003
- 6 Haferlach T, **Kohlmann A**, Kern W, Schnittger S, Dugas M, Schoch C. Method for distinguishing AML subtype inv(3)(q21q26)/t(3;3)(q21q26) from other AML subtypes. European Patent Application EP 03025345.4, Date of Filing: 4.11.2003
- 7 Haferlach T, **Kohlmann A**, Kern W, Schnittger S, Dugas M, Schoch C. Method for distinguishing leukemia subtypes. European Patent Application EP 03025336.3, Date of Filing: 4.11.2003
- 8 Haferlach T, **Kohlmann A**, Kern W, Schnittger S, Dugas M, Schoch C. Method for distinguishing AML-specific FLT3 length mutations from TKD mutations. European Patent Application EP 03025341.3, Date of Filing: 4.11.2003
- 9 Haferlach T, **Kohlmann A**, Kern W, Schnittger S, Dugas M, Schoch C. Method for distinguishing CBF-positive AML subtypes from CBF-negative

AML subtypes. European Patent Application EP 03025335.5, Date of Filing: 4.11.2003

- 10 Haferlach T, **Kohlmann A**, Kern W, Schnittger S, Dugas M, Schoch C. Method for distinguishing AML subtypes with different gene dosages. European Patent Application EP 03025342.1, Date of Filing: 4.11.2003
- 11 Haferlach T, **Kohlmann A**, Kern W, Schnittger S, Dugas M, Schoch C. Method for distinguishing AML subtypes with recurring genetic aberrations. EP 03025343.9 vom 04. 11. 03, Date of Filing: 4.11.2003
- 12 Haferlach T, **Kohlmann A**, Kern W, Schnittger S, Dugas M, Schoch C. Method for distinguishing MLL-PTD-positive AML from other AML subtypes. European Patent Application EP 03025339.7, Date of Filing: 4.11.2003
- 13 Haferlach T, **Kohlmann A**, Kern W, Schnittger S, Dugas M, Schoch C. Method for distinguishing AML subtypes with aberrant and prognostically intermediate karyotypes. European Patent Application EP 03025344.7, Date of Filing: 4.11.2003
- 14 Haferlach T, **Kohlmann A**, Kern W, Schnittger S, Dugas M, Schoch C. Method for distinguishing prognostically definable AML. European Patent Application EP 03025338.9, Date of Filing: 4.11.2003

Danksagung

An erster Stelle möchte ich mich bei meinem Doktorvater Professor Dr. Dr. Torsten Haferlach bedanken. Vielen herzlichen Dank für die interessante Themenstellung und die herausragende Betreuung. Die ständige Bereitschaft meine Arbeit zu diskutieren, freundschaftliche Unterstützung in allen Belangen, sowie vor allem das mir entgegengebrachte Vertrauen haben entscheidend zum Gelingen dieser Arbeit beigetragen.

Herrn Professor Dr. Thomas Cremer möchte ich danken für die Übernahme des Erstgutachtens und die Vertretung meiner Promotion an der Biologischen Fakultät der Ludwig-Maximilians-Universität München.

Herrn Professor Dr. Heinrich Leonhardt gilt mein Dank für die Übernahme des Zweitgutachtens.

Mein besonderer Dank gilt zudem:

- PD Dr. Claudia Schoch, PD Dr. Wolfgang Kern und PD Dr. Susanne Schnittger für die ausgezeichnete Zusammenarbeit, die kritischen Diskussionen meiner Ergebnisse und die schönen Momente auf zahlreichen Kongressen im In- und Ausland.
- dem Team des Labors für Leukämie-Diagnostik, das meine Arbeit über die letzten Jahre begleitete und eine extrem motivierende Atmosphäre vermittelt hat.
- PD Dr. Martin Dugas und Dr. Sylvia Merk für die gute Zusammenarbeit und die vielen Diskussionen und Ratschläge was die Auswertung von Microarraydaten betrifft.
- Dr. Matthias Prucha und Dr. Wieland Keilholz (Affymetrix) für die hilfreiche Unterstützung bei Fragen zum GeneChip System.
- Frank, Dirk, Thorsten, Nicole, Dagi und Andrea, die mich schon seit vielen Jahren auf meinem wissenschaftlichen Lebensweg begleiten und mir immer in entscheidenden Fragen eine große Hilfe waren.
- den Roche Diagnostics Mitarbeitern Prof. Dr. Bärbel Porstmann, Dr. Fabrice Schoumacher, Dr. Friedemann Krause, Dr. Helmut Burtscher, Ute Bär und Dr. Anja Wiese für die erfolgreiche Zusammenarbeit.
- PD Dr. Roland Eils und Dr. Benedikt Brors (DKFZ Heidelberg) für die Kooperation und die Etablierung der Multiple-tree Klassifikationsmethode bei definierten AML Subtypen.
- Manu, Christian, Daniel, Steffi und Axel für die schöne Zeit in München außerhalb des Labors.
- Andy, Dani, Judith, Olli, Tommi, Katja, David, Erminia, Emmi, Tim, Locke, Christine, Sellu und Sonja, weil ich mich immer auf sie verlassen kann.
- meinen Eltern und meiner Schwester, die immer für mich da sind und mich all die letzten Jahre so immens unterstützten.

Lebenslauf

Name: Kohlmann
Vorname: Alexander
Anschrift: Ledererstr. 8, 82131 Gauting
Geburtsdatum: 02. Juli 1975
Geburtsort: Neumarkt i. d. OPf.
Familienstand: ledig

Ausbildung

9/1981 – 7/1985 Grundschole Neumarkt
9/1985 – 7/1994 Ostendorfer-Gymnasium Neumarkt – Abitur
10/1994 – 10/1995 Zivildienst: Beifahrer im Rettungsdienst beim Bayerischen Roten Kreuz, Kreisverband Neumarkt
11/1995 – 3/2001 Biologiestudium an der Bayerischen Julius-Maximilians-Universität in Würzburg; Diplomarbeit angefertigt bei der Roche Diagnostics GmbH, Penzberg, Pharma Research Oncology; Thema: Analyse der CD40-regulierten Genexpression in B-Zellen
seit 4/2001 Promotion an der Ludwig-Maximilians-Universität in München im Labor für spezielle Leukämie-Diagnostik, Universitätsklinikum Großhadern

Praktische Tätigkeiten

5/1995 Praktikum für Rettungssanitäter, Klinikum Neumarkt
6/1998 – 8/1998 Studentische Hilfskraft am Institut für Molekulare Pflanzenphysiologie und Biophysik an der Julius-Maximilians-Universität in Würzburg
11/1998 – 4/1999 Forschungspraktikum bei der Roche Diagnostics GmbH, Penzberg, Pharma Research; Thema: Konstruktion einer retroviralen Verpackungszelllinie
1/2001 – 3/2001 Wissenschaftlicher Mitarbeiter bei der Roche Diagnostics GmbH, Penzberg, Pharma Research; Thema: Validierung von CD40-regulierten Genen

Erklärung:

Hiermit versichere ich, dass die vorliegende Promotionsarbeit das Ergebnis meiner eigenständigen Arbeit ist, und dass ich diese Dissertation persönlich verfasst habe. Zudem habe ich keine anderen als die angegebenen Quellen und Hilfsmittel verwendet.

München, den 1. Dezember 2004

Alexander Kohlmann